Wei Qiu
Kurt Schumacher Str. 48
67663 Kaiserslautern
Deutschland

Transmit power reduction
in MIMO multi-user mobile radio downlinks
by the rationale receiver orientation

deutscher Titel:
Sendeleistungsreduktion durch das Übertragungskonzept Empfängerorientierung in Mehrteilnehmer-Mobilfunkabwärtsstrecken mit MIMO-Antennen

Vom Fachbereich Elektrotechnik und Informationstechnik

der Technischen Universität Kaiserslautern

zur Verleihung des akademischen Grades

Doktor der Ingenieurwissenschaften (Dr.–Ing.)

genehmigte Dissertation

von

M.Sc. Wei Qiu

D 386

Tag der Einreichung: 22.12.2004
Tag der mündlichen Prüfung: 23.02.2005

Dekan des Fachbereichs
Elektrotechnik und
Informationstechnik: Prof. Dr.–Ing. G. Huth

Vorsitzender der
Prüfungskommission: Prof. Dr.-Ing. R. Urbansky

1. Berichterstatter: Prof. Dr.–Ing. habil. Dr.–Ing. E.h. P.W. Baier
2. Berichterstatter: Prof. Dr.–Ing. A. Klein

Vorwort

Die vorliegende Arbeit entstand in der Zeit von September 2001 bis Dezember 2004 im Rahmen meiner Tätigkeit als wissenschaftlicher Mitarbeiter Prof. Dr.–Ing. habil. Dr.–Ing. E.h. P.W. Baiers am Lehrstuhl für hochfrequente Signalübertragung und -verarbeitung der Technischen Universität Kaiserslautern. Ich möchte all jenen danken, die mich bei der Entstehung dieser Arbeit unterstützt haben.

Mein besonderer Dank ergeht an Herrn Prof. Baier für die Anregung, die Betreuung und die Förderung meiner Arbeit. Durch seine stete Diskussionsbereitschaft sowie durch zahlreiche Ratschläge und Hinweise hat er wesentlich zum Gelingen dieser Arbeit beigetragen.

Frau Prof. Dr.–Ing. A. Klein von der TU Darmstadt danke ich für das Interesse an meiner Arbeit und für die Übernahme des Korreferats. Weiterhin danke ich dem Vorsitzenden der Promotionskommission, Herrn Prof. Dr.–Ing. R. Urbansky.

Den jetzigen und den ehemaligen Kollegen am Lehrstuhl für hochfrequente Signalübertragung und –verarbeitung danke ich für eine angenehme Arbeitsatmosphäre und für viele fruchtbare Diskussionen, die mir oftmals weitergeholfen haben. Ein besonderer Dank ergeht an die Herren Dr.–Ing. M. Meurer und Dr.–Ing. H. Tröger für die erfolgreiche Zusammenarbeit in gemeinsamen Projekten und viele hilfreiche Hinweise. Ebenso danke ich allen Studenten, die im Rahmen ihrer Studien-, Diplom- und Masterarbeiten sowie als wissenschaftliche Hilfskräfte unter meiner Anleitung Beiträge zu dieser Arbeit geleistet haben.

Teile meiner Dissertation entstanden im Rahmen der Kooperation des Lehrstuhls für hochfrequente Signalübertragung und -verarbeitung mit der Fa. Siemens, u.a. im EU-Projekt FLOWS (Flexible Convergence of Wireless Standards and Services). Für diese Förderung sowie zahlreiche Anregungen aus der industriellen Praxis sei den Herren Dipl.–Ing. H. von der Neyen und Dipl.–Ing. G. Lehmann herzlich gedankt. Andere Teile der Arbeit entstanden im Rahmen eines Forschungsvorhabens im DFG-Schwerpunktprogramm AKOM (Adaptivität in heterogenen Kommunikationsnetzen mit drahtlosem Zugang). Dafür danke ich der DFG herzlich.

Der Technischen Universität Kaiserslautern danke ich für die Möglichkeit, die leistungsfähigen Rechner des Regionalen Hochschulrechenzentrums Kaiserslautern (RHRK) für meine Forschungsarbeiten zu benutzen. Den Mitarbeitern des RHRK gilt mein Dank für die Beratung in Software- und Hardwarefragen.

Nicht zuletzt möchte ich mich bei meiner Frau, meiner Familie und meinen Freunden bedanken, die mir immer ein großer Rückhalt waren. Ganz besonders herzlich danke ich meinen Eltern. Sie haben mir das Studium der Elektrotechnik ermöglicht und mir immer ihre uneingeschränkte Unterstützung zukommen lassen. Ihnen widme ich diese Arbeit.

Kaiserslautern, im Februar 2005 Wei Qiu

VII

Contents

Chapter 1

Introduction

1.1 Classification of mobile radio communication systems

The thesis deals with radio communication systems. Throughout the thesis, the band-pass signals of the radio communication systems are represented by their equivalent low-pass signals as in [Kle96]. The transmitted and received data symbols are arranged in complex column vectors. Complex vectors and matrices are represented by underlined bold face symbols.

Fig. 1.1a shows the block diagram of a communication system [Rup93], which involves four main parts:

- the transmitter,
- the channel,
- the noise adder, and
- the receiver.

Following the system representation introduced in [Trö03], the output signals of the transmitter, the channel and the noise adder as well as the noise are represented by the complex vectors $\underline{t}$, $\underline{e}$, $\underline{r}$ and $\underline{n}$, respectively. The transmit data symbols stacked in the data vector $\underline{d}$ are fed into the transmitter. Generally, in the transmitter the data symbols constituting $\underline{d}$ are subject to Forward Error Correction (FEC) Coding and modulated to form the transmit signal $\underline{t}$, which is fed into the channel. The channel is the physical medium that is used to transfer the transmit signal $\underline{t}$ from the transmitter to the receiver. At the channel output $\underline{t}$ causes the undisturbed receive signal $\underline{e}$. In the case of radio communications, the channel consists as shown in Fig. 1.1b of three parts:

- the transmit antenna,
- the free space and
- the receive antenna, at which, in addition to the undisturbed receive signal $\underline{e}$, the noise signal $\underline{n}$ impinges.

As an essential feature of the transmission systems of Fig. 1.1, the undisturbed receive signal $\underline{e}$ is corrupted by the additive noise $\underline{n}$, which leads to the disturbed receive signal

$$\underline{r} = \underline{e} + \underline{n}. \tag{1.1}$$

The signal $\underline{r}$ arriving at the receiver is in general passed to the demodulator and the FEC decoder in the receiver, which attempt to reconstruct the original vector $\underline{d}$ of the data

a)

b)
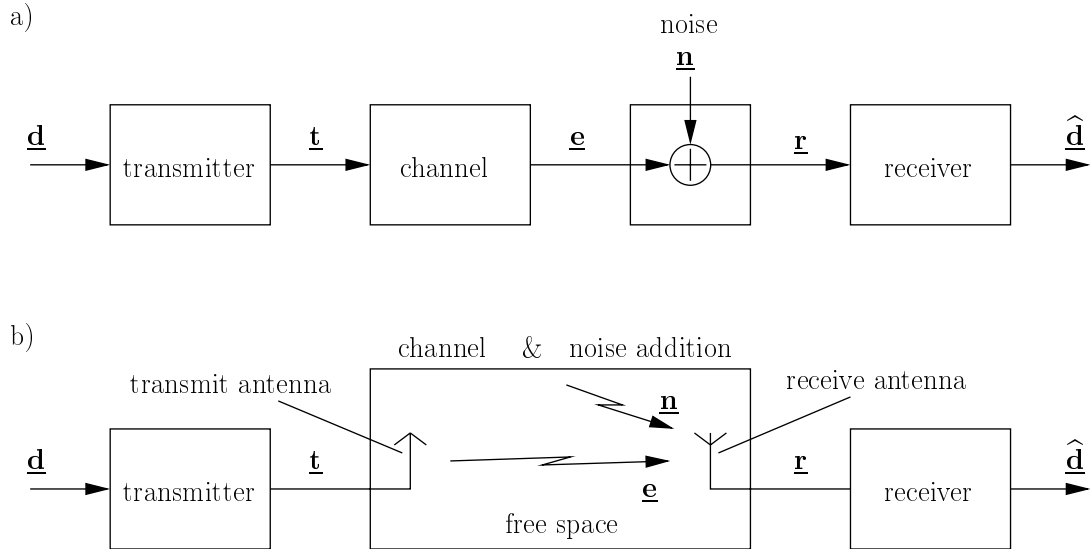
Fig. 1.1. Block diagram of a communication system
    a) general case
    b) radio communication case

symbols to form a data estimate $\widehat{\underline{\mathbf{d}}}$. It is aspired that the data estimate $\widehat{\underline{\mathbf{d}}}$ is as accurate as possible compared to $\underline{\mathbf{d}}$ under certain conditions given e.g. by restrictions of the available transmit energy and the system bandwidth. The more accurate the data estimate $\widehat{\underline{\mathbf{d}}}$, the better the performance of the communication system.

For a given channel and given characteristics of the additive noise $\underline{\mathbf{n}}$ the performance of a communication system depends on the FEC encoder and the modulator applied in the transmitter as well as on the demodulator and the FEC decoder utilized in the receiver [Pro95]. In other words, the system performance depends on the signal processing algorithms applied in the transmitter and the receiver. The characteristics of these algorithms are decisive for the required computational effort, i.e. for the cost of the required hardware and the required primary power. In this thesis only the digital signal processing is considered.

The beginning of data communications with electromagnetic waves can be traced back to the 19th century. Carl Friedrich Gauss and Wilhelm Weber hook up the world's first electromagnetic single-needle telegraph link between 1833 and 1835 [Asc84]. They run two wires 1500m across roofs between the university observatory and the physics laboratory in Göttingen. Later, Carl August von Steinheil continued the work of Gauss and further developed the practical electromagnetic telegraphy. The radio communication technology, i.e. the communication without fixed lines, started with the experiments made by the Italian physicist Guglielmo Marconi in Bologna in 1895 [Asc84]. For his achievements, he received the Nobel Price for physics in 1909.

From the first experimental data communication systems to today's modern commercial communication systems, the system design generally starts from the transmitter (Tx), i.e. the signal processing algorithm in the transmitter is a priori selected, and then the signal processing algorithm in the receiver is a posteriori determined to obtain the corresponding data estimate. Therefore, in these conventional communication systems, the transmitter can be considered the master and the receiver can be considered the slave. Consequently, such systems can be termed transmitter (Tx) oriented. In the case of Tx orientation, the a priori selected transmitter algorithm can be chosen with a view to arrive at particularly simple transmitter implementations. This advantage has to be countervailed by a higher implementation complexity of the a posteriori determined receiver algorithm.

Opposed to the conventional scheme of Tx orientation, the design of communication systems can alternatively start from the receiver (Rx). Then, the signal processing algorithm in the receiver is a priori determined, and the transmitter algorithm results a posteriori. Such an unconventional approach to system design can be termed receiver (Rx) oriented. In the case of Rx orientation, the receiver algorithm can be a priori selected in such a way that the receiver complexity is minimum, and the a posteriori determined transmitter has to tolerate more implementation complexity.

In summary, the conventional scheme of Tx orientation allows simple transmitters and leads to more complex receivers, whereas, vice versa, the scheme of Rx orientation allows simple receivers and leads to more complex transmitters. In practical communication systems the implementation complexity corresponds to the weight, volume, cost etc of the equipment. Therefore, the complexity is an important aspect which should be taken into account, when building practical communication systems. The terms Tx orientation and Rx orientation were coined by the author of this thesis and by his colleagues [MBQ04].

In both Tx and Rx oriented communication systems, in order to obtain a satisfying system performance, the channel knowledge is an important issue and should be taken into account when a posteriori determining the algorithms, that is the channel knowledge should be considered

- at the receiver in the case of Tx orientation and
- at the transmitter in the case of Rx orientation.

In the case of Tx orientation, this knowledge can be obtained at the receiver by sending training signals to the receiver, which are before made known to the receiver. Based on the knowledge of these signals and of the corresponding received signals, the receiver can estimate the channel impulse response [Ste95]. In the case of Rx orientation, the channel knowledge should be available at the transmitter. There it can be generally obtained in such a way that this knowledge is first determined at the receiver, e.g. as done in the case of Tx orientation, and then fed back to the transmitter. In general, this seems not to be an easily solvable task, and, therefore, limits the application of Rx orientation.

In mobile radio communication systems, the complexity of the mobile terminals (MTs) should be as low as possible, whereas more complicated implementations can be tolerated

in the base station (BS). Having in mind the above mentioned complexity features of the rationales Tx orientation and Rx orientation, this means that in the uplink (UL), i.e. in the radio link from the MT to the BS, the quasi natural choice would be Tx orientation, which leads to low cost transmitters at the MTs, whereas in the downlink (DL), i.e. in the radio link from the BS to the MTs, the rationale Rx orientation would be the favorite alternative, because this results in simple receivers at the MTs.

As mentioned above, in the case of Tx orientation channel knowledge would be desirable at the MTs, whereas in the case of Rx orientation such knowledge should be available at the BSs. This means that, in the case of mobile radio systems, the above proposed combination of Tx orientation in the UL and Rx orientation in the DL is particularly easily feasible, if the utilized duplexing scheme is TDD (Time Division Duplexing). In the case of TDD the UL and the DL use the same frequency band in temporally separated periods so that, due to the reciprocity theorem [Par92], both links experience the same channel impulse responses as long as the time elapsing between UL and DL transmissions is not too large. Therefore, the channel knowledge needed by the BS receivers in the Tx oriented UL and obtainable for instance based on the transmission of training signals by the MTs can be used also as the channel knowledge required for the Rx oriented DL transmission. This approach to exploiting channel knowledge available in the BS for DL transmission has the additional advantage that no resources have to be sacrificed for the transmission of training signals in the DL, which tends, anyhow, capacity-wise to be the more crucial one of the two links [BMWT00]. In FDD (Frequency Division Duplexing) systems, the UL and DL occupy two different frequency bands, and, therefore, the channel properties of UL and DL are different. Consequently, in FDD systems the channel knowledge is not as easily obtained at the transmitter as in TDD systems. However, also solutions to this problem exist [JBMW02].

Tx orientation in the UL of mobile radio systems has been well studied in the past [Kle96, Ver98], whereas Rx orientation in the DL of such systems only recently began to attract some attention [MBQ04]. In this thesis, investigations of certain aspects of Rx orientation in the DL are the topics of interest. In these investigations perfect channel knowledge is assumed to be available at the BS.

1.2   Requirement of low transmit energy

Modern mobile radio communication systems are cellular systems [Cal88], in which the whole geographical service area is subdivided into many non-overlapping cells. In each cell a BS is situated which simultaneously supports a number of MTs located in this cell. This simultaneous support of multiple MTs by the BS is organized according to the well-known basic multiple access principles FDMA (Frequency Division Multiple Access), TDMA (Time Division Multiple Access) and CDMA (Code Division Multiple Access), with practical multiple access schemes being usually hybrids, i.e. combinations of at least

two of the basic multiple access principles [Bai94, BK95, Bai96, BJK96, FST+96, OP98, HKK+00]. In FDMA the user signals are assigned to different frequency domains, and, therefore, are spectrally disjoint. The disjointness of the user signals offered by FDMA is virtually unaffected by the multipath mobile radio channels, as long as the impact of the Doppler effect can be neglected. In TDMA the disjointness of user signals is achieved by arranging them in different time domains. The disjointness of TDMA user signals is impaired due to the delay spread of the multipath mobile radio channels only moderately, if appropriate guard intervals are provided between successive TDMA bursts. However, in CDMA, because many user signals are active in the same time and frequency domain, user signals transmitted even in a perfectly disjoint way by using orthogonal CDMA codes tend to loose their disjointness due to the frequency selectivity of the mobile radio channels [Bai96, Ver98]. This degraded disjointness of user signals in the case of CDMA leads to interference between them, which is termed multiple access interference (MAI). The MAI between the user signals of one and the same cell is termed intracell MAI [Lee90]. Intracell MAI is a limiting factor for the single cell performance of mobile radio systems [Ste92], and, therefore, should be eliminated or at least reduced. The elimination of intracell MAI in ULs following the rationale Tx orientation has been well studied [Naß95, Kle96, Bla98, Ver98] and can be solved by resorting to Joint Detection (JD) techniques, by which all user signals of a cell are detected simultaneously in the receiver of the BS by exploiting the a priori knowledge about the used CDMA codes and the channel impulse responses. However, it was only recently that the elimination of intracell MAI in the DL with Rx orientation began to attract some attention and Joint Transmission (JT) techniques were envisaged [BMWT00, MBQ04], in which all user signals of a cell are jointly generated in the transmitter of the BS under consideration of the a priori knowledge about the used CDMA codes and the channel impulse responses.

Frequency reuse is an essential feature of cellular mobile radio systems and means that the cells are grouped into clusters and the frequencies allotted to the cells of a certain cluster are again used in other clusters [Cal88, Lee90]. Due to this frequency reuse, in each cell of a cluster interfering signals originating from the cells which use the same frequency in other clusters are received. This kind of interference is termed intercell MAI [Lee90] and is present irrespective of the applied multiple access scheme, because disjointness of the user signals in general cannot be maintained across cluster borders. Intercell MAI limits the capacity of the mobile radio systems, and, therefore, should be eliminated or kept as low as possible. There are two basic possibilities to eliminate or mitigate intercell MAI:

- Intercell MAI could be eliminated by jointly detecting/generating the user signals over cluster borders in the receiver/transmitter by exploiting the a priori knowledge about the used CDMA codes and the channel impulse responses in a way similar to that followed when mitigating intracell MAI. Because, now, the user signals over cluster borders would be jointly processed, the a priori knowledge should include all the used CDMA codes and the channel impulse responses with respect to the user signals over cluster borders. Consequently, a huge organizational and computational complexity would be required both for the achievement of the a priori knowledge and for the joint processing of all user signals over cluster borders. This is not

feasible due to the limits of implementation cost and signaling effort in practical systems.

- Restricted by said limits of the implementation complexity of practical systems, only the user signals within each cell can be jointly processed without consideration of intercell MAI or at most with consideration of the statistical properties of intercell MAI, e.g. the spatial-temporal correlations of intercell MAI [Wec02]. Therfore, the intercell interference always exists. The detrimental effect of intercell MAI grows with its average energy. In order to keep the detrimental effect of intercell MAI low, another way to attack this problem would be to keep the average energy of the intercell MAI as low as possible. This energy of the intercell MAI grows with the radiated energies within each cell, because these energies are the reason of intercell MAI. Therefore, reducing the radiated energies within each cell can mitigate the detrimental effect of intercell MAI. Concerning the DL which, as stated at the end of Section 1.1, is the link of interest in this thesis, this means that the transmit energy radiated by the BSs should be as low as possible.

Low transmit energy is required also with respect to the growing electro-phobia of the public. In the past ten years, the number of mobile phone users went up worldwide very quickly. This omnipresence of mobile phones has lead to increased concerns about possible health hazards by electromagnetic irradiation. Research into possible biological effects of electromagnetic fields has been carried out in government, academic and industrial laboratories all over the world [KBL97, HNP+99, IEE01]. Whatever the outcome of the latest research will be, the debate on the health impacts of mobile communications will continue. Such issues are very difficult and time-consuming to resolve. How to respond appropriately to public fears, identifying any real hazard while avoiding unproductive controversy, is not a purely scientific matter, but a question with deep social aspects. Anyway, low transmit energy leads to weak electromagnetic irradiation and will reduce the risk of possible health hazards, and, therefore, can somewhat relax the problem of electro-phobia of the public.

As a short summary of Section 1.2, the major goal of designing the DL based on the rationale Rx orientation consists in reducing the transmit energy, when a posteriori designing the transmitter algorithm for a given single cell transmission quality.

1.3   State-of-the-art and open questions

Although ideas similar to Rx orientation came up more than ten years ago [EN93], it was only recently that this rationale, especially for the mobile radio downlinks, was clearly formulated [BMWT00, JU00, MBQ04]. In the meantime more and more academic and industrial research projects concern this rationale, and a systematical study has begun. However, due to the late perception of Rx orientation, up to now the available references are limited.

The first proposals of Rx orientation for mobile radio downlinks concerned linear transmission schemes [EN93, BMWT00, JU00, JKG+02] with modulators based on the rationales Transmit Matched Filter (TxMF) [EN93, ESN95, JN98, ESN99, NBF00, CLM01, NB01], Transmit Minimum Mean Square Error (TxMMSE) Filter [JKG+02, JKUN02, BM03, MBQ04] or Transmit Zero Forcing (TxZF) Filter [VM98, MBW+00, BMWT00, MBL+00, JU00, QTM02], see also Table 1.1. These three linear schemes differ from each other by the way in which the problem of intracell interference is addressed when designing the transmit signals. The intracell interference

- is totally neglected in the case of the Transmit Matched Filter (TxMF),
- is admitted to a certain degree and beneficially balanced against the received noise in the case of the Transmit Minimum Mean Square Error (TxMMSE) Filter, and
- is strictly eliminated in the case of the Transmit Zero Forcing (TxZF) Filter.

For the assessment of the linear transmission schemes appropriate criteria are required. Due to the fact that the energy radiated by the transmitter is an important technical and even social issue as mentioned in Subsection 1.2, besides of bit error probabilities or signal-to-noise-plus-interference ratios, as another suitable criterion the energy efficiency is proposed in [TWMB01, BQT+03]. The energy efficiency characterizes how efficiently the energy radiated by the transmitter is transferred as useful energy to the receiver output. A large energy efficiency means efficient transmission of the radiated energy, and, therefore, low transmit energy is required at the transmitter when a certain useful energy has to be produced at the receiver output. Quite generally, the energy efficiency decreases with an increasing degree of mitigation of intracell interference, because such an increase goes along with growing constraints on the design of the transmit signals. In the case of the TxMF the intracell interference is totally neglected, and, therefore, no such constraints exist. The TxMMSE Filter and the TxZF Filter imply such constraints, which are more stringent in the case of the TxZF Filter than in the case of the TxMMSE Filter. This means that, when proceeding from the TxMF over the TxMMSE Filter to the TxZF Filter, the energy efficiency tends to go down [Trö03]. To summarize, there seems to be a rule telling us, the larger the energy efficiency, the more distinct the impact of intracell interference. Or in other words, striving for high transmission quality in linear Rx oriented schemes goes along with a sacrifice of transmit energy, and, therefore, leads to possibly high transmit energy.

An important asset with respect to increasing the spectrum efficiency of radio transmission systems is the use of multiple antennas instead of single antennas at the transmitter and/or the receiver [Tel99, FG98, GSS+03]. The inclusion of multiple antennas in linear Rx oriented transmission schemes would be straightforward [QTM02] and has the potential of reducing the transmit energy. Up to now, the previous investigations in this field focus only on the beneficial effect of using multiple antennas at the transmitter. In [Trö03] it was shown by simulation results that the utilization of multiple transmit antennas increases the energy efficiency, and, therefore, reduces the transmit energy in the considered radio scenarios. Later, again concerning the linear schemes with multiple transmit antennas, an analysis based on an approximate assumption for a special radio scenario was made

Table 1.1. Important contributions on Rx orientation

quantization scheme	classification	references	remarks
conventional	linear	[EN93] [ESN95] [JN98] [ESN99] [CLM01][NBF00][NB01]	TxMF
		[MBW$^+$00] [BMWT00] [MBL$^+$00][JU00][VM98] [MTJ02][TWMB01] [QTM02][MTWB01]	TxZF Filter
		[JKG$^+$02] [JKUN02] [BM03] [MBQ04]	TxMMSE Filter
	non-linear	[WM03][WMS03] [IHRF03][IRF03]	exploit the discreteness of the modulation alphabet
multiply connected	non-linear	[FWLH02b][FWLH02c] [FWLH02a] [WF03a][WF03b][PHS03]	lattice-structured quantization scheme

available in [MWQ04]. However, the investigations of the linear Rx oriented transmission schemes with multiple antennas at both the transmitter the receiver, i.e. with MIMO (Multiple Input Multiple Output) antenna structures, are still open and would be also important research issues.

Non-linear Rx oriented transmission schemes, which exploit the discreteness of the modulation alphabet, also attained attention [WM03, WMS03, IHRF03, IRF03]. However, it turned out [WM03, WMS03] that these non-linear schemes do not offer any improvements with respect to the problem of possibly high transmit energy occurring in linear Rx oriented transmit schemes.

Motivated by the idea of Tomlinson-Harashima Precoding (THP) [Tom71, HM72] already published more than 30 years ago, non-linear Rx oriented transmission schemes combined with lattice-structured [Fis02], or more generally, multiply connected quantization schemes [QMBW04] at the receiver attracted increasing attention with respect to reducing the required transmit energy in mobile radio downlinks. In conventional quantization schemes, which are the usual case for the linear schemes, each of the message elements corresponds to a single decision region. For an error free transmission of a message element carried by a certain data symbol, the estimate at the receiver output should land in the corresponding decision region. In contrast to the conventional quantization schemes, multiply connected quantization schemes offer several, or even infinitely many partial decision regions for each of these message elements. Then, the estimate at

the receiver landing in any one of the corresponding partial decision regions of the transmitted message will lead to an error free transmission. Consequently, if a certain number of data symbols carrying a set of message elements have to be transmitted, instead of only one, as in the case of conventional quantization schemes, now many possible transmit signals aiming at different combinations of the corresponding partial decision regions exist. Each of them requires a different value of the transmit energy. Now, the crux of the non-linear Rx oriented transmission scheme with multiply connected quantization schemes consists in finding a specific transmit signal out of all these possible transmit signals so that the required transmit energy becomes as low as possible. The optimum solution with respect to the minimum transmit energy can only be found by exhaustive search over all these possible transmit signals. In mobile radio systems this would lead to a prohibitively expensive computational complexity. Therefore, less complex suboptimum solutions are aspired. The first suboptimum solutions [FWLH02a, FWLH02b, FWLH02c] concern the extension of THP for a lattice-structured quantization scheme, which showed a very low computational complexity, but also a rather moderate reduction of the transmit energy. Later, again under consideration of lattice-structured quantization schemes, Peel et al. proposed the sphere encoding algorithm [PHS03] to find the transmit signal among a restricted number of possible transmit signals. The performance of the proposed scheme was shown near optimum, however, the complexity is still a problem. All the important contributions on non-linear Rx orientation combined with multiply connected quantization schemes are listed in Table 1.1. All these contributions seem to have

- either a good performance, but also a high computational complexity, or
- a low computational complexity, but also a highly degraded performance compared to the optimum solution.

Questions on the solutions in between of these two extreme cases, which allow a free balance between the computational complexity and the performance, are still open. Further, as mentioned above, all these non-linear schemes are only suitable for lattice-structured quantization schemes. Therefore, another possible open question is how to generalize these schemes for arbitrary multiply connected quantization schemes.

1.4   Goals and contents of the thesis

From the many open questions mentioned in Section 1.3, two questions of major importance are considered in this thesis, namely

- linear Rx oriented transmission schemes combined with MIMO antenna structures, and
- solutions of non-linear Rx oriented transmission schemes combined with multiply connected quantization schemes in between of the two mentioned extreme cases.

Concerning these two questions, the following goals are pursued:

- To establish simple point-to-point and broadcast MIMO channel models.

- Mathematical description of linear Rx oriented MIMO broadcast systems.

- Investigation of the effect of MIMO antenna structures on linear Rx oriented transmission schemes by numerical and/or analytical results.

- Introduction of multiply connected quantization schemes and exploitation of their potential with respect to the transmit energy reduction.

- Design of general non-linear Rx oriented broadcast systems with group-wise signal generation at the transmitter based on multiply connected quantization schemes, which allows free balance between the performance and the required complexity.

- Investigation of the performance of the proposed non-linear Rx oriented transmission scheme.

- Presentation of rules for an advantageous system design.

In addition to the introduction, this thesis consists of six chapters. The content of these chapters corresponds to the goals mentioned above.

In Chapter 2 the point-to-point and broadcast MIMO channels are introduced. In particular two variants of broadcast MIMO channels are presented, namely channels with totally uncorrelated and channels with fully correlated partial MIMO branches. These two types of broadcast MIMO channels are used for system evaluations of the linear and non-linear Rx oriented transmission schemes considered in this thesis.

Based on the description of the general structure of a data transmission system, general linear and non-linear Rx oriented transmission systems are presented at the beginning of Chapter 3. As a part of the receiver, the generalized multiply connected quantization schemes are introduced. Then, the chapter briefly recapitulates the linear Rx oriented transmission schemes with TxMF, TxZF Filter and TxMMSE Filter. The rest of the chapter develops the performance criterion energy efficiency and the related criterion Tx efficiency and recapitulates the analytical results obtained in [MWQ04].

Chapter 4 has two goals. First, the TxZF Filter algorithm and the corresponding performance criteria developed in Chapter 3 for general linear Rx oriented transmission systems are adapted to MIMO broadcast systems. Then, the performance of such MIMO broadcast systems is studied by numerical and/or analytical results for the two types of broadcast MIMO channels introduced in Chapter 2.

The non-linear Rx oriented transmission scheme with group-wise signal generation at the transmitter are proposed in Chapter 5. This scheme is termed Transmit Non-linear Zero Forcing (TxNZF) Filter by the author. After revealing the basic idea of reducing the transmit energy by combination of the linear scheme TxZF Filter with unconventional multiply connected quantization schemes in the receivers, the group-wise construction of the transmit signal is presented. Then, the performance of TxNZF Filter is given. After that, possibilities to reduce the computational complexity of TxNZF Filter are presented. Finally, a general view on the proposed TxNZF Filter is considered. Different variants

of non-linear Rx oriented transmission schemes based on the generalized TxNZF Filter
are discussed in relation to the non-linear schemes with multiply connected quantization
schemes proposed by other authors.

Chapter 6 summarizes the thesis.

Chapter 2

MIMO channel models

2.1 Introduction

As stated in Section 1.3, MIMO is an important feature with respect to the transmit power reduction of mobile radio systems. For the purpose of performance evaluation of mobile radio systems with MIMO antenna structures, MIMO channel models are required. Besides the temporal dimension as in conventional SISO (Single Input Single Output) channel modelling, the multiple antennas introduce additionally the spatial dimension, which should also be considered in MIMO channel modelling. An important issue concerning the spatial dimension of MIMO is the degree of correlation of the impulse responses of the channels between different pairs of transmit and receive antennas. These channel impulse responses are termed antenna specific. The correlation depends on the configuration of the antenna structures and the topography and morphography of the propagation area, etc. Recently, much work concerning MIMO channel modelling for different scenarios has been reported [BAWT01, GBP02, SBE+02, XCHV04, XWL+04, BT04, YBO+04], and the standardization of MIMO channel models is also going on [LNSE01]. In this thesis, we do not try to address all these MIMO channel models. Rather, we consider only two quasi extreme cases, namely on the one side scenarios with spatially totally uncorrelated and on the other side scenarios with spatially fully correlated antenna specific channel impulse responses. These two models will be introduced in Section 2.3 and will be employed in this thesis when evaluating the performance of mobile radio systems. Evaluating the performance of mobile radio systems for these two extreme channel models would give an impression on the performance of mobile radio systems in the case of other MIMO channel models which cover the scenarios in between of these two extreme cases.

This chapter is organized as follows: Section 2.2 introduces the general MIMO point-to-point and MIMO broadcast channels, and in Section 2.3 the MIMO broadcast channel models for the two above mentioned extreme scenarios are presented.

2.2 MIMO point-to-point and broadcast channels

In a point-to-point system a transmitter serves only a single receiver. When both the transmitter and the receiver are equipped with multiple antennas, then we use the term MIMO point-to-point system. The structure of a MIMO point-to-point system is shown in Fig. 2.1. The channel between the transmitter and the receiver of this system is called MIMO point-to-point channel. When a transmitter simultaneously supports several receivers, we have a broadcast system. The broadcast system with multiple antennas
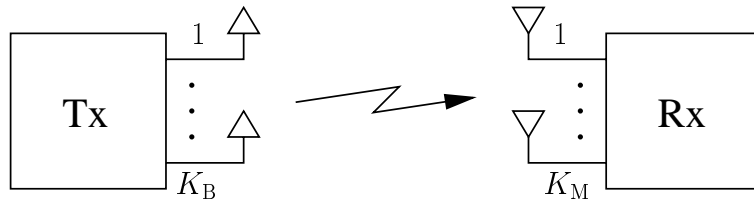
Fig. 2.1. MIMO point-to-point system
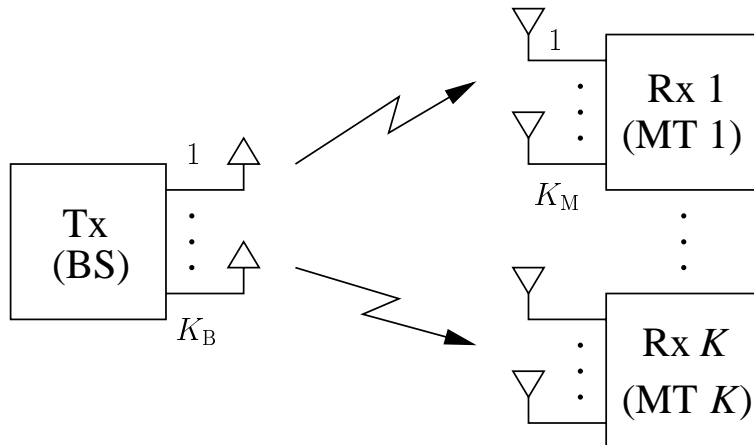
Fig. 2.2. MIMO broadcast system

at both the transmitter and the receivers is termed MIMO broadcast system, whose structure is depicted in Fig. 2.2. The channel between the transmitter and the receivers of this system is termed MIMO broadcast channel. The MIMO point-to-point channel can be treated as a special case of the MIMO broadcast channel. Therefore, only the MIMO broadcast channel is modelled in the following. The structure shown in Fig. 2.2 corresponds to mobile radio downlinks, which are considered in this thesis. Therefore, instead of the terms transmitter and receiver the acronyms BS and MT, respectively, are used in the following. It is assumed that the BS supports K MTs. The number of transmit (Tx) antennas at the BS is termed K_B, and the number of receive (Rx) antennas at each MT is termed K_M, see Fig. 2.2.

The MIMO broadcast channel consists of K partial MIMO channels which characterize the MIMO channels between the BS and the MT k, $k = 1 \ldots K$, see Fig. 2.3. Each of the K partial MIMO channels comprises $K_B K_M$ SISO channels, namely one SISO channel between each pair of Tx antenna k_B at the BS and Rx antenna k_M at the MT k. Modelling these SISO channels alone is well known [Bel63]. These channels can be modelled in the equivalent lowpass domain by the delay continuous antenna specific impulse responses $\underline{h}^{(k,k_B,k_M)}(\tau)$, $k = 1 \ldots K$, $k_B = 1 \ldots K_B$, $k_M = 1 \ldots K_M$, or in time discrete form [Ste95,
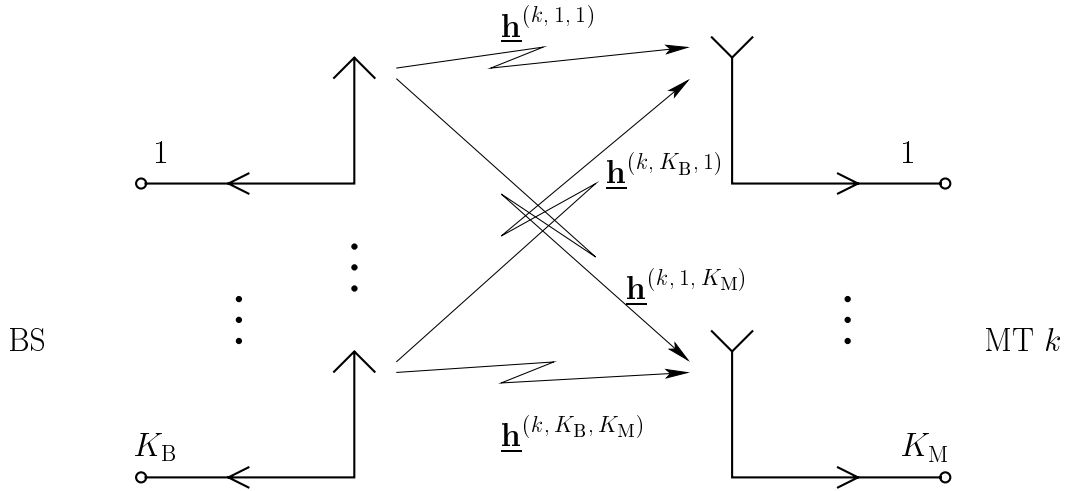
Fig. 2.3. Partial MIMO channels between the BS and MT k

Kle96] by the complex vectors

$$\underline{\mathbf{h}}^{(k,\,k_{\mathrm{B}},\,k_{\mathrm{M}})} \;=\; \left(\underline{h}_1^{(k,\,k_{\mathrm{B}},\,k_{\mathrm{M}})}\ldots\underline{h}_W^{(k,\,k_{\mathrm{B}},\,k_{\mathrm{M}})}\right)^{\mathrm{T}} \in \mathbb{C}^{W\times 1},$$
$$k = 1\ldots K,\; k_{\mathrm{B}} = 1\ldots K_{\mathrm{B}},\; k_{\mathrm{M}} = 1\ldots K_{\mathrm{M}}. \qquad (2.1)$$

For simplicity, these vectors are termed antenna specific impulse responses in what follows. In [Ste95] it is shown how the dimension W of these vectors depends on the excess delay of the radio channels and the system bandwidth.

2.3 Considered variants of MIMO broadcast channels

2.3.1 Correlations

The basic structure of the considered MIMO broadcast channel models is given in Fig. 2.2, and these models can be quantitatively described by the $KK_{\mathrm{B}}K_{\mathrm{M}}$ antenna specific channel impulse responses $\underline{\mathbf{h}}^{(k,\,k_{\mathrm{B}},\,k_{\mathrm{M}})}$ of (2.1). In order to fill these channel models with live, the components $\underline{h}_w^{(k,\,k_{\mathrm{B}},\,k_{\mathrm{M}})}$ of the antenna specific channel impulse responses have to be given numerical values. In the following we assume that the data symbols to be transmitted are grouped in consecutive blocks. The block dimension is chosen such that during the transmission of each such block the radio channels can be considered as fixed, that is time variance manifests itself only if different data blocks are considered. The transmission period of each data block is termed one snapshot, and in order to take into account time

variance, in each block the components $\underline{h}_w^{(k,k_{\mathrm{B}},k_{\mathrm{M}})}$ of $\underline{\mathbf{h}}^{(k,k_{\mathrm{B}},k_{\mathrm{M}})}$ of (2.1) have to be anew determined. The question is now, how this determination is performed in this thesis, and this question will be answered in what follows.

All elements $\underline{h}_w^{(k,k_{\mathrm{B}},k_{\mathrm{M}})}$ with the same index w are obtained by a random access to a Gaussian set $\mathbb{H}_w$ of complex numbers with zero expectation and the variance σ_w^2 of the real and imaginary parts. In general, the sets for different w may differ in their variance σ_w^2 so that W different sets $\mathbb{H}_w$, $w = 1 \ldots W$, are required.

When it comes to the determination of the components of $\underline{\mathbf{h}}^{(k,k_{\mathrm{B}},k_{\mathrm{M}})}$, first of all we assume that the components $\underline{h}_w^{(k,k_{\mathrm{B}},k_{\mathrm{M}})}$ and $\underline{h}_{w'}^{(k',k'_{\mathrm{B}},k'_{\mathrm{M}})}$ of the antenna specific channel impulse responses $\underline{\mathbf{h}}^{(k,k_{\mathrm{B}},k_{\mathrm{M}})}$ and $\underline{\mathbf{h}}^{(k',k'_{\mathrm{B}},k'_{\mathrm{M}})}$ of two different MTs k and k', $k \neq k'$, are obtained by independent accesses to the sets $\mathbb{H}_w$, $w = 1 \ldots W$, so that these elements are uncorrelated. This means, if we designate averaging over infinitely many snapshots by $\mathrm{E}\{\cdot\}$, that

$$\mathrm{E}\left\{\underline{h}_w^{(k,k_{\mathrm{B}},k_{\mathrm{M}})}\underline{h}_{w'}^{(k',k'_{\mathrm{B}},k'_{\mathrm{M}})^*}\right\} = 0 \text{ for } k \neq k' \tag{2.2}$$

holds. (2.2) implies

$$\mathrm{E}\left\{\underline{\mathbf{h}}^{(k,k_{\mathrm{B}},k_{\mathrm{M}})}\underline{\mathbf{h}}^{(k',k'_{\mathrm{B}},k'_{\mathrm{M}})^{\mathrm{H}}}\right\} = \mathbf{0} \text{ for } k \neq k'. \tag{2.3}$$

Next we assume that any two elements $\underline{h}_w^{(k,k_{\mathrm{B}},k_{\mathrm{M}})}$ and $\underline{h}_{w'}^{(k,k'_{\mathrm{B}},k'_{\mathrm{M}})}$ for different values w and w' but for the same MT k are obtained by independent accesses to the sets $\mathbb{H}_w$ and $\mathbb{H}_{w'}$ so that

$$\mathrm{E}\left\{\underline{h}_w^{(k,k_{\mathrm{B}},k_{\mathrm{M}})}\underline{h}_{w'}^{(k,k'_{\mathrm{B}},k'_{\mathrm{M}})^*}\right\} = 0 \text{ for } w \neq w' \tag{2.4}$$

holds. Due to (2.4) the matrix $\mathrm{E}\left\{\underline{\mathbf{h}}^{(k,k_{\mathrm{B}},k_{\mathrm{M}})}\underline{\mathbf{h}}^{(k,k'_{\mathrm{B}},k'_{\mathrm{M}})^{\mathrm{H}}}\right\}$ is a diagonal matrix. If (2.4) is valid, the channels are said to exhibit uncorrelated scattering (US) [Bel63].

Let us now consider the elements $\underline{h}_w^{(k,k_{\mathrm{B}},k_{\mathrm{M}})}$ and $\underline{h}_w^{(k,k'_{\mathrm{B}},k'_{\mathrm{M}})}$ of MT k for the case $k'_{\mathrm{B}} \neq k_{\mathrm{B}}$ and/or $k'_{\mathrm{M}} \neq k_{\mathrm{M}}$. Here we consider two cases 1 and 2 in the thesis. In case 1 the elements $\underline{h}_w^{(k,k_{\mathrm{B}},k_{\mathrm{M}})}$ and $\underline{h}_w^{(k,k'_{\mathrm{B}},k'_{\mathrm{M}})}$ are obtained by independent accesses to the set $\mathbb{H}_w$. Then

$$\mathrm{E}\left\{\underline{h}_w^{(k,k_{\mathrm{B}},k_{\mathrm{M}})}\underline{h}_w^{(k,k'_{\mathrm{B}},k'_{\mathrm{M}})^*}\right\} = 0 \text{ for } k'_{\mathrm{B}} \neq k_{\mathrm{B}} \text{ and/or } k'_{\mathrm{M}} \neq k_{\mathrm{M}} \tag{2.5}$$

holds, and we have totally uncorrelated antenna specific channel impulse responses $\underline{\mathbf{h}}^{(k,k_{\mathrm{B}},k_{\mathrm{M}})}$ and $\underline{\mathbf{h}}^{(k,k'_{\mathrm{B}},k'_{\mathrm{M}})}$, $k'_{\mathrm{B}} \neq k_{\mathrm{B}}$ and/or $k'_{\mathrm{M}} \neq k_{\mathrm{M}}$. In case 2 the two elements $\underline{h}_w^{(k,k_{\mathrm{B}},k_{\mathrm{M}})}$ and $\underline{h}_w^{(k,k'_{\mathrm{B}},k'_{\mathrm{M}})}$ are obtained by one and the same access to the set $\mathbb{H}_w$ in such a way that these elements differ only by a complex factor. Then

$$\mathrm{E}\left\{\underline{h}_w^{(k,k_{\mathrm{B}},k_{\mathrm{M}})}\underline{h}_w^{(k,k'_{\mathrm{B}},k'_{\mathrm{M}})^*}\right\} \neq 0 \text{ for } k'_{\mathrm{B}} \neq k_{\mathrm{B}} \text{ and/or } k'_{\mathrm{M}} \neq k_{\mathrm{M}}, \tag{2.6}$$

is valid, and we have fully correlated antenna specific channel impulse responses $\underline{\mathbf{h}}^{(k, k_\mathrm{B}, k_\mathrm{M})}$ and $\underline{\mathbf{h}}^{(k, k_\mathrm{B}^{'}, k_\mathrm{M}^{'})}$, $k_\mathrm{B}^{'} \neq k_\mathrm{B}$ and/or $k_\mathrm{M}^{'} \neq k_\mathrm{M}$. The above introduced cases 1 and 2 constitute the two extreme scenarios mentioned in Section 2.1.

(2.2), (2.4) and (2.5) should be understood in such a way that the expectations are zero even if the involved components of the channel impulse responses are non-zero.

2.3.2   Situations with totally uncorrelated antenna specific MIMO channels

As mentioned in Section 2.1, the correlation between the channel impulse responses of different pairs of Tx and Rx antennas depends on the configuration of the applied multiple antennas. The larger the distance between the antenna elements at the BS and the MTs, the lower the degree of correlation between the related channel impulse responses. Multi-antenna structures with large distances between the antenna elements are more closely considered in [BPJ97] and are there termed macro antenna structures. If such macro structures are employed both at the BS and the MTs, the antenna specific channel impulse responses $\underline{\mathbf{h}}^{(k, k_\mathrm{B}, k_\mathrm{M})}$ and $\underline{\mathbf{h}}^{(k, k_\mathrm{B}^{'}, k_\mathrm{M}^{'})}$, $k_\mathrm{B}^{'} \neq k_\mathrm{B}$ and/or $k_\mathrm{M}^{'} \neq k_\mathrm{M}$, tend to be uncorrelated, that is (2.5) holds.

2.3.3   Situations with fully correlated antenna specific MIMO channels

If in a multi-antenna structure the antenna elements are situated close to each other, then in the transmit case the wavefronts launched by the antenna elements differ only by their phases. In the receive case all antenna elements experience the same impinging wave-fronts, which differ again only in their phases from antenna element to antenna element. Multi-antenna structures with such closely spaced antenna elements are also considered in [BPJ97] and are there termed micro structures. If micro structures are employed both at the BS and the MTs, then the antenna specific channel impulse responses $\underline{\mathbf{h}}^{(k, k_\mathrm{B}, k_\mathrm{M})}$ and $\underline{\mathbf{h}}^{(k, k_\mathrm{B}^{'}, k_\mathrm{M}^{'})}$, $k_\mathrm{B}^{'} \neq k_\mathrm{B}$ and/or $k_\mathrm{M}^{'} \neq k_\mathrm{M}$, of (2.1) due to being based on the same wavefronts, tend to be fully correlated so that (2.6) holds. In what follows we describe the micro antenna structures assumed at the BS and the MTs in this thesis, and also the assumed arrangement of the MTs around the BS.

We first describe the geometrical configuration of the antenna elements at the BS as considered in this thesis under reference to Fig. 2.4:

- At the BS a uniform circular array with K_B omni-directional transmit antenna elements (TAEs), namely $\mathrm{TAE}^{(k_\mathrm{B})}$, $k_\mathrm{B} = 1 \ldots K_\mathrm{B}$, is provided around the reference point (RP), which is the center of the array. In what follows, it is assumed that the distance between two adjacent TAEs is one half of the carrier wavelength λ.
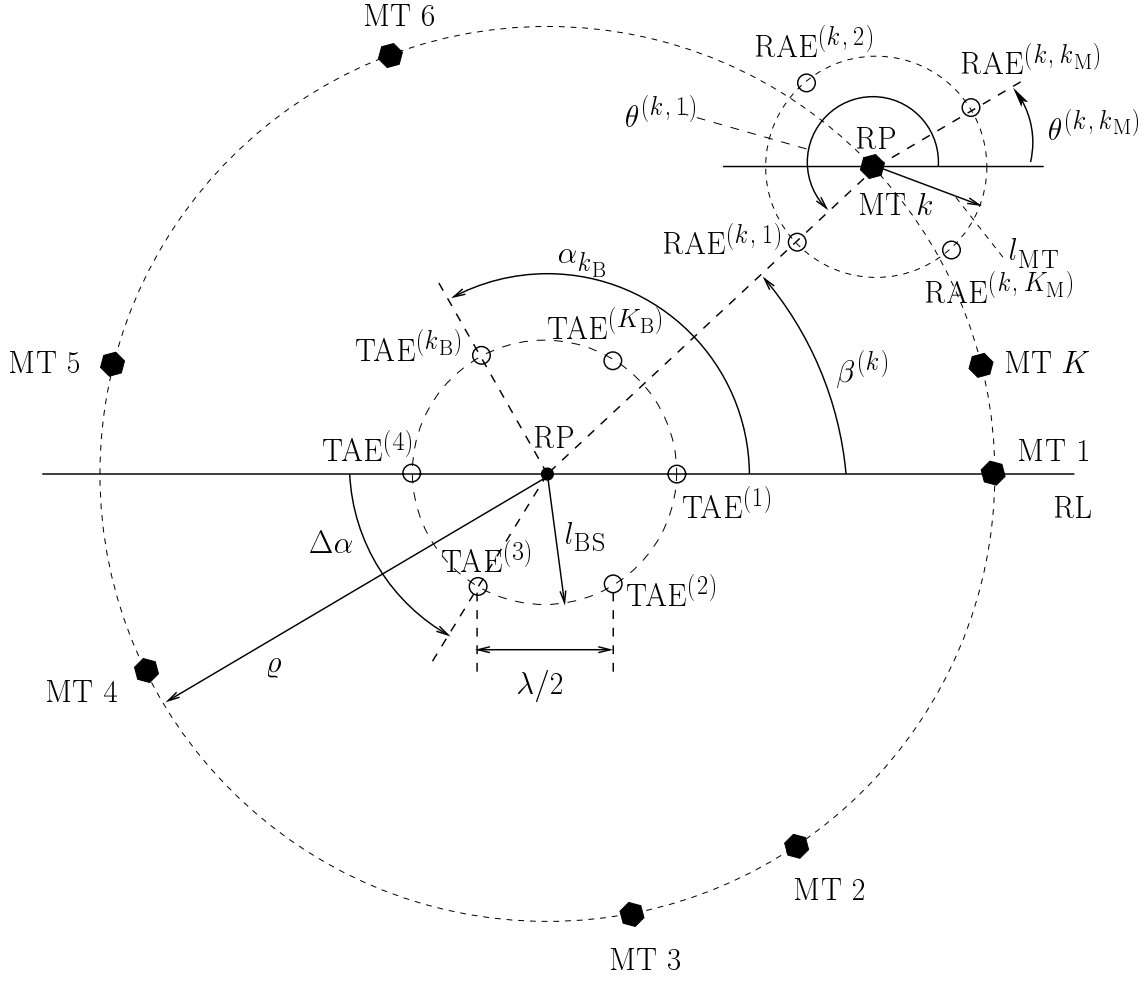
Fig. 2.4. Antenna configuration of the broadcast MIMO systems with fully corre-
      lated partial MIMO channels

- Each $\text{TAE}^{(k_{\text{B}})}$, $k_{\text{B}} = 1 \ldots K_{\text{B}}$, is placed under an azimuth angle $\alpha_{k_{\text{B}}}$, see Fig. 2.4.
  The angle between two adjacent TAEs is

$$\Delta\alpha = \alpha_{k_{\text{B}}} - \alpha_{k_{\text{B}}-1} = \frac{2\pi}{K_{\text{B}}}. \tag{2.7}$$

We set

$$\alpha_1 = 0. \tag{2.8}$$

Then, the azimuth angle of $\text{TAE}^{(k_{\text{B}})}$ becomes

$$
\begin{aligned}
\alpha_{k_{\text{B}}} &= (k_{\text{B}} - 1) \cdot \Delta\alpha + \alpha_1 \\
&= 2\pi \frac{k_{\text{B}} - 1}{K_{\text{B}}} + \alpha_1 \\
&= 2\pi \frac{k_{\text{B}} - 1}{K_{\text{B}}}.
\end{aligned}
\tag{2.9}
$$

- The radius of the circular array at the BS is

$$l_{\mathrm{BS}} = \frac{\lambda}{4 \sin\left(\frac{\pi}{K_{\mathrm{B}}}\right)}. \tag{2.10}$$

We now consider the location of the MTs and the geometrical configurations of the antenna elements at the MTs, see again Fig. 2.4:

- The MTs k, $k = 1 \ldots K$, are distributed around the RP of the BS. At each MT a circular array with K_{M} receive antenna elements (RAEs), namely $\mathrm{RAE}^{(k, k_{\mathrm{M}})}$, $k_{\mathrm{M}} = 1 \ldots K_{\mathrm{M}}$, is employed around the RP of the MT k. The distance between the RP of the BS and the RP of each MT is ϱ. The azimuth angle of the MT k is $\beta^{(k)}$, see Fig. 2.4.

- $\mathrm{RAE}^{(k, k_{\mathrm{M}})}$, $k_{\mathrm{M}} = 1 \ldots K_{\mathrm{M}}$, of the MT k is placed at an azimuth angle $\theta^{(k, k_{\mathrm{M}})}$. The angle between two adjacent RAEs is

$$\Delta\theta^{(k)} = \theta^{(k, k_{\mathrm{M}})} - \theta^{(k, k_{\mathrm{M}}-1)} = \frac{2\pi}{K_{\mathrm{M}}}. \tag{2.11}$$

We set
$$\theta^{(k, 1)} = \pi + \beta^{(k)}, \ k = 1 \ldots K. \tag{2.12}$$

Then, the azimuth angle of $\mathrm{RAE}^{(k, k_{\mathrm{M}})}$ becomes

$$\begin{aligned}
\theta^{(k, k_{\mathrm{M}})} &= (k_{\mathrm{M}} - 1) \cdot \Delta\theta^{(k)} + \theta^{(k, 1)} \\
&= 2\pi \frac{k_{\mathrm{M}} - 1}{K_{\mathrm{M}}} + \pi + \beta^{(k)}, \ k = 1 \ldots K.
\end{aligned} \tag{2.13}$$

- The radius of the circular arrays at the MTs is

$$l_{\mathrm{MT}} = \frac{\lambda}{4 \sin\left(\frac{\pi}{K_{\mathrm{M}}}\right)}. \tag{2.14}$$

We assume that the MTs are located in the far field of the BS, i.e. for the radius ϱ, see Fig. 2.4,

$$\varrho \gg l_{\mathrm{BS}} \tag{2.15}$$

and

$$\varrho \gg l_{\mathrm{MT}}, \tag{2.16}$$

hold. Moreover, we only consider the case that the mobile radio channels for each pair of $\mathrm{TAE}^{(k_{\mathrm{B}})}$, $k_{\mathrm{B}} = 1 \ldots K_{\mathrm{B}}$, and $\mathrm{RAE}^{(k, k_{\mathrm{M}})}$, $k_{\mathrm{M}} = 1 \ldots K_{\mathrm{M}}$, are single directional channels in which the waves propagate along the corresponding Line-of-Sights (LOSs). Then, the channel impulse responses $\underline{\mathbf{h}}^{(k, k_{\mathrm{B}}, k_{\mathrm{M}})}$ of (2.1) for different pairs of $\mathrm{TAE}^{(k_{\mathrm{B}})}$ and $\mathrm{RAE}^{(k, k_{\mathrm{M}})}$ of the MT k differ from each other only by different phase factors termed steering factors [MM80]. The steering factors depend only on the geometrical configuration. In this case

the channel impulse responses belonging to a certain MT are fully correlated. In the following we will model these channel impulse responses.

Fig. 2.5 shows the downlink wave propagation between $\mathrm{TAE}^{(k_\mathrm{B})}$ and $\mathrm{RAE}^{(k,k_\mathrm{M})}$ in the LOS direction, i.e. along the direction with azimuth angle $\beta^{(k)}$. Let us assume that virtual omni-antennas are placed in the RP of the BS and the RP of the MT k. The corresponding directional channel impulse response between the RP of the BS and the RP of the MT k along the LOS is termed

$$\underline{\mathbf{h}}_\mathrm{R}^{(k)} = \left(\underline{h}_{\mathrm{R},1}^{(k)} \cdots \underline{h}_{\mathrm{R},W}^{(k)} \right)^\mathrm{T}. \tag{2.17}$$

From the geometrical relations shown in Fig. 2.5 follows that the radiation from $\mathrm{TAE}^{(k_\mathrm{B})}$
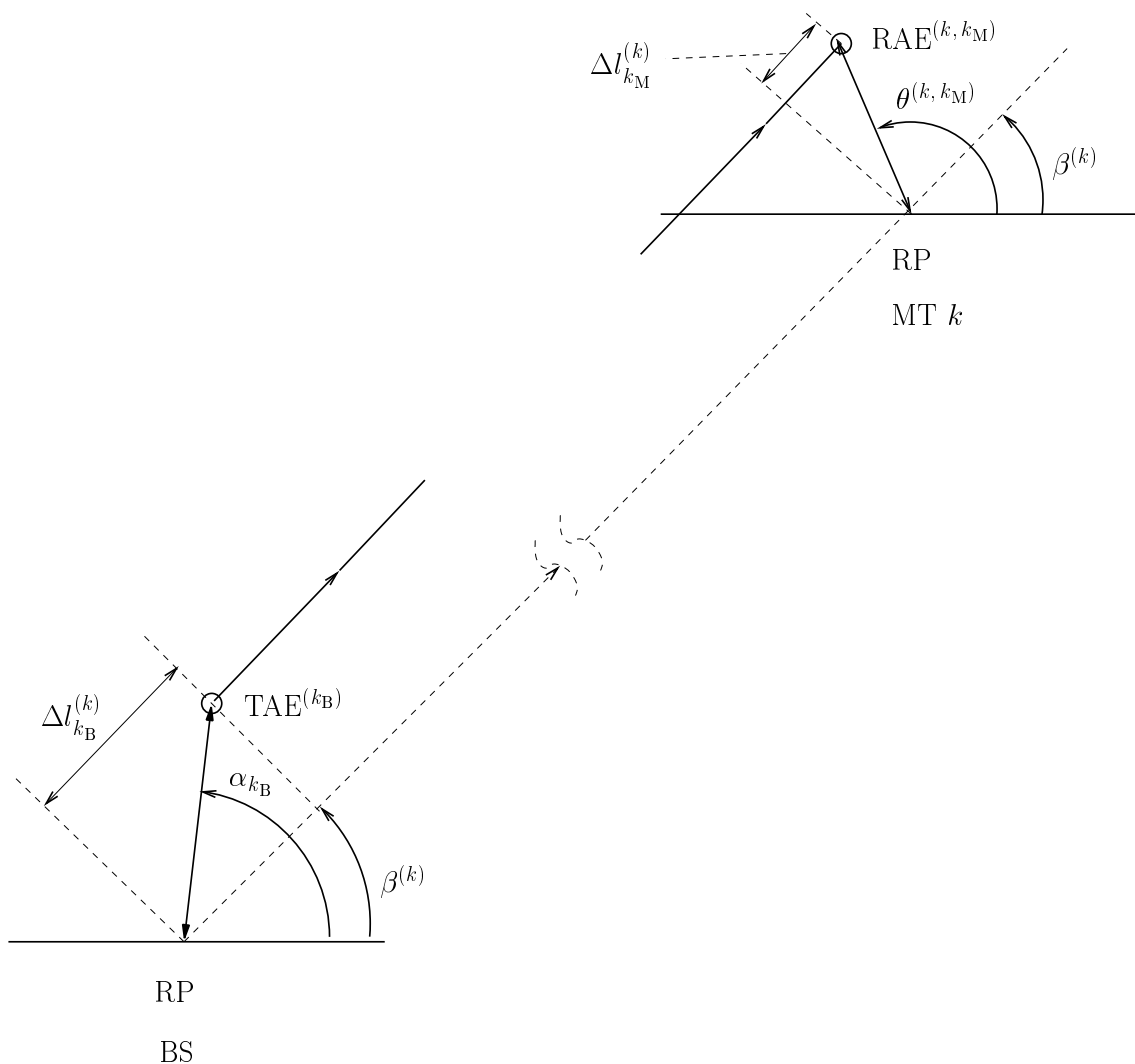
Fig. 2.5. The downlink wave propagation between $\mathrm{TAE}^{(k_\mathrm{B})}$ and $\mathrm{RAE}^{(k,k_\mathrm{M})}$ in the direction of LOS

has a path delay

$$\Delta l_{k_{\mathrm{B}}}^{(k)} = l_{\mathrm{BS}} \cos\left(\alpha_{k_{\mathrm{B}}} - \beta^{(k)}\right) \tag{2.18}$$

compared to the radiation from the RP of the BS along the LOS, which causes a phase lag

$$
\begin{aligned}
\Psi_{\mathrm{Tx}}^{(k,k_{\mathrm{B}})} &= \frac{2\pi}{\lambda}\Delta l_{k_{\mathrm{B}}}^{(k)} \\
&= \frac{2\pi}{\lambda} l_{\mathrm{BS}} \cos\left(\alpha_{k_{\mathrm{B}}} - \beta^{(k)}\right) \\
&= \frac{\pi}{2\sin\left(\frac{\pi}{K_{\mathrm{B}}}\right)} \cos\left(\alpha_{k_{\mathrm{B}}} - \beta^{(k)}\right).
\end{aligned}
\tag{2.19}
$$

With $\Psi_{\mathrm{Tx}}^{(k,k_{\mathrm{B}})}$ of (2.19) we can form the phase factor

$$\underline{a}_{\mathrm{Tx}}^{(k,k_{\mathrm{B}})} = e^{\mathrm{j}\Psi_{\mathrm{Tx}}^{(k,k_{\mathrm{B}})}}. \tag{2.20}$$

$\underline{a}_{\mathrm{Tx}}^{(k,k_{\mathrm{B}})}$ of (2.20) is termed Tx steering factor [MM80]. Similarly, the arrival of the waves at the $\mathrm{RAE}^{(k,k_{\mathrm{M}})}$ has a path advance

$$\Delta l_{k_{\mathrm{M}}}^{(k)} = l_{\mathrm{MT}} \cos\left(\theta^{(k,k_{\mathrm{M}})} - \beta^{(k)}\right) \tag{2.21}$$

compared to the arrival of the waves at the RP of the MT k, which causes a phase advance

$$
\begin{aligned}
\Psi_{\mathrm{Rx}}^{(k,k_{\mathrm{M}})} &= -\frac{2\pi}{\lambda} l_{\mathrm{MT}} \cos\left(\theta^{(k,k_{\mathrm{M}})} - \beta^{(k)}\right) \\
&= -\frac{\pi}{2\sin\left(\frac{\pi}{K_{\mathrm{M}}}\right)} \cos\left(\theta^{(k,k_{\mathrm{M}})} - \beta^{(k)}\right).
\end{aligned}
\tag{2.22}
$$

With $\Psi_{\mathrm{Rx}}^{(k,k_{\mathrm{M}})}$ of (2.22) we can form the phase factor

$$\underline{a}_{\mathrm{Rx}}^{(k,k_{\mathrm{M}})} = e^{\mathrm{j}\Psi_{\mathrm{Rx}}^{(k,k_{\mathrm{M}})}}. \tag{2.23}$$

$\underline{a}_{\mathrm{Rx}}^{(k,k_{\mathrm{M}})}$ of (2.23) is termed Rx steering factor. With (2.17), (2.20) and (2.23), the channel impulse response between $\mathrm{TAE}^{(k_{\mathrm{B}})}$ and $\mathrm{RAE}^{(k,k_{\mathrm{M}})}$ can be expressed as

$$\underline{\mathbf{h}}^{(k,k_{\mathrm{B}},k_{\mathrm{M}})} = \underline{a}_{\mathrm{Tx}}^{(k,k_{\mathrm{B}})}\, \underline{a}_{\mathrm{Rx}}^{(k,k_{\mathrm{M}})}\, \underline{\mathbf{h}}_{\mathrm{R}}^{(k)}. \tag{2.24}$$

(2.24) shows that the impulse responses of all $K_{\mathrm{B}}K_{\mathrm{M}}$ channels between the K_{B} TAEs of the BS and the K_{M} RAEs of each MT differ only by a complex factor of magnitude one from each other.

Chapter 3

General transmission system

3.1   Structure

The following considerations are an extension and generalization of considerations made in [BQT$^+$03]. Fig. 3.1 shows the general structure of a data transmission system. It is assumed that N_t data symbols $\underline{d}_n$, $n = 1 \ldots N_\mathrm{t}$, have to be transmitted from the transmitter (Tx) to the receiver (Rx). These data symbols are stacked in the data vector

$$\underline{\mathbf{d}} = \left(\underline{d}_1 \ldots \underline{d}_{N_\mathrm{t}}\right)^\mathrm{T} \tag{3.1}$$

of dimension N_t, which corresponds to one of the data blocks mentioned in Subsection 2.3.1. We do not consider channel encoding and decoding in this thesis. This means that $\underline{\mathbf{d}}$ of (3.1) occurs at the output of the channel encoder at the Tx, and that the estimate of $\underline{\mathbf{d}}$ generated in the Rx has to be further processed by a channel decoder. The elements $\underline{d}_n$, $n = 1 \ldots N_\mathrm{t}$, of $\underline{\mathbf{d}}$ of (3.1) are taken from a finite Tx sided symbol alphabet

$$\mathbb{V} = \{\underline{v}_1 \ldots \underline{v}_M\} \tag{3.2}$$

of cardinality M, and, therefore, we have

$$\underline{\mathbf{d}} \in \mathbb{V}^{N_\mathrm{t} \times 1}. \tag{3.3}$$

With the dimension N_t of $\underline{\mathbf{d}}$ of (3.1) and the cardinality M of $\mathbb{V}$ of (3.2), M^{N_t} different realizations $\underline{\mathbf{d}}^{(R)}$, $R = 1 \ldots M^{N_\mathrm{t}}$, of $\underline{\mathbf{d}}$ are possible. If we consider QPSK (Quadrature Phase Shift Keying), then we have

$$\mathbb{V} = \frac{1}{\sqrt{2}} \{1 + \mathrm{j}, -1 + \mathrm{j}, -1 - \mathrm{j}, 1 - \mathrm{j}\}. \tag{3.4}$$

In what follows $\underline{\mathbf{d}}$ of (3.1) is assumed to be wide sense stationary with zero mean and the covariance matrix

$$\mathbf{R}_\mathrm{d} = \mathrm{E}\left\{\underline{\mathbf{d}}\,\underline{\mathbf{d}}^\mathrm{H}\right\} = 2\sigma_\mathrm{d}^2\,\mathbf{I}^{(N_\mathrm{t})} = E_\mathrm{d}\,\mathbf{I}^{(N_\mathrm{t})}. \tag{3.5}$$

The task of the Tx consists in transforming $\underline{\mathbf{d}}$ of (3.1) into a transmit signal

$$\underline{\mathbf{t}} = \left(\underline{t}_1 \ldots \underline{t}_Q\right)^\mathrm{T} \in \mathbb{C}^{Q \times 1}, \tag{3.6}$$

where Q is termed spreading factor. This transformation can be described by the Tx operator $\mathcal{M}\{\cdot\}$:

$$\underline{\mathbf{t}} = \mathcal{M}\{\underline{\mathbf{d}}\}. \tag{3.7}$$

$\mathcal{M}\{\cdot\}$ of (3.7) has to assign to each of the M^{N_t} realizations $\underline{\mathbf{d}}^{(R)}$ of $\underline{\mathbf{d}}$ a unique transmit signal $\underline{\mathbf{t}}^{(R)}$, $R = 1 \ldots M^{N_\mathrm{t}}$.

additive noise

Tx   channel $\underline{\mathbf{n}}$ Rx

$\underline{\mathbf{d}}$ → $\mathcal{M}\{\cdot\}$ → $\underline{\mathbf{t}}$ → $\underline{\mathbf{H}}$ → $\underline{\mathbf{e}}$ → ⊕ → $\underline{\mathbf{r}}$ → $\mathcal{D}_{\text{dis}}\{\cdot\}$ → $\widehat{\underline{\mathbf{d}}}_{\text{dis}}$
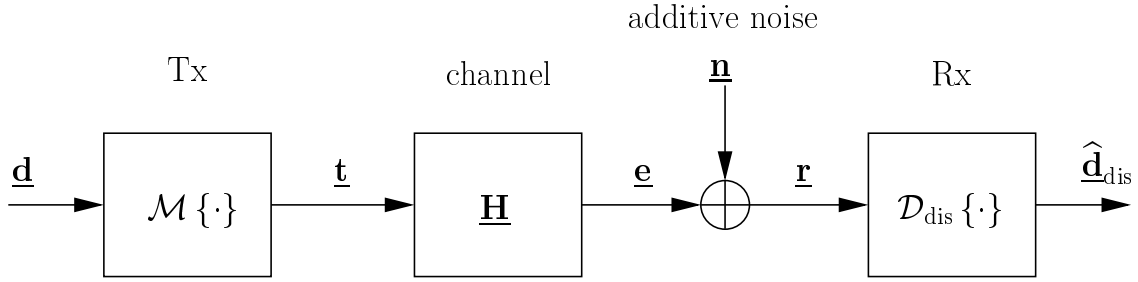
Fig. 3.1. General structure of data transmission systems

The assignment of $\underline{\mathbf{t}}$ to $\underline{\mathbf{d}}$ by (3.7) could be in a general sense termed channel encoding even though, as mentioned above, channel encoding is not considered in this thesis. Generally the assignment by (3.7) is non-linear and could be for instance implemented in the form of a look-up table. In special cases to be considered in Subsection 3.3 and in Chapter 4 of this thesis, this assignment is linear. Then, $\mathcal{M}\{\cdot\}$ can be substituted by a $Q \times N_{\text{t}}$ matrix $\underline{\mathbf{M}}$ termed modulator matrix, and (3.7) can be rewritten as the matrix-vector product

$$\underline{\mathbf{t}} = \underline{\mathbf{M}}\,\underline{\mathbf{d}} \ \in \ \mathbb{C}^{Q \times 1}. \tag{3.8}$$

The energy invested to transmit the signal $\underline{\mathbf{t}}$ of (3.7), which is termed transmit energy in the following, becomes

$$T = \frac{1}{2}\,\underline{\mathbf{t}}^{\text{H}}\underline{\mathbf{t}}. \tag{3.9}$$

Concerning the factor $\frac{1}{2}$ in (3.9), which will occur in an analogue way also in other equations throughout the thesis, we refer to the bandpass−lowpass transformation as described in [SJ67] and to the conventions made in that reference.

The radio channel between the Tx and the Rx is assumed to be linear and is represented by a channel matrix $\underline{\mathbf{H}}$ of dimension $Z \times Q$ [BQT$^+$03]. After having passed the radio channel, the transmit signal $\underline{\mathbf{t}}$ of (3.6) leads to the receive signal

$$\underline{\mathbf{e}} = \underline{\mathbf{H}}\,\underline{\mathbf{t}} \in \mathbb{C}^{Z \times 1} \tag{3.10}$$

at the channel output. $\underline{\mathbf{e}}$ of (3.10) is termed undisturbed receive signal and is assumed to be corrupted by continuous valued additive noise

$$\underline{\mathbf{n}} = \left(\underline{n}_1 \ldots \underline{n}_Z\right)^{\text{T}} \in \mathbb{C}^{Z \times 1}. \tag{3.11}$$

In what follows, we assume that $\underline{\mathbf{n}}$ of (3.11) is stationary with the expectation zero and the covariance matrix

$$\mathbf{R}_{\text{n}} = 2\,\sigma^2\,\mathbf{I}^{(Z)}. \tag{3.12}$$

With $\underline{\mathbf{e}}$ of (3.10) and $\underline{\mathbf{n}}$ of (3.11), the disturbed receive signal at the Rx input becomes

$$\underline{\mathbf{r}} = \underline{\mathbf{e}} + \underline{\mathbf{n}} \in \mathbb{C}^{Z \times 1}, \tag{3.13}$$

see also (1.1). Due to its generation by (3.7) and (3.10) the undisturbed receive signal $\underline{\mathbf{e}}$ is discrete valued. However, because $\underline{\mathbf{n}}$ in (3.13) is continuous valued, the disturbed receive signal $\underline{\mathbf{r}}$ is continuous valued.

The task of the Rx consists in assigning to each disturbed receive signal $\underline{\mathbf{r}}$ of (3.13) an estimate

$$\widehat{\underline{\mathbf{d}}}_{\mathrm{dis}} = \left(\widehat{\underline{d}}_{\mathrm{dis},\,1} \ldots \widehat{\underline{d}}_{\mathrm{dis},\,N_{\mathrm{t}}} \right)^{\mathrm{T}} \in \mathbb{V}^{N_{\mathrm{t}} \times 1} \tag{3.14}$$

of the transmit data vector $\underline{\mathbf{d}}$ of (3.1), with the subscript "dis" indicating that $\widehat{\underline{\mathbf{d}}}_{\mathrm{dis}}$ of (3.14) is discrete valued. This assignment procedure is non-linear because to each disturbed continuous valued receive signal $\underline{\mathbf{r}}$ exactly one out of $M^{N_{\mathrm{t}}}$ possible vectors $\widehat{\underline{\mathbf{d}}}_{\mathrm{dis}}$ has to be assigned [Pro95], and in a general sense could be termed channel decoding. The assignment procedure can be described by the Rx operator $\mathcal{D}_{\mathrm{dis}} \{\cdot\}$ operating on $\underline{\mathbf{r}}$ of (3.13):

$$\widehat{\underline{\mathbf{d}}}_{\mathrm{dis}} = \mathcal{D}_{\mathrm{dis}} \{\underline{\mathbf{r}}\} . \tag{3.15}$$

The transmission may be correct or erroneous:

$$\widehat{\underline{\mathbf{d}}}_{\mathrm{dis}} \begin{cases} = \underline{\mathbf{d}} \rightarrow & \text{exact transmission,} \\[2mm] \neq \underline{\mathbf{d}} \rightarrow & \text{transmission error.} \end{cases} \tag{3.16}$$

For a given channel characterized by $\underline{\mathbf{H}}$ and given properties of the noise $\underline{\mathbf{n}}$ the art of transmission system design consists in determining $\mathcal{M} \{\cdot\}$ of (3.7) and $\mathcal{D}_{\mathrm{dis}} \{\cdot\}$ of (3.15) in such a way that

- the system complexity and
- the transmit energy radiated from the Tx for a certain probability of transmission errors, as mentioned in Chapter 1,

become as low as possible. Usually a compromise between these two contradictory demands has to be found.

In conventional systems, that is in systems which follow the rationale Tx orientation, see Section 1.1, the system design starts from the Tx side, i.e. firstly the Tx operator $\mathcal{M} \{\cdot\}$ is given, and then the Rx operator $\mathcal{D}_{\mathrm{dis}} \{\cdot\}$ has to be a posteriori adapted under consideration of $\underline{\mathbf{H}}$ and $\mathcal{M} \{\cdot\}$. In contrast to this situation, in systems which follow the rationale Rx orientation, when designing the systems in the first step the Rx operator $\mathcal{D}_{\mathrm{dis}} \{\cdot\}$ is given, and then in the second step the Tx operator $\mathcal{M} \{\cdot\}$ has to be a posteriori adapted under consideration of $\underline{\mathbf{H}}$ and $\mathcal{D}_{\mathrm{dis}} \{\cdot\}$. As mentioned in Section 1.1, the latter rationale is the one being of interest in this thesis.

3.2 From non-linear to linear Rx oriented transmission systems

In Rx oriented transmission systems, for the a priori given Rx operator $\mathcal{D}_{\mathrm{dis}} \{\cdot\}$ of (3.15) there exist a variety of choices. This thesis focuses on the application of the Rx orientation

in mobile radio downlinks, in which a simply structured and, therefore, low cost Rx operator $\mathcal{D}_{\mathrm{dis}}\{\cdot\}$ is aspired as mentioned in Section 1.1. In order to fulfill this requirement, this thesis adopts an approach frequently followed in Tx oriented systems in order to reach such a simply structured Rx operator $\mathcal{D}_{\mathrm{dis}}\{\cdot\}$. In this approach the Rx operator $\mathcal{D}_{\mathrm{dis}}\{\cdot\}$ is composed according to the structure shown in Fig. 3.2 by concatenating a linear Rx operator $\underline{\mathbf{D}} \in \mathbb{C}^{N_{\mathrm{t}} \times Z}$ and a quantizer with the quantization function $\mathrm{Q}(\cdot)$, where the latter constitutes the non-linearity of $\mathcal{D}_{\mathrm{dis}}\{\cdot\}$. With this type of Rx operator, the estimate $\underline{\widehat{\mathbf{d}}}_{\mathrm{dis}}$ of (3.15) is produced in a two-step manner:

- In a first step a continuous valued, that is linear estimate

$$\underline{\widehat{\mathbf{d}}} = \left(\underline{\widehat{d}}_1 \ldots \underline{\widehat{d}}_{N_{\mathrm{t}}}\right)^{\mathrm{T}} = \underline{\mathbf{D}}\,\underline{\mathbf{r}} \in \mathbb{C}^{N_{\mathrm{t}} \times 1} \qquad (3.17)$$

  of $\underline{\mathbf{d}}$ of (3.1) is generated by linear filtering of $\underline{\mathbf{r}}$ of (3.13). The linear Rx operator $\underline{\mathbf{D}}$ is termed demodulator matrix.

- In a second step, each continuous valued component $\underline{\widehat{d}}_n$, $n = 1 \ldots N_{\mathrm{t}}$, of the estimate $\underline{\widehat{\mathbf{d}}}$ of (3.17) is mapped on one of the elements $\underline{w}_m$, $m = 1 \ldots M$, of a Rx sided discrete valued alphabet

$$\mathbb{W} = \{\underline{w}_1 \ldots \underline{w}_M\} \qquad (3.18)$$

  by means of the quantization function $\mathrm{Q}(\cdot)$:

$$\underline{\widehat{d}}_{\mathrm{dis},n} = \mathrm{Q}\left(\underline{\widehat{d}}_n\right) \in \mathbb{W}. \qquad (3.19)$$

As a precondition to make such a two-step approach reasonable, the generation of the Tx signal $\underline{\mathbf{t}}$ from the data vector $\underline{\mathbf{d}}$, see (3.7), has to be performed in a way which via (3.17) enables a linear estimate $\underline{\widehat{\mathbf{d}}}$ which componentwise corresponds to $\underline{\mathbf{d}}$ of (3.1). This means that each component $\underline{\widehat{d}}_n$ of $\underline{\widehat{\mathbf{d}}}$ of (3.17) would yield the corresponding component $\underline{\widehat{d}}_{\mathrm{dis},n}$ of $\underline{\widehat{\mathbf{d}}}_{\mathrm{dis}}$ by quantization according to (3.19).
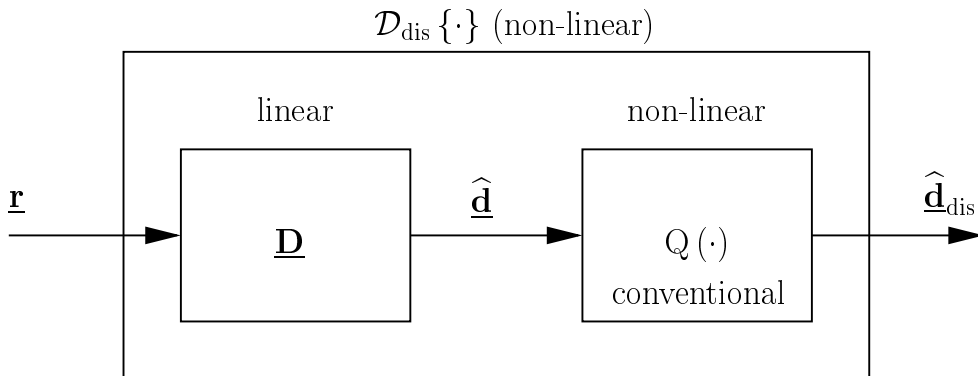
Fig. 3.2. Composing $\mathcal{D}_{\mathrm{dis}}\{\cdot\}$ of (3.15) by concatenating the linear operator $\underline{\mathbf{D}}$ and a quantizer $\mathrm{Q}(\cdot)$ with simply connected decision regions $\mathbb{G}_m$

Concerning the just described second step, this is the procedure followed in conventional quantization schemes, in which, in addition, $\mathbb{W}$ of (3.18) is usually chosen equal to $\mathbb{V}$ of (3.2). In the case of such conventional schemes the quantization can be illustrated in the complex plane as shown in Fig. 3.3 for an example with M equal to 4. For each of the M realizations $\underline{v}_m$, $m = 1 \ldots M$, of the transmitted data symbols $\underline{d}_n$ a simply connected decision region $\mathbb{G}_m$ is defined in the complex plane, and within each of these M decision regions a representative

$$\underline{g}_m = \underline{w}_m \tag{3.20}$$

is chosen. Now, if a continuous valued data estimate $\widehat{\underline{d}}_n$ falls into the decision region $\mathbb{G}_m$, then the output of the quantizer is set to $\underline{g}_m$, which is usually equal to $\underline{w}_m$ and $\underline{v}_m$. This quantization function can be described by

$$\widehat{\underline{d}}_n \in \mathbb{G}_m \rightarrow \widehat{\underline{d}}_{\text{dis},\,n} = \mathrm{Q}\left(\widehat{\underline{d}}_n\right) = \underline{g}_m = \underline{w}_m = \underline{v}_m. \tag{3.21}$$

Now, the two steps described by (3.17) and (3.19) can be written in the comprehensive form

$$\widehat{\mathbf{d}}_{\text{dis}} = \mathcal{D}_{\text{dis}}(\underline{\mathbf{r}}) = \mathrm{Q}\left(\widehat{\underline{\mathbf{d}}}\right) = \mathrm{Q}\left(\underline{\mathbf{D}}\,\underline{\mathbf{r}}\right), \tag{3.22}$$

where the notation $\mathrm{Q}\left(\widehat{\underline{\mathbf{d}}}\right)$ in (3.22) means that the quantization function $\mathrm{Q}\left(\cdot\right)$ of (3.19) is applied to each of the N_{t} components of the linear estimate $\widehat{\underline{\mathbf{d}}}$. With (3.22), (3.7), (3.10) and (3.13), one obtains the relation

$$\widehat{\underline{\mathbf{d}}}_{\text{dis}} = \mathrm{Q}\big(\underbrace{\underline{\mathbf{D}}\,\underline{\mathbf{H}}}_{\underline{\mathbf{B}}}\,\mathcal{M}\left(\underline{\mathbf{d}}\right) + \underline{\mathbf{D}}\,\underline{\mathbf{n}}\big) \tag{3.23}$$

between $\widehat{\underline{\mathbf{d}}}_{\text{dis}}$ of (3.14) and $\underline{\mathbf{d}}$ of (3.1). $\underline{\mathbf{B}}$ in (3.23) is termed system matrix.

Once the Rx operator $\mathcal{D}_{\text{dis}}\left\{\cdot\right\}$, namely the demodulator matrix $\underline{\mathbf{D}}$ of (3.17) and the quantizer $\mathrm{Q}\left(\cdot\right)$ of (3.19), are a priori determined, the Tx operator $\mathcal{M}\left\{\cdot\right\}$ of (3.7) has to be a posteriori adapted under consideration of $\mathcal{D}_{\text{dis}}\left\{\cdot\right\}$ and $\underline{\mathbf{H}}$ to meet the system requirements as mentioned in Section 3.1. Meanwhile quite well known techniques to design $\mathcal{M}\left\{\cdot\right\}$ are the linear techniques, in which a linear Tx operator, see (3.8),

$$\underline{\mathbf{M}} = f\left(\underline{\mathbf{D}}, \underline{\mathbf{H}}\right) \in \mathbb{C}^{Q \times N_{\text{t}}} \tag{3.24}$$

is determined based on the chosen demodulator matrix $\underline{\mathbf{D}}$ and the channel matrix $\underline{\mathbf{H}}$, whereas the quantizer $\mathrm{Q}\left(\cdot\right)$ in the structure shown in Fig. 3.2 is not considered when determining $\underline{\mathbf{M}}$. Without the quantizer $\mathrm{Q}\left(\cdot\right)$, we arrive at the general structure of a linear transmission system shown in Fig. 3.4. This system can be described by

$$\widehat{\underline{\mathbf{d}}} = \underline{\mathbf{D}}\,\underline{\mathbf{r}} = \underline{\mathbf{D}}\left(\underline{\mathbf{H}}\,\underline{\mathbf{M}}\,\underline{\mathbf{d}} + \underline{\mathbf{n}}\right). \tag{3.25}$$

Linear transmission systems following the rationale Rx orientation are termed linear Rx oriented transmission systems. In the remaining sections of Chapter 3 such linear Rx oriented transmission systems will be considered.
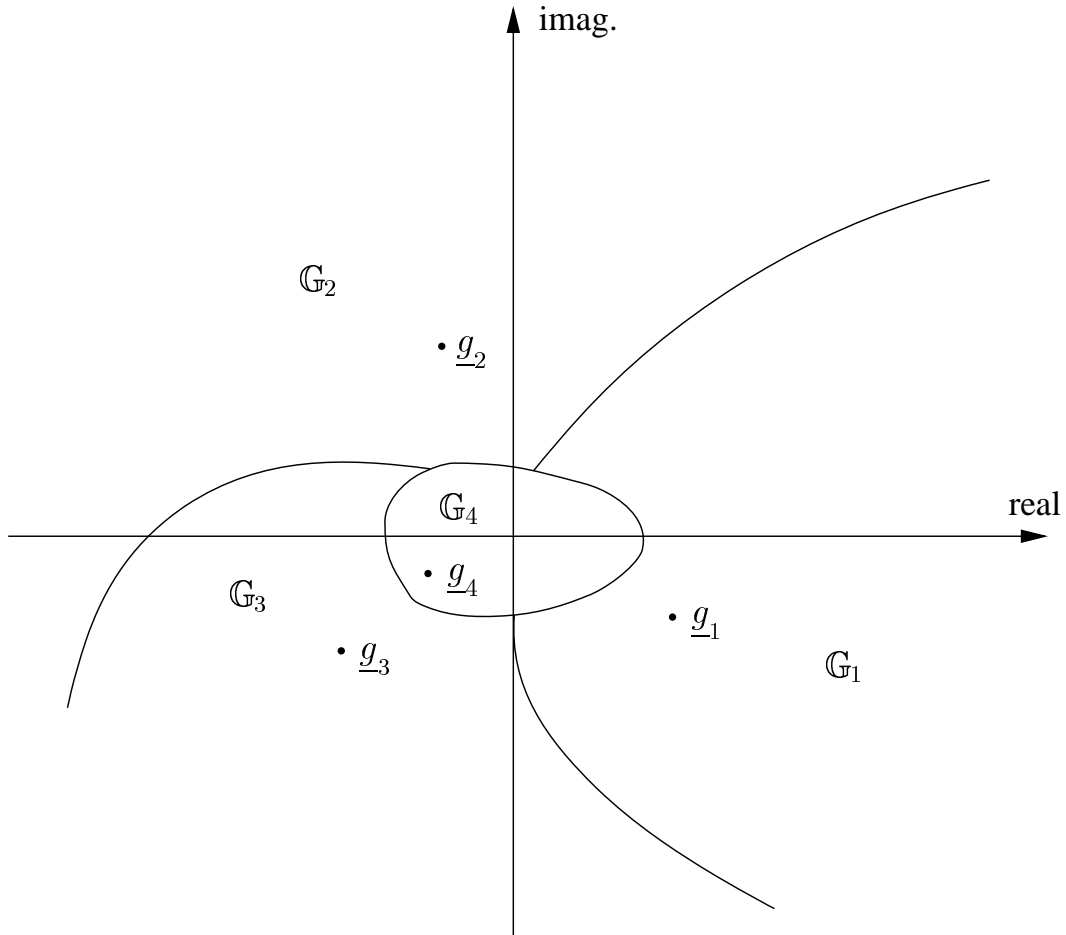
Fig. 3.3. Example of a conventional simply connected quantization scheme
Q(·) with cardinality $M = 4$
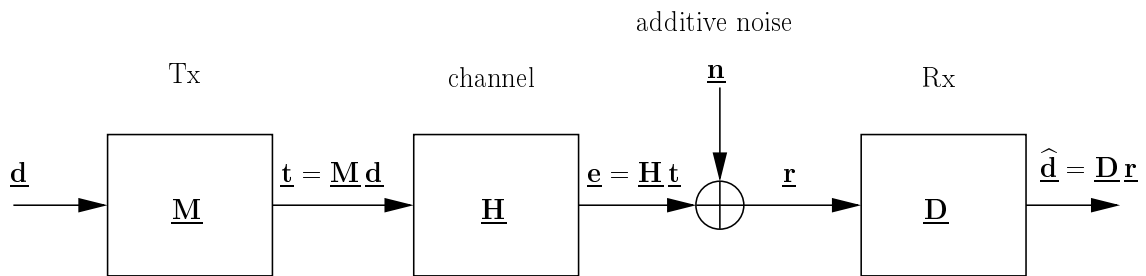
Fig. 3.4. General structure of a linear transmission system

The author of this thesis extends the above recapitulated conception of conventional
quantizers, that is of quantizers with simply connected decision regions, to quantizers
with multiply connected decision regions in order to achieve certain benefits with respect
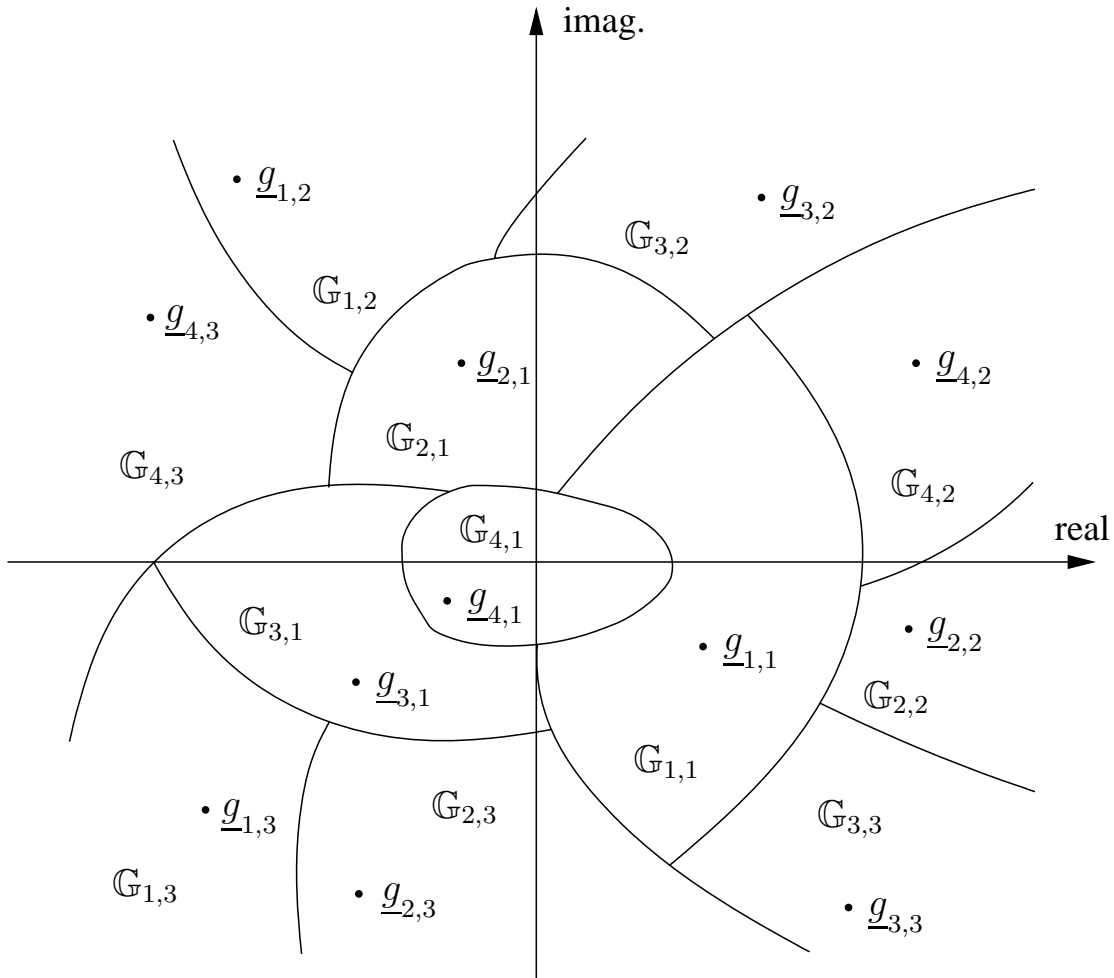
Fig. 3.5. Example of an unconventional 3-fold connected quantization scheme $Q(\cdot)$, that is $P = 3$, with cardinality $M = 4$

to the system performance, see Chapter 5. In doing so he also generalizes the conception of lattice-structured decision regions [Fis02]. The author names these novel quantizers as unconventional quantizers.

Concerning the quantization function $Q\left(\widehat{\underline{d}}_n\right)$ of (3.19) to each possible Tx sided realization $\underline{v}_m, m = 1 \ldots M$, of a data symbol $\underline{d}_n, n = 1 \ldots N_t$, in contrast to the considerations made up to now, instead of only one now P representatives $\underline{g}_{m,p}, p = 1 \ldots P$, could be assigned. The entirety of these P representatives $\underline{g}_{m,p}, p = 1 \ldots P$, valid for a certain realization $\underline{v}_m$ of a data symbol constitutes the data symbol specific set

$$\mathbb{V}_{q,m} = \left\{ \underline{g}_{m,1} \cdots \underline{g}_{m,P} \right\}. \tag{3.26}$$

Each representative $\underline{g}_{m,p}, p = 1 \ldots P, m = 1 \ldots M$, is located in a region $\mathbb{G}_{m,p}$ [Bai86], which is termed partial decision regions in the following. In total we have MP such re-

gions, which are assumed to completely tile the complex plane and to be non-overlapping. With the P partial decision regions $\mathbb{G}_{m,p}$, $p = 1 \ldots P$, corresponding to the realization $\underline{v}_m$ of a data symbol, one obtains the respective total decision region

$$\mathbb{G}_m = \bigcup_{p=1}^{P} \mathbb{G}_{m,p}. \tag{3.27}$$

$\mathbb{G}_m$ of (3.27) consists of P non-connected partial decision regions. Therefore, $\mathbb{G}_m$ is termed a P-fold, or generally multiply connected decision region. For the special case P equal to one, $\mathbb{G}_m$ becomes simply connected, and we obtain a simply connected quantization scheme as shown in Fig. 3.3.

Fig. 3.5 shows an example of an unconventional 3-fold connected quantization scheme with cardinality $M = 4$. For given representatives $\underline{g}_{m,p}$ an important question is how the partial decision regions $\mathbb{G}_{m,p}$ around these representatives should be chosen. If all continuous valued estimates $\widehat{\underline{d}}_n$ would be corrupted by the same Gaussian noise, then the optimum decision regions would be the Voronoi regions [CS82].

In the case of applying a unconventional quantizer, the useful portion of $\widehat{\underline{\mathbf{d}}}$ in the structure shown in Fig. 3.2 has no longer to be assigned to $\underline{\mathbf{d}}$ in a unique way. Rather, a specific $\underline{\mathbf{d}}$ can be represented by any one out of a selection of P^{N_t} useful portions in $\widehat{\underline{\mathbf{d}}}$. In order to emphasize this difference between systems with conventional and unconventional quantization schemes, we use in the latter case instead of $\widehat{\underline{\mathbf{d}}}$ the quantity $\widehat{\underline{\mathbf{g}}}$, see Fig. 3.6.

In systems with such a linear Tx operator $\mathcal{M}\{\cdot\}$ equal to $\underline{\mathbf{M}}$, the conventional quantization schemes are chosen in the following.
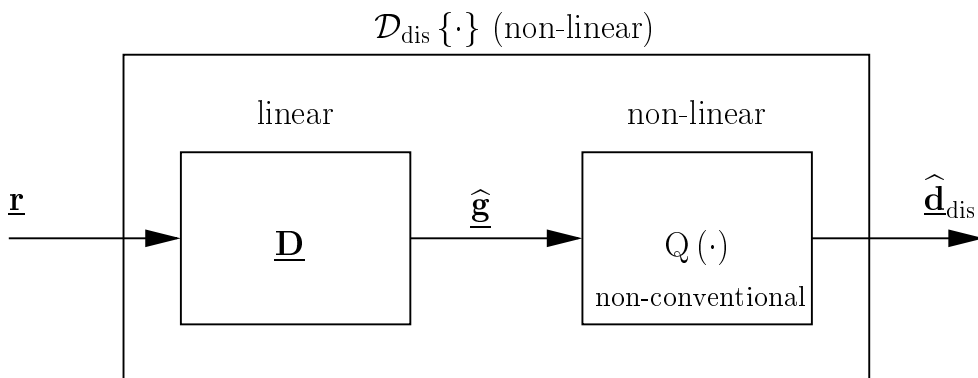
Fig. 3.6. Composing $\mathcal{D}_{\text{dis}}\{\cdot\}$ of (3.15) by concatenating the linear operator $\underline{\mathbf{D}}$ and a quantizer $Q(\cdot)$ with multiply connected decision regions $\mathbb{G}_m$

3.3 Linear Rx oriented transmission systems

3.3.1 General

With respect to the design of linear Rx oriented transmission systems to be described by (3.25), the first question is how the demodulator matrix $\underline{\mathbf{D}}$ should be chosen; quite generally, this choice means that a total of $N_t Z$ elements $\underline{D}_{n,z}$, $n = 1 \ldots N_t$, $z = 1 \ldots Z$, should be chosen, which gives a lot of chances to make good or bad decisions. After having chosen $\underline{\mathbf{D}}$, the next question is in which way the modulator matrix $\underline{\mathbf{M}}$ should be a posteriori determined. This question will be addressed in Subsection 3.3.2.

Subsection 3.3.3 describes the singular value decomposition (SVD) of $\underline{\mathbf{H}}$ and representation of $\underline{\mathbf{D}}$ by the left side singular vectors of $\underline{\mathbf{H}}$, which is a preparation for the definition of criteria in Subsection 3.3.4.

Once $\underline{\mathbf{D}}$ and $\underline{\mathbf{M}}$ are determined, the system performance enabled by these matrices should be evaluated. Such an evaluation is the topic of Subsection 3.3.4, in which criteria for a performance evaluation will be proposed. Up to now the question how to choose a priori the demodulator matrix $\underline{\mathbf{D}}$ was not addressed. In this Subsection some hints concerning this choice will be also given.

The statistical considerations of the criteria introduced in Subsection 3.3.4 will be addressed in Subsections 3.3.5 and 3.3.6.

3.3.2 A posteriori determination of the modulator matrix $\underline{\mathbf{M}}$

Linear approaches meanwhile quite well known to determining $\underline{\mathbf{M}}$ based on given matrices $\underline{\mathbf{H}}$ and $\underline{\mathbf{D}}$ are the TxMF and the TxZF Filter mentioned in Section 1.3. In [BQT$^+$03, MBQ04] the author contributes to the elaboration and consistent description of these filters. Other options for Rx orientation are various kinds of TxMMSE Filters also mentioned in Section 1.3 and considered by the author in [MBQ04].

In the case of the TxMF the modulator matrix results according to [MBQ04]

$$\underline{\mathbf{M}} = (\underline{\mathbf{D}}\,\underline{\mathbf{H}})^{\mathrm{H}} = \underline{\mathbf{B}}^{\mathrm{H}} \tag{3.28}$$

from $\underline{\mathbf{D}}$ and $\underline{\mathbf{H}}$. As already mentioned in connection with (3.23), the matrix $\underline{\mathbf{B}}$ is termed system matrix. As shown in [MBQ04], the choice of $\underline{\mathbf{M}}$ according to (3.28) allows an optimum exploitation of the transmit energy T of (3.9). However, interference between different symbols $\underline{d}_n$ of the data vector $\underline{\mathbf{d}}$ of (3.1), that is intersymbol interference (ISI) occurs, which in the case of the TxMF remains out of consideration and yet may have a severe impact on the system performance.

In the case of the TxZF Filter the modulator matrix is determined according to [MBQ04]

$$\underline{\mathbf{M}} = (\underline{\mathbf{D}}\,\underline{\mathbf{H}})^{\mathrm{H}} \left[\underline{\mathbf{D}}\,\underline{\mathbf{H}}\,(\underline{\mathbf{D}}\,\underline{\mathbf{H}})^{\mathrm{H}} \right]^{-1} = \underline{\mathbf{B}}^{\mathrm{H}} \left(\underline{\mathbf{B}}\,\underline{\mathbf{B}}^{\mathrm{H}} \right)^{-1}. \tag{3.29}$$

As explained in [MBQ04], by this choice of $\underline{\mathbf{M}}$ the ISI typical of the TxMF and mentioned in the previous paragraph is totally eliminated. However, the utilization of the invested transmit energy T of (3.9) is non-optimum. Quite analogue to an observation made already in [Kle96] for linear Tx oriented systems we incur the problem that ISI elimination costs useful energy or enhances the impact of the received noise.

In one version of the TxMMSE Filter, which leads to a closed form expression for $\underline{\mathbf{M}}$, we set out from a given average transmit energy $\overline{T}$ — average because T of (3.9) varies depending on the realization $\underline{\mathbf{d}}^{(R)}$, $R = 1 \ldots M^{N_{\mathrm{t}}}$, of $\underline{\mathbf{d}}$, see Section 3.1. Then, with a scalar κ, by designating the nth column of a matrix in brackets by $[\,\cdot\,]_n$, and with σ_{d}^2 of (3.5) and σ^2 of (3.12) the modulator matrix is given by [MBQ04, BZT$^+$04]

$$\underline{\mathbf{M}} = \kappa\,(\underline{\mathbf{D}}\,\underline{\mathbf{H}})^{\mathrm{H}} \left[\underline{\mathbf{D}}\,\underline{\mathbf{H}}\,(\underline{\mathbf{D}}\,\underline{\mathbf{H}})^{\mathrm{H}} + \frac{\sigma^2}{\overline{T}} \mathrm{trace}\,(\underline{\mathbf{D}}\,\underline{\mathbf{D}}^{\mathrm{H}})\,\mathbf{I}^{(N_{\mathrm{t}})} \right]^{-1},$$

$$\text{s.t. } \sigma_{\mathrm{d}}^2 \sum_{n=1}^{N_{\mathrm{t}}} \|[\underline{\mathbf{M}}]_n\|^2 = \overline{T} \text{ by proper choice of } \kappa. \tag{3.30}$$

The TxMMSE Filter of (3.30) allows an advantageous compromise between the detrimental impact of ISI typical of the TxMF and the reduced energy efficiency typical of the TxZF Filter, and maximizes the mean SNIR (Signal-to-Noise-plus-Interference Ratio)

$$\gamma = \frac{\sum_{n=1}^{N_{\mathrm{t}}} \left| [\underline{\mathbf{D}}\,\underline{\mathbf{H}}\,\underline{\mathbf{M}}]_{n,n} \right|^2 \sigma_{\mathrm{d}}^2}{\sum_{n=1}^{N_{\mathrm{t}}} \left\{ \|[\underline{\mathbf{D}}^{\mathrm{T}}]_n\|^2 \sigma^2 + \|[\overline{\mathrm{diag}}\,(\underline{\mathbf{D}}\,\underline{\mathbf{H}}\,\underline{\mathbf{M}})]_n\|^2 \sigma_{\mathrm{d}}^2 \right\}} \tag{3.31}$$

as shown in [BZT$^+$04].

In order to illustrate and compare the performances of the TxMF of (3.28), the TxZF Filter of (3.29) and the TxMMSE Filter of (3.30), the author shows in Fig. 3.6 the average SNIR γ of (3.31) versus the ratio $\overline{T}/\sigma^2$ of the average transmit energy $\overline{T}$ and the noise variance σ^2 of (3.12). This ratio is termed pseudo SNR (Signal-to-Noise Ratio), because it relates the energy $\overline{T}$ radiated by the Tx to the noise variance σ^2 observed at the Rx. The shown curves were determined by the author for certain system parameters described in [BZT$^+$04]. The curves show that the performance of the TxMMSE Filter converges to the performance of the TxMF for low values $\overline{T}/\sigma^2$ and to the performance of the TxZF Filter for high values of $\overline{T}/\sigma^2$. For medium values of $\overline{T}/\sigma^2$ the TxMMSE Filter outperforms both the TxMF and the TxZF Filter.

A heuristic approach to the TxMMSE Filter would be given by the choice of $\underline{\mathbf{M}}$ according to

$$\underline{\mathbf{M}} \sim (\underline{\mathbf{D}}\,\underline{\mathbf{H}})^{\mathrm{H}} \left[\underline{\mathbf{D}}\,\underline{\mathbf{H}}\,(\underline{\mathbf{D}}\,\underline{\mathbf{H}})^{\mathrm{H}} + \frac{\sigma^2}{\overline{T}} \mathbf{I}^{(N_{\mathrm{t}})} \right]^{-1}. \tag{3.32}$$
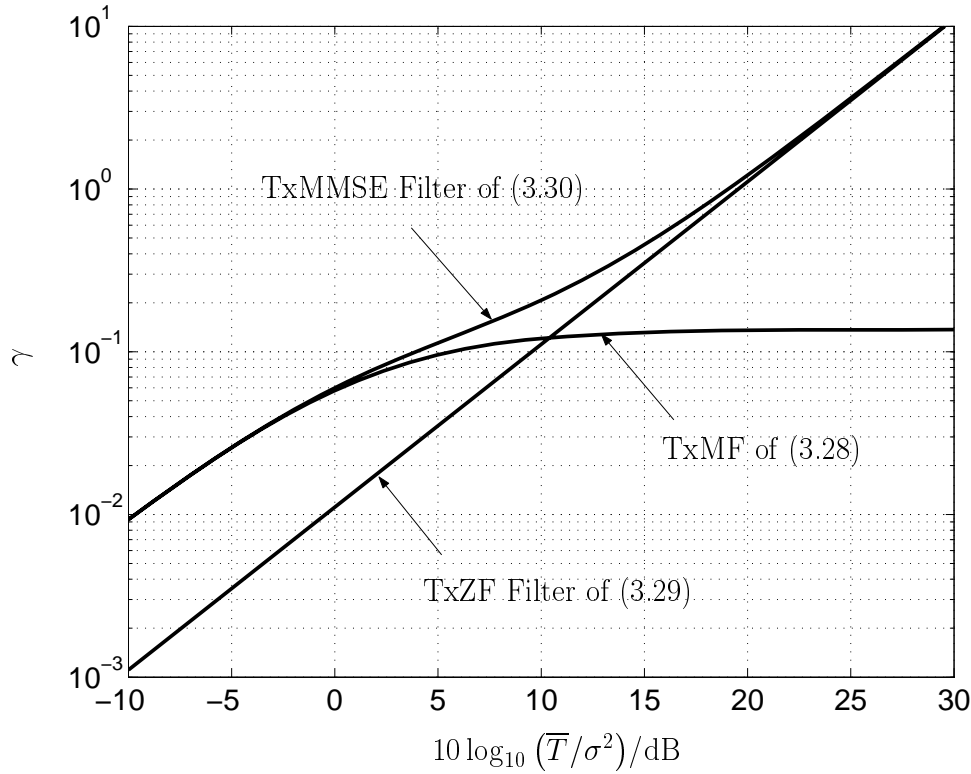
Fig. 3.7. Average SNIR γ at the Rx versus the pseudo SNR $\overline{T}/\sigma^2$ [BZT$^+$04]

Also this TxMMSE Filter would converge to the TxMF for low pseudo SNRs $\overline{T}/\sigma^2$ and to the TxZF Filter for high pseudo SNRs $\overline{T}/\sigma^2$, but does not exactly maximize the SNIR γ as the TxMMSE Filter of (3.30) does. In investigations not included in this thesis, the author could show that the performance of the heuristic TxMMSE Filter of (3.32) is comparable to that of the exact TxMMSE Filter of (3.30).

In (3.28) to (3.30) the nth row $\left(\left[\underline{\mathbf{D}}^{\text{T}}\right]_n\right)^{\text{T}}$ of $\underline{\mathbf{D}}$ and the nth column $[\underline{\mathbf{M}}]_n$ of $\underline{\mathbf{M}}$ correspond to the transmission of the data symbol $\underline{d}_n$ of $\underline{\mathbf{d}}$ of (3.1). If in the case of the TxMF of (3.28) or the TxZF Filter of (3.29) the row $\left(\left[\underline{\mathbf{D}}^{\text{T}}\right]_n\right)^{\text{T}}$ is multiplied by the scalar $\underline{s}_n$, then the column $[\underline{\mathbf{M}}]_n$ changes by the scalar $1/\underline{s}_n$ in order to keep (3.28) and (3.29) fulfilled. Therefore, multiplication of $\left(\left[\underline{\mathbf{D}}^{\text{T}}\right]_n\right)^{\text{T}}$ by $\underline{s}_n$ means that the transmit energy

$$T_n = \frac{1}{2}\left\|[\underline{\mathbf{M}}]_n\right\|^2 |\underline{d}_n|^2 = \frac{1}{2}\left[\underline{\mathbf{M}}^{\text{H}}\underline{\mathbf{M}}\right]_{n,n} |\underline{d}_n|^2 \tag{3.33}$$

of the data symbol $\underline{d}_n$ is reduced by the factor $1/|\underline{s}_n|^2$. Consequently, by a row-wise scaling of $\underline{\mathbf{D}}$ the invested transmit energy T_n can by symbol-wise adjusted.

In the further course of this thesis we do not consider the TxMMSE Filter but restrict ourselves to the TxMF and TxZF Filter.

3.3.3   Singular value decomposition (SVD) of $\underline{\mathbf{H}}$ and representation of $\underline{\mathbf{D}}$ by the left side singular vectors of $\underline{\mathbf{H}}$

By performing singular value decomposition (SVD) [Lue96], the $Z \times Q$ channel matrix $\underline{\mathbf{H}}$ of (3.10) can be expressed by two unitary matrices

$$\underline{\mathbf{U}} = (\underline{\mathbf{u}}_1 \ldots \underline{\mathbf{u}}_Z) \in \mathbb{C}^{Z \times Z} \tag{3.34}$$

and

$$\underline{\mathbf{V}} = \left(\underline{\mathbf{v}}_1 \ldots \underline{\mathbf{v}}_Q\right) \in \mathbb{C}^{Q \times Q} \tag{3.35}$$

and a $Z \times Q$ matrix $\boldsymbol{\Sigma}$ as

$$\underline{\mathbf{H}} = \underline{\mathbf{U}}\,\boldsymbol{\Sigma}\,\underline{\mathbf{V}}^{\mathrm{H}}. \tag{3.36}$$

The Z columns $\underline{\mathbf{u}}_z$, $z = 1 \ldots Z$, of $\underline{\mathbf{U}}$ of (3.34) and the Q columns $\underline{\mathbf{v}}_q$, $q = 1 \ldots Q$, of $\underline{\mathbf{V}}$ of (3.35) are termed left or right side singular vectors of $\underline{\mathbf{H}}$, respectively. In the case $Z > Q$, $\boldsymbol{\Sigma}$ in (3.36) has the form

$$\boldsymbol{\Sigma} = \begin{pmatrix} \sqrt{\lambda_1} & \ldots & 0 \\ \vdots & \ddots & \vdots \\ 0 & \ldots & \sqrt{\lambda_Q} \\ \vdots & \ddots & \vdots \\ 0 & \ldots & 0 \end{pmatrix}, \tag{3.37}$$

and in the case $Z < Q$, $\boldsymbol{\Sigma}$ in (3.36) has the form

$$\boldsymbol{\Sigma} = \begin{pmatrix} \sqrt{\lambda_1} & \ldots & 0 & \ldots & 0 \\ \vdots & \ddots & \vdots & \ddots & \vdots \\ 0 & \ldots & \sqrt{\lambda_Z} & \ldots & 0 \end{pmatrix}. \tag{3.38}$$

In the case $Z = Q$, $\boldsymbol{\Sigma}$ in (3.36) is a diagonal matrix. The elements $\sqrt{\lambda_q}$ of (3.37) or (3.38) are non-negative and are termed singular values [Lue96] of the channel matrix $\underline{\mathbf{H}}$. In general,

$$G = \min(Z, Q) \tag{3.39}$$

singular values exist. Let us assume that they are sorted so that

$$\sqrt{\lambda_1} \geq \sqrt{\lambda_2} \geq \cdots \geq \sqrt{\lambda_G} \geq 0 \tag{3.40}$$

holds. Then $\sqrt{\lambda_1}$ is termed principal singular value. The singular vectors $\underline{\mathbf{u}}_1$ of (3.34) and $\underline{\mathbf{v}}_1$ of (3.35) belonging to $\sqrt{\lambda_1}$ are termed principal singular vectors.

The rank of the channel matrix $\underline{\mathbf{H}}$ is equal to the number of non-zero valued singular values $\sqrt{\lambda_q}$, $q = 1 \ldots G$, of $\underline{\mathbf{H}}$, i.e. with G of (3.39)

$$\mathrm{rank}(\underline{\mathbf{H}}) \leq G \tag{3.41}$$

is valid.

The Gram matrices $\underline{\mathbf{H}}^{\mathrm{H}}\underline{\mathbf{H}}$ and $\underline{\mathbf{H}}\,\underline{\mathbf{H}}^{\mathrm{H}}$ of $\underline{\mathbf{H}}$ are hermitian matrices. Their SVDs degenerate to eigenvalue decompositions (EVD) [Lue96]. With $\underline{\mathbf{U}}$ of (3.34), $\underline{\mathbf{V}}$ of (3.35) and $\mathbf{\Sigma}$ of (3.37) or (3.38) we can obtain

$$\underline{\mathbf{H}}^{\mathrm{H}}\underline{\mathbf{H}} = \underline{\mathbf{V}}\,\mathbf{\Sigma}^{\mathrm{T}}\mathbf{\Sigma}\,\underline{\mathbf{V}}^{\mathrm{H}} \tag{3.42}$$

and

$$\underline{\mathbf{H}}\,\underline{\mathbf{H}}^{\mathrm{H}} = \underline{\mathbf{U}}\,\mathbf{\Sigma}\,\mathbf{\Sigma}^{\mathrm{T}}\underline{\mathbf{U}}^{\mathrm{H}}, \tag{3.43}$$

respectively.

We now come to the representation of $\underline{\mathbf{D}}$ by the left side singular vectors $\underline{\mathbf{u}}_z$, $z = 1\ldots Z$, of $\underline{\mathbf{H}}$. With $\underline{\mathbf{U}}$ of (3.34) and the matrix

$$\underline{\mathbf{G}} = \begin{pmatrix} \underline{g}_{1,1} & \cdots & \underline{g}_{1,Z} \\ \vdots & \ddots & \vdots \\ \underline{g}_{N_{\mathrm{t}},1} & \cdots & \underline{g}_{N_{\mathrm{t}},Z} \end{pmatrix} \in \mathbb{C}^{N_{\mathrm{t}} \times Z} \tag{3.44}$$

we can express the a priori determined demodulator matrix $\underline{\mathbf{D}}$, see Subsection 3.3.2, in the form [Lue96]

$$\underline{\mathbf{D}} = \underline{\mathbf{G}}\,\underline{\mathbf{U}}^{\mathrm{H}}. \tag{3.45}$$

Without restricting generality we assume that $\underline{\mathbf{D}}$ and, consequently, $\underline{\mathbf{G}}$ fulfill

$$\mathrm{diag}\left(\underline{\mathbf{D}}\,\underline{\mathbf{D}}^{\mathrm{H}}\right) = \mathrm{diag}\left(\underline{\mathbf{G}}\,\underline{\mathbf{U}}^{\mathrm{H}}\underline{\mathbf{U}}\,\underline{\mathbf{G}}^{\mathrm{H}}\right) = \mathrm{diag}\left(\underline{\mathbf{G}}\,\underline{\mathbf{G}}^{\mathrm{H}}\right) = \mathbf{I}^{(N_{\mathrm{t}})}. \tag{3.46}$$

In order to illustrate (3.36) and (3.45), we present a numerical example in what follows. For simplicity we assume that all occurring matrices are real. The channel matrix considered in the example reads

$$\underline{\mathbf{H}} = \overbrace{\begin{pmatrix} -0.08 & 0.64 & -0.10 & 0.00 \\ -0.69 & 0.43 & 0.30 & 0.53 \\ 0.08 & 0.01 & -0.25 & 0.05 \\ 0.11 & 0.16 & 0.89 & -0.09 \\ -0.57 & 0.02 & -0.01 & -0.55 \end{pmatrix}}^{Q=4} \left.\vphantom{\begin{pmatrix}1\\1\\1\\1\\1\end{pmatrix}}\right\} Z = 5. \tag{3.47}$$

By SVD of $\underline{\mathbf{H}}$ of (3.47) we obtain

$$\underline{\mathbf{U}} = \begin{pmatrix} -0.29 & 0.30 & 0.13 & -0.90 & 0.12 \\ -0.82 & 0.31 & 0.26 & 0.40 & -0.07 \\ 0.15 & 0.18 & 0.15 & -0.09 & -0.96 \\ -0.44 & -0.83 & -0.18 & -0.19 & -0.23 \\ -0.16 & 0.32 & -0.93 & 0.01 & -0.11 \end{pmatrix}, \tag{3.48}$$

$$\mathbf{\Sigma} = \begin{pmatrix} \sqrt{1.3} & 0 & 0 & 0 \\ 0 & \sqrt{0.8} & 0 & 0 \\ 0 & 0 & \sqrt{0.6} & 0 \\ 0 & 0 & 0 & \sqrt{0.3} \\ 0 & 0 & 0 & 0 \end{pmatrix} \tag{3.49}$$

and

$$\underline{\mathbf{V}} = \begin{pmatrix} 0.57 & -0.55 & 0.43 & -0.44 \\ -0.54 & 0.22 & 0.19 & -0.79 \\ -0.56 & -0.80 & -0.15 & 0.12 \\ -0.26 & 0.08 & 0.87 & 0.41 \end{pmatrix}. \tag{3.50}$$

Concerning the demodulator matrix $\underline{\mathbf{D}}$ we consider two cases, firstly

$$
\begin{aligned}
\underline{\mathbf{D}} &= \begin{pmatrix} -0.29 & -0.82 & 0.15 & -0.44 & -0.16 \\ -0.29 & -0.82 & 0.15 & -0.44 & -0.16 \\ -0.29 & -0.82 & 0.15 & -0.44 & -0.16 \\ -0.29 & -0.82 & 0.15 & -0.44 & -0.16 \end{pmatrix} \\
&= \underbrace{\begin{pmatrix} 1 & 0 & 0 & 0 & 0 \\ 1 & 0 & 0 & 0 & 0 \\ 1 & 0 & 0 & 0 & 0 \\ 1 & 0 & 0 & 0 & 0 \end{pmatrix}}_{\underline{\mathbf{G}}} \cdot \underbrace{\begin{pmatrix} -0.29 & -0.82 & 0.15 & -0.44 & -0.16 \\ 0.30 & 0.31 & 0.18 & -0.83 & 0.32 \\ 0.13 & 0.26 & 0.15 & -0.18 & -0.93 \\ -0.90 & 0.40 & -0.09 & -0.19 & 0.01 \\ 0.12 & -0.07 & -0.96 & -0.23 & -0.11 \end{pmatrix}}_{\underline{\mathbf{U}}^{\mathrm{H}}},
\end{aligned}
\tag{3.51}
$$

and secondly

$$
\begin{aligned}
\underline{\mathbf{D}} &= \begin{pmatrix} -0.49 & -0.27 & -0.69 & 0.12 & 0.43 \\ -0.02 & 0.86 & 0.52 & -0.04 & 0.04 \\ -0.53 & 0.11 & 0.09 & -0.77 & 0.33 \\ -0.59 & -0.55 & 0.06 & 0.16 & -0.56 \end{pmatrix} \\
&= \underbrace{\begin{pmatrix} 0.14 & -0.31 & -0.66 & 0.38 & 0.55 \\ -0.61 & 0.39 & 0.26 & 0.32 & -0.55 \\ 0.36 & 0.63 & -0.20 & 0.65 & -0.01 \\ 0.66 & -0.64 & 0.28 & 0.27 & -0.06 \end{pmatrix}}_{\underline{\mathbf{G}}} \cdot \underbrace{\begin{pmatrix} -0.29 & -0.82 & 0.15 & -0.44 & -0.16 \\ 0.30 & 0.31 & 0.18 & -0.83 & 0.32 \\ 0.13 & 0.26 & 0.15 & -0.18 & -0.93 \\ -0.90 & 0.40 & -0.09 & -0.19 & 0.01 \\ 0.12 & -0.07 & -0.96 & -0.23 & -0.11 \end{pmatrix}}_{\underline{\mathbf{U}}^{\mathrm{H}}}.
\end{aligned}
$$
$$\tag{3.52}$$

In the first case all rows of $\underline{\mathbf{D}}$ are equal to $\underline{\mathbf{u}}_1^{\mathrm{H}}$. In the second case each row of $\underline{\mathbf{D}}$ is a linear combination of $\underline{\mathbf{u}}_1^{\mathrm{H}} \ldots \underline{\mathbf{u}}_Z^{\mathrm{H}}$.

3.3.4   Performance criteria energy efficiency and Tx efficiency

A suitable performance criterion for linear Rx oriented transmission systems concerns the degree to which the energy T_n radiated for a symbol $\underline{d}_n$, see (3.33), is transformed into useful energy R_n at the output of the Rx. In this subsection a quantitative measure for this energy transfer will be defined based on [Trö03] and on considerations made by the author and his colleagues in [BQT+03].

Let us first answer the question which signal $\underline{t}$ of (3.6) with a given energy T of (3.9) should be radiated into a channel with the channel matrix $\underline{H}$ in order to produce at the channel output a signal $\underline{e}$ of (3.10) with maximum energy. We term this radiated signal $\underline{t}_{opt}$, and it is given by

$$\underline{t}_{opt} = \max_{\substack{\underline{t} \in \mathbb{C}^{Q \times 1} \\ \frac{1}{2}\underline{t}^H\underline{t} = T = \text{const}}} \left\{ \underline{e}^H\underline{e} = \underline{t}^H\underline{H}^H\underline{H}\,\underline{t} \right\}. \tag{3.53}$$

The undisturbed receive signal resulting in $\underline{t}_{opt}$ of (3.53) is

$$\underline{e}_{opt} = \underline{H}\,\underline{t}_{opt}, \tag{3.54}$$

which has maximum energy

$$R_{opt} = \frac{1}{2}\underline{e}_{opt}^H\underline{e}_{opt}. \tag{3.55}$$

According to [BQT$^+$03, QTMJ03], with the principal right side singular vector $\underline{v}_1$ of $\underline{H}$ we should choose

$$\underline{t}_{opt} = \sqrt{2\,T}\,\underline{v}_1 \tag{3.56}$$

in order to obtain R_{opt} of (3.55). Then, the corresponding undisturbed receive signal becomes

$$\underline{e}_{opt} = \underline{H}\,\underline{t}_{opt} = \underline{U}\,\underline{\Sigma}\,\underline{V}^H\,\underline{v}_1 = \sqrt{2\,\lambda_1\,T}\,\underline{u}_1, \tag{3.57}$$

and this signal has the maximum possible receive energy [BQT$^+$03, QTMJ03]

$$R_{opt} = \lambda_1\,T. \tag{3.58}$$

From (3.58) follows that the ratio of the received and transmit energies is equal to

$$r_{opt} = \frac{R_{opt}}{T} = \lambda_1. \tag{3.59}$$

Next we consider the TxMF. We are interested in the relation between the transmit energy T_n of (3.33) of the data symbol $\underline{d}_n$ and the corresponding useful receive energy R_n. In the case of the TxMF we obtain from (3.28) with (3.45) and (3.36)

$$\underline{M} = (\underline{D}\,\underline{H})^H = \left(\underline{G}\,\underline{U}^H\underline{U}\,\underline{\Sigma}\,\underline{V}^H\right)^H = \underline{V}\,\underline{\Sigma}^T\underline{G}^H \tag{3.60}$$

and

$$\underline{M}^H\underline{M} = \left(\underline{V}\,\underline{\Sigma}^T\underline{G}^H\right)^H\,\underline{V}\,\underline{\Sigma}^T\underline{G}^H = \underline{G}\,\underline{\Sigma}\,\underline{\Sigma}^T\underline{G}^H. \tag{3.61}$$

From (3.61) follows [Trö03]

$$\left[\underline{M}^H\underline{M}\right]_{n,n} = \left[\underline{G}\,\underline{\Sigma}\,\underline{\Sigma}^T\underline{G}^H\right]_{n,n} = \sum_{q=1}^{G} \lambda_q\,\left|\underline{g}_{n,q}\right|^2. \tag{3.62}$$

$$\underline{\mathbf{M}}^{\mathrm{H}}\underline{\mathbf{M}} = \underline{\mathbf{G}} \cdot \boldsymbol{\Sigma} \cdot \boldsymbol{\Sigma}^{\mathrm{T}} \cdot \underline{\mathbf{G}}^{\mathrm{H}}$$

$$\underline{\mathbf{G}} = \begin{bmatrix} \underline{g}_{1,1} & \underline{g}_{1,2} & \underline{g}_{1,3} & \underline{g}_{1,4} & \underline{g}_{1,5} \\ \underline{g}_{2,1} & \underline{g}_{2,2} & \underline{g}_{2,3} & \underline{g}_{2,4} & \underline{g}_{2,5} \end{bmatrix}$$

$$\boldsymbol{\Sigma} = \begin{bmatrix} \sqrt{\lambda_1} & 0 & 0 \\ 0 & \sqrt{\lambda_2} & 0 \\ 0 & 0 & \sqrt{\lambda_3} \\ 0 & 0 & 0 \\ 0 & 0 & 0 \end{bmatrix}$$

$$\boldsymbol{\Sigma}^{\mathrm{T}} = \begin{bmatrix} \sqrt{\lambda_1} & 0 & 0 & 0 & 0 \\ 0 & \sqrt{\lambda_2} & 0 & 0 & 0 \\ 0 & 0 & \sqrt{\lambda_3} & 0 & 0 \end{bmatrix}$$

$$\underline{\mathbf{G}}^{\mathrm{H}} = \begin{bmatrix} \underline{g}^*_{1,1} & \underline{g}^*_{2,1} \\ \underline{g}^*_{1,2} & \underline{g}^*_{2,2} \\ \underline{g}^*_{1,3} & \underline{g}^*_{2,3} \\ \underline{g}^*_{1,4} & \underline{g}^*_{2,4} \\ \underline{g}^*_{1,5} & \underline{g}^*_{2,5} \end{bmatrix}$$

$$= \underline{\mathbf{G}} \cdot \boldsymbol{\Sigma}\,\boldsymbol{\Sigma}^{\mathrm{T}} \cdot \underline{\mathbf{G}}^{\mathrm{H}}$$

$$= \begin{bmatrix} \underline{g}_{1,1} & \underline{g}_{1,2} & \underline{g}_{1,3} & \underline{g}_{1,4} & \underline{g}_{1,5} \\ \underline{g}_{2,1} & \underline{g}_{2,2} & \underline{g}_{2,3} & \underline{g}_{2,4} & \underline{g}_{2,5} \end{bmatrix} \cdot \begin{bmatrix} \lambda_1 & 0 & 0 & 0 & 0 \\ 0 & \lambda_2 & 0 & 0 & 0 \\ 0 & 0 & \lambda_3 & 0 & 0 \\ 0 & 0 & 0 & 0 & 0 \\ 0 & 0 & 0 & 0 & 0 \end{bmatrix} \cdot \begin{bmatrix} \underline{g}^*_{1,1} & \underline{g}^*_{2,1} \\ \underline{g}^*_{1,2} & \underline{g}^*_{2,2} \\ \underline{g}^*_{1,3} & \underline{g}^*_{2,3} \\ \underline{g}^*_{1,4} & \underline{g}^*_{2,4} \\ \underline{g}^*_{1,5} & \underline{g}^*_{2,5} \end{bmatrix}$$

$$= \underline{\mathbf{G}} \cdot \boldsymbol{\Sigma}\,\boldsymbol{\Sigma}^{\mathrm{T}}\underline{\mathbf{G}}^{\mathrm{H}}$$

$$= \begin{bmatrix} \underline{g}_{1,1} & \underline{g}_{1,2} & \underline{g}_{1,3} & \underline{g}_{1,4} & \underline{g}_{1,5} \\ \underline{g}_{2,1} & \underline{g}_{2,2} & \underline{g}_{2,3} & \underline{g}_{2,4} & \underline{g}_{2,5} \end{bmatrix} \cdot \begin{bmatrix} \lambda_1 \underline{g}^*_{1,1} & \lambda_1 \underline{g}^*_{2,1} \\ \lambda_2 \underline{g}^*_{1,2} & \lambda_2 \underline{g}^*_{2,2} \\ \lambda_3 \underline{g}^*_{1,3} & \lambda_3 \underline{g}^*_{2,3} \\ 0 & 0 \\ 0 & 0 \end{bmatrix} = \begin{pmatrix} \sum_{q=1}^{3} \lambda_q \left| \underline{g}_{1,q} \right|^2 & \sum_{q=1}^{3} \lambda_q \underline{g}_{1,q} \underline{g}^*_{2,q} \\ \sum_{q=1}^{3} \lambda_q \underline{g}_{2,q} \underline{g}^*_{1,q} & \sum_{q=1}^{3} \lambda_q \left| \underline{g}_{2,q} \right|^2 \end{pmatrix}$$

Fig. 3.8. Visualization of $\left[\underline{\mathbf{M}}^{\mathrm{H}}\underline{\mathbf{M}} \right]_{n,n} = \sum_{q=1}^{Q} \lambda_q^2 \left| \underline{g}_{n,q} \right|^2$ of (3.62) for $Z = 5$, $Q = 3$ and $N_{\mathrm{t}} = 2$

In Fig. 3.8 (3.62) is visualized for an example with Z equal to 5, Q equal to 3 and N_{t} equal to 2, which implies G equal to 3, see (3.39). With (3.62) we obtain from (3.33) for the transmit energy of the data symbol $\underline{d}_n$

$$T_{\mathrm{MF},\,n} = \frac{1}{2}|\underline{d}_n|^2 \sum_{q=1}^{G} \lambda_q \left| \underline{g}_{n,\,q} \right|^2 . \tag{3.63}$$

Let us now determine the receive energy $R_{\mathrm{MF},\,n}$ of the data symbol $\underline{d}_n$. To this purpose we resort to the expression

$$
\begin{aligned}
\underline{\mathbf{D}}\,\underline{\mathbf{H}}\,\underline{\mathbf{M}} &= \underline{\mathbf{D}}\,\underline{\mathbf{H}}\,(\underline{\mathbf{D}}\,\underline{\mathbf{H}})^{\mathrm{H}} = \underline{\mathbf{D}}\,\underline{\mathbf{H}}\,\underline{\mathbf{H}}^{\mathrm{H}}\underline{\mathbf{D}}^{\mathrm{H}} \\
&= \underbrace{\underline{\mathbf{G}}\,\underline{\mathbf{U}}^{\mathrm{H}}}_{\underline{\mathbf{D}}}\,\underbrace{\underline{\mathbf{U}}\,\boldsymbol{\Sigma}\,\underline{\mathbf{V}}^{\mathrm{H}}}_{\underline{\mathbf{H}}}\,\underbrace{\underline{\mathbf{V}}\,\boldsymbol{\Sigma}^{\mathrm{T}}\,\underline{\mathbf{U}}^{\mathrm{H}}}_{\underline{\mathbf{H}}^{\mathrm{H}}}\,\underbrace{\underline{\mathbf{U}}\,\underline{\mathbf{G}}^{\mathrm{H}}}_{\underline{\mathbf{D}}^{\mathrm{H}}} = \underline{\mathbf{G}}\,\boldsymbol{\Sigma}\,\boldsymbol{\Sigma}^{\mathrm{T}}\underline{\mathbf{G}}^{\mathrm{H}},
\end{aligned}
\tag{3.64}
$$

in which we substitute $\underline{\mathbf{D}}$ according to (3.45) and $\underline{\mathbf{H}}$ according to (3.36). With (3.64) the receive energy of the data symbol $\underline{d}_n$ can be expressed as

$$R_{\mathrm{MF},\,n} = \frac{1}{2}|\underline{d}_n|^2 \left[\underline{\mathbf{D}}\,\underline{\mathbf{H}}\,\underline{\mathbf{M}}\right]_{n,n}^2 = \frac{1}{2}|\underline{d}_n|^2 \left[\underline{\mathbf{G}}\,\boldsymbol{\Sigma}\,\boldsymbol{\Sigma}^{\mathrm{T}}\underline{\mathbf{G}}^{\mathrm{H}}\right]_{n,n}^2 . \tag{3.65}$$

With (3.61) and (3.62) follows from (3.65)

$$R_{\mathrm{MF},\,n} = \frac{1}{2}|\underline{d}_n|^2 \left(\sum_{q=1}^{G} \lambda_q \left| \underline{g}_{n,\,q} \right|^2 \right)^2 . \tag{3.66}$$

With (3.66) and (3.63) we obtain the ratio

$$r_{\mathrm{MF},\,n} = \frac{R_{\mathrm{MF},n}}{T_{\mathrm{MF},n}} = \left[\underline{\mathbf{G}}\,\boldsymbol{\Sigma}\,\boldsymbol{\Sigma}^{\mathrm{T}}\underline{\mathbf{G}}^{\mathrm{H}}\right]_{n,n} = \sum_{q=1}^{G} \lambda_q \left| \underline{g}_{n,\,q} \right|^2 \tag{3.67}$$

of the transmitted and received energies of the data symbol $\underline{d}_n$. (3.67) tells us that this ratio, which should be as large as possible, depends

- on the one hand on the radio channel, which is described by its G singular values $\sqrt{\lambda_q}$, and
- on the other hand on the choice of the demodulator matrix $\underline{\mathbf{D}}$ with respect to $\underline{\mathbf{H}}$, that is with respect to the Z left side singular vectors $\underline{\mathbf{u}}_z$, $z = 1 \ldots Z$, of the channel matrix $\underline{\mathbf{H}}$.

Said choice of $\underline{\mathbf{D}}$ with respect to $\underline{\mathbf{H}}$ is described by the matrix $\underline{\mathbf{G}}$ of (3.44). For given singular values $\sqrt{\lambda_q}$ the ratio $r_{\mathrm{MF},\,n}$ of (3.67) would attain the maximum value λ_1, if we would choose as in the example of Fig. 3.8

$$\left| \underline{g}_{n,\,q} \right| = \begin{cases} 1 & \text{for } q = 1, \\ 0 & \text{else.} \end{cases} \tag{3.68}$$

However, in this case the receiver could not discern the different data symbols $\underline{d}_n$, $n = 1 \ldots N_t$, so that such a choice of $\underline{\mathbf{D}}$ would be futile. The ratio $r_{\text{MF},n}$ would become minimum, if in the case $Z > Q$ we would choose

$$\left| \underline{g}_{n,q} \right| = 0 \text{ for } q \leq Q \tag{3.69}$$

and in the case $Z \leq Q$

$$\left| \underline{g}_{n,q} \right| = \begin{cases} 1 & \text{for } q = Z, \\ 0 & \text{else.} \end{cases} \tag{3.70}$$

In the case $Z > Q$, the choice of $\underline{\mathbf{D}}$ according to (3.69) would result in zero receive energy $R_{\text{MF},n}$ of (3.66).

In the case of Rx orientation, no channel knowledge is available at the Rx. Therefore, the Rx does not have the chance to choose $\underline{\mathbf{D}}$ in such a way that, with respect to the ratio $r_{\text{MF},n}$ of (3.67), $\underline{\mathbf{D}}$ best fits to the channel.

In the next step we consider the ratio of the received and transmitted energies observed in the case of the TxZF Filter. In this case due to (3.29)

$$\underline{\mathbf{D}}\,\underline{\mathbf{H}}\,\underline{\mathbf{M}} = \underline{\mathbf{D}}\,\underline{\mathbf{H}}\,\underbrace{(\underline{\mathbf{D}}\,\underline{\mathbf{H}})^{\text{H}} \left[\underline{\mathbf{D}}\,\underline{\mathbf{H}}\,(\underline{\mathbf{D}}\,\underline{\mathbf{H}})^{\text{H}} \right]^{-1}}_{\underline{\mathbf{M}}} = \mathbf{I}^{(N_t)} \tag{3.71}$$

holds. Therefore, the symbol $\underline{d}_n$ is represented by the receive energy

$$R_{\text{ZF},n} = \frac{1}{2} |\underline{d}_n|^2. \tag{3.72}$$

Concerning the transmit energy $T_{\text{ZF},n}$ of (3.33) in the case of TxZF Filter we consider the Gram matrix $\underline{\mathbf{M}}^{\text{H}}\underline{\mathbf{M}}$. With (3.29), (3.45) and (3.36) this matrix can be written as

$$\begin{aligned} \underline{\mathbf{M}}^{\text{H}}\underline{\mathbf{M}} &= \left((\underline{\mathbf{D}}\,\underline{\mathbf{H}})^{\text{H}} \left[\underline{\mathbf{D}}\,\underline{\mathbf{H}}\,(\underline{\mathbf{D}}\,\underline{\mathbf{H}})^{\text{H}} \right]^{-1} \right)^{\text{H}} (\underline{\mathbf{D}}\,\underline{\mathbf{H}})^{\text{H}} \left[\underline{\mathbf{D}}\,\underline{\mathbf{H}}\,(\underline{\mathbf{D}}\,\underline{\mathbf{H}})^{\text{H}} \right]^{-1} \\ &= \left(\underline{\mathbf{D}}\,\underline{\mathbf{H}}\,(\underline{\mathbf{D}}\,\underline{\mathbf{H}})^{\text{H}} \right)^{-1} = \left(\underline{\mathbf{G}}\,\mathbf{\Sigma}\,\mathbf{\Sigma}^{\text{T}}\underline{\mathbf{G}}^{\text{H}} \right)^{-1}. \end{aligned} \tag{3.73}$$

Now, with (3.33) and (3.73), we obtain

$$\begin{aligned} T_{\text{ZF},n} &= \frac{1}{2} |\underline{d}_n|^2 \left[\left(\underline{\mathbf{D}}\,\underline{\mathbf{H}}\,\underline{\mathbf{H}}^{\text{H}}\underline{\mathbf{D}}^{\text{H}} \right)^{-1} \right]_{n,n} = \frac{1}{2} |\underline{d}_n|^2 \left[\left(\underline{\mathbf{B}}\,\underline{\mathbf{B}}^{\text{H}} \right)^{-1} \right]_{n,n} \\ &= \frac{1}{2} |\underline{d}_n|^2 \left[\left(\underline{\mathbf{G}}\,\mathbf{\Sigma}\,\mathbf{\Sigma}^{\text{T}}\underline{\mathbf{G}}^{\text{H}} \right)^{-1} \right]_{n,n}, \end{aligned} \tag{3.74}$$

and with $R_{\text{ZF},n}$ of (3.72) and $T_{\text{ZF},n}$ of (3.74) we can form the energy ratio

$$\begin{aligned} r_{\text{ZF},n} &= \frac{R_{\text{ZF},n}}{T_{\text{ZF},n}} = \frac{1}{\left[\left(\underline{\mathbf{D}}\,\underline{\mathbf{H}}\,\underline{\mathbf{H}}^{\text{H}}\underline{\mathbf{D}}^{\text{H}} \right)^{-1} \right]_{n,n}} = \frac{1}{\left[\left(\underline{\mathbf{B}}\,\underline{\mathbf{B}}^{\text{H}} \right)^{-1} \right]_{n,n}} \\ &= \frac{1}{\left[\left(\underline{\mathbf{G}}\,\mathbf{\Sigma}\,\mathbf{\Sigma}^{\text{T}}\underline{\mathbf{G}}^{\text{H}} \right)^{-1} \right]_{n,n}} = \left(\left[\left(\underline{\mathbf{G}}\,\mathbf{\Sigma}\,\mathbf{\Sigma}^{\text{T}}\underline{\mathbf{G}}^{\text{H}} \right)^{-1} \right]_{n,n} \right)^{-1}. \end{aligned} \tag{3.75}$$

The reciprocal value

$$t_{\mathrm{ZF},\,n} = \frac{1}{r_{\mathrm{ZF},\,n}} = \left[\left(\underline{\mathbf{B}}\,\underline{\mathbf{B}}^{\mathrm{H}}\right)^{-1}\right]_{n,n} \tag{3.76}$$

of $r_{\mathrm{ZF},\,n}$ of (3.75) is the normalized Tx energy required for the radiation of the data symbol $\underline{d}_n$. According to the considerations made above, $r_{\mathrm{ZF},\,n}$ of (3.75) similarly to $r_{\mathrm{MF},\,n}$ of (3.67) depends on the matrix $\underline{\mathbf{G}}$ of (3.44) and on the singular values $\sqrt{\lambda_q}$, $q = 1 \ldots G$, of $\underline{\mathbf{H}}$. However, whereas this dependence could be expressed in closed form in the case of the TxMF, see (3.67), such a closed form expression is not possible for $r_{\mathrm{ZF},\,n}$ of (3.75), because a matrix inversion is involved. As soon as $\underline{\mathbf{G}}\,\boldsymbol{\Sigma}\,\boldsymbol{\Sigma}^{\mathrm{T}}\underline{\mathbf{G}}^{\mathrm{H}}$ is not a diagonal matrix, its inverse cannot be expressed by the singular values $\sqrt{\lambda_q}$ and the elements $\underline{g}_{n,z}$ of the matrix $\underline{\mathbf{G}}$ analytically. What, however, can be said based on considerations made in [Pap00] in the following: For the expression $\left[\underline{\mathbf{G}}\,\boldsymbol{\Sigma}\,\boldsymbol{\Sigma}^{\mathrm{T}}\underline{\mathbf{G}}^{\mathrm{H}}\right]_{n,n}$ occurring in (3.65) and the expression $\left(\left[\left(\underline{\mathbf{G}}\,\boldsymbol{\Sigma}\,\boldsymbol{\Sigma}^{\mathrm{T}}\underline{\mathbf{G}}^{\mathrm{H}}\right)^{-1}\right]_{n,n}\right)^{-1}$ holds

$$\left[\underline{\mathbf{G}}\,\boldsymbol{\Sigma}\,\boldsymbol{\Sigma}^{\mathrm{T}}\underline{\mathbf{G}}^{\mathrm{H}}\right]_{n,n} \geq \left(\left[\left(\underline{\mathbf{G}}\,\boldsymbol{\Sigma}\,\boldsymbol{\Sigma}^{\mathrm{T}}\underline{\mathbf{G}}^{\mathrm{H}}\right)^{-1}\right]_{n,n}\right)^{-1}. \tag{3.77}$$

Therefore,

$$r_{\mathrm{MF},\,n} \geq r_{\mathrm{ZF},\,n} \tag{3.78}$$

is true, that is the energy ratio $r_{\mathrm{ZF},\,n}$ of the TxZF Filter is generally lower than the energy ratio $r_{\mathrm{MF},\,n}$ of the TxMF, and this is the price to be paid for the elimination of ISI by the TxZF Filter.

Now we come to the performance measure of the TxZF Filter. As such a measure, the author proposes in accordance with [BQT$^+$03] the ratio

$$\eta_n = \frac{r_{\mathrm{ZF},\,n}}{r_{\mathrm{opt}}} = \frac{1}{\lambda_1 \left[\left(\underline{\mathbf{D}}\,\underline{\mathbf{H}}\,\underline{\mathbf{H}}^{\mathrm{H}}\underline{\mathbf{D}}^{\mathrm{H}}\right)^{-1}\right]_{n,n}} = \frac{1}{\lambda_1 \left[\left(\underline{\mathbf{G}}\,\boldsymbol{\Sigma}\,\boldsymbol{\Sigma}^{\mathrm{T}}\underline{\mathbf{G}}^{\mathrm{H}}\right)^{-1}\right]_{n,n}} \leq 1 \tag{3.79}$$

of $r_{\mathrm{ZF},\,n}$ of (3.75) and r_{opt} of (3.59) and terms this ratio energy efficiency of the transmission of symbol $\underline{d}_n$. With $r_{\mathrm{MF},\,n}$ of (3.67), η_n of (3.79) can be rewritten as

$$\eta_n = \underbrace{\frac{r_{\mathrm{MF},\,n}}{r_{\mathrm{opt}}}}_{\substack{\eta_{\mathrm{Rx},\,n} \leq 1 \text{ due to mis-}\\ \text{match between } \underline{\mathbf{D}} \text{ and} \\ \underline{\mathbf{H}}}} \cdot \underbrace{\frac{r_{\mathrm{ZF},\,n}}{r_{\mathrm{MF},\,n}}}_{\substack{\eta_{\mathrm{Tx},\,n} \leq 1 \text{ due to} \\ \text{ISI elimination}}} . \tag{3.80}$$

On the right hand side of (3.80) the first fraction considers the mismatch between $\underline{\mathbf{D}}$ and $\underline{\mathbf{H}}$, and the second fraction represents the price to be paid for ISI elimination.

Table 3.1. Energy ratios and energy efficiencies for $\underline{\mathbf{G}}$ of (3.51)

n	$r_{\mathrm{MF},n}$	$r_{\mathrm{ZF},n}$	η_n	$\eta_{\mathrm{Tx},n}$
1	1.3	0	0	0
2	1.3	0	0	0
3	1.3	0	0	0
4	1.3	0	0	0

Table 3.2. Energy ratios and energy efficiencies for $\underline{\mathbf{G}}$ of (3.52)

n	$r_{\mathrm{MF},n}$	$r_{\mathrm{ZF},n}$	η_n	$\eta_{\mathrm{Tx},n}$
1	0.41	0.13	0.10	0.32
2	0.68	0.07	0.05	0.10
3	0.64	0.38	0.29	0.59
4	0.96	0.13	0.10	0.14

The second fraction

$$
\begin{aligned}
\eta_{\mathrm{Tx},n} &= \frac{r_{\mathrm{ZF},n}}{r_{\mathrm{MF},n}} = \frac{1}{\left[\left(\underline{\mathbf{D}}\,\underline{\mathbf{H}}\,\underline{\mathbf{H}}^{\mathrm{H}}\underline{\mathbf{D}}^{\mathrm{H}}\right)^{-1}\right]_{n,n}\left[\underline{\mathbf{D}}\,\underline{\mathbf{H}}\,\underline{\mathbf{H}}^{\mathrm{H}}\underline{\mathbf{D}}^{\mathrm{H}}\right]_{n,n}} \\
&= \frac{1}{\left[\left(\underline{\mathbf{B}}\,\underline{\mathbf{B}}^{\mathrm{H}}\right)^{-1}\right]_{n,n}\left[\underline{\mathbf{B}}\,\underline{\mathbf{B}}^{\mathrm{H}}\right]_{n,n}} \\
&= \frac{1}{\left[\left(\underline{\mathbf{G}}\,\boldsymbol{\Sigma}\,\boldsymbol{\Sigma}^{\mathrm{T}}\underline{\mathbf{G}}^{\mathrm{H}}\right)^{-1}\right]_{n,n}\left[\underline{\mathbf{G}}\,\boldsymbol{\Sigma}\,\boldsymbol{\Sigma}^{\mathrm{T}}\underline{\mathbf{G}}^{\mathrm{H}}\right]_{n,n}}
\end{aligned} \tag{3.81}
$$

is termed transmission (Tx) efficiency. This quantity characterizes energy-wise the performance of the TxZF Filter relative to the TxMF under the condition that both filters use the same demodulator matrix.

In order to illustrate the above considerations by numerical examples, we return to the channel matrix $\underline{\mathbf{H}}$ of (3.47) and to the matrices $\underline{\mathbf{G}}$ of (3.51) and (3.52), respectively. With $\boldsymbol{\Sigma}$ of (3.49) we obtain

$$r_{\mathrm{opt}} = \lambda_1 = 1.3. \tag{3.82}$$

For the energy ratios $r_{\mathrm{MF},n}$ and $r_{\mathrm{ZF},n}$ of (3.80), for the energy efficiencies η_n of (3.80) and for the Tx efficiencies $\eta_{\mathrm{Tx},n}$ of (3.81) we obtain the values listed in Tables 3.1 and 3.2. The numerical results presented in these tables confirm the verbal statements made in the course of Subsection 3.3.4. Furthermore, from the values $r_{\mathrm{MF},n}$ and $r_{\mathrm{ZF},n}$ in Table 3.2 it becomes apparent that a large value $r_{\mathrm{MF},n}$ may correspond to a small value $r_{\mathrm{ZF},n}$, see the case n equal to 2 in Table 3.2. Obviously, in such cases the price for ISI elimination is particularly high.

3.3.5   Statistical consideration of the Tx efficiency

In real world situations with time variant channels the channel matrix $\underline{\mathbf{H}}$ in (3.10) can be assumed to be randomly changing. When we a priori determine the demodulator matrix $\underline{\mathbf{D}}$ in (3.17), this choice of $\underline{\mathbf{D}}$ can be regarded as a random choice, because the channel properties are not taken into account. In this subsection we are interested in some general statements on the Tx efficiencies $\eta_{\mathrm{Tx},n}$ in the case of randomly varying matrices $\underline{\mathbf{H}}$ and randomly chosen demodulator matrices $\underline{\mathbf{D}}$. To be more precise, we are interested in the mean and variance of the Tx efficiencies $\eta_{\mathrm{Tx},n}$. The following considerations resort to an analysis elaborated in [MWQ04] based on random matrix theory [Meh91] and briefly recapitulate the results presented in this reference. It should be mentioned that the results in [MWQ04] are only valid for an approximate assumption made in below. In Chapter 4 these results will be argued and verified by simulation results.

Concerning the randomly varying channel matrix $\underline{\mathbf{H}}$ we assume that the components $\underline{H}_{z,q}$, $z = 1 \ldots Z$, $q = 1 \ldots Q$, of $\underline{\mathbf{H}}$ are independent complex Gaussian variables with zero expectation. Concerning the randomly chosen demodulator matrix, we assume that all elements $\underline{D}_{n,z}$, $n = 1 \ldots N_{\mathrm{t}}$, $z = 1 \ldots Z$, of $\underline{\mathbf{D}}$ are independent binary variables. Under these assumptions the elements of the matrix $\underline{\mathbf{B}}$ in (3.81) are uncorrelated. In addition, as explained in [MWQ04], these elements can be considered approximately as independent identically distributed Gaussian variables with zero mean and variance σ_{b}^2. Under the latter assumption and with the function

$$\mathrm{B}(y,x) = \int_0^1 t^{y-1}(1-t)^{x-1}\mathrm{d}t = \frac{\Gamma(y) \cdot \Gamma(x)}{\Gamma(y+x)} \tag{3.83}$$

the probability density function (pdf) of $\eta_{\mathrm{Tx},n}$ of (3.81) becomes [MWQ04]

$$\mathrm{p}_{\eta_{\mathrm{Tx},n}}(\eta) \approx \begin{cases} \dfrac{\eta^{Q-N_{\mathrm{t}}}(1-\eta)^{N_{\mathrm{t}}-2}}{\mathrm{B}(Q-N_{\mathrm{t}}+1, N_{\mathrm{t}}-1)}, & 0 \leq \eta \leq 1, \\ \\ 0, & \text{else.} \end{cases} \tag{3.84}$$

From (3.83) we can obtain the mth moment of $\eta_{\mathrm{Tx},n}$, which reads

$$\mathrm{E}\{(\eta_{\mathrm{Tx},n})^m\} \approx \frac{\Gamma(Q-N_{\mathrm{t}}+m+1)}{\Gamma(Q-N_{\mathrm{t}}+1)} \cdot \frac{\Gamma(Q)}{\Gamma(Q+m)}. \tag{3.85}$$

Using (3.85), the mean

$$\overline{\eta}_{\mathrm{Tx}} = \mathrm{E}\{\eta_{\mathrm{Tx},n}\} \approx \frac{Q-(N_{\mathrm{t}}-1)}{Q} \tag{3.86}$$

and the variance

$$\mathrm{var}\{\eta_{\mathrm{Tx},n}\} = \mathrm{E}\{(\eta_{\mathrm{Tx},n})^2\} - (\overline{\eta}_{\mathrm{Tx}})^2 \approx \frac{[Q-(N_{\mathrm{t}}-1)](N_{\mathrm{t}}-1)}{Q^2(Q+1)} \tag{3.87}$$

of $\eta_{\mathrm{Tx},n}$ of (3.81) follow.

Obviously, $\overline{\eta}_{\mathrm{Tx}}$ of (3.86) depends on the difference of two quantities, namely

- the number Q of degrees of freedom for the transmit signal design, i.e., the number of elements of the total transmit signal $\underline{\mathbf{t}}$ of (3.8), and

- the number $(N_{\mathrm{t}} - 1)$ of restrictions due to interference avoidance, when designing the contribution of each data symbol $\underline{d}_n$, $n = 1 \ldots N_{\mathrm{t}}$, to $\underline{\mathbf{t}}$.

If the number Q of degrees of freedom is large compared to $(N_{\mathrm{t}} - 1)$, then $\overline{\eta}_{\mathrm{Tx}}$ tends to be close to one; otherwise it is between zero and one. For a fixed system load

$$l = \frac{N_{\mathrm{t}}}{Q} \tag{3.88}$$

(3.86) and (3.87) can be rewritten as

$$\overline{\eta}_{\mathrm{Tx}} \approx 1 - \left(l - 1/Q \right) \tag{3.89}$$

and

$$\mathrm{var}\left\{ \eta_{\mathrm{Tx},n} \right\} \approx \frac{\left(1 - l + \frac{1}{Q} \right) \left(l - \frac{1}{Q} \right)}{1 + Q}, \tag{3.90}$$

respectively. (3.89) and (3.90) disclose, if the system load l is kept constant and Q is quite large, $\eta_{\mathrm{Tx},n}$ tends to the asymptotic transmit efficiency $\eta_{\mathrm{Tx}}^{\infty}$ with its mean

$$\overline{\eta}_{\mathrm{Tx}}^{\infty} = \lim_{Q \to \infty} \overline{\eta}_{\mathrm{Tx}} = 1 - l \tag{3.91}$$

and its variance

$$\mathrm{var}\left\{ \eta_{\mathrm{Tx}}^{\infty} \right\} = \lim_{Q \to \infty} \mathrm{var}\left(\eta_{\mathrm{Tx},n} \right) = 0, \tag{3.92}$$

respectively. Therefore, for large systems with given system load l the mean of the asymptotic transmit efficiency $\overline{\eta}_{\mathrm{Tx}}^{\infty}$ is only a function of the system load l, while the variance $\mathrm{var}\left(\eta_{\mathrm{Tx}}^{\infty} \right)$ of $\eta_{\mathrm{Tx},n}$ asymptotically goes to zero, resulting in the pdf

$$\mathrm{p}_{\eta_{\mathrm{Tx}}^{\infty}}\left(\eta \right) = \delta\left(\eta - (1 - l) \right) \tag{3.93}$$

of the asymptotic transmit efficiency $\eta_{\mathrm{Tx}}^{\infty}$.

3.3.6   Statistical consideration of the Tx energy

Let us again assume that the matrices $\underline{\mathbf{H}}$ and $\underline{\mathbf{D}}$ vary stochastically according to the assumptions made in Subsection 3.3.5. Such variations entail fluctuations of the Tx energy $T_{\mathrm{ZF},n}$ of (3.74) to be radiated for the transmission of the data symbol $\underline{d}_n$. Following an argumentation similar to that behind (3.86) and (3.87) [MWQ04], one can obtain with the variance σ_{b}^2 of the elements of $\underline{\mathbf{B}}$

$$\overline{T}_{\mathrm{ZF}} = \mathrm{E}\left\{ T_{\mathrm{ZF},n} \right\} \approx \frac{E_{\mathrm{d}}}{2\sigma_{\mathrm{b}}^2} \cdot \frac{1}{Q - N_{\mathrm{t}}} \tag{3.94}$$

and

$$\mathrm{var}\left\{ T_{\mathrm{ZF},n} \right\} \approx \frac{E_{\mathrm{d}}^2}{4\sigma_{\mathrm{b}}^4} \cdot \frac{1}{\left(Q - N_{\mathrm{t}} \right)^2 \left(Q - N_{\mathrm{t}} + 1 \right)}. \tag{3.95}$$

for the mean and variance of $T_{\mathrm{ZF},n}$, respectively. (3.94) and (3.95) show that

- $\overline{T}_{\mathrm{ZF}}$ and $\mathrm{var}\left\{T_{\mathrm{ZF},n}\right\}$ decrease with increasing σ_{b}^2, that is with decreasing channel attenuation, that

- both these quantities decrease with increasing differences between N_{t} and Q, respectively, and that

- in the case N_{t} equal to Q, that is for full system load, both these quantities tend to infinity.

(3.94) and (3.95) are approximations which are valid under the assumption that the elements of the system matrix $\underline{\mathbf{B}}$ of (3.23) are not only uncorrelated, but also statistically independent. These approximate results will also be argued and verified by simulations in Chapter 4.

Chapter 4

Linear Rx oriented MIMO broadcast systems with TxZF Filter

4.1 Introduction

In this chapter we consider linear Rx oriented MIMO broadcast systems, in which the BS has K_B Tx antennas and each of the K MTs has K_M Rx antennas, see Fig. 2.2. For the generation of the transmit signal $\underline{\mathbf{t}}$ the rationale TxZF Filter introduced in Section 3.3 is selected. Chapter 4 has two goals:

- Adaptation of the TxZF Filter algorithm and the corresponding performance criteria developed in Section 3.3 for general linear Rx oriented transmission systems to MIMO broadcast systems.

- Exemplary quantitative study of the performance of such MIMO broadcast systems under the assumption of totally uncorrelated or fully correlated channels, see Chapter 2.

4.2 Adaptation of the general system model of Section 3.3

As already stated in Section 2.2, see also Fig. 2.2, we consider a downlink situation where a BS supports K MTs numbered with $k = 1 \ldots K$. The BS is equipped with K_B Tx antennas, and each of the K MTs employs K_M Rx antennas. Fig. 4.1 illustrates this situation by a block diagram, which will be explained and mathematically described in what follows based on former publications of the author [BQT$^+$03].

It is assumed that N data symbols have to be transmitted from the BS to each MT k, $k = 1 \ldots K$. The N data symbols intended for MT k are arranged in the MT specific data vector

$$\underline{\mathbf{d}}^{(k)} = \left(\underline{d}_1^{(k)} \ldots \underline{d}_N^{(k)} \right)^\mathrm{T} \in \mathbb{V}^{N \times 1}. \tag{4.1}$$

The K MT specific data vectors $\underline{\mathbf{d}}^{(k)}$ of (4.1) are stacked to the total data vector

$$\underline{\mathbf{d}} = \left(\underline{\mathbf{d}}^{(1)\,\mathrm{T}} \ldots \underline{\mathbf{d}}^{(K)\,\mathrm{T}} \right)^\mathrm{T} = \left(\underline{d}_1 \ldots \underline{d}_n \ldots \underline{d}_{N_\mathrm{t}} \right)^\mathrm{T} \in \mathbb{V}^{N_\mathrm{t} \times 1} \tag{4.2}$$

of dimension

$$N_\mathrm{t} = KN. \tag{4.3}$$
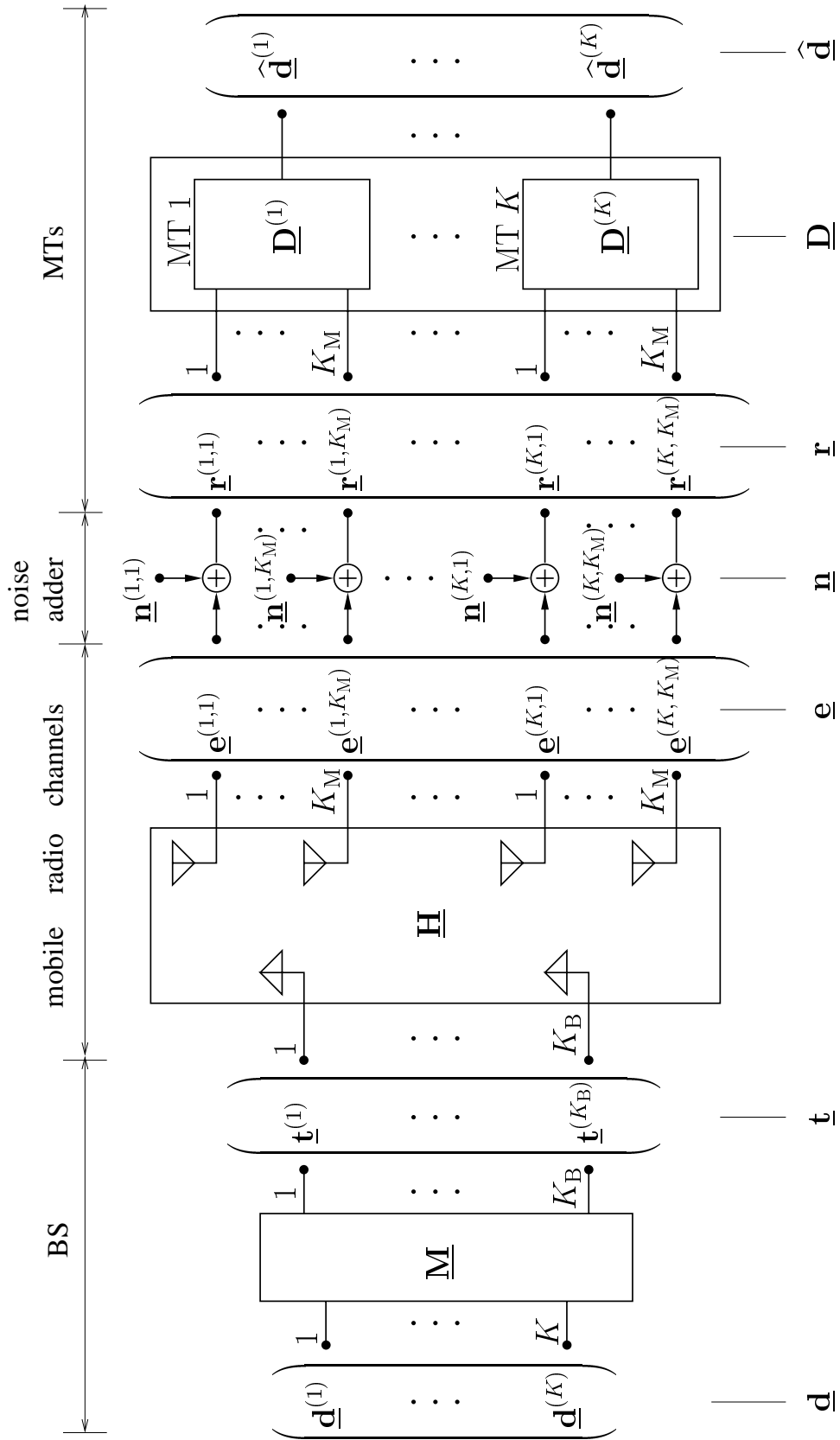
Fig. 4.1. Structure of linear MIMO broadcast systems

$\underline{\mathbf{d}}$ of (4.2) corresponds to $\underline{\mathbf{d}}$ of (3.1) and is assumed to fulfill (3.5). By linear modulation based on $\underline{\mathbf{d}}$ of (4.2) and the K_{B} antenna specific modulator matrices

$$\underline{\mathbf{M}}^{(k_{\mathrm{B}})} \in \mathbb{C}^{Q_{\mathrm{t}} \times (KN)},\ k_{\mathrm{B}} = 1 \ldots K_{\mathrm{B}}, \tag{4.4}$$

K_{B} transmit antenna specific transmit signals

$$\underline{\mathbf{t}}^{(k_{\mathrm{B}})} = \left(\underline{t}_1^{(k_{\mathrm{B}})} \ldots \underline{t}_{Q_{\mathrm{t}}}^{(k_{\mathrm{B}})}\right)^{\mathrm{T}} = \underline{\mathbf{M}}^{(k_{\mathrm{B}})}\, \underline{\mathbf{d}} \in \mathbb{C}^{Q_{\mathrm{t}} \times 1},\ k_{\mathrm{B}} = 1 \ldots K_{\mathrm{B}}, \tag{4.5}$$

are generated for the individual Tx antennas. The K_{B} transmit signals $\underline{\mathbf{t}}^{(k_{\mathrm{B}})}$ of (4.5) can be stacked to form the signal

$$\underline{\mathbf{t}} \;=\; \left(\underline{\mathbf{t}}^{(1)\,\mathrm{T}} \ldots \underline{\mathbf{t}}^{(K_{\mathrm{B}})\,\mathrm{T}}\right)^{\mathrm{T}} = \underbrace{\left(\underline{\mathbf{M}}^{(1)\,\mathrm{T}} \ldots \underline{\mathbf{M}}^{(K_{\mathrm{B}})\,\mathrm{T}}\right)^{\mathrm{T}}}_{\underline{\mathbf{M}} \in \mathbb{C}^{(K_{\mathrm{B}} Q_{\mathrm{t}}) \times 1}} \underline{\mathbf{d}} = \underline{\mathbf{M}}\,\underline{\mathbf{d}} \in \mathbb{C}^{(K_{\mathrm{B}} Q_{\mathrm{t}}) \times 1} \tag{4.6}$$

of dimension

$$Q = K_{\mathrm{B}} Q_{\mathrm{t}}, \tag{4.7}$$

where Q corresponds to the quantity Q introduced in the general system model in Section 3.3. $\underline{\mathbf{t}}$ is termed total transmit signal and corresponds to $\underline{\mathbf{t}}$ of (3.8). $\underline{\mathbf{M}}$ in (4.6) is termed total modulator matrix and corresponds to $\underline{\mathbf{M}}$ of (3.8). Via (4.6) the N_{t} components of $\underline{\mathbf{d}}$ of (4.2) are mapped on the $K_{\mathrm{B}}Q_{\mathrm{t}}$ components of $\underline{\mathbf{t}}$. In what follows we assume

$$Q = K_{\mathrm{B}} Q_{\mathrm{t}} > N_{\mathrm{t}}, \tag{4.8}$$

which can be interpreted as a spreading of the data symbols $\underline{d}_n$ of (4.2). This spreading consists of a spatial spreading over the K_{B} Tx antennas quantified in (4.8) by K_{B} and a spectral spreading quantified in (4.8) by Q_{t}. To be precise, we have a spectral spreading by a factor of Q_{t}, if the transmission period for each data symbol $\underline{d}_n$ is fixed, and if this data symbol is then represented by Q_{t} successive elements of $\underline{\mathbf{t}}^{(k_{\mathrm{B}})}$ of (4.5). If we would temporally extend the transmission period of $\underline{d}_n$ by a factor of Q_{t}, then we would have a temporal spreading.

The channel between the transmit antenna k_{B} of the BS and the receive antenna k_{M} of MT k is characterized by the channel impulse response $\underline{\mathbf{h}}^{(k,\,k_{\mathrm{B}},\,k_{\mathrm{M}})} \in \mathbb{C}^{W \times 1}$. With this channel impulse response and the dimension Q_{t} of $\underline{\mathbf{t}}^{(k_{\mathrm{B}})}$ of (4.5) the MT and antenna specific channel matrix

$$\begin{aligned}
\underline{\mathbf{H}}^{(k,\,k_{\mathrm{B}},\,k_{\mathrm{M}})} &= \left(\underline{H}_{i,\,j}^{(k,\,k_{\mathrm{B}},\,k_{\mathrm{M}})}\right) \in \mathbb{C}^{(Q_{\mathrm{t}} + W - 1) \times Q_{\mathrm{t}}}, \\
&\quad i = 1 \ldots Q_{\mathrm{t}} + W - 1,\ j = 1 \ldots Q_{\mathrm{t}}, \\[2mm]
\underline{H}_{i,\,j}^{(k,\,k_{\mathrm{B}},\,k_{\mathrm{M}})} &= \begin{cases} \underline{h}_{i-j+1}^{(k,\,k_{\mathrm{B}},\,k_{\mathrm{M}})} & 1 \le i - j + 1 \le W, \\[1mm] 0 & \text{else}, \end{cases} \\
&\quad k = 1 \ldots K,\ k_{\mathrm{B}} = 1 \ldots K_{\mathrm{B}}, \\
&\quad k_{\mathrm{M}} = 1 \ldots K_{\mathrm{M}},
\end{aligned} \tag{4.9}$$

is established, which is a Toeplitz matrix [Lue96]. In total $K K_\mathrm{B} K_\mathrm{M}$ such matrices exist. With the K_B matrices $\underline{\mathbf{H}}^{(k, k_\mathrm{B}, k_\mathrm{M})}$ obtained from (4.9) for each $k_\mathrm{B} = 1 \ldots K_\mathrm{B}$ and for given values k, k_M and with (4.6) the undisturbed signal received by Rx antenna k_M of MT k is termed MT and antenna specific receive signal and can be expressed as

$$
\begin{aligned}
\underline{\mathbf{e}}^{(k, k_\mathrm{M})} &= \sum_{k_\mathrm{B}=1}^{K_\mathrm{B}} \underline{\mathbf{H}}^{(k, k_\mathrm{B}, k_\mathrm{M})} \, \underline{\mathbf{t}}^{(k_\mathrm{B})} = \underbrace{\left(\underline{\mathbf{H}}^{(k, 1, k_\mathrm{M})} \cdots \underline{\mathbf{H}}^{(k, K_\mathrm{B}, k_\mathrm{M})} \right)}_{\underline{\mathbf{H}}^{(k, k_\mathrm{M})} \, \in \, \mathbb{C}^{(Q_\mathrm{t}+W-1)\times(K_\mathrm{B} Q_\mathrm{t})}} \underline{\mathbf{t}} \\
&= \underline{\mathbf{H}}^{(k, k_\mathrm{M})} \, \underline{\mathbf{t}} = \underline{\mathbf{H}}^{(k, k_\mathrm{M})} \, \underline{\mathbf{M}} \, \underline{\mathbf{d}} \in \mathbb{C}^{(Q_\mathrm{t}+W-1)\times 1}.
\end{aligned}
\tag{4.10}
$$

Stacking the K_M signals $\underline{\mathbf{e}}^{(k, k_\mathrm{M})}$, $k_\mathrm{M} = 1 \ldots K_\mathrm{M}$, of (4.10) received by MT k yields the space-time receive signal

$$
\begin{aligned}
\underline{\mathbf{e}}^{(k)} &= \left(\underline{\mathbf{e}}^{(k, 1)\,\mathrm{T}} \cdots \underline{\mathbf{e}}^{(k, K_\mathrm{M})\,\mathrm{T}} \right)^\mathrm{T} \\
&= \underbrace{\left(\underline{\mathbf{H}}^{(k, 1)\,\mathrm{T}} \cdots \underline{\mathbf{H}}^{(k, K_\mathrm{M})\,\mathrm{T}} \right)^\mathrm{T}}_{\underline{\mathbf{H}}^{(k)} \, \in \, \mathbb{C}^{[K_\mathrm{M}(Q_\mathrm{t}+W-1)]\times(K_\mathrm{B} Q_\mathrm{t})}} \underline{\mathbf{t}} = \underline{\mathbf{H}}^{(k)} \, \underline{\mathbf{M}} \, \underline{\mathbf{d}} \in \mathbb{C}^{[K_\mathrm{M}(Q_\mathrm{t}+W-1)]\times 1}
\end{aligned}
\tag{4.11}
$$

of MT k. $\underline{\mathbf{e}}^{(k)}$ and $\underline{\mathbf{H}}^{(k)}$ of (4.11) are termed MT specific undisturbed receive signal and MT specific channel matrix, respectively. The K signals $\underline{\mathbf{e}}^{(k)}$, $k = 1 \ldots K$, of (4.11) can be arranged in a vector

$$
\begin{aligned}
\underline{\mathbf{e}} &= \left(\underline{\mathbf{e}}^{(1)\,\mathrm{T}} \cdots \underline{\mathbf{e}}^{(K)\,\mathrm{T}} \right)^\mathrm{T} \\
&= \underbrace{\left(\underline{\mathbf{H}}^{(1)\,\mathrm{T}} \cdots \underline{\mathbf{H}}^{(K)\,\mathrm{T}} \right)^\mathrm{T}}_{\underline{\mathbf{H}} \, \in \, \mathbb{C}^{[K K_\mathrm{M}(Q_\mathrm{t}+W-1)]\times(K_\mathrm{B} Q_\mathrm{t})}} \underline{\mathbf{t}} = \underline{\mathbf{H}} \, \underline{\mathbf{M}} \, \underline{\mathbf{d}} \in \mathbb{C}^{[K K_\mathrm{M}(Q_\mathrm{t}+W-1)]\times 1}.
\end{aligned}
\tag{4.12}
$$

$\underline{\mathbf{e}}$ and $\underline{\mathbf{H}}$ of (4.12) are termed total undisturbed receive signal and total channel matrix, respectively.

In Fig. 4.2 the establishment of the MT specific channel matrix $\underline{\mathbf{H}}^{(k)}$ of (4.11) by the matrices $\underline{\mathbf{H}}^{(k, k_\mathrm{B}, k_\mathrm{M})}$ of (4.9) and the matrices $\underline{\mathbf{H}}^{(k, k_\mathrm{M})}$ of (4.10) is visualized. Correspondingly, Fig. 4.3 shows the establishment of the total channel matrix $\underline{\mathbf{H}}$ of (4.12).

The signal $\underline{\mathbf{e}}^{(k, k_\mathrm{M})}$ of (4.10) is disturbed by the MT and antenna specific noise signal

$$
\underline{\mathbf{n}}^{(k, k_\mathrm{M})} = \left(\underline{n}_1^{(k, k_\mathrm{M})} \cdots \underline{n}_{Q_\mathrm{t}+W-1}^{(k, k_\mathrm{M})} \right)^\mathrm{T} \in \mathbb{C}^{(Q_\mathrm{t}+W-1)\times 1},
\tag{4.13}
$$

which yields the disturbed MT and antenna specific receive signal

$$
\underline{\mathbf{r}}^{(k, k_\mathrm{M})} = \underline{\mathbf{e}}^{(k, k_\mathrm{M})} + \underline{\mathbf{n}}^{(k, k_\mathrm{M})} = \underline{\mathbf{H}}^{(k, k_\mathrm{M})} \, \underline{\mathbf{M}} \, \underline{\mathbf{d}} + \underline{\mathbf{n}}^{(k, k_\mathrm{M})} \in \mathbb{C}^{(Q_\mathrm{t}+W-1)\times 1}.
\tag{4.14}
$$

The signal $\underline{\mathbf{e}}^{(k)}$ of (4.11) is disturbed by the MT specific noise signal

$$
\underline{\mathbf{n}}^{(k)} = \left(\underline{\mathbf{n}}^{(k, 1)\,\mathrm{T}} \cdots \underline{\mathbf{n}}^{(k, K_\mathrm{M})\,\mathrm{T}} \right)^\mathrm{T} \in \mathbb{C}^{[K_\mathrm{M}(Q_\mathrm{t}+W-1)]\times 1},
\tag{4.15}
$$
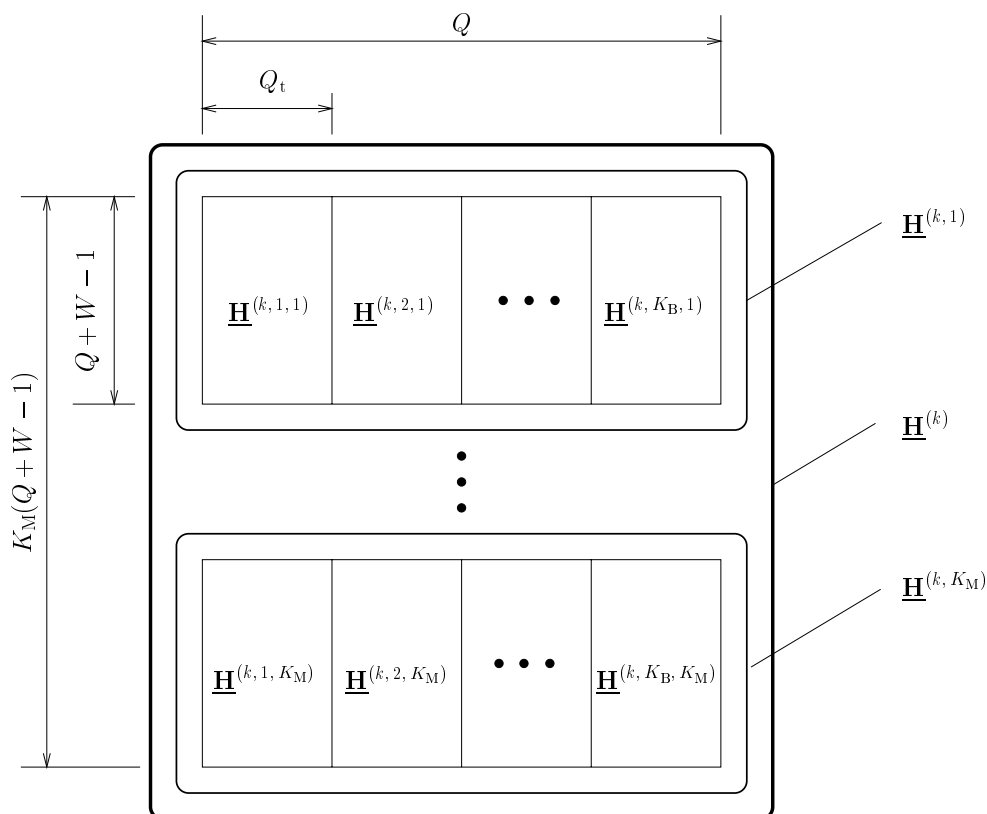
Fig. 4.2. Visualization of the establishment of the MT specific channel matrix $\underline{\mathbf{H}}^{(k)}$
of (4.11)
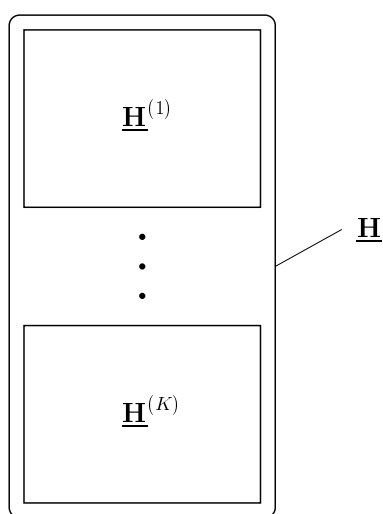
Fig. 4.3. Visualization of the establishment of the total channel matrix $\underline{\mathbf{H}}$ of (4.12)

which yields the disturbed MT specific receive signal

$$\underline{\mathbf{r}}^{(k)} = \underline{\mathbf{e}}^{(k)} + \underline{\mathbf{n}}^{(k)} = \underline{\mathbf{H}}^{(k)}\underline{\mathbf{M}}\,\underline{\mathbf{d}} + \underline{\mathbf{n}}^{(k)}. \tag{4.16}$$

The signal $\underline{\mathbf{e}}$ of (4.12) is disturbed by the total noise signal

$$\underline{\mathbf{n}} = \left(\underline{\mathbf{n}}^{(1)\,\mathrm{T}} \ldots \underline{\mathbf{n}}^{(K)\,\mathrm{T}}\right)^{\mathrm{T}} \in \mathbb{C}^{[KK_{\mathrm{M}}(Q_{\mathrm{t}}+W-1)]\times 1}, \tag{4.17}$$

which yields the disturbed total receive signal

$$\underline{\mathbf{r}} = \underline{\mathbf{e}} + \underline{\mathbf{n}} = \underline{\mathbf{H}}\,\underline{\mathbf{M}}\,\underline{\mathbf{d}} + \underline{\mathbf{n}} \in \mathbb{C}^{[KK_{\mathrm{M}}(Q_{\mathrm{t}}+W-1)]\times 1}. \tag{4.18}$$

(4.18) mathematically describes the linear transmission model of Fig. 4.1 from the data input to the Rx antenna outputs. With (4.18) we succeeded to frame the signal transmission from the data input to the Rx antenna outputs in the structure shown in Fig. 4.1 with the formalism of the general linear transmission system considered in Section 3.3. Now, the next step should be to adapt also data detection correspondingly.

The demodulation process to be performed at the K MTs can be described with $\underline{\mathbf{r}}$ of (4.18) by a demodulator matrix $\underline{\mathbf{D}}$ similarly to (3.17) in the form

$$\widehat{\underline{\mathbf{d}}} = \underline{\mathbf{D}}\,\underline{\mathbf{r}} = \underbrace{\underline{\mathbf{D}}\,\underline{\mathbf{H}}}_{\underline{\mathbf{B}}}\,\underline{\mathbf{M}}\,\underline{\mathbf{d}} + \underline{\mathbf{D}}\,\underline{\mathbf{n}} \in \mathbb{C}^{N_{\mathrm{t}}\times 1}. \tag{4.19}$$

Because the dimensions of $\underline{\mathbf{d}}$ of (4.2) and $\underline{\mathbf{r}}$ of (4.18) are N_{t} and

$$Z = KK_{\mathrm{M}}(Q_{\mathrm{t}} + W - 1), \tag{4.20}$$

respectively, again

$$\underline{\mathbf{D}} \in \mathbb{C}^{Z\times N_{\mathrm{t}}} \tag{4.21}$$

holds, see (3.17). Therefore, the a priori determination of $\underline{\mathbf{D}}$ requires the choice of the ZN_{t} components $\underline{D}_{z,\,n}$, $z = 1\ldots Z$, $n = 1\ldots N_{\mathrm{t}}$, of $\underline{\mathbf{D}}$. With (4.14) and (4.16) $\underline{\mathbf{r}}$ of (4.18) can be displayed as

$$\underline{\mathbf{r}} = \left(\underline{\mathbf{r}}^{(1,\,1)\,\mathrm{T}} \ldots \underline{\mathbf{r}}^{(1,\,K_{\mathrm{M}})\,\mathrm{T}}, \ldots, \underline{\mathbf{r}}^{(K,\,1)\,\mathrm{T}} \ldots \underline{\mathbf{r}}^{(K,\,K_{\mathrm{M}})\,\mathrm{T}}\right)^{\mathrm{T}}. \tag{4.22}$$

Having this representation in mind, $\underline{\mathbf{D}}$ in (4.19) can be expressed by the $K^2 K_{\mathrm{M}}$ MT and antenna specific demodulator matrices

$$\underline{\mathbf{D}}^{(k,\,k',\,k_{\mathrm{M}})} \in \mathbb{C}^{N\times(Q+W-1)} \tag{4.23}$$

as

$$\underline{\mathbf{D}} = \begin{pmatrix} \underline{\mathbf{D}}^{(1,\,1,\,1)} & \ldots & \underline{\mathbf{D}}^{(1,\,1,\,K_{\mathrm{M}})}, & \ldots, & \underline{\mathbf{D}}^{(1,\,K,\,1)} & \ldots & \underline{\mathbf{D}}^{(1,\,K,\,K_{\mathrm{M}})} \\ \vdots & \ddots & \vdots & & \vdots & \ddots & \vdots \\ \underline{\mathbf{D}}^{(K,\,1,\,1)} & \ldots & \underline{\mathbf{D}}^{(K,\,1,\,K_{\mathrm{M}})}, & \ldots, & \underline{\mathbf{D}}^{(K,\,K,\,1)} & \ldots & \underline{\mathbf{D}}^{(K,\,K,\,K_{\mathrm{M}})} \end{pmatrix}. \tag{4.24}$$

In $\underline{\mathbf{D}}^{(k,\,k',\,k_{\mathrm{M}})}$ of (4.23) the superscript k designates the MT at which the data estimate is determined, and the superscript k' stands for the MT the receive signal of which is processed at MT k.

4.3 Cooperative and non-cooperative MTs

Concerning the K MTs assigned to the BS we have to discern between the two situations of cooperative and non-cooperative MTs. In the case of co-operative MTs it is assumed that each of the K MTs k, $k = 1 \ldots K$, has at its disposal not only its own disturbed MT specific receive signal $\underline{\mathbf{r}}^{(k)}$ of (4.16), but also the disturbed MT specific receive signals $\underline{\mathbf{r}}^{(k')}$, $k \neq k'$, from all other $K - 1$ MTs k', $k' = 1 \ldots K$, $k' \neq k$. This means that at each MT the total disturbed receive signal $\underline{\mathbf{r}}$ of (4.18) would be available. Such a cooperation between the MTs would require that communication channels between the different MTs exist, which allow the transmission of the disturbed MT specific receive signals $\underline{\mathbf{r}}^{(k)}$ between MTs. This would be a very impractical situation which is not feasible in real world systems. In practical systems each MT k, $k = 1 \ldots K$, disposes only of its own disturbed MT specific receive signal $\underline{\mathbf{r}}^{(k)}$ of (4.16). In this case the MTs are said to be non-cooperative, and only this case will be considered in detail in this thesis.

In the case of cooperative MTs, where at each MT the disturbed total receive signal $\underline{\mathbf{r}}$ of (4.18) would be available, and in order to consider all components of $\underline{\mathbf{r}}$ at each MT when estimating the data, it would be obvious to choose a full demodulator matrix $\underline{\mathbf{D}}$ of (4.24). The question is now, how $\underline{\mathbf{D}}$ should be chosen in the case of non-cooperative MTs, where at each MT k only the disturbed MT specific receive signal $\underline{\mathbf{r}}^{(k)}$ is available. The answer is that in such a situation the signals $\underline{\mathbf{r}}^{(k')}$, $k' = k$, not available at MT k should be multiplied by zero when performing demodulation at MT k. Considering $\underline{\mathbf{D}}$ as displayed in (4.24), such a multiplication by zero can be effected by setting

$$\underline{\mathbf{D}}^{(k, k', k_{\mathrm{M}})} = \mathbf{0} \text{ for } k \neq k'. \tag{4.25}$$

Then, for simplicity, we can write

$$\underline{\mathbf{D}}^{(k, k', k_{\mathrm{M}})} = \underline{\mathbf{D}}^{(k, k_{\mathrm{M}})} \text{ for } k \neq k' \tag{4.26}$$

with the elements being $\underline{D}_{n, m}^{(k, k_{\mathrm{M}})}$, $n = 1 \ldots N$, $m = 1 \ldots Q_{\mathrm{t}} + W - 1$. With these $K K_{\mathrm{M}}$ MT and antenna specific demodulator matrices we can form the MT specific demodulator matrices

$$\underline{\mathbf{D}}^{(k)} = \left(\underline{\mathbf{D}}^{(k, 1)} \ldots \underline{\mathbf{D}}^{(k, K_{\mathrm{M}})} \right) \in \mathbb{C}^{N \times [K_{\mathrm{M}} (Q_{\mathrm{t}} + W - 1)]}. \tag{4.27}$$

Now, with these matrices we can write the demodulator matrix for the case of non-cooperative MTs as a blockdiagonal matrix:

$$\underline{\mathbf{D}} = \mathrm{blockdiag} \left(\underline{\mathbf{D}}^{(1)} \ldots \underline{\mathbf{D}}^{(K)} \right). \tag{4.28}$$

In Fig. 4.4 the matrix $\underline{\mathbf{D}}$ of (4.28) is visualized for the case N equal to 2, $Q_{\mathrm{t}} + W - 1$ equal to 3, K_{M} equal to 2 and K equal to 2. In the case with non-cooperative MTs, the system matrix $\underline{\mathbf{B}}$ in (4.12) becomes

$$\underline{\mathbf{B}} = \underline{\mathbf{D}} \, \underline{\mathbf{H}} = \left(\left(\underline{\mathbf{D}}^{(1)} \underline{\mathbf{H}}^{(1)} \right)^{\mathrm{T}} \ldots \left(\underline{\mathbf{D}}^{(K)} \underline{\mathbf{H}}^{(K)} \right)^{\mathrm{T}} \right)^{\mathrm{T}} = \left(\underline{\mathbf{B}}^{(1)^{\mathrm{T}}} \ldots \underline{\mathbf{B}}^{(K)^{\mathrm{T}}} \right)^{\mathrm{T}}. \tag{4.29}$$

Fig. 4.4. Visualization of $\underline{\mathbf{D}}$ of (4.24) for the case $N = 2$, $Q_t + W - 1 = 3$, $K_M = 2$ and $K = 2$

$\underline{\mathbf{B}}^{(k)}$ in (4.29) is termed MT specific system matrix.

When a priori determining $\underline{\mathbf{D}}$, in the case of cooperative MTs $K N_t K_M (Q_t + W - 1)$ complex elements $\underline{D}_{n,z}$ have to be chosen, whereas in the case of non-cooperative MTs this number would be only $N_t K_M (Q_t + W - 1)$. Of course, also in the case of cooperative MTs $\underline{\mathbf{D}}$ could be chosen according to (4.28). However, such a choice would mean an unnecessary restriction when designing the system.

4.4 Energy efficiency and Tx efficiency

In the case of linear Rx oriented MIMO broadcast systems with TxZF Filter the expression (3.79) for the energy efficiencies η_n could be used in a straightforward manner as performance measures. However, in the case of non-cooperative MTs these performance measures would be unfair for the following reason: $R_{\max}$ as defined by (3.58) would be the maximum possible receive energy over all K MTs; however, if the MTs are non-cooperative, this energy could not be really collected on the receive side. Therefore, the conception of energy efficiency will be somewhat modified in what follows in order to arrive at a fair performance criterion.

Let us designate the principal singular value of the MT specific channel matrix $\underline{\mathbf{H}}^{(k)}$ of (4.11) as $\lambda_1^{(k)}$. If we then would consider only the point-to-point transmission between the

BS ad MT k, then for this link we would obtain instead of r_{opt} of (3.59) the ratio

$$r_{\text{opt}}^{(k)} = \lambda_1^{(k)} = \frac{R_{\max}^{(k)}}{T^{(k)}} \tag{4.30}$$

of the energy $T^{(k)}$ radiated by the BS for MT k and the maximum possible energy $R_{\max}^{(k)}$ received by MT k. If we now introduce $r_{\text{opt}}^{(k)}$ of (4.30) into (3.79), then we obtain the energy efficiency of the nth data symbol $\underline{d}_n^{(k)}$ of MT k according to

$$\eta_n^{(k)} = \frac{1}{\lambda_1^{(k)} \left[\left(\underline{\mathbf{B}}\, \underline{\mathbf{B}}^{\text{H}} \right)^{-1} \right]_{(k-1)N+n,\, (k-1)N+n}}, \; n = 1 \ldots N. \tag{4.31}$$

With (3.80) the Tx efficiency of this data symbol becomes

$$\eta_{\text{Tx},\, n}^{(k)} = \frac{r_{\text{ZF},\, n}^{(k)}}{r_{\text{MF},\, n}^{(k)}} = \frac{1}{\left[\left(\underline{\mathbf{B}}\, \underline{\mathbf{B}}^{\text{H}} \right)^{-1} \right]_{v,\, v} \left[\underline{\mathbf{B}}\, \underline{\mathbf{B}}^{\text{H}} \right]_{v,\, v}}, \; v = (k-1)N + n. \tag{4.32}$$

Intuitively it should be expected that in the case of cooperative MTs the energy efficiencies $\eta_n^{(k)}$ of (4.31) and the Tx efficiencies $\eta_{\text{Tx},\, n}^{(k)}$ of (4.32) are larger than in the case of non-cooperative MTs. By means of a simple example it will be demonstrated that this expectation is plausible. We consider the case

$$K_{\text{B}} = K_{\text{M}} = 1, \; K = 2, \; Q_{\text{t}} = N_{\text{t}} = KN = 4, \; W = 3, \tag{4.33}$$

and assume the two MT specific channel matrices

$$\underline{\mathbf{H}}^{(1)} = \begin{pmatrix} -0.2507 & 0 & 0 & 0 \\ -0.9653 & -0.2507 & 0 & 0 \\ 0.0726 & -0.9653 & -0.2507 & 0 \\ 0 & 0.0726 & -0.9653 & -0.2507 \\ 0 & 0 & 0.0726 & -0.9653 \\ 0 & 0 & 0 & 0.0726 \end{pmatrix} \tag{4.34}$$

and

$$\underline{\mathbf{H}}^{(2)} = \begin{pmatrix} 0.1714 & 0 & 0 & 0 \\ -0.6833 & 0.1714 & 0 & 0 \\ 0.7098 & -0.6833 & 0.1714 & 0 \\ 0 & 0.7098 & -0.6833 & 0.1714 \\ 0 & 0 & 0.7098 & -0.6833 \\ 0 & 0 & 0 & 0.7098 \end{pmatrix}. \tag{4.35}$$

These matrices have the principal singular values

$$\lambda_1^{(1)} = 1.2620 \tag{4.36}$$

and

$$\lambda_1^{(2)} = 2.0848, \tag{4.37}$$

Table 4.1. Energy ratios $r^{(k)}_{\mathrm{ZF},n}$ and energy efficiencies $\eta^{(k)}_n$ for cooperative MTs

(k,n)	$r^{(k)}_{\mathrm{ZF},n}$	$\eta^{(k)}_n$
1,1	2.7907	2.2112
1,2	2.1761	1.7243
2,1	1.6397	0.7865
2,2	1.3937	0.6685

Table 4.2. Energy ratios $r^{(k)}_{\mathrm{ZF},n}$ and energy efficiencies $\eta^{(k)}_n$ for non-cooperative MTs

(k,n)	$r^{(k)}_{\mathrm{ZF},n}$	$\eta^{(k)}_n$
1,1	0.1784	0.1414
1,2	0.3783	0.2998
2,1	0.1632	0.0783
2,2	0.0126	0.0060

respectively. The total channel matrix

$$\underline{\mathbf{H}} = \begin{pmatrix} \underline{\mathbf{H}}^{(1)} \\ \underline{\mathbf{H}}^{(2)} \end{pmatrix} \tag{4.38}$$

has the principal singular value

$$\lambda_1 = 2.7907. \tag{4.39}$$

In the case of cooperative MTs we choose with the left sided singular vectors $\underline{\mathbf{u}}_n$, $n = 1 \ldots N_{\mathrm{t}}$, of the total channel matrix $\underline{\mathbf{H}}$ the total demodulator matrix

$$\underline{\mathbf{D}} = \begin{pmatrix} \underline{\mathbf{u}}_1^{\mathrm{H}} \\ \underline{\mathbf{u}}_2^{\mathrm{H}} \\ \underline{\mathbf{u}}_3^{\mathrm{H}} \\ \underline{\mathbf{u}}_4^{\mathrm{H}} \end{pmatrix} = \begin{pmatrix} \underline{u}_{1,1}^* & \underline{u}_{1,2}^* & \underline{u}_{1,3}^* & \underline{u}_{1,4}^* & \underline{u}_{1,5}^* & \underline{u}_{1,6}^* \\ \underline{u}_{2,1}^* & \underline{u}_{2,2}^* & \underline{u}_{2,3}^* & \underline{u}_{2,4}^* & \underline{u}_{2,5}^* & \underline{u}_{2,6}^* \\ \underline{u}_{3,1}^* & \underline{u}_{3,2}^* & \underline{u}_{3,3}^* & \underline{u}_{3,4}^* & \underline{u}_{3,5}^* & \underline{u}_{3,6}^* \\ \underline{u}_{4,1}^* & \underline{u}_{4,2}^* & \underline{u}_{4,3}^* & \underline{u}_{4,4}^* & \underline{u}_{4,5}^* & \underline{u}_{4,6}^* \end{pmatrix}. \tag{4.40}$$

In the case of non-cooperative MTs we choose

$$\underline{\mathbf{D}} = \begin{pmatrix} \underline{u}_{1,1}^* & \underline{u}_{1,2}^* & \underline{u}_{1,3}^* & 0 & 0 & 0 \\ \underline{u}_{2,1}^* & \underline{u}_{2,2}^* & \underline{u}_{2,3}^* & 0 & 0 & 0 \\ 0 & 0 & 0 & \underline{u}_{3,4}^* & \underline{u}_{3,5}^* & \underline{u}_{3,6}^* \\ 0 & 0 & 0 & \underline{u}_{4,4}^* & \underline{u}_{4,5}^* & \underline{u}_{4,6}^* \end{pmatrix}. \tag{4.41}$$

Tables 4.1 and 4.2 show the energy ratios $r^{(k)}_{\mathrm{ZF},n}$ and the energy efficiencies $\eta^{(k)}_n$ for the two cases, and by comparison we see the superior performance of the system with cooperative MTs. The choices of $\underline{\mathbf{D}}$ according to (4.40) and (4.41) would require channel knowledge at the MTs and, therefore, do not comply with the rationale Rx orientation. However, this does not hamper the comparison being of interest here.

4.5 Statistical consideration of the Tx efficiency

4.5.1 Introduction

In this Section 4.5 we consider the statistical properties of the Tx efficiencies $\eta_{\mathrm{Tx},n}^{(k)}$ of (4.32) for the scenarios with totally uncorrelated and fully correlated channel impulse responses $\underline{\mathbf{h}}^{(k,k_{\mathrm{B}},k_{\mathrm{M}})}$ as described in Section 2.3. The Tx efficiencies characterize energy-wise the performance of TxZF Filter relative to the TxMF under the condition that both filters use the same a priori given demodulator matrix. As mentioned in Subsection 3.3.2, TxMF allows an optimum exploitation of the transmit energy for a given demodulator matrix. Therefore, Tx efficiencies represent the price to be paid for interference elimination. The purpose of the statistical considerations made in this Section 4.5 is to show the effects of the multiple Tx and Rx antennas on the Tx efficiencies $\eta_{\mathrm{Tx},n}^{(k)}$ for the considered two extreme scenarios, and therefore, to give the impression on these effects for the scenarios in between of these two extreme scenarios. The statistical properties of $\eta_{\mathrm{Tx},n}^{(k)}$ for the scenarios with totally uncorrelated channel impulse responses are studied in Subsection 4.5.2, in which the approximate analysis obtained in Section 3.3.5 are extended to MIMO broadcast systems introduced in this Chapter 4 and are verified by simulation results. Some complementarities on the approximate assumption made in Section 3.3.5 are also made. The statistical properties of $\eta_{\mathrm{Tx},n}^{(k)}$ for the scenarios with fully correlated channel impulse responses are only presented by simulation results in Subsection 4.5.3 due to the lack of closed form analysis.

4.5.2 Scenarios with totally uncorrelated channel impulse responses

We resume and extend the considerations made in Subsection 3.3.5 for the scenarios with totally uncorrelated channel impulse responses $\underline{\mathbf{h}}^{(k,k_{\mathrm{B}},k_{\mathrm{M}})}$ as described in Subsections 2.3.1 and 2.3.2. Let us assume that the elements $\underline{h}_{w}^{(k,k_{\mathrm{B}},k_{\mathrm{M}})}$ of the channel impulse responses $\underline{\mathbf{h}}^{(k,k_{\mathrm{B}},k_{\mathrm{M}})}$ are independent Gaussian variables with zero mean and the variance

$$\mathrm{var}\left\{\mathrm{Re}\left\{\underline{h}_{w}^{(k,k_{\mathrm{B}},k_{\mathrm{M}})}\right\}\right\} = \mathrm{var}\left\{\mathrm{Im}\left\{\underline{h}_{w}^{(k,k_{\mathrm{B}},k_{\mathrm{M}})}\right\}\right\} = \sigma_{w}^{2},\ w = 1 \ldots W, \tag{4.42}$$

for the real and imaginary parts. Let us further assume that all elements $D_{n,m}^{(k,k_{\mathrm{M}})}$ of the matrices $\underline{\mathbf{D}}^{(k)}$ of (4.27) are independent real binary variables taking the values from the set

$$\mathbb{V} = \left\{ \frac{1}{\sqrt{K_{\mathrm{M}}(Q_{\mathrm{t}}+W-1)}}, \frac{-1}{\sqrt{K_{\mathrm{M}}(Q_{\mathrm{t}}+W-1)}} \right\}. \tag{4.43}$$

That means each row of $\underline{\mathbf{D}}^{(k)}$ is normalized to have unit energy. Then we obtain in analogy to (3.86) and (3.87) [MWQ04] approximately the mean

$$\overline{\eta}_{\mathrm{Tx}} = \mathrm{E}\left\{\eta_{\mathrm{Tx},n}^{(k)}\right\} \approx \frac{K_{\mathrm{B}}Q_{\mathrm{t}} - (N_{\mathrm{t}}-1)}{K_{\mathrm{B}}Q_{\mathrm{t}}} \tag{4.44}$$

and the variance

$$\text{var}\left\{\eta_{\text{Tx},n}^{(k)}\right\} \approx \frac{\left[K_{\text{B}}Q_{\text{t}} - (N_{\text{t}} - 1)\right](N_{\text{t}} - 1)}{\left(K_{\text{B}}Q_{\text{t}}\right)^2 \left(K_{\text{B}}Q_{\text{t}} + 1\right)} \tag{4.45}$$

of the Tx efficiencies $\eta_{\text{Tx},n}^{(k)}$ of (4.32). According to (4.44) and (4.45), if the spreading factor $Q = K_{\text{B}}Q_{\text{t}}$ of (4.7) increases, $\overline{\eta}_{\text{Tx}}$ goes up and $\text{var}\left\{\eta_{\text{Tx},n}^{(k)}\right\}$ goes down. In the limit we obtain

$$\lim_{K_{\text{B}}Q_{\text{t}} \to \infty} \left(\overline{\eta}_{\text{Tx}}\right) \approx 1 \tag{4.46}$$

and

$$\lim_{K_{\text{B}}Q_{\text{t}} \to \infty} \left(\text{var}\left\{\eta_{\text{Tx},n}^{(k)}\right\}\right) \approx 0, \tag{4.47}$$

respectively. Here we see the beneficial effect of the multiple Tx antennas. However, the influence of the number K_{M} of Rx antennas cannot be observed by the approximate results in (4.44) and (4.45), which will be complemented by the simulation results presented later.

As a precondition for the validity of the expressions (4.44) and (4.45), the elements

$$\begin{aligned}
\underline{b}_{n,\,(k_{\text{B}}-1)Q_{\text{t}}+q}^{(k)} &= \sum_{k_{\text{M}}=1}^{K_{\text{M}}} \sum_{w=1}^{W} D_{n,\,w+q-1}^{(k,\,k_{\text{M}})} \underline{h}_{w}^{(k,\,k_{\text{B}},\,k_{\text{M}})}, \\
&\quad k = 1\ldots K,\ k_{\text{B}} = 1\ldots K_{\text{B}},\ n = 1\ldots N,\ q = 1\ldots Q_{\text{t}}, \tag{4.48}
\end{aligned}$$

of all MT specific system matrix $\underline{\mathbf{B}}^{(k)}$ in (4.29) should be again statistically independent, which is not strictly the case and is valid only when the number K_{M} of Rx antennas tends to infinitely large. In the following we will compare the results obtained by these formulas with simulation results.

In said simulations we set the parameters

$$K = 6,\ N = 1,\ N_{\text{t}} = KN = 6,\ Q_{\text{t}} = 16 \tag{4.49}$$

and vary the parameters K_{B} and K_{M}. Fig. 4.5 shows the simulated $\overline{\eta}_{\text{Tx}}$ versus K_{B} with K_{M} as the curve parameter. It turns out that

- the analytical result obtained from (4.44) coincides with the simulation result, and that
- $\overline{\eta}_{\text{Tx}}$ virtually does not depend on K_{M}.

Fig. 4.6 shows the simulated $\text{var}\left\{\eta_{\text{Tx},n}^{(k)}\right\}$ versus K_{B} with K_{M} as the curve parameter, where we also include the closed form result of (4.45) as a dashed curve. It can be stated that

- $\text{var}\left\{\eta_{\text{Tx},n}^{(k)}\right\}$ decreases with increasing number K_{M} of Rx antennas, and that
- the coincidence of the analytical and simulated curves improves with increasing K_{M} and becomes perfect for $K_{\text{M}} \to \infty$.

This behavior verifies the effect that statistical independence of the elements of $\underline{\mathbf{B}}$ which was assumed when deriving (4.44) and (4.45) is fulfilled the better the larger K_{M} is as mentioned before.
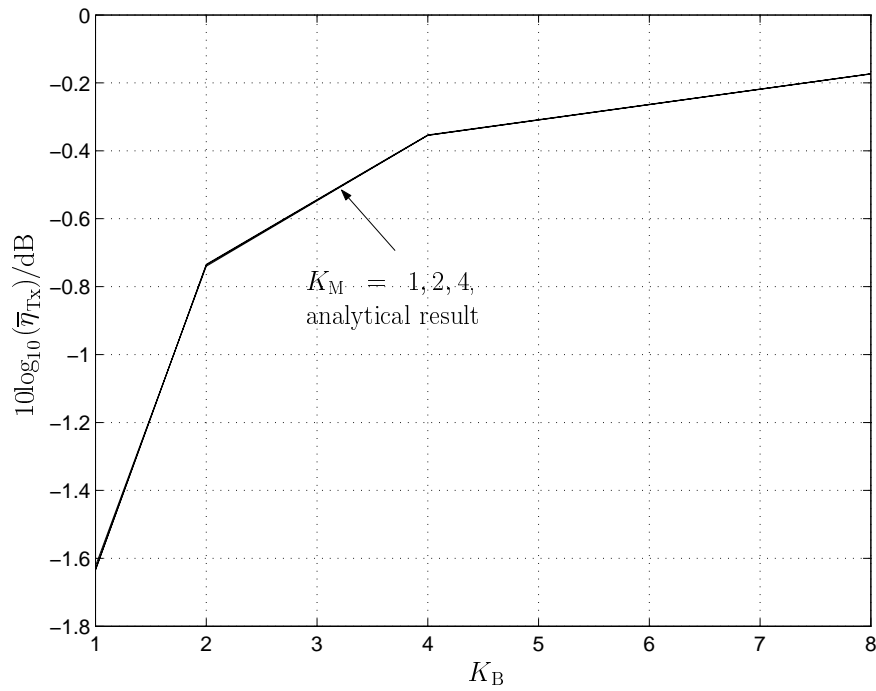
Fig. 4.5. Average Tx efficiency $\overline{\eta}_{\text{Tx}}$ versus K_{B} for the scenarios with totally uncorrelated channel impulse responses; parameters: $K = 6$, $N = 1$, $N_{\text{t}} = KN = 6$, $Q_{\text{t}} = 16$

Fig. 4.6. Variance of Tx efficiency $\eta_{\text{Tx},n}^{(k)}$ versus K_{B} for the scenarios with totally uncorrelated channel impulse responses; parameters: $K = 6$, $N = 1$, $N_{\text{t}} = KN = 6$, $Q_{\text{t}} = 16$

4.5.3   Scenarios with fully correlated channel impulse responses

In the scenarios with fully correlated channel impulse responses $\underline{\mathbf{h}}^{(k,k_{\mathrm{B}},k_{\mathrm{M}})}$ as described in Subsections 2.3.1 and 2.3.3, the components $\underline{h}_{\mathrm{R},w}^{(k)}$, $w = 1 \ldots W$, of the reference channel impulse response $\underline{\mathbf{h}}_{\mathrm{R}}^{(k)}$ of (2.17) are assumed to be i.i.d complex Gaussian variables with zero mean and the variance

$$\mathrm{var}\left\{\mathrm{Re}\left\{\underline{h}_{\mathrm{R},w}^{(k)}\right\}\right\} = \mathrm{var}\left\{\mathrm{Im}\left\{\underline{h}_{\mathrm{R},w}^{(k)}\right\}\right\} = \sigma_w^2, \; w = 1 \ldots W, \qquad (4.50)$$

for the real and imaginary parts. The MTs are assumed to uniformly distributed around the BS with the corresponding azimuth angles being i.i.d. variables uniformly distributed within $[-\pi, \pi)$. The antenna arrays at the BS and the MTs are assumed to be randomly rotated around their RP, where the corresponding azimuth angles of any one of the antenna elements are also assumed to be i.i.d. variables uniformly distributed within $[-\pi, \pi)$. The same assumption as made in Subsection 4.5.2 is valid for the MT specific demodulator matrix $\underline{\mathbf{D}}^{(k)}$.

For the simulations we set the same parameters in (4.49) and vary the parameters K_{B} and K_{M}. Figs. 4.7 and 4.8 show the simulated $\overline{\eta}_{\mathrm{Tx}}$ and $\mathrm{var}\left\{\eta_{\mathrm{Tx},n}^{(k)}\right\}$ versus K_{B} with K_{M} as the curve parameter, respectively. It turns out that the curves obtained for the scenarios with totally uncorrelated channel impulse responses and for the scenarios with fully correlated channel impulse responses are very similar and only slight degradations are observed in the latter case, that is that

- $\overline{\eta}_{\mathrm{Tx}}$ goes up and $\mathrm{var}\left\{\eta_{\mathrm{Tx},n}^{(k)}\right\}$ goes down with increasing number K_{B} of Tx antennas, that
- $\overline{\eta}_{\mathrm{Tx}}$ again virtually does not depend on K_{M}, however, is slightly smaller than $\overline{\eta}_{\mathrm{Tx}}$ for the scenarios with totally uncorrelated channel impulse responses, that
- $\mathrm{var}\left\{\eta_{\mathrm{Tx},n}^{(k)}\right\}$ decreases with increasing number K_{M} of Rx antennas and tends to be an asymptotic value, and that
- $\mathrm{var}\left\{\eta_{\mathrm{Tx},n}^{(k)}\right\}$ for the scenarios with fully correlated channels impulse responses is larger than $\mathrm{var}\left\{\eta_{\mathrm{Tx},n}^{(k)}\right\}$ for the scenarios with totally uncorrelated channel impulse responses.

4.5.4   General conclusions on the Tx efficiency

The results obtained in Subsections 4.5.2 and 4.5.3 give the following impressions on the Tx efficiencies $\eta_{\mathrm{Tx},n}^{(k)}$ for the scenarios in between of the two extreme scenarios:

- Both multiple Tx and Rx antennas show beneficial effects on the Tx efficiencies for all scenarios with different degree of correlation between channel impulse responses.
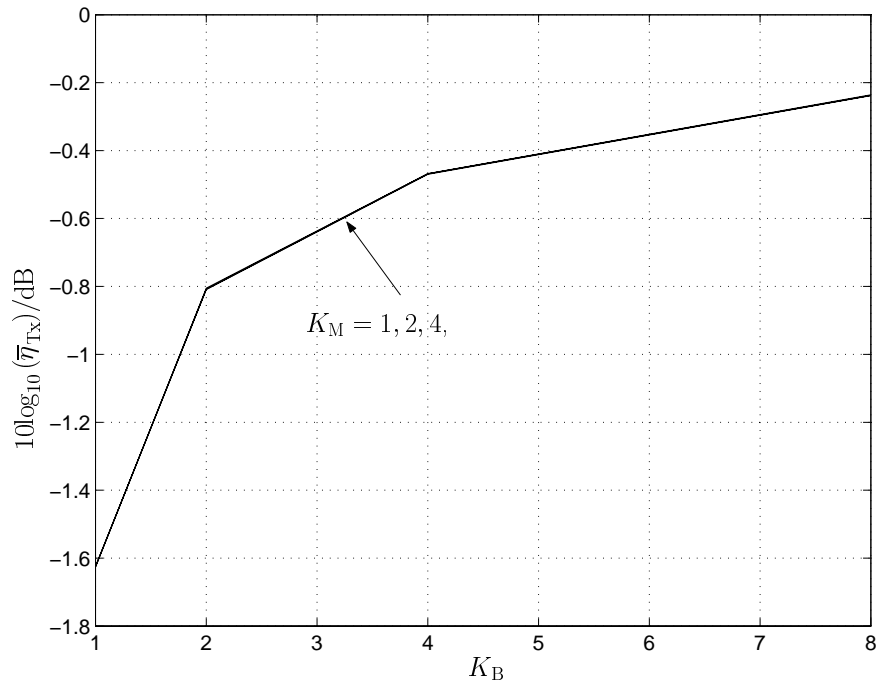
Fig. 4.7. Average Tx efficiency $\overline{\eta}_{\mathrm{Tx}}$ versus K_{B} for the scenarios with fully correlated channel impulse responses; parameters: $K = 6$, $N = 1$, $N_{\mathrm{t}} = KN = 6$, $Q_{\mathrm{t}} = 16$
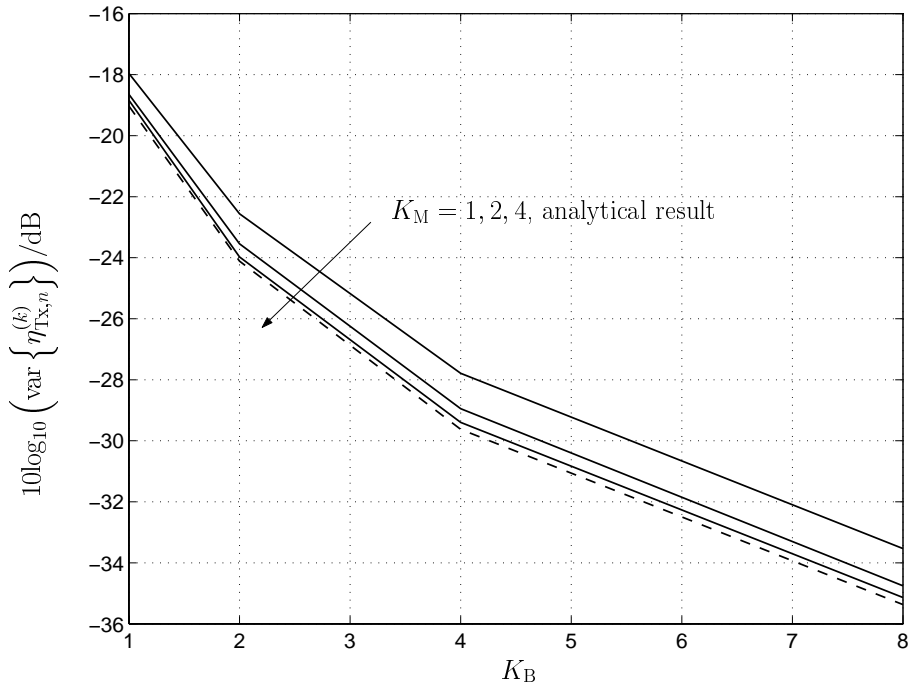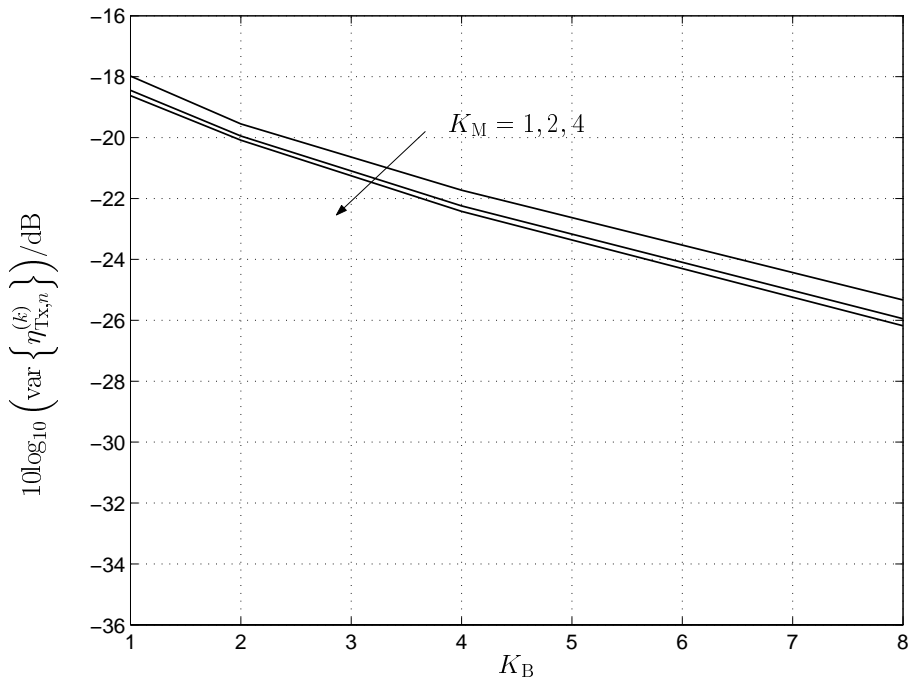

Fig. 4.8. Variance of Tx efficiency $\eta_{\mathrm{Tx},n}^{(k)}$ versus K_{B} for the scenarios with fully correlated channel impulse responses; parameters: $K = 6$, $N = 1$, $N_{\mathrm{t}} = KN = 6$, $Q_{\mathrm{t}} = 16$

- With increasing number K_{B} of Tx antennas, the mean $\overline{\eta}_{\mathrm{Tx}}$ of Tx efficiencies increases and its variance $\mathrm{var}\left\{\eta_{\mathrm{Tx},\,n}^{(k)}\right\}$ decreases.

- The multiple Rx antennas show the beneficial effect only on the variance $\mathrm{var}\left\{\eta_{\mathrm{Tx},\,n}^{(k)}\right\}$ of the Tx efficiencies and virtually have no influence on its mean $\overline{\eta}_{\mathrm{Tx}}$.

- When going from the scenarios with totally uncorrelated channel impulse responses to the scenarios with fully correlated channel impulse responses, i.e. increasing the correlation degree of the channel impulse responses, the degree of the beneficial effects of both multiple Tx and Rx antennas tends to go down.

4.6 Statistical consideration of the Tx energy

4.6.1 Introduction

The study on the Tx efficiencies shows the effects of the multiple Tx and Rx antennas on the price for interference elimination, which is only one aspect with respect to the transmit energy reduction. Therefore, in this Section 4.6 we consider the statistical properties of the Tx energies $T_{\mathrm{ZF},\,n}^{(k)}$ of (3.74) for the scenarios with totally uncorrelated and fully correlated channel impulse responses $\underline{\mathbf{h}}^{(k,\,k_{\mathrm{B}},\,k_{\mathrm{M}})}$ as described in Section 2.3. The purpose of such considerations is similar to that made in Section 4.5 and is to show the effects of the multiple Tx and Rx antennas on the Tx energies $T_{\mathrm{ZF},\,n}^{(k)}$ for the considered two extreme scenarios, and therefore, to give the impression on the these effects for the scenarios in between of the two extreme scenarios. The statistical properties of $T_{\mathrm{ZF},\,n}^{(k)}$ for the scenarios with totally uncorrelated channel impulse responses are studied in Subsection 4.6.2, in which the approximate analysis obtained in Section 3.3.6 are extended to MIMO broadcast systems introduced in this Chapter 4 and are complemented and verified by simulation results. The statistical properties of $T_{\mathrm{ZF},\,n}^{(k)}$ for the scenarios with fully correlated channel impulse responses are presented by simulation results in Subsection 4.6.3.

4.6.2 Scenarios with totally uncorrelated channel impulse responses

The expressions (3.94) and (3.95) can be extended in order to be applicable to the MIMO systems studied in this chapter. The same assumptions made in Subsection 4.5.2 are valid in this subsection. By such an extension we obtain [MWQ04] with the variance

$$\sigma_{\mathrm{b}}^2 = \mathrm{var}\left\{\underline{b}_{n,\,(k_{\mathrm{B}}-1)Q_{\mathrm{t}}+q}^{(k)}\right\} = \frac{1}{Q_{\mathrm{t}}+W-1}\sum_{w=1}^{W}\sigma_w^2 \tag{4.51}$$

of the elements $\underline{b}^{(k)}_{n,\,(k_{\mathrm{B}}-1)Q_{\mathrm{t}}+q}$ of (4.48)

$$\overline{T}_{\mathrm{ZF}} = \mathrm{E}\left\{T^{(k)}_{\mathrm{ZF},n}\right\} \approx \frac{E_{\mathrm{d}}}{2\sigma_{\mathrm{b}}^2} \cdot \frac{1}{K_{\mathrm{B}}Q_{\mathrm{t}} - N_{\mathrm{t}}} \tag{4.52}$$

and

$$\mathrm{var}\left\{T^{(k)}_{\mathrm{ZF},n}\right\} \approx \frac{E_{\mathrm{d}}^2}{4\sigma_{\mathrm{b}}^4} \cdot \frac{1}{(K_{\mathrm{B}}Q_{\mathrm{t}} - N_{\mathrm{t}})^2(K_{\mathrm{B}}Q_{\mathrm{t}} - N_{\mathrm{t}} + 1)}. \tag{4.53}$$

According to (4.52) and (4.53) both the mean $\overline{T}_{\mathrm{ZF}}$ and the variance $\mathrm{var}\left\{T^{(k)}_{\mathrm{ZF},n}\right\}$ go down with increasing number K_{B} of Tx antennas. If we increase K_{B} more and more, the Tx energy required to achieve a certain quality of the detected data symbol becomes smaller and smaller. Again, the approximate results give no observation on the influence of the number K_{M} of Rx antennas. In the following we will first study a very simple case, where a single data symbol is transmitted for a single MT, to give an impression on the influence of K_{M} on the Tx energy. Then, simulation results will be presented.

In the case with a single data symbol transmitted for a single MT, we obtain with (3.74) the corresponding Tx energy

$$T^{(1)}_{\mathrm{ZF},1} = \frac{1}{2}\left|\underline{d}_n\right|^2 \left[\left(\underline{\mathbf{B}}\,\underline{\mathbf{B}}^{\mathrm{H}}\right)^{-1}\right]_{n,n} = \frac{E_{\mathrm{d}}}{2}\Big(\underbrace{\sum_{p=1}^{K_{\mathrm{B}}Q_{\mathrm{t}}}\left|\underline{b}^{(1)}_{1,p}\right|^2}_{X}\Big)^{-1}. \tag{4.54}$$

Let us first consider the variable X in (4.54). With the assumptions made for the scenarios for totally uncorrelated channel impulse responses in Subsection 4.5.2 the mean

$$\mathrm{E}\left\{X\right\} = \frac{2K_{\mathrm{B}}Q_{\mathrm{t}}}{(Q_{\mathrm{t}} + W - 1)}\sum_{w=1}^{W}\sigma_w^2 \tag{4.55}$$

and the variance

$$\mathrm{var}\left\{X\right\} = \frac{4K_{\mathrm{B}}Q_{\mathrm{t}}}{(Q_{\mathrm{t}} + W - 1)^2}\left[\frac{Q_{\mathrm{t}} - 1}{K_{\mathrm{M}}}\sum_{w=1}^{W}\sigma_w^4 + \sum_{w=1}^{W}\sum_{w'=1}^{W}\sigma_w^2\sigma_{w'}^2\right] \tag{4.56}$$

of the variable X in (4.54) can be derived as shown in the appendix A.1. It can be seen from (4.55) that the number K_{M} of Rx antennas has no influence on the mean of X. However, with (4.56), the variance of X decreases with the increasing number K_{M} of Rx antennas. When the number K_{M} of Rx antennas tends to infinitely large, the variance of X decreases to an asymptotic value

$$\mathrm{var}\left\{X\right\}^{(\infty)} = \frac{4K_{\mathrm{B}}Q_{\mathrm{t}}}{(Q_{\mathrm{t}} + W - 1)^2}\sum_{w=1}^{W}\sum_{w'=1}^{W}\sigma_w^2\sigma_{w'}^2. \tag{4.57}$$

Consequently, with (4.54) increasing the number K_{M} of Rx antennas decreases the mean [AS65]

$$\mathrm{E}\left\{T^{(1)}_{\mathrm{ZF},1}\right\} = \mathrm{E}\left\{\frac{E_{\mathrm{d}}}{2X}\right\} \tag{4.58}$$
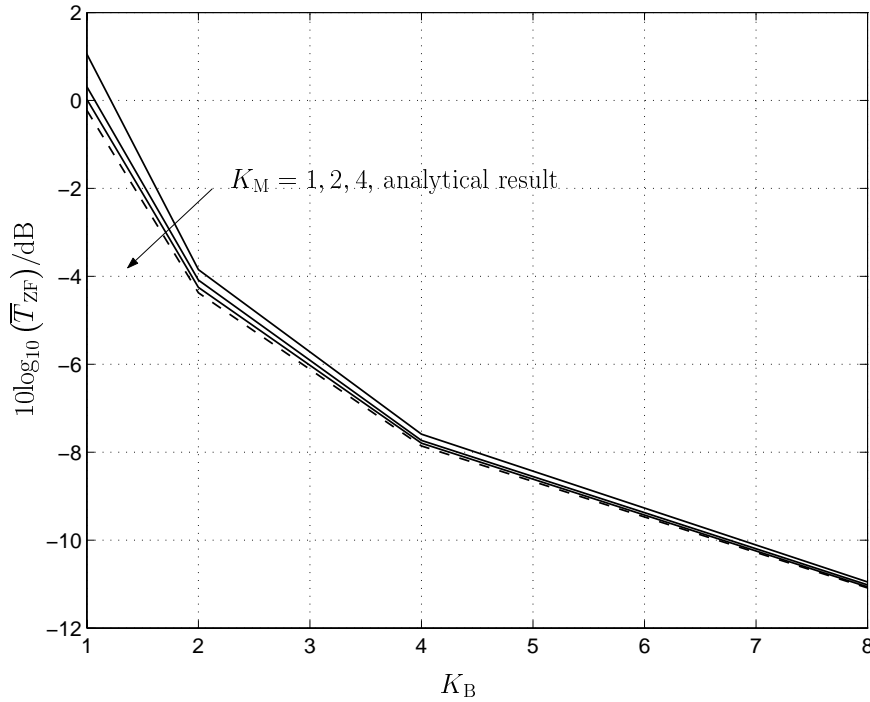
Fig. 4.9. Average symbol specific transmit energy $\overline{T}_{\mathrm{ZF}}$ versus K_{B} for the scenarios with totally uncorrelated channel impulse responses; parameters: $K = 6$, $N = 1$, $N_{\mathrm{t}} = KN = 6$, $Q_{\mathrm{t}} = 16$

of the symbol specific Tx energy $T_{\mathrm{ZF},1}^{(1)}$ and also decreases its variance [AS65]

$$\mathrm{var}\left\{T_{\mathrm{ZF},1}^{(1)}\right\} = \mathrm{var}\left\{\frac{E_{\mathrm{d}}}{2X}\right\}. \tag{4.59}$$

When K_{M} tends to be infinitely large, both the mean $\mathrm{E}\left\{T_{\mathrm{ZF},1}^{(1)}\right\}$ of (4.58) and the variance $\mathrm{var}\left\{T_{\mathrm{ZF},1}^{(1)}\right\}$ of (4.59) tend to their asymptotic values. This conclusion is also valid for $T_{\mathrm{ZF},n}^{(k)}$ of the general case. The simulation results in what follows will confirm this observation.

For the Tx energies $T_{\mathrm{ZF},n}^{(k)}$ simulations are performed for the parameters given in (4.49). The results are shown in Figs. 4.9 and 4.10. In these figures also the analytical results of (4.52) and (4.53), respectively, are included. It can be seen from these curves that

- when increasing the number K_{B} of Tx antennas both $\overline{T}_{\mathrm{ZF}}$ and $\mathrm{var}\left\{T_{\mathrm{ZF},n}^{(k)}\right\}$ go down, that
- increasing K_{M} decreases both $\overline{T}_{\mathrm{ZF}}$ and $\mathrm{var}\left\{T_{\mathrm{ZF},n}^{(k)}\right\}$ as expected by the analysis of the simple case, and that
- the coincidence of the analytical and simulated curves improves with increasing K_{M}.
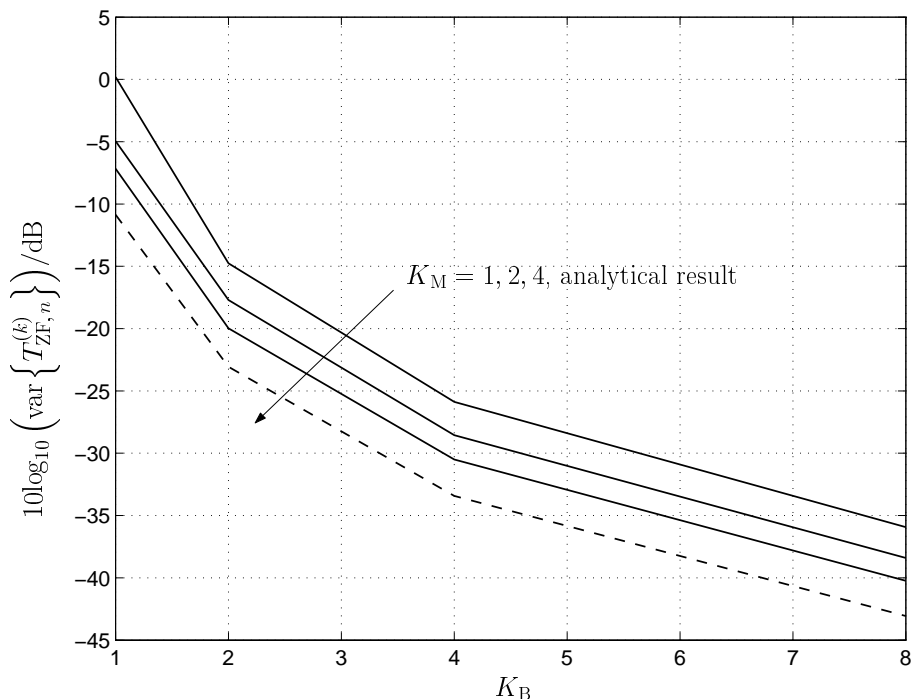
Fig. 4.10. Variance of the symbol specific transmit energy $T_{\mathrm{ZF},n}^{(k)}$ versus K_{B} for the scenarios with totally uncorrelated channel impulse responses; parameters: $K = 6$, $N = 1$, $N_{\mathrm{t}} = KN = 6$, $Q_{\mathrm{t}} = 16$

4.6.3   Scenarios with fully correlated channel impulse responses

Let us again consider the simple case mentioned in Subsection 4.6.2 to gain an impression of the influence of multiple Rx antennas on the symbol specific transmit energy $T_{\mathrm{ZF},n}^{(k)}$ for the scenarios with fully correlated channel impulse responses. With the assumptions made in Subsection 4.5.3 for the case with fully correlated channel impulse responses, we can obtain the mean

$$\mathrm{E}\left\{X\right\} = \frac{2K_{\mathrm{B}}Q_{\mathrm{t}}}{Q_{\mathrm{t}} + W - 1} \sum_{w=1}^{W} \sigma_w^2 \qquad (4.60)$$

and the variance

$$\mathrm{var}\left\{X\right\} = \frac{4K_{\mathrm{B}}Q_{\mathrm{t}}^2}{(Q_{\mathrm{t}} + W - 1)^2} \left[\frac{K_{\mathrm{M}} - 1}{K_{\mathrm{M}}Q_{\mathrm{t}}} \left(1 + \frac{2(Q_{\mathrm{t}} - W)(W - 1)}{Q_{\mathrm{t}}} \right) \sum_{w=1}^{W} \sum_{w''=1}^{W} \sigma_w^2 \sigma_{w'}^2 \right.$$
$$\left. + \left(K_{\mathrm{B}} + \frac{K_{\mathrm{M}} - 1}{K_{\mathrm{M}}Q_{\mathrm{t}}} \right) \sum_{w=1}^{W} \sigma_w^4 \right] \qquad (4.61)$$

for X in (4.54) as derived in Appendix A.2. It can be seen from (4.60) that the number K_{M} of Rx antennas has no influence on the mean of X. However, with (4.61), unlike for the scenarios with totally uncorrelated channel impulse responses the variance of X

increases with an increasing number K_M of Rx antennas. When the number K_M of Rx antennas tends to be infinitely large, then the variance of X increases to an asymptotic value

$$
\text{var}\,\{X\}^{(\infty)} \;\; = \;\; \frac{4K_B Q_t^2}{(Q_t + W - 1)^2}\left[\frac{1}{Q_t}\left(1 + \frac{2(Q_t - W)(W - 1)}{Q_t}\right)\sum_{w=1}^{W}\sum_{w''=1}^{W}\sigma_w^2\sigma_{w'}^2\right.
$$
$$
\left. + \left(K_B + \frac{1}{Q_t}\right)\sum_{w=1}^{W}\sigma_w^4\right]. \tag{4.62}
$$

Consequently, increasing the number K_M of Rx antennas increases the mean [AS65]

$$
\text{E}\left\{T_{\text{ZF},1}^{(1)}\right\} = \text{E}\left\{\frac{E_d}{2X}\right\} \tag{4.63}
$$

of the symbol specific Tx energy $T_{\text{ZF},1}^{(1)}$ and also increases its variance [AS65]

$$
\text{var}\left\{T_{\text{ZF},1}^{(1)}\right\} = \text{var}\left\{\frac{1}{X}\right\}. \tag{4.64}
$$

When K_M tends to be infinitely large, both the mean and the variance tend to their asymptotic values. This conclusion is also valid for the general case and will be verified by the simulation results performed in what follows.

The simulations are performed again for the parameters given in (4.49). The results are shown in Figs. 4.11 and 4.12. It can be stated from these curves that

- both $\overline{T}_{\text{ZF}}$ and var $\left\{T_{\text{ZF},n}^{(k)}\right\}$ go down with increasing number K_B of Tx antennas, and

- multiple Rx antennas has a slightly detrimental effect on the Tx energies $T_{\text{ZF},n}^{(k)}$ as expected by the analysis of the simple case, i.e., increasing the number K_M of Rx antennas leads to slight increasing of both $\overline{T}_{\text{ZF}}$ and var $\left\{T_{\text{ZF},n}^{(k)}\right\}$.

4.6.4   General conclusions on the Tx energy

The results obtained in Subsections 4.6.2 and 4.6.3 give the following impressions on the Tx energies $T_{\text{ZF},n}^{(k)}$ for the scenarios in between of the two extreme scenarios:

- Multiple Tx antennas show beneficial effects on the Tx energy for all scenarios with different degree of correlation between channel impulse responses.

- With increasing number K_B of Tx antennas, both the mean value $\overline{T}_{\text{ZF}}$ and the variance var $\left\{T_{\text{ZF},n}^{(k)}\right\}$ of Tx energies decreases.
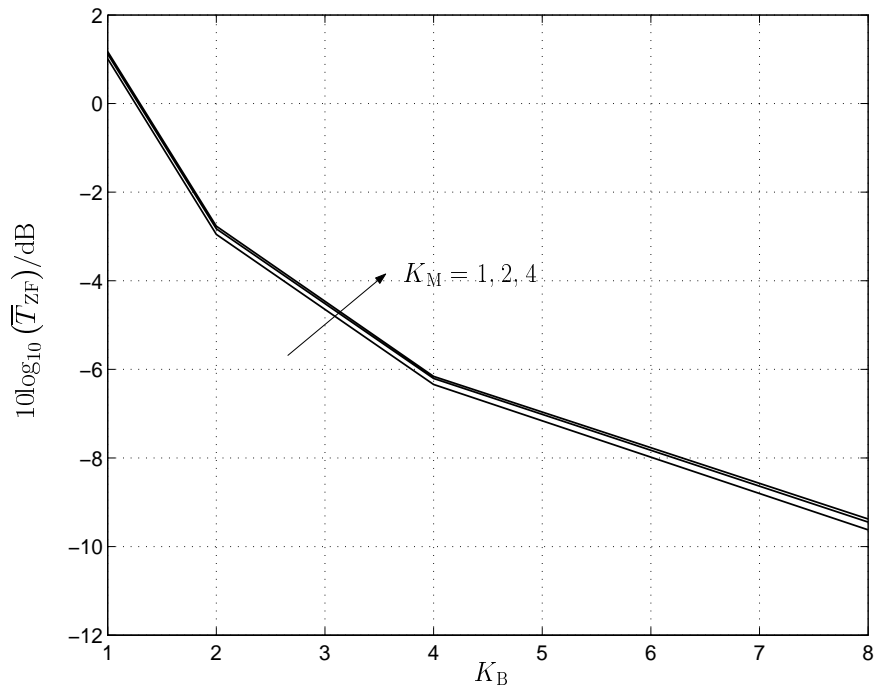
Fig. 4.11. Average transmit energy $\overline{T}_{\mathrm{ZF}}$ versus K_{B} for the scenarios with fully correlated channel impulse responses; parameters: $K = 6$, $N = 1$, $N_{\mathrm{t}} = KN = 6$, $Q_{\mathrm{t}} = 16$
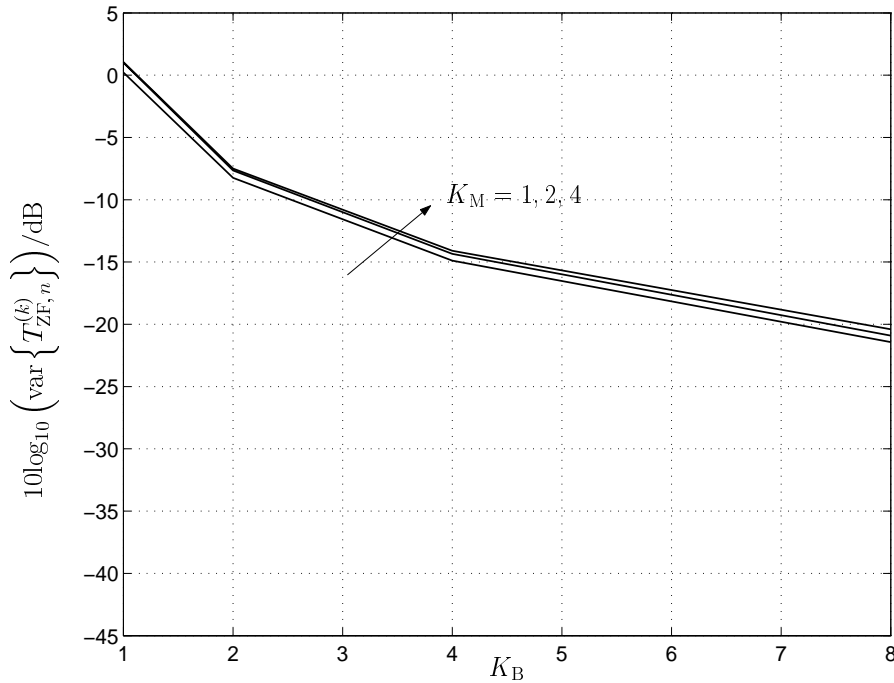
Fig. 4.12. Variance of transmit energy $T_{\mathrm{ZF},\,n}^{(k)}$ versus K_{B} for the scenarios with fully correlated channel impulse responses; parameters: $K = 6$, $N = 1$, $N_{\mathrm{t}} = KN = 6$, $Q_{\mathrm{t}} = 16$

- When going from the scenarios with totally uncorrelated channel impulse responses to the scenarios with fully correlated channel impulse responses, i.e. increasing the correlation degree of the channel impulse responses, the degree of the beneficial effects of multiple Tx antennas tends to go down.

- The multiple Rx antennas do not always show the beneficial effects, these beneficial effects disappear when the channel impulse responses are highly correlated.

Chapter 5

Non-linear Rx oriented MIMO broadcast systems

5.1   Goal minimum required Tx energy

In this chapter we consider Rx oriented MIMO broadcast systems with a structure as shown in Fig. 5.1. In the receiver we employ an unconventional quantizer, see Figs. 3.5 and 3.6. The considered structure consists of a linear inner part constituted by $\underline{\mathbf{H}}$, the noise addition and $\underline{\mathbf{D}}$, and non-linear parts on the Tx and Rx sides. $\underline{\mathbf{D}}$ and $Q(\cdot)$ are a priori given, and the Tx operator $\mathcal{M}\{\cdot\}$ is a posteriori determined based on the knowledge of $\underline{\mathbf{D}}$, $Q(\cdot)$ and $\underline{\mathbf{H}}$, see Fig. 5.1. As far as the linear inner part of the structure shown in Fig. 5.1 is concerned, this part can be further displayed quite analogously to the corresponding parts in Fig. 4.1.

Let us assume that a specific realization $\underline{\mathbf{d}}^{(R)}$, $R = 1 \ldots M^{N_{\mathrm{t}}}$, of $\underline{\mathbf{d}}$ of (4.2) has to be transmitted. Then, in the case of P-fold connected decision regions, see Section 3.2, one out of $P^{N_{\mathrm{t}}}$ possible signals $\underline{\mathbf{t}}^{(R)}$ has to be radiated into the channel. Each of these $P^{N_{\mathrm{t}}}$ Tx signals generates a different useful part $\mathbf{g}$ in the signal $\widehat{\mathbf{g}}$ at the output of the demodulator. For instance, if the component $\underline{d}_n$ of $\underline{\mathbf{d}}$ of (4.2) has the realization $\underline{v}_m$, then for the useful part of the corresponding component of $\widehat{\underline{g}}_n$ of $\widehat{\mathbf{g}}$ should

$$\underline{g}_n \in \mathbb{V}_{\mathrm{q},\, m} \text{ if } \underline{d}_n = \underline{v}_m \tag{5.1}$$

hold.

The issue of Chapter 5 is the minimization of the Tx energy T of (3.9) required for the transmission of the data vector $\underline{\mathbf{d}}$ of (4.2) with a given receive quality. Each of the $P^{N_{\mathrm{t}}}$ Tx signals $\underline{\mathbf{t}}^{(R)}$ suited for the transmission of the realization $\underline{\mathbf{d}}^{(R)}$ of $\underline{\mathbf{d}}$ has a different energy T. In order to minimize T, one could determine T for all $P^{N_{\mathrm{t}}}$ possible Tx signals $\underline{\mathbf{t}}^{(R)}$ and then, finally, use the signal $\underline{\mathbf{t}}^{(R)}$ with the smallest energy T. However, such an exhaustive search would be prohibitively expensive. In the following, the author develops a cost efficient suboptimum algorithm for reducing the Tx energy by suitably chosen Tx signals $\underline{\mathbf{t}}$. This approach is termed Transmit Non-linear Zero Forcing (TxNZF) Filter by the author.

In Section 5.2 the concept TxNZF Filter will be developed and mathematically described. In Section 5.3 the performance of TxNZF Filter will be illustrated by computer simulations. In Section 5.4 possibilities to reduce the computational complexity of TxNZF Filter will be presented. Finally, Section 5.5 generalizes the concept TxNZF Filter.
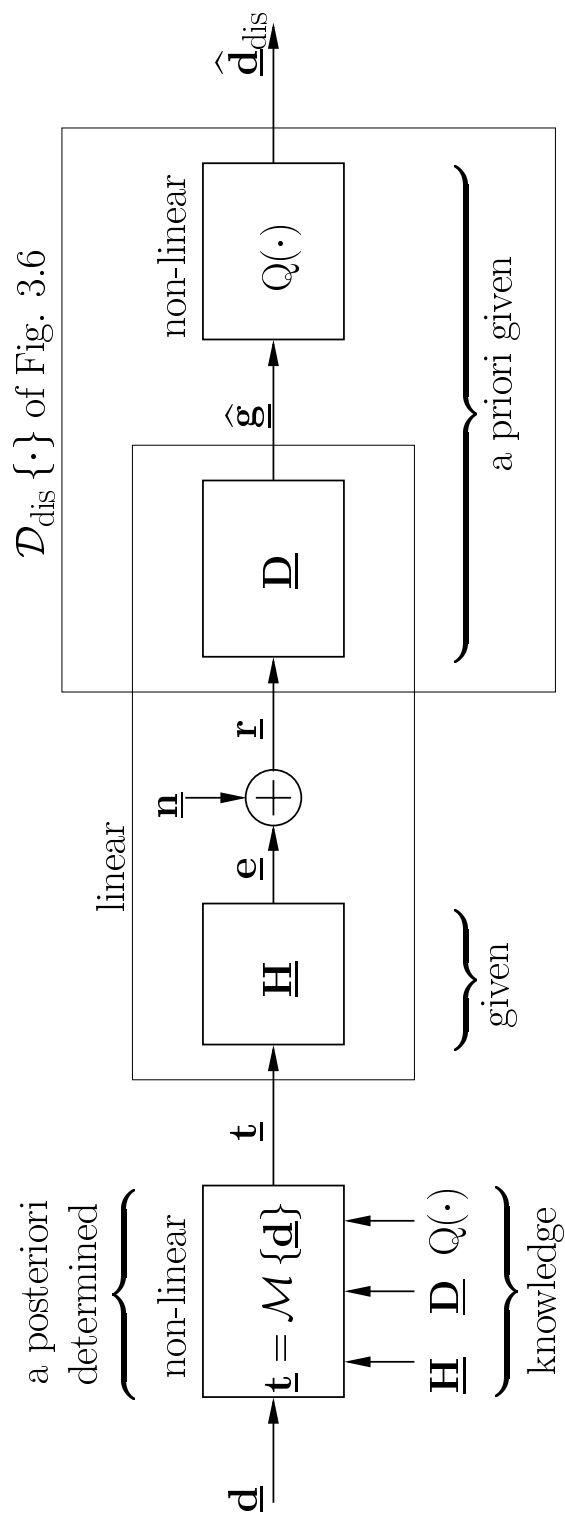
Fig. 5.1. Basic structure of the considered non-linear Rx oriented MIMO broadcast system

5.2   Description of Transmit Non-linear Zero Forcing (TxNZF) Filter

5.2.1   Group-wise generation of the transmit signal $\underline{t}$ under consideration of a multiply connected quantization scheme

The crux of TxNZF Filter consists in a group-wise generation of the transmit signals for the data symbols $\underline{d}_n$, $n = 1 \ldots N_{\mathrm{t}}$. For this reason the set

$$\mathbb{D} = \left\{ \underline{d}_1 \ldots \underline{d}_{N_{\mathrm{t}}} \right\} \tag{5.2}$$

containing all data symbols $\underline{d}_n$, $n = 1 \ldots N_{\mathrm{t}}$, to be transmitted from the BS to the K MTs is subdivided into G disjoint non-empty subsets $\mathbb{D}_g$, $g = 1 \ldots G$, termed data groups so that $\mathbb{D}$ is equal to

$$\mathbb{D} = \bigcup_{g=1}^{G} \mathbb{D}_g . \tag{5.3}$$

Fig. 5.2 shows an example for such a subdivision for the case N_{t} equal to 8 and G equal to 4. In the following all the group specific vectors and matrices are designated by the group number g as a superscript and by the notation G as a subscript. For each data group g, $g = 1 \ldots G$, a group specific transmit signal $\underline{\mathbf{t}}_{\mathrm{G}}^{(g)}$ should be generated. By superposition of all G group specific transmit signals $\underline{\mathbf{t}}_{\mathrm{G}}^{(g)}$, $g = 1 \ldots G$, one obtains the total transmit signal

$$\underline{\mathbf{t}} = \sum_{g=1}^{G} \underline{\mathbf{t}}_{\mathrm{G}}^{(g)} . \tag{5.4}$$
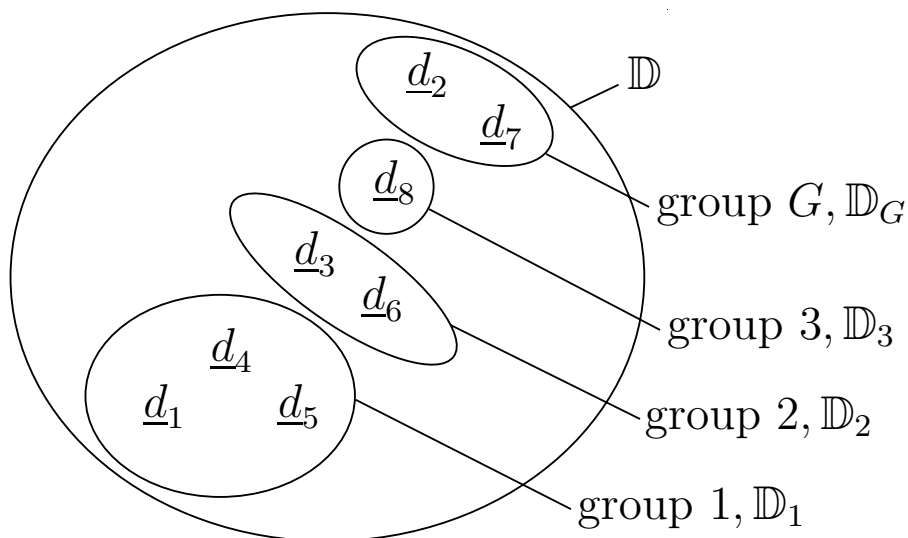
Fig. 5.2. Exemplary subdivision of set $\mathbb{D}$ of all data symbols into disjoint subsets $\mathbb{D}_g$, $g = 1 \ldots G$, termed data groups for the case $N_{\mathrm{t}} = 8$ and $G = 4$

$$\mathbf{S}_{\mathrm{G}}^{(1)} = \begin{pmatrix} 1\ 0\ 0\ 0\ 0\ 0\ 0\ 0 \\ 0\ 0\ 0\ 1\ 0\ 0\ 0\ 0 \\ 0\ 0\ 0\ 0\ 1\ 0\ 0\ 0 \end{pmatrix}, \ \mathbf{S}_{\mathrm{G}}^{(2)} = \begin{pmatrix} 0\ 0\ 1\ 0\ 0\ 0\ 0\ 0 \\ 0\ 0\ 0\ 0\ 0\ 1\ 0\ 0 \end{pmatrix},$$

$$\mathbf{S}_{\mathrm{G}}^{(3)} = \begin{pmatrix} 0\ 0\ 0\ 0\ 0\ 0\ 0\ 1 \end{pmatrix}, \quad \mathbf{S}_{\mathrm{G}}^{(4)} = \begin{pmatrix} 0\ 1\ 0\ 0\ 0\ 0\ 0\ 0 \\ 0\ 0\ 0\ 0\ 0\ 0\ 1\ 0 \end{pmatrix}.$$

Fig. 5.3. Exemplary selection matrices $\mathbf{S}_{\mathrm{G}}^{(g)}$, $g = 1 \ldots 4$, for the exemplary subdivision of the data symbols in Fig. 5.2

Now, let us consider the generation of each group specific transmit signal $\underline{\mathbf{t}}_{\mathrm{G}}^{(g)}$ of (5.4). To ease the mathematical description of the generation of $\underline{\mathbf{t}}_{\mathrm{G}}^{(g)}$, we first reorganize the related vectors and matrices used for TxNZF Filter. The data symbols $\underline{d}_n \in \mathbb{D}_g$ assigned to one and the same data group g are combined to the group specific data vector

$$\underline{\mathbf{d}}_{\mathrm{G}}^{(g)} = \left(\underline{d}_{\mathrm{G},1}^{(g)} \ldots \underline{d}_{\mathrm{G}, \|\mathbb{D}_g\|}^{(g)} \right)^{\mathrm{T}} \in \mathbb{V}^{\|\mathbb{D}_g\| \times 1}. \tag{5.5}$$

The mapping between the total data vector $\underline{\mathbf{d}}$ of (3.3) and $\underline{\mathbf{d}}_{\mathrm{G}}^{(g)}$ of (5.5) can be expressed by a $\|\mathbb{D}_g\| \times N_{\mathrm{t}}$-matrix $\mathbf{S}_{\mathrm{G}}^{(g)}$ as

$$\underline{\mathbf{d}}_{\mathrm{G}}^{(g)} = \mathbf{S}_{\mathrm{G}}^{(g)} \underline{\mathbf{d}}. \tag{5.6}$$

$\mathbf{S}_{\mathrm{G}}^{(g)}$ of (5.6) is termed group specific selection matrix and has the following properties:

- In each row of $\mathbf{S}_{\mathrm{G}}^{(g)}$ all elements are zero except of exactly one element which is one.

- Each column of $\mathbf{S}_{\mathrm{G}}^{(g)}$ contains at most only one non-zero element.

Even if a fixed subdivision $\mathbb{D}_g$, $g = 1 \ldots G$, of $\mathbb{D}$ of (5.2) is considered, generally different possibilities exist for the choice of the group specific selection matrix $\mathbf{S}_{\mathrm{G}}^{(g)}$ of (5.6) due to different sorting orders of the data symbols $\underline{d}_n \in \mathbb{D}_g$. In Fig. 5.3 an example for possible group specific selection matrices $\mathbf{S}_{\mathrm{G}}^{(g)}$, $g = 1 \ldots 4$, corresponding to the exemplary subdivision of data symbols in Fig. 5.2 is visualized.

Based on $\mathbf{S}_{\mathrm{G}}^{(g)}$ of (5.6) the group specific system matrices

$$\underline{\mathbf{B}}_{\mathrm{G}}^{(g)} = \mathbf{S}_{\mathrm{G}}^{(g)} \underline{\mathbf{B}}, \ g = 1 \ldots G, \tag{5.7}$$

are established which contain all rows of $\underline{\mathbf{B}}$ of (3.23), which are related to the data symbols $\underline{d}_n \in \mathbb{D}_g$ assigned to group g, $g = 1 \ldots G$. Fig. 5.4 shows an example of the group specific system matrices $\underline{\mathbf{B}}_{\mathrm{G}}^{(g)}$, $g = 1 \ldots G$, for the group specific selection matrices $\mathbf{S}_{\mathrm{G}}^{(g)}$, $g = 1 \ldots 4$, of Fig. 5.3 corresponding to the exemplary subdivision of Fig. 5.2. The group specific continuous valued estimate signal $\widehat{\underline{\mathbf{g}}}_{\mathrm{G}}^{(g)}$ of $\underline{\mathbf{d}}_{\mathrm{G}}^{(g)}$ of (5.6) and its useful part $\underline{\mathbf{g}}_{\mathrm{G}}^{(g)}$ follow by

$$\widehat{\underline{\mathbf{g}}}_{\mathrm{G}}^{(g)} = \mathbf{S}_{\mathrm{G}}^{(g)} \widehat{\underline{\mathbf{g}}} \tag{5.8}$$
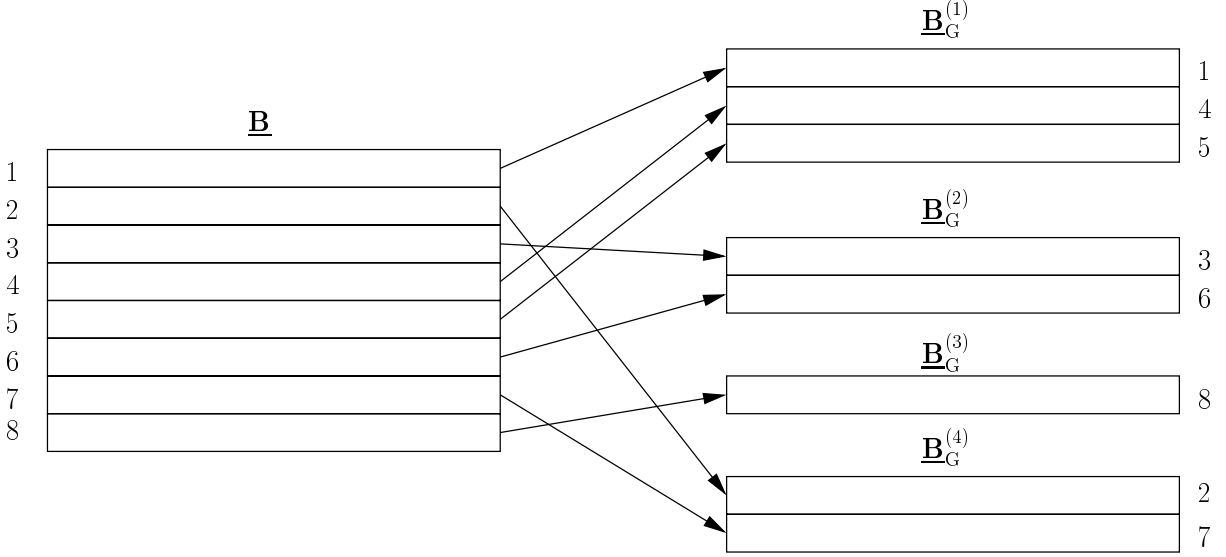
Fig. 5.4. Exemplary group specific system matrices $\underline{\mathbf{B}}_{\mathrm{G}}^{(g)}$, $g = 1 \ldots G$, for the group specific selection matrices $\mathbf{S}_{\mathrm{G}}^{(g)}$, $g = 1 \ldots 4$, of Fig. 5.3 corresponding to the exemplary subdivision of Fig. 5.2

and

$$\underline{\mathbf{g}}_{\mathrm{G}}^{(g)} = \mathbf{S}_{\mathrm{G}}^{(g)} \, \underline{\mathbf{g}} \tag{5.9}$$

using the continuous valued estimate signal $\widehat{\underline{\mathbf{g}}}$ of the total data vector $\underline{\mathbf{d}}$ of (3.3) and its useful part $\underline{\mathbf{g}}$, respectively. We aim at designing the transmit signal $\underline{\mathbf{t}}$ of (5.4) so that in the noisefree case all the continuous valued estimate signal $\widehat{\underline{\mathbf{g}}}$ is the useful part, i.e.

$$\widehat{\underline{\mathbf{g}}} = \underline{\mathbf{g}} \text{ for } \underline{\mathbf{n}} = 0 \tag{5.10}$$

holds. Substitution (5.10) into (5.8) and (5.9) yields

$$\widehat{\underline{\mathbf{g}}}_{\mathrm{G}}^{(g)} = \underline{\mathbf{g}}_{\mathrm{G}}^{(g)} \tag{5.11}$$

for the noisefree case. Quite generally, each component $\underline{g}_{\mathrm{G},n}^{(g)}$ of $\underline{\mathbf{g}}_{\mathrm{G}}^{(g)}$ of (5.11), which represents a specific data symbol $\underline{d}_n \in \mathbb{D}_g$, comes about as the sum of an interference component $\underline{i}_{\mathrm{G},n}^{(g)}$ resulting from the transmission of other data symbols and a component $\underline{\Delta}_{\mathrm{G},n}^{(g)}$ intended for the transmission of this data symbol. Then, we can write

$$\underline{\Delta}_{\mathrm{G},n}^{(g)} = \underline{g}_{\mathrm{G},n}^{(g)} - \underline{i}_{\mathrm{G},n}^{(g)}, n = 1 \ldots \|\mathbb{D}_g\|, \tag{5.12}$$

and term $\underline{\Delta}_{\mathrm{G},n}^{(g)}$ as the correction component necessary to obtain $\underline{g}_{\mathrm{G},n}^{(g)}$ under the influence of the interference $\underline{i}_{\mathrm{G},n}^{(g)}$. In the case with TxZF Filter the interference components $\underline{i}_{\mathrm{G},n}^{(g)}$ are a priori nulled by zero forcing, whereas in the case of TxNZF Filter these components are

deliberately conceded. As will be shown below, they depend on the representatives $\underline{g}_{m,p}$ of the transmit data symbols $\underline{d}_{\mathrm{G},n}^{(g)}$ and influence the choice of the correction components $\underline{\Delta}_{\mathrm{G},n}^{(g)}$. This way of generating $\underline{\Delta}_{\mathrm{G},n}^{(g)}$ constitutes the non-linear feature of TxNZF Filter.

In the case of P-fold connected decision regions utilized in the case of TxNZF Filter, for a given value $\underline{i}_{\mathrm{G},n}^{(g)}$ of the interference and a given symbol alphabet $\underline{v}_m$ of the data symbol $\underline{d}_{\mathrm{G},n}^{(g)}$, according to (5.12) and (5.1) , P options for $\underline{\Delta}_{\mathrm{G},n}^{(g)}$ exist. With a view to radiate minimum energy for $\underline{d}_{\mathrm{G},n}^{(g)}$, the one with the smallest magnitude $\left|\underline{\Delta}_{\mathrm{G},n}^{(g)}\right|$ would be chosen, that is

$$\underline{d}_{\mathrm{G},n}^{(g)} = \underline{v}_m \Longrightarrow \underline{g}_{\mathrm{G},n}^{(g)} = \underline{g}_{m,p'}, \ \underline{\Delta}_{\mathrm{G},n}^{(g)} = \underline{g}_{m,p'} - \underline{i}_{\mathrm{G},n}^{(g)}, \ p' = \arg \min_{p \in \{1...P\}} \left\| \underline{g}_{m,p} - \underline{i}_{\mathrm{G},n}^{(g)} \right\|. \quad (5.13)$$

Of course, there are other ways to choose $\underline{\Delta}_{\mathrm{G},n}^{(g)}$, which will be addressed in Section 5.5.

By stacking $\underline{i}_{\mathrm{G},n}^{(g)}$, $n = 1 \ldots \|\mathbb{D}_g\|$, and $\underline{\Delta}_{\mathrm{G},n}^{(g)}$, $n = 1 \ldots \|\mathbb{D}_g\|$, of (5.13) to the vectors

$$\underline{\mathbf{i}}_{\mathrm{G}}^{(g)} = \left(\underline{i}_{\mathrm{G},1}^{(g)} \ldots \underline{i}_{\mathrm{G},\|\mathbb{D}_g\|}^{(g)} \right)^{\mathrm{T}} \quad (5.14)$$

and

$$\underline{\boldsymbol{\Delta}}_{\mathrm{G}}^{(g)} = \left(\underline{\Delta}_{\mathrm{G},1}^{(g)} \ldots \underline{\Delta}_{\mathrm{G},\|\mathbb{D}_g\|}^{(g)} \right)^{\mathrm{T}}, \quad (5.15)$$

respectively, the $\|\mathbb{D}_g\|$ relations of (5.12) are combined to

$$\underline{\boldsymbol{\Delta}}_{\mathrm{G}}^{(g)} = \underline{\mathbf{g}}_{\mathrm{G}}^{(g)} - \underline{\mathbf{i}}_{\mathrm{G}}^{(g)}. \quad (5.16)$$

The basic principle of generating the group specific transmit signal $\underline{\mathbf{t}}_{\mathrm{G}}^{(g)}$ of (5.4) in TxNZF Filter is as follows:

- The group specific transmit signals $\underline{\mathbf{t}}_{\mathrm{G}}^{(g)}$, $g = 1 \ldots G$, of (5.4) are generated one by one, starting with $\underline{\mathbf{t}}_{\mathrm{G}}^{(1)}$. This sorting order implies no lack of generality as any sorting order could be achieved by appropriately relabeling the groups g, $g = 1 \ldots G$. Later, we will show that a proper sorting order of the groups could be beneficial.

- The group specific transmit signal $\underline{\mathbf{t}}_{\mathrm{G}}^{(g)}$ of (5.4) for a certain group g, $g = 1 \ldots G$, is designed in such a way that $\underline{\mathbf{t}}_{\mathrm{G}}^{(g)}$

  - produces no interferences to all data symbols $\underline{d}_n \in \mathbb{D}_{g'}$, $g' < g$, of the previous processed groups,
  - produces no interferences to all data symbols $\underline{d}_n \in \mathbb{D}_g$ assigned to that group, while it generates the corresponding correction components $\underline{\Delta}_{\mathrm{G},n}^{(g)}$ of (5.16) at the demodulator output and
  - may produce interferences to all data symbols $\underline{d}_n \in \mathbb{G}_{g'}$, $g' > g$, of groups to be processed in the following.

As a consequence of this procedure, the interference $\underline{\mathbf{i}}_{\mathrm{G}}^{(g)}$ of (5.14) only results from the transmission of the group specific transmit signals $\underline{\mathbf{t}}_{\mathrm{G}}^{(g')}$, $g' < g$, i.e., can be calculated to be (step 1)

$$\underline{\mathbf{i}}_{\mathrm{G}}^{(g)} = \begin{cases} \mathbf{0}, & g = 1, \\[2ex] \underline{\mathbf{B}}_{\mathrm{G}}^{(g)} \sum_{g'=1}^{g-1} \underline{\mathbf{t}}_{\mathrm{G}}^{(g')}, & g > 1. \end{cases} \tag{5.17}$$

With $\underline{\mathbf{i}}_{\mathrm{G}}^{(g)}$ of (5.17), following (5.13), the correction component $\underline{\boldsymbol{\Delta}}_{\mathrm{G}}^{(g)}$ has to be adjusted (step 2). Let us designate by $[\cdot]_j^i$ a matrix consisting of columns i to j of the matrix in brackets. With the cumulative matrices

$$\underline{\mathbf{B}}_g = \left(\underline{\mathbf{B}}_{\mathrm{G}}^{(1)\,\mathrm{T}} \ldots \underline{\mathbf{B}}_{\mathrm{G}}^{(g)\,\mathrm{T}} \right)^{\mathrm{T}}, \, g = 1 \ldots G, \tag{5.18}$$

and the a posteriori determined group specific modulator matrices

$$\underline{\mathbf{M}}_{\mathrm{G}}^{(g)} = \left[\underline{\mathbf{B}}_g^{\mathrm{H}} \left(\underline{\mathbf{B}}_g \underline{\mathbf{B}}_g^{\mathrm{H}} \right)^{-1} \right]_{\|\mathbb{G}_1 \cup \ldots \cup \mathbb{G}_g\|}^{\|\mathbb{G}_1 \cup \ldots \cup \mathbb{G}_{g-1}\|+1} \tag{5.19}$$

the group specific transmit signal $\underline{\mathbf{t}}_{\mathrm{G}}^{(g)}$ of group g can be calculated (step 3) as

$$\underline{\mathbf{t}}_{\mathrm{G}}^{(g)} = \underline{\mathbf{M}}_{\mathrm{G}}^{(g)} \underline{\boldsymbol{\Delta}}_{\mathrm{G}}^{(g)}. \tag{5.20}$$

$\underline{\mathbf{M}}_{\mathrm{G}}^{(g)}$ of (5.19) is derived as shown in the Appendix A.3. Repeating the steps 1 to 3 for all groups g, $g = 1 \ldots G$, G group specific transmit signals $\underline{\mathbf{t}}_{\mathrm{G}}^{(g)}$ are determined. Then, based on (5.6) and (5.20) follows the total transmit signal (step 4)

$$\underline{\mathbf{t}}_{\mathrm{G}} = \sum_{g=1}^{G} \underline{\mathbf{t}}_{\mathrm{G}}^{(g)} = \sum_{g=1}^{G} \underline{\mathbf{M}}_{\mathrm{G}}^{(g)} \, \underline{\boldsymbol{\Delta}}_{\mathrm{G}}^{(g)} \tag{5.21}$$

by (5.4).

The energy of the total transmit signal $\underline{\mathbf{t}}$ of (5.4) becomes

$$T = \frac{1}{2}\underline{\mathbf{t}}^{\mathrm{H}}\underline{\mathbf{t}} = \sum_{g=1}^{G} \underbrace{\frac{1}{2}\underline{\mathbf{t}}_{\mathrm{G}}^{(g)\,\mathrm{H}} \underline{\mathbf{t}}_{\mathrm{G}}^{(g)}}_{T_{\mathrm{G}}^{(g)}}. \tag{5.22}$$

Surprisingly, the energy T of the total transmit signal is only the sum of the energies $T_{\mathrm{G}}^{(g)}$ of the group specific transmit signals $\underline{\mathbf{t}}_{\mathrm{G}}^{(g)}$. This results from the fact that due to the design strategy followed in the case of TxNZF Filter the group specific transmit signals $\underline{\mathbf{t}}_{\mathrm{G}}^{(g)}$ and $\underline{\mathbf{t}}_{\mathrm{G}}^{(g')}$ of two different groups g and g', $g \neq g'$, respectively, are orthogonal.

The entire algorithm constituted by the steps 1 to 4 forms the mapping of the total data vector $\underline{\mathbf{d}}$ on the total transmit signal $\underline{\mathbf{t}}$ in the case of TxNZF Filter. Therefore, these steps describe the corresponding Tx operator $\mathcal{M}\{\cdot\}$ of (3.7). $\mathcal{M}\{\cdot\}$ is illustrated in a self explanatory comprehensive form by the Nassi-Shneiderman diagram [NS73] of Fig. 5.5.

$$
\boxed{
\begin{array}{l}
\text{for } g := 1 \ldots G \\[4pt]
\hline
\begin{array}{c}
g = 1 \\
\text{Y} \diagdown \qquad\qquad\qquad \diagup \text{N}
\end{array} \\[4pt]
\hline
\begin{array}{c|c}
\underline{\mathbf{i}}_{\mathrm{G}}^{(g)} := \mathbf{0} & \underline{\mathbf{i}}_{\mathrm{G}}^{(g)} := \underline{\mathbf{B}}_{\mathrm{G}}^{(g)} \sum_{g'=1}^{g-1} \underline{\mathbf{t}}_{\mathrm{G}}^{(g')}
\end{array} \\[4pt]
\hline
\text{Calculation of } \underline{\boldsymbol{\Delta}}_{\mathrm{G}}^{(g)} \text{ by } (5.13) \\[4pt]
\hline
\text{Determination of } \underline{\mathbf{M}}_{\mathrm{G}}^{(g)} \text{ by } (5.19) \\[4pt]
\hline
\underline{\mathbf{t}}_{\mathrm{G}}^{(g)} := \underline{\mathbf{M}}_{\mathrm{G}}^{(g)} \underline{\boldsymbol{\Delta}}_{\mathrm{G}}^{(g)} \\[4pt]
\hline
\underline{\mathbf{t}} = \sum_{g=1}^{G} \underline{\mathbf{t}}_{\mathrm{G}}^{(g)}
\end{array}
}
$$
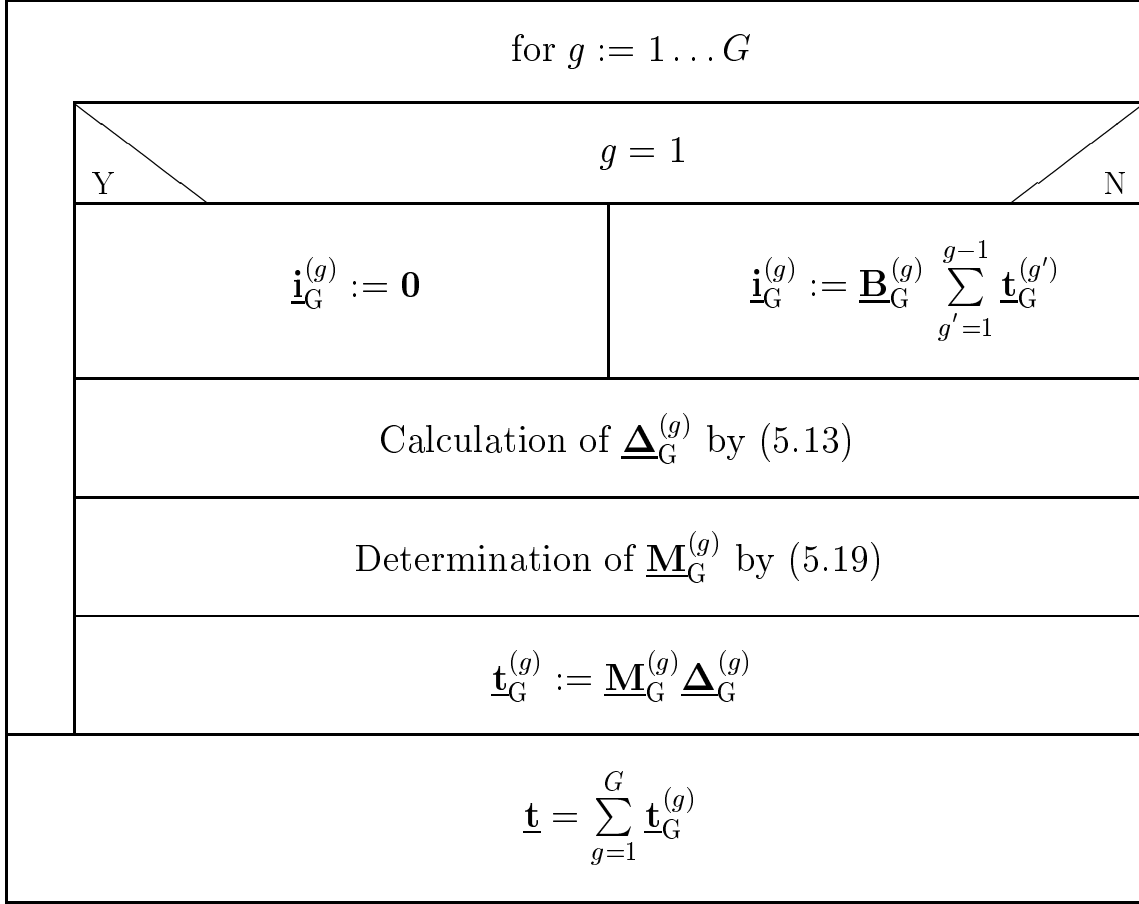
Fig. 5.5. Nassi-Shneiderman diagram describing the Tx operator $\mathcal{M}\{\cdot\}$ for TxNZF Filter, i.e., the generation of the transmit signal $\underline{\mathbf{t}}$ in the case of TxNZF Filter

5.2.2 Benefits and potentials of TxNZF Filter

TxNZF Filter has a high potential with respect to the achievable transmission performance –, e.g. for a required transmission quality to reduce the necessary transmit energy T of (3.9). This potential mainly results from the reduced constraints while designing the transmit signal $\underline{\mathbf{t}}$. When designing the group specific transmit signal $\underline{\mathbf{t}}_{\mathrm{G}}^{(g)}$ of group g, for each data symbol $\underline{d}_n \in \mathbb{D}_g$ only interferences produced to $(\|\mathbb{D}_1 \cup \ldots \cup \mathbb{D}_g\| - 1)$ other data symbols $\underline{d}_{n'} \in \mathbb{D}_{g'}$, $g' \le g$, $n' \ne n$, have to be taken into account. That means that the number of interference constraints for designing of the group specific transmit signal $\underline{\mathbf{t}}_{\mathrm{G}}^{(g)}$ is $(\|\mathbb{D}_1 \cup \ldots \cup \mathbb{D}_g\| - 1)$. For these interference constraints of data groups g, $g = 1 \ldots G$,

$$(\|\mathbb{D}_1\| - 1) < \cdots < (\|\mathbb{D}_1 \cup \ldots \cup \mathbb{D}_{G-1}\| - 1) < (\|\mathbb{D}_1 \cup \ldots \cup \mathbb{D}_G\| - 1) = N_{\mathrm{t}} - 1 \quad (5.23)$$

holds. Therefore, based on the knowledge obtained in Chapters 3 and 4, we can see

$$\overline{\eta}_{\mathrm{Tx}}^{(1)} > \overline{\eta}_{\mathrm{Tx}}^{(2)} > \cdots > \overline{\eta}_{\mathrm{Tx}}^{(G)} \tag{5.24}$$

and can conclude:

- the average Tx efficiency $\overline{\eta}_{\mathrm{Tx}}^{(g)}$ of TxNZF Filter is always larger than or at least equal to $\overline{\eta}_{\mathrm{Tx}}$ of TxZF Filter.

- groups g which are processed first, i.e., which have low group indices g, are processed with Tx efficiencies $\overline{\eta}_{\mathrm{Tx}}^{(g)}$ of almost one.

- groups g which are processed last, i.e., which have rather high group indices close to G are processed with lower Tx efficiencies $\overline{\eta}_{\mathrm{Tx}}^{(g)}$. However, $\overline{\eta}_{\mathrm{Tx}}^{(g)}$ is never smaller than $\overline{\eta}_{\mathrm{Tx}}$ of TxZF Filter.

These conclusions are a strong motivation to have a closer look at a rather usual situation in typical mobile radio systems, where the channel attenuations for the channels between the BS and the different MTs k, $k = 1 \ldots K$, differ significantly from each other – sometimes by orders of magnitude –, which is usually the case due to shadowing and/or largely different distances between the BS and the MTs. In what follows we use as a measure corresponding to the channel attenuations but being not the channel attenuations the quantities

$$\alpha^{(k)} = \left(\sum_{k_{\mathrm{M}}=1}^{K_{\mathrm{M}}} \sum_{k_{\mathrm{B}}=1}^{K_{\mathrm{B}}} \left\| \underline{\mathbf{h}}^{(k, k_{\mathrm{B}}, k_{\mathrm{M}})} \right\|^2 \right)^{-1}. \tag{5.25}$$

Let us assume that the K MTs are labeled in such a way that

$$\alpha^{(1)} \geq \alpha^{(2)} \geq \cdots \geq \alpha^{(K)} \tag{5.26}$$

is valid. Then, a favorable choice for the subdivision of $\mathbb{D}$ would be to introduce G equal to K groups, where each group g, $g = 1 \ldots G$, corresponds to a single MT g and combines the data symbols $\underline{d}_n$, $n = (k-1)N \ldots kN$, of that MT g, i.e.,

$$\mathbb{D}_g = \left\{ \underline{d}_{(k-1)N+1} \cdots \underline{d}_{kN} \right\}. \tag{5.27}$$

When doing so, in the case of TxNZF Filter there is the tendency that the energies $T_{\mathrm{G}}^{(g)}$ of the group specific transmit signals $\underline{\mathbf{t}}_{\mathrm{G}}^{(g)}$, $g = 1 \ldots G$, increase with decreasing g due to the necessity to overcome the increasing channel attenuations. However, as explained above, also the Tx efficiencies $\eta_{\mathrm{Tx},\,n}^{(g)}$ increase with decreasing g so that the group specific transmit signals $\underline{\mathbf{t}}_{\mathrm{G}}^{(g)}$ of basically high energies are endowed with high Tx efficiencies. This combination of originally high required transmit energies and high Tx efficiencies is one of the keys to the aspired reduction of the required transmit energy T typical of TxNZF Filter.
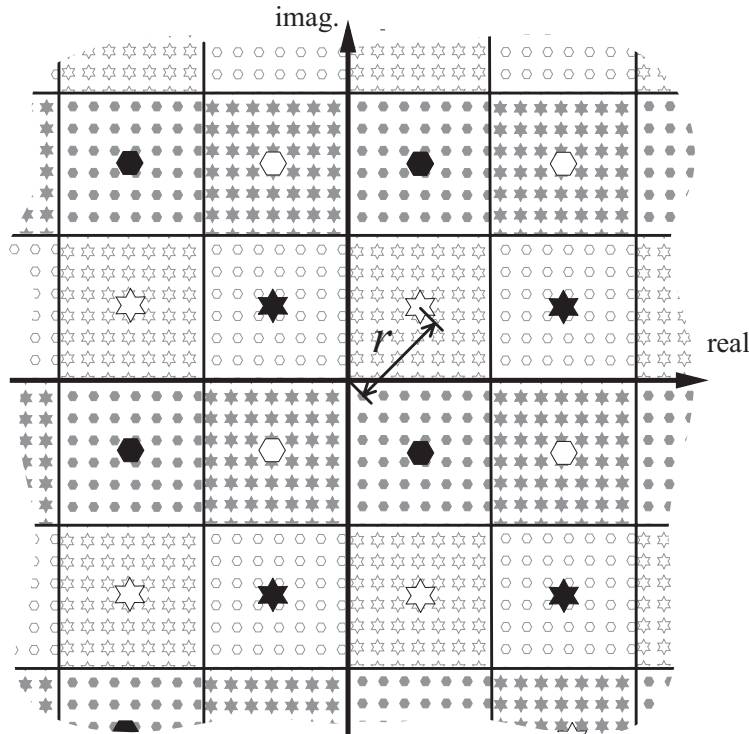
Fig. 5.6. Quadratic multiply connected quantization scheme

5.3 Performance analysis of TxNZF Filter by simulations

In this section, we will study the performance of TxNZF Filter with the subdivision $\mathbb{D}_g$ of (5.27) by simulations for exemplary scenarios with totally uncorrelated channel impulse responses, see Sections 2.3.1 and 2.3.2. In this way we can illustrate the advantage of TxNZF Filter over TxZF Filter with respect to the required transmit energy. The system parameters considered in these simulations are listed in Table 5.1. A large number of statistically independent snapshots is evaluated according to the following side conditions:

Table 5.1. System parameters for the simulations

M	N	Q_t	K	K_B	K_M	W
4	4	16	8	2	1	5

- The $N(Q_t + W - 1)$ elements of $\underline{\mathbf{D}}^{(k)}$ of (4.27) are derived from an orthonormal set of N binary sequences of dimension $Q_t + W - 1$. The N rows of $\underline{\mathbf{D}}^{(k)}$ are obtained by scrambling the N sequences of this set by a random MT specific scrambling code of dimension $Q_t + W - 1$. The elements of this scrambling code have magnitude one.

- The KK_BW elements of the channel impulse responses $\underline{\mathbf{h}}^{(k,k_B,1)}$ are obtained by randomly generating independent bivariate Gaussian numbers with zero mean and identical variance. However, in order to model the different channel attenuations $\alpha^{(k)}$ of (5.25) the generated channel impulse responses $\underline{\mathbf{h}}^{(k,k_B,1)}$ are normalized in such a way that

$$\left\| \underline{\mathbf{h}}^{(1,k_B,1)} \right\|^2 = 1, \ k_B = 1 \ldots K_B, \tag{5.28}$$

and

$$10 \log_{10} \left(\frac{\left\| \underline{\mathbf{h}}^{(k,k_B,1)} \right\|^2}{\left\| \underline{\mathbf{h}}^{(k-1,k_B,1)} \right\|^2} \right) = \begin{cases} 0 \text{ dB} & \text{(case 1)}, \\ 3 \text{ dB} & \text{(case 2)}, \\ 6 \text{ dB} & \text{(case 3)}, \\ \quad k = 2 \ldots K, \end{cases} \tag{5.29}$$

hold.

- The multiply connected quantization scheme considered in the simulations is a quadratic multiply connected quantization scheme as depicted in Fig. 5.6. For the sake of comparability the considered simply connected quantization scheme corresponds to the modulation scheme QPSK. The multiply connected and the simply connected quantization schemes are made consistent in the sense that the four representatives of the multiply connected quantization scheme closest to the origin and the four representatives of the simply connected quantization scheme are chosen identical with the distance

$$r = 1, \tag{5.30}$$

see Fig. 5.6.

The average required transmit energy of TxZF Filter obtained by averaging over many snapshots characterized by randomly determined $\underline{\mathbf{h}}^{(k,k_B,1)}$ and $\underline{\mathbf{D}}^{(k)}$, see above, is termed $\overline{T}_{\text{TxZF}}$. Figs. 5.7 to 5.9 show for the three cases of (5.29) the cumulative distribution functions of the ratio $T/\overline{T}_{\text{TxZF}}$ for the TxZF Filter and the TxNZF Filter, respectively. As expected, the TxNZF Filter does with significantly lower transmit energies than the TxZF Filter. This superiority of TxNZF Filter increases with increasing differences between consecutive channel attenuations $\alpha^{(k)}$, $k = 1 \ldots K$, of (5.25) and (5.26), because, when proceeding from MT k to MT $k+1$, see the explanation in Subsection 5.2.2, the decrease of the Tx efficiency $\eta_{\text{Tx},n}^{(k)}$ is more and more mitigated by an simultaneously decreasing channel attenuation.

It is well known [CS85] that in the case of two consistently chosen simply connected and multiply connected quantization schemes subject to identical noise with the power σ^2,
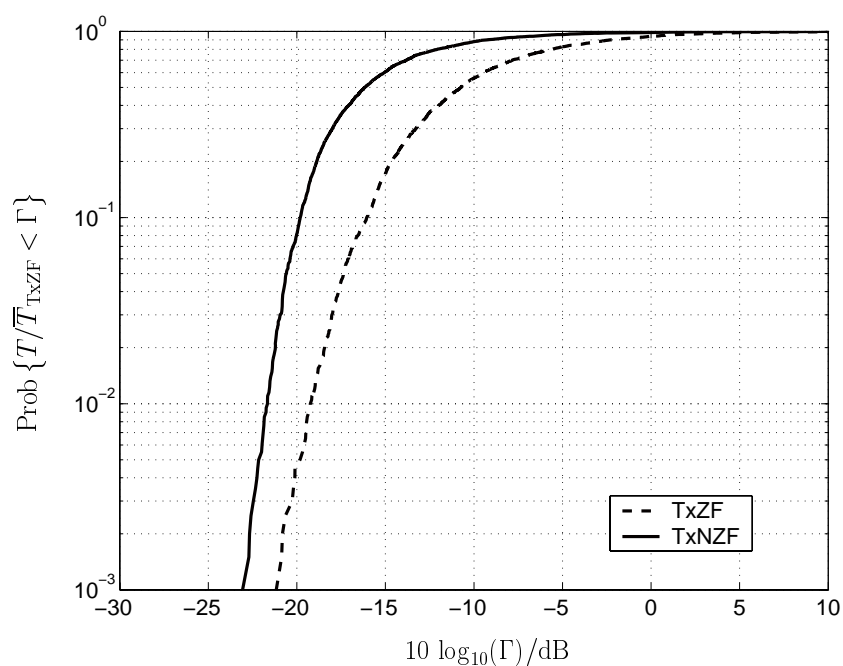
Fig. 5.7. Cumulative distribution functions of the normalized required transmit energy $T/\overline{T}_{\mathrm{TxZF}}$, case 1
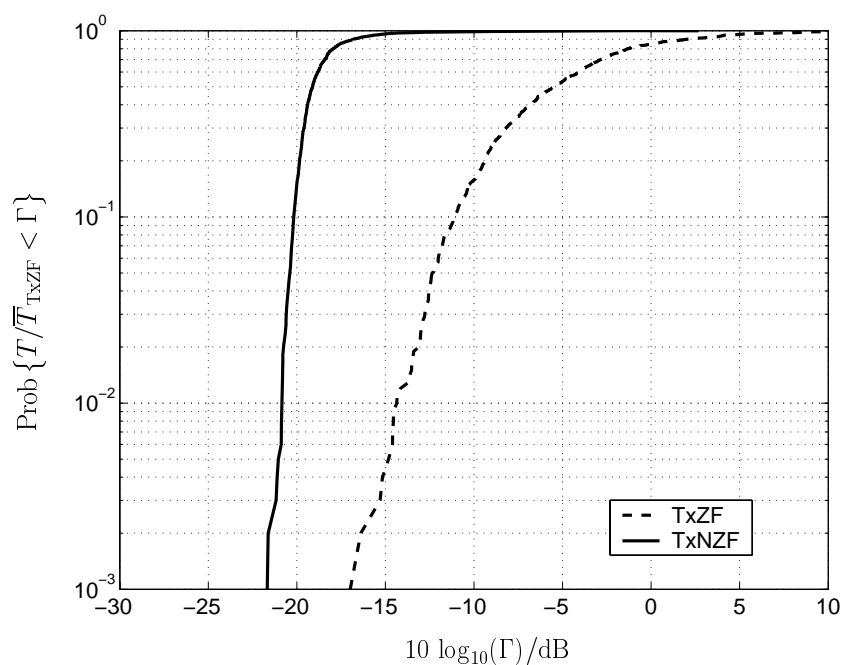
Fig. 5.8. Cumulative distribution functions of the normalized required transmit energy $T/\overline{T}_{\mathrm{TxZF}}$, case 2
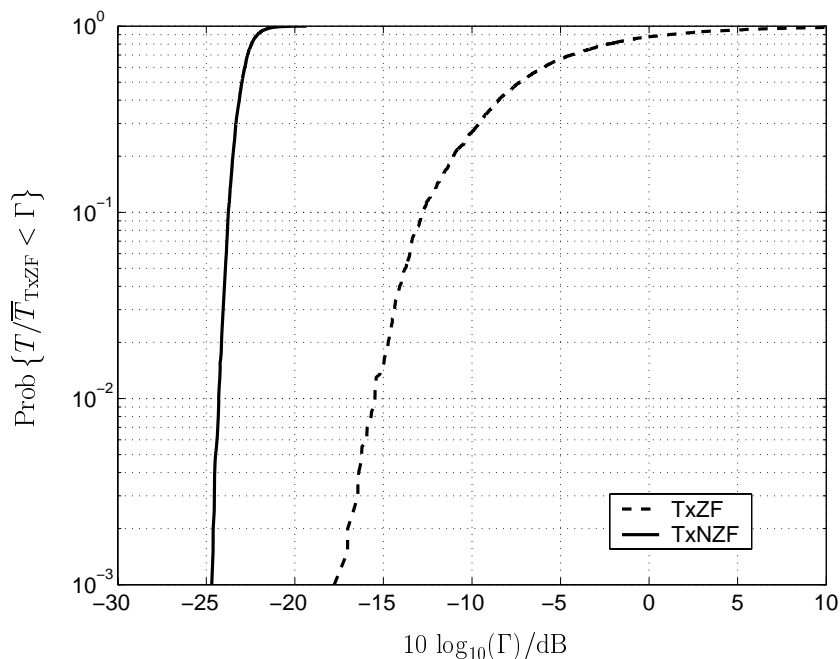
Fig. 5.9. Cumulative distribution functions of the normalized required trans-
mit energy $T/\overline{T}_{\mathrm{TxZF}}$, case 3

the latter exhibits a somewhat larger error probability, because the demodulator output
signals are more prone to land in a wrong decision region. With the quantity

$$\Pi = \frac{r^2}{2\sigma^2} \tag{5.31}$$

Fig. 5.10 illustrates the BER loss of the selected unconventional multiply connected quan-
tization scheme over the conventional simply connected quantization scheme.

To a certain degree this effect counteracts the energy advantage of the TxNZF Filter over
the TxZF Filter illustrated in Figs. 5.7 to 5.9 and should be studied. To this purpose we
again consider the cases 1 to 3 of (5.29). We designate the average of the transmit energy
T as $\overline{T}$ and assume that the total received noise $\underline{\mathbf{n}}$ of (4.17) is white and Gaussian with
zero mean and the variance σ^2 [BQT$^+$03]. Then, the pseudo SNR, which is defined as the
ratio of the average transmitted bit energy to σ^2, becomes

$$\gamma = \frac{\overline{T}/\left[\mathrm{ld}(M)KN\right]}{\sigma^2}. \tag{5.32}$$

In Figs. 5.11 to 5.13, the bit error rate P_{b} is shown versus γ of (5.32) for the cases 1 to 3
of (5.29). From these curves we can conclude the following:

- For sufficiently large values of γ of (5.32), TxNZF Filter always outperforms TxZF
  Filter.

- As in the case of the required transmit energies, see Figs. 5.7 to 5.9, the superi-
  ority of TxNZF Filter increases with increasing differences of consecutive channel
  attenuations $\alpha^{(k)}$ of (5.25) and (5.26).
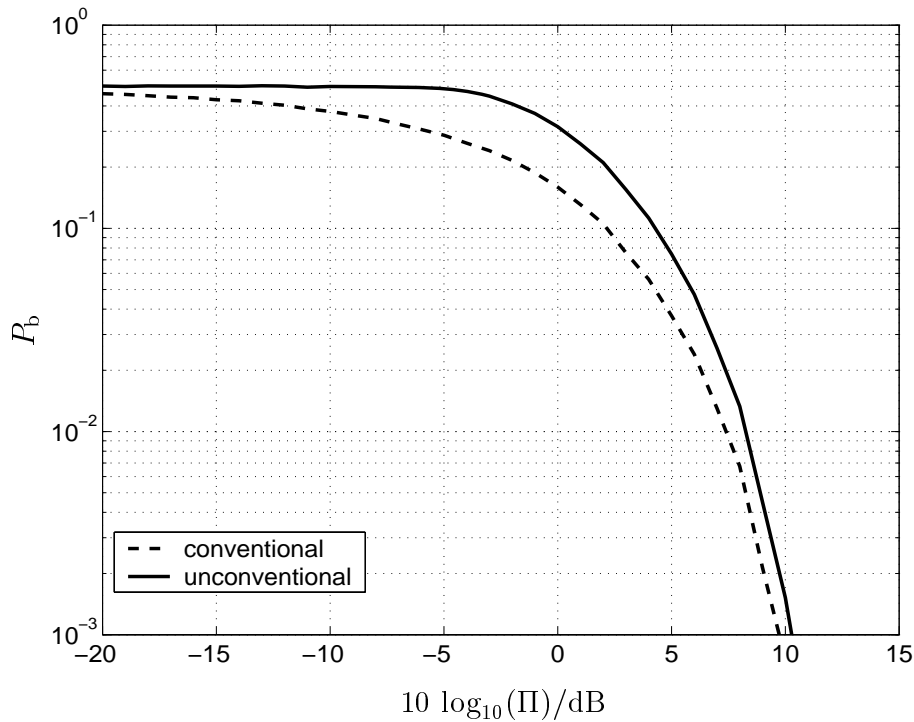
Fig. 5.10. BER loss of the selected unconventional multiply connected quantization scheme over the conventional simply connected quantization scheme

- As becoming apparent by Fig. 5.11, at low values of γ of (5.32) and low increments of the channel attenuations $\alpha^{(k)}$ of (5.25) and (5.26), TxZF Filter may outperform TxNZF Filter. However, this occurs only for values of P_b so large that they are of no practical interest.

The results presented above give a first impression on the potential performance gains of TxNZF Filter over TxZF Filter.

5.4 Cost efficient implementation of TxNZF Filter

In this Section 5.4 we will consider the implementation aspects of the TxNZF Filter. The goal of this section is not to give a complete implementation algorithm of TxNZF Filter but to give some hints which could be used to implement TxNZF Filter in a cost efficient way.

As knowing from Section 5.2 the construction of the transmit signal for TxNZF Filter consists in

- finding the group specific correction vector $\underline{\boldsymbol{\Delta}}_{\mathrm{G}}^{(g)}$ of (5.16) taking the multiply connected quantization scheme into account,
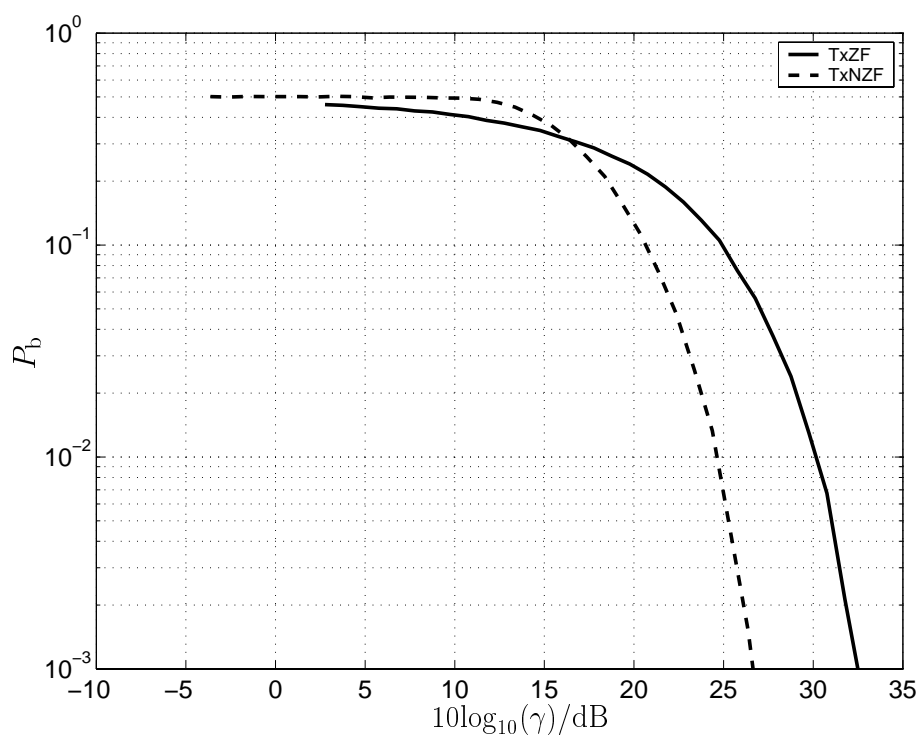
Fig. 5.11. Bit error rate P_b vesus the pseudo SNR γ of (5.32), case 1
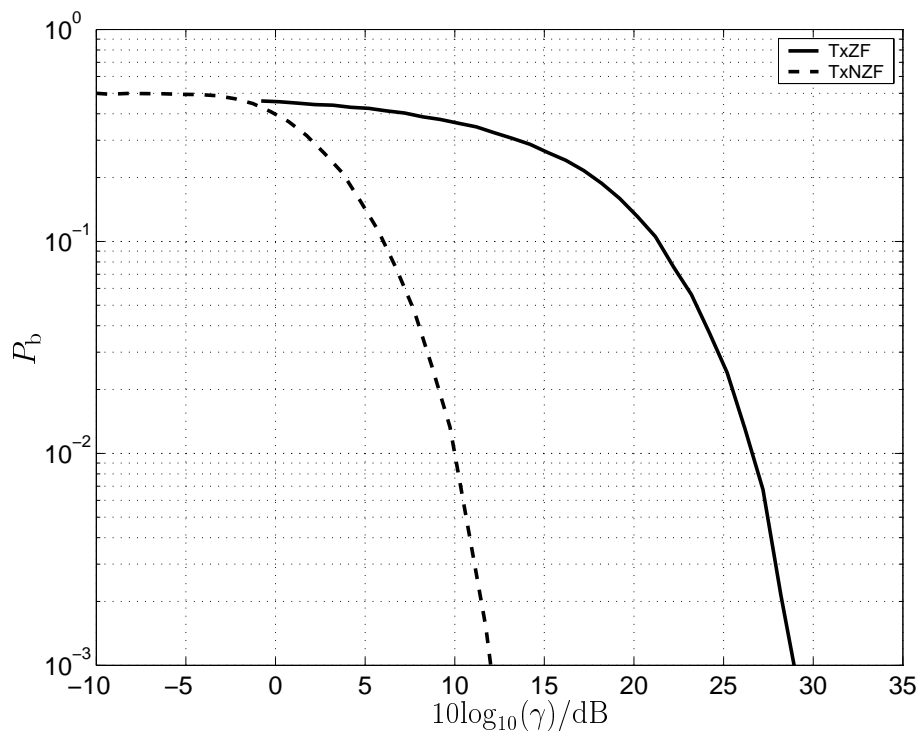
Fig. 5.12. Bit error rate P_b vesus the pseudo SNR γ of (5.32), case 2
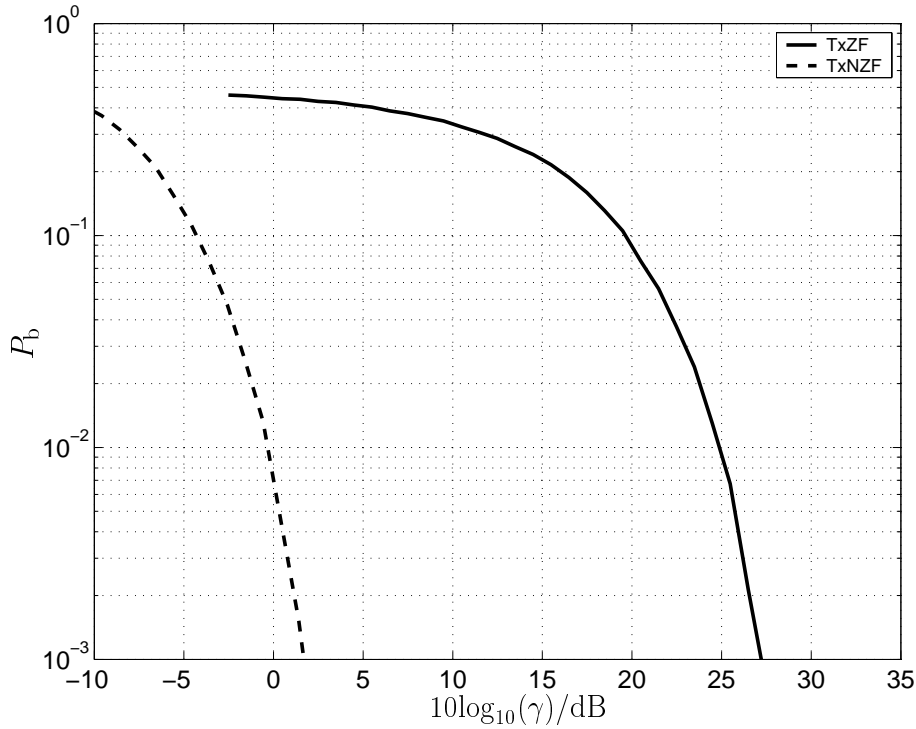
Fig. 5.13. Bit error rate P_b vesus the pseudo SNR γ of (5.32), case 3

- a posteriori determining the group specific modulator matrix

$$\underline{\mathbf{M}}_\mathrm{G}^{(g)} = \left[\underline{\mathbf{B}}_g^\mathrm{H}\left(\underline{\mathbf{B}}_g\,\underline{\mathbf{B}}_g^\mathrm{H}\right)^{-1}\right]_{\|\mathbb{G}_1\cup\ldots\cup\mathbb{G}_g\|}^{\|\mathbb{G}_1\cup\ldots\cup\mathbb{G}_{g-1}\|+1} \qquad (5.33)$$

of (5.19) and

- generating the group specific transmit signal

$$\underline{\mathbf{t}}_\mathrm{G}^{(g)} = \underline{\mathbf{M}}_\mathrm{G}^{(g)}\,\underline{\boldsymbol{\Delta}}_\mathrm{G}^{(g)} \qquad (5.34)$$

of (5.20)

iteratively for the group specific data vectors $\underline{\mathbf{d}}_\mathrm{G}^{(g)}$, $g = 1\ldots G$, of (5.5). Without consideration of the computational complexity for finding the group specific correction vectors $\underline{\boldsymbol{\Delta}}_\mathrm{G}^{(g)}$ in quadratic multiply connected quantization scheme of Fig. 5.6, which is trivial due to (5.13). The determination of G group specific modulator matrices $\underline{\mathbf{M}}_\mathrm{G}^{(g)}$, $g = 1\ldots G$, of (5.33) has the dominant computational complexity for the transmit signal design of the TxNZF Filter. In the following a cost efficient determination of the group specific modulator matrices $\underline{\mathbf{M}}_\mathrm{G}^{(g)}$, $g = 1\ldots G$, is proposed, which leads to a low complex implementation of the TxNZF Filter.

The group specific modulator matrix $\underline{\mathbf{M}}_\mathrm{G}^{(g)}$ of (5.33) is a partial matrix of the pseudo-inverse of the $\|\mathbb{D}_1\cup\cdots\cup\mathbb{D}_g\| \times Q$ cumulative system matrix $\underline{\mathbf{B}}_g$ of (5.18). It is assumed that

$$\|\mathbb{D}_1\cup\cdots\cup\mathbb{D}_G\| = N_\mathrm{t} \le Q \qquad (5.35)$$

holds. Then, $\underline{\mathbf{B}}_g$, $g = 1 \ldots G$, are wide matrices. By applying QR-decomposition $\underline{\mathbf{B}}_g$ of (5.18) can be expressed with a $(\|\mathbb{D}_1 \cup \cdots \cup \mathbb{D}_g\|) \times (\|\mathbb{D}_1 \cup \cdots \cup \mathbb{D}_g\|)$ low triangular matrix $\underline{\mathbf{R}}_g$ and a $Q \times Q$ unitary matrix $\underline{\mathbf{Q}}_g$ as

$$\underline{\mathbf{B}}_g = \left(\underline{\mathbf{R}}_g, \mathbf{0}^{\|\mathbb{D}_1 \cup \cdots \cup \mathbb{D}_g\| \times (Q - \|\mathbb{D}_1 \cup \cdots \cup \mathbb{D}_g\|)} \right) \underline{\mathbf{Q}}_g. \tag{5.36}$$

If we define a $\|\mathbb{D}_1 \cup \cdots \cup \mathbb{D}_g\| \times Q$ partial matrix

$$\underline{\mathbf{Q}}_{\text{eff}, g} = \left(\mathbf{I}^{(\|\mathbb{D}_1 \cup \cdots \cup \mathbb{D}_g\|)}, \mathbf{0}^{(\|\mathbb{D}_1 \cup \cdots \cup \mathbb{D}_g\|) \times (Q - \|\mathbb{D}_1 \cup \cdots \cup \mathbb{D}_g\|)} \right) \underline{\mathbf{Q}}_g, \tag{5.37}$$

which contains the first $\|\mathbb{D}_1 \cup \cdots \cup \mathbb{D}_g\|$ rows of the matrix $\underline{\mathbf{Q}}_g$ in (5.37), then, (5.36) can be equivalently written as

$$\underline{\mathbf{B}}_g = \underline{\mathbf{R}}_g \, \underline{\mathbf{Q}}_{\text{eff}, g}, \tag{5.38}$$

which is termed effective QR-decomposition of $\underline{\mathbf{B}}_g$ in the following. Substituting (5.38) into (5.33), we obtain

$$
\begin{aligned}
\underline{\mathbf{M}}_{\text{G}}^{(g)} &= \left[\left(\underline{\mathbf{R}}_g \, \underline{\mathbf{Q}}_{\text{eff}, g} \right)^{\text{H}} \left[\underline{\mathbf{R}}_g \, \underline{\mathbf{Q}}_{\text{eff}, g} \left(\underline{\mathbf{R}}_g \, \underline{\mathbf{Q}}_{\text{eff}, g} \right)^{\text{H}} \right]^{-1} \right]_{\|\mathbb{D}_1 \cup \cdots \cup \mathbb{D}_g\|}^{\|\mathbb{D}_1 \cup \cdots \cup \mathbb{D}_{g-1}\| + 1} \\
&= \left[\underline{\mathbf{Q}}_{\text{eff}, g}^{\text{H}} \, \underline{\mathbf{R}}_g^{\text{H}} \left(\underline{\mathbf{R}}_g \, \underline{\mathbf{Q}}_{\text{eff}, g} \, \underline{\mathbf{Q}}_{\text{eff}, g}^{\text{H}} \, \underline{\mathbf{R}}_g^{\text{H}} \right)^{-1} \right]_{\|\mathbb{D}_1 \cup \cdots \cup \mathbb{D}_g\|}^{\|\mathbb{D}_1 \cup \cdots \cup \mathbb{D}_{g-1}\| + 1}.
\end{aligned}
\tag{5.39}
$$

Noticing that $\underline{\mathbf{Q}}_{\text{eff}, g}$ of (5.37) is a part of the unitary matrix $\underline{\mathbf{Q}}_g$ of (5.36) and satisfies the relation

$$\underline{\mathbf{Q}}_{\text{eff}, g} \, \underline{\mathbf{Q}}_{\text{eff}, g}^{\text{H}} = \mathbf{I}^{(\|\mathbb{D}_1 \cup \cdots \cup \mathbb{D}_g\|)}, \tag{5.40}$$

and that $\underline{\mathbf{R}}_g$ is a invertible matrix, (5.39) can be further written as

$$
\begin{aligned}
\underline{\mathbf{M}}_{\text{G}}^{(g)} &= \left[\underline{\mathbf{Q}}_{\text{eff}, g}^{\text{H}} \, \underline{\mathbf{R}}_g^{\text{H}} \left(\underline{\mathbf{R}}_g \, \mathbf{I}^{(\|\mathbb{D}_1 \cup \cdots \cup \mathbb{D}_g\|)} \, \underline{\mathbf{R}}_g^{\text{H}} \right)^{-1} \right]_{\|\mathbb{D}_1 \cup \cdots \cup \mathbb{D}_g\|}^{\|\mathbb{D}_1 \cup \cdots \cup \mathbb{D}_{g-1}\| + 1} \\
&= \left[\underline{\mathbf{Q}}_{\text{eff}, g}^{\text{H}} \, \underline{\mathbf{R}}_g^{-1} \right]_{\|\mathbb{D}_1 \cup \cdots \cup \mathbb{D}_g\|}^{\|\mathbb{D}_1 \cup \cdots \cup \mathbb{D}_{g-1}\| + 1}.
\end{aligned}
\tag{5.41}
$$

With (5.41) the pseudo-inverse necessary to find each $\underline{\mathbf{M}}_{\text{G}}^{(g)}$, $g = 1 \ldots G$, can be performed in three steps:

- performing QR-decomposition of $\underline{\mathbf{B}}_g$ of (5.18) to obtain the low triangular matrix $\underline{\mathbf{R}}_g$ and the matrix $\underline{\mathbf{Q}}_{\text{eff}, g}$,
- determination of the inverse of the low triangular matrix $\underline{\mathbf{R}}_g$, $-$ which can be performed in a quite simple manner due to the triangular structure of $\underline{\mathbf{R}}_g$ $-$, and
- multiplication of $\underline{\mathbf{Q}}_{\text{eff}, g}^{\text{H}}$ and $\underline{\mathbf{R}}_g^{-1}$.

It is not necessary to perform the QR-decompositions separately for all $\underline{\mathbf{B}}_g$, $g = 1 \ldots G$, of (5.18) and to determine the inverses of all $\underline{\mathbf{R}}_g$, $g = 1 \ldots G$, of (5.36). The reason is as follows:

The cumulative system matrix $\underline{\mathbf{B}}_g$ of (5.18) can be constructed by the $(\|\mathbb{D}_1 \cup \cdots \cup \mathbb{D}_{g-1}\| \times Q)$ cumulative system matrix $\underline{\mathbf{B}}_{g-1}$ and the group specific system matrix $\underline{\mathbf{B}}_{\mathrm{G}}^{(g)}$ as:

$$\underline{\mathbf{B}}_g = \begin{pmatrix} \underline{\mathbf{B}}_{g-1} \\ \underline{\mathbf{B}}^{(g)} \end{pmatrix}. \tag{5.42}$$

The effective QR-decomposition of $\underline{\mathbf{B}}_g$ can be rewritten as

$$
\begin{aligned}
\underline{\mathbf{B}}_g &= \underline{\mathbf{R}}_g \, \underline{\mathbf{Q}}_{\mathrm{eff},\,g} \\[2mm]
&= \begin{pmatrix} \left([\underline{\mathbf{R}}_g^{\mathrm{T}}]_{\|\mathbb{D}_1 \cup \cdots \cup \mathbb{D}_{g-1}\|}^{1} \right)^{\mathrm{T}} \\ \left([\underline{\mathbf{R}}_g^{\mathrm{T}}]_{\|\mathbb{D}_1 \cup \cdots \cup \mathbb{D}_g\|}^{\|\mathbb{D}_1 \cup \cdots \cup \mathbb{D}_{g-1}\|+1} \right)^{\mathrm{T}} \end{pmatrix} \underline{\mathbf{Q}}_{\mathrm{eff},\,g} \\[2mm]
&= \begin{pmatrix} \left([\underline{\mathbf{R}}_g^{\mathrm{T}}]_{\|\mathbb{D}_1 \cup \cdots \cup \mathbb{D}_{g-1}\|}^{1} \right)^{\mathrm{T}} \underline{\mathbf{Q}}_{\mathrm{eff},\,g} \\ \left([\underline{\mathbf{R}}_g^{\mathrm{T}}]_{\|\mathbb{D}_1 \cup \cdots \cup \mathbb{D}_g\|}^{\|\mathbb{D}_1 \cup \cdots \cup \mathbb{D}_{g-1}\|+1} \right)^{\mathrm{T}} \underline{\mathbf{Q}}_{\mathrm{eff},\,g} \end{pmatrix}.
\end{aligned}
\tag{5.43}
$$

The upper partial matrix $\left([\underline{\mathbf{R}}_g^{\mathrm{T}}]_{\|\mathbb{D}_1 \cup \cdots \cup \mathbb{D}_{g-1}\|}^{1} \right)^{\mathrm{T}} \underline{\mathbf{Q}}_{\mathrm{eff},\,g}$ in (5.43) has the dimension $(\|\mathbb{D}_1 \cup \cdots \cup \mathbb{D}_{g-1}\|) \times Q$. Comparing (5.42) and (5.43), we obtain

$$\underline{\mathbf{B}}_{g-1} = \left([\underline{\mathbf{R}}_g^{\mathrm{T}}]_{\|\mathbb{D}_1 \cup \cdots \cup \mathbb{D}_{g-1}\|}^{1} \right)^{\mathrm{T}} \underline{\mathbf{Q}}_{\mathrm{eff},\,g}. \tag{5.44}$$

Noticing that $\underline{\mathbf{R}}_g$ is a low triangular matrix, the left $(\|\mathbb{D}_1 \cup \cdots \cup \mathbb{D}_{g-1}\|) \times (\|\mathbb{D}_1 \cup \cdots \cup \mathbb{D}_{g-1}\|)$ partial matrix $\left[\left([\underline{\mathbf{R}}_g^{\mathrm{T}}]_{\|\mathbb{D}_1 \cup \cdots \cup \mathbb{D}_{g-1}\|}^{1} \right)^{\mathrm{T}} \right]_{\|\mathbb{D}_1 \cup \cdots \cup \mathbb{D}_{g-1}\|}^{1}$ of $\left([\underline{\mathbf{R}}_g^{\mathrm{T}}]_{\|\mathbb{D}_1 \cup \cdots \cup \mathbb{D}_{g-1}\|}^{1} \right)^{\mathrm{T}}$ is also a low triangular matrix and the rest part of this matrix contains all zeros. Therefore, (5.44) can be equivalently written as

$$
\begin{aligned}
\underline{\mathbf{B}}_{g-1} &= \left(\left[\left([\underline{\mathbf{R}}_g^{\mathrm{T}}]_{\|\mathbb{D}_1 \cup \cdots \cup \mathbb{D}_{g-1}\|}^{1} \right)^{\mathrm{T}} \right]_{\|\mathbb{D}_1 \cup \cdots \cup \mathbb{D}_{g-1}\|}^{1} , \mathbf{0}^{(\|\mathbb{D}_1 \cup \cdots \cup \mathbb{D}_{g-1}\|) \times (Q - \|\mathbb{D}_1 \cup \cdots \cup \mathbb{D}_{g-1}\|)} \right) \\[2mm]
&\quad \cdot \begin{pmatrix} \left([\underline{\mathbf{Q}}_{\mathrm{eff},\,g}^{\mathrm{T}}]_{\|\mathbb{D}_1 \cup \cdots \cup \mathbb{D}_{g-1}\|}^{1} \right)^{\mathrm{T}} \\ \left([\underline{\mathbf{Q}}_{\mathrm{eff},\,g}^{\mathrm{T}}]_{\|\mathbb{D}_1 \cup \cdots \cup \mathbb{D}_g\|}^{\|\mathbb{D}_1 \cup \cdots \cup \mathbb{D}_{g-1}\|+1} \right)^{\mathrm{T}} \end{pmatrix} \\[2mm]
&= \left[\left([\underline{\mathbf{R}}_g^{\mathrm{T}}]_{\|\mathbb{D}_1 \cup \cdots \cup \mathbb{D}_{g-1}\|}^{1} \right)^{\mathrm{T}} \right]_{\|\mathbb{D}_1 \cup \cdots \cup \mathbb{D}_{g-1}\|}^{1} \left([\underline{\mathbf{Q}}_{\mathrm{eff},\,g}^{\mathrm{T}}]_{\|\mathbb{D}_1 \cup \cdots \cup \mathbb{D}_{g-1}\|}^{1} \right)^{\mathrm{T}}.
\end{aligned}
\tag{5.45}
$$

Consequently, comparing (5.38) and (5.45) the effective QR-decomposition of $\underline{\mathbf{B}}_{g-1}$ is obtained with the resulting low triangular matrix

$$\underline{\mathbf{R}}_{g-1} = \left[\left([\underline{\mathbf{R}}_g^{\mathrm{T}}]_{\|\mathbb{D}_1 \cup \cdots \cup \mathbb{D}_{g-1}\|}^{1} \right)^{\mathrm{T}} \right]_{\|\mathbb{D}_1 \cup \cdots \cup \mathbb{D}_{g-1}\|}^{1} \tag{5.46}$$
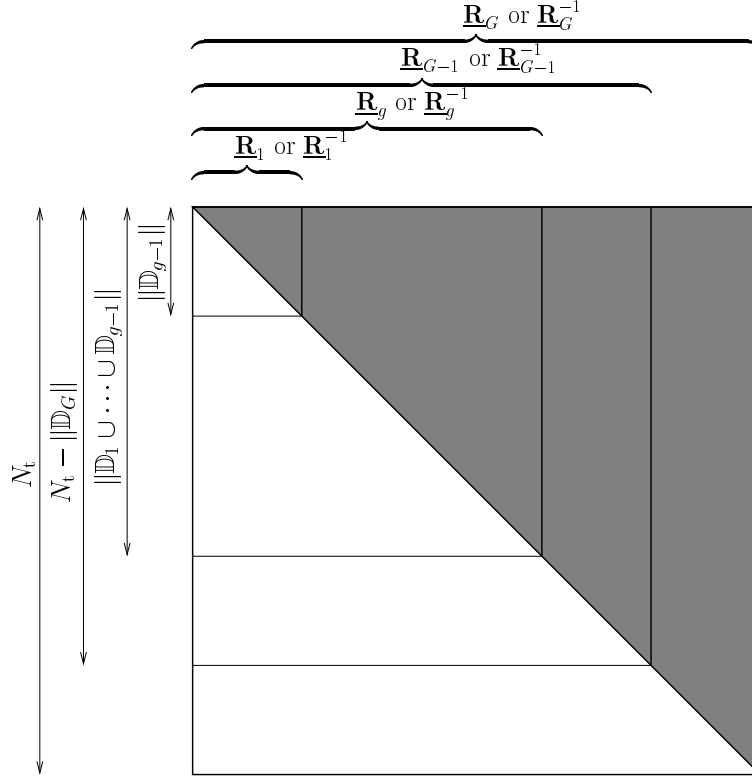
Fig. 5.14. Construction of $\underline{\mathbf{R}}_g$ (or $\underline{\mathbf{R}}_g^{-1}$), $g = 1 \ldots G - 1$, from $\underline{\mathbf{R}}_G$ (or $\underline{\mathbf{R}}_G^{-1}$)

and the effective matrix

$$\underline{\mathbf{Q}}_{\mathrm{eff},\,g-1} = \left(\left[\underline{\mathbf{Q}}_{\mathrm{eff},\,g}^{\mathrm{T}} \right]_{\|\mathbb{D}_1 \cup \cdots \cup \mathbb{D}_{g-1}\|}^{1} \right)^{\mathrm{T}}. \tag{5.47}$$

(5.46) and (5.47) tell us that the effective QR-decompositions of the cumulative system matrices $\underline{\mathbf{B}}_{g'}$, $g' = 1 \ldots g$, of (5.18) can be obtained from the effective QR-decomposition of the cumulative system matrix $\underline{\mathbf{B}}_g$. That means that, only the calculation of effective QR-decomposition of the largest cumulative system matrix $\underline{\mathbf{B}}_G$ is necessary, if we want to find the effective QR-decompositions of all the other cumulative matrices $\underline{\mathbf{B}}_g$, $g = 1 \ldots G$. Fig. 5.14 and Fig. 5.15 show the construction of $\underline{\mathbf{R}}_g$ and $\underline{\mathbf{Q}}_{\mathrm{eff},\,g}$, $g = 1 \ldots G - 1$, based on $\underline{\mathbf{R}}_G$ and $\underline{\mathbf{Q}}_{\mathrm{eff},\,G}$, respectively.

Concerning the inverse of the low triangular matrix $\underline{\mathbf{R}}_g$, we have

$$\underline{\mathbf{R}}_g \, \underline{\mathbf{R}}_g^{-1} = \mathbf{I}^{(\|\mathbb{D}_1 \cup \cdots \cup \mathbb{D}_g\|)}. \tag{5.48}$$

Therefore, the first $\|\mathbb{D}_1 \cup \cdots \cup \mathbb{D}_{g-1}\|$ rows of $\underline{\mathbf{R}}_g$ and the first $\|\mathbb{D}_1 \cup \cdots \cup \mathbb{D}_{g-1}\|$ columns of $\underline{\mathbf{R}}_g^{-1}$ satisfy the relation

$$\left(\left[\underline{\mathbf{R}}_g^{\mathrm{T}} \right]_{\|\mathbb{D}_1 \cup \cdots \cup \mathbb{D}_{g-1}\|}^{1} \right)^{\mathrm{T}} \left[\underline{\mathbf{R}}_g^{-1} \right]_{\|\mathbb{D}_1 \cup \cdots \cup \mathbb{D}_{g-1}\|}^{1} = \mathbf{I}^{(\|\mathbb{D}_1 \cup \cdots \cup \mathbb{D}_{g-1}\|)}. \tag{5.49}$$
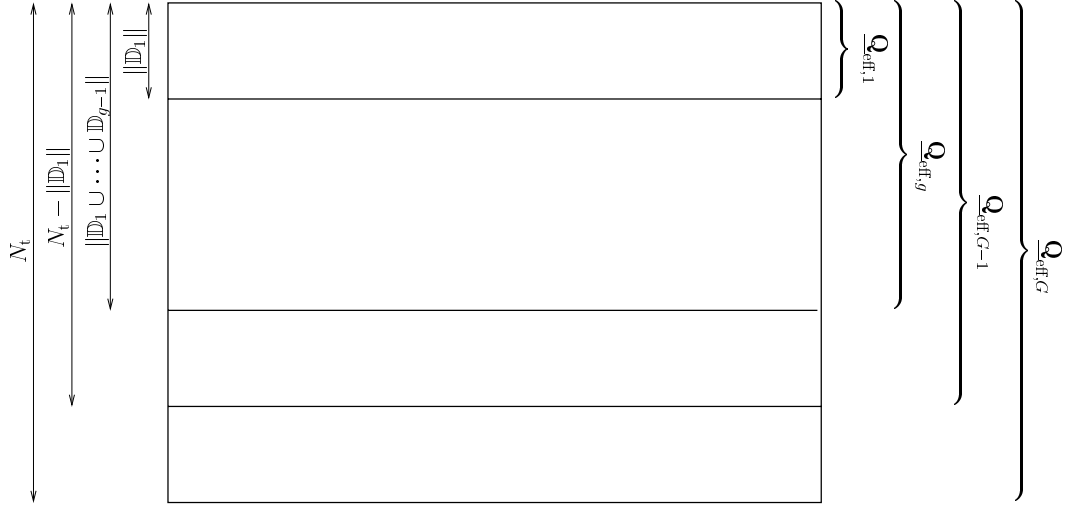
Fig. 5.15. Construction of $\underline{\mathbf{Q}}_{\mathrm{eff},\,g}$, $g = 1 \ldots G - 1$, from $\underline{\mathbf{Q}}_{\mathrm{eff},\,G}$

Again, because the elements in the last $Q - \|\mathbb{D}_1 \cup \cdots \cup \mathbb{D}_{g-1}\|$ columns of $\left([\underline{\mathbf{R}}_g^{\mathrm{T}}]^1_{\|\mathbb{D}_1 \cup \cdots \cup \mathbb{D}_{g-1}\|} \right)^{\mathrm{T}}$ are all zeros, (5.49) can be equivalently written as

$$
\underbrace{\left[\left([\underline{\mathbf{R}}_g^{\mathrm{T}}]^1_{\|\mathbb{D}_1 \cup \cdots \cup \mathbb{D}_{g-1}\|} \right)^{\mathrm{T}} \right]^1_{\|\mathbb{D}_1 \cup \cdots \cup \mathbb{D}_{g-1}\|}}_{\underline{\mathbf{R}}_{g-1}} \cdot \left(\left[\left([\underline{\mathbf{R}}_g^{-1}]^1_{\|\mathbb{D}_1 \cup \cdots \cup \mathbb{D}_{g-1}\|} \right)^{\mathrm{T}} \right]^1_{\|\mathbb{D}_1 \cup \cdots \cup \mathbb{D}_{g-1}\|} \right)^{\mathrm{T}}
$$
$$
= \mathbf{I}^{(\|\mathbb{D}_1 \cup \cdots \cup \mathbb{D}_{g-1}\|)}. \tag{5.50}
$$

It is clear from (5.50) that

$$
\underline{\mathbf{R}}_{g-1}^{-1} = \left(\left[\left([\underline{\mathbf{R}}_g^{-1}]^1_{\|\mathbb{D}_1 \cup \cdots \cup \mathbb{D}_{g-1}\|} \right)^{\mathrm{T}} \right]^1_{\|\mathbb{D}_1 \cup \cdots \cup \mathbb{D}_{g-1}\|} \right)^{\mathrm{T}} \tag{5.51}
$$

holds. (5.51) tell us that once the inverse of $\underline{\mathbf{R}}_G$ is calculated, the inverses of the matrices $\underline{\mathbf{R}}_g$, $g = 1 \ldots G - 1$, can be obtained by picking out the respective parts of the inverse $\underline{\mathbf{R}}_G^{-1}$ following (5.51), see Fig. 5.14.

In summary, the group specific modulator matrix $\underline{\mathbf{M}}_{\mathrm{G}}^{(g)}$ of (5.33) can be find out in a low complexity way, which is described as follows:

- In a first step, the effective QR-decomposition of $\underline{\mathbf{B}}_G$ is performed to get the low triangular matrix $\underline{\mathbf{R}}_G$ and the effective matrix $\underline{\mathbf{Q}}_{\mathrm{eff},\,G}$.
- In a second step, each low triangular matrices $\underline{\mathbf{R}}_g$, $g = 1 \ldots G - 1$, is obtained by picking out the respective part of $\underline{\mathbf{R}}_G$ following (5.44), see Fig. 5.14. The matrices $\underline{\mathbf{Q}}_{\mathrm{eff},\,g}$, $g = 1 \ldots G - 1$, are obtained by picking out parts of $\underline{\mathbf{Q}}_{\mathrm{eff},\,G}$ following (5.47), see Fig. 5.15.

- In a third step, $\underline{\mathbf{R}}_G^{-1}$ is calculated in a very effective way based on its triangular structure, and therefore, $\underline{\mathbf{R}}_g^{-1}$, $g = 1 \ldots G-1$, are obtained following (5.51), see Fig. 5.14.

- Finally, with (5.41) all the group specific modulator matrices $\underline{\mathbf{M}}_G^{(g)}$, $g = 1 \ldots G$, are obtained by a simple multiplication.

5.5   A general view of the TxNZF Filter

The purpose of this section is to give a general view on the TxNZF Filter and to show that the TxNZF Filter can be served as a framework of several precoding techniques which allows free balance between performance and computational complexity. For this purpose, in this section, the TxNZF Filter introduced in Section 5.2 will be first described in an alternative way with block diagram of Fig. 5.16, and then, different variants of non-linear Rx oriented transmission schemes based on this block diagram are discussed in relation to other well known non-linear schemes combined with unconventional quantization scheme.

The entire algorithm of Fig. 5.5 can be described in an alternative way with block diagram of Fig. 5.16, and is explained in what follows.

$\underline{\mathbf{d}}$ is the total data vector, c.f. (3.1). $\mathbf{S}_G$ is termed permutation matrix and is defined as

$$\mathbf{S}_G = \left(\mathbf{S}_G^{(1)\,\mathrm{T}} \ldots \mathbf{S}_G^{(G)\,\mathrm{T}} \right)^{\mathrm{T}} \tag{5.52}$$

of the combination of all group specific selection matrices $\mathbf{S}_G^{(g)}$, $g = 1 \ldots G$, of (5.6). Multiplying $\underline{\mathbf{d}}$ by $\mathbf{S}_G$ sorts the elements of $\underline{\mathbf{d}}$ into concatenated data groups $\underline{\mathbf{d}}_G^{(g)}$, $g = 1 \ldots G$, i.e.

$$\underline{\mathbf{d}}_G = \mathbf{S}_G \underline{\mathbf{d}} = \left(\underline{\mathbf{d}}_G^{(1)\,\mathrm{T}} \ldots \underline{\mathbf{d}}_G^{(G)\,\mathrm{T}} \right)^{\mathrm{T}} \in \mathbb{V}^{N_t \times 1} \tag{5.53}$$

holds. The rest part of the block diagram illustrates an iterative procedure, which is constructed by three parts: the feedback part with feedback matrix $\underline{\mathbf{F}}_G$, the forward part with forward matrix $\underline{\mathbf{M}}_G$ and non-linear generation part with group-wise generation function $\mathcal{V}_G^{(g)}\{\cdot\}$, $g = 1 \ldots G$. This procedure consists of G steps with p, $p = 1 \ldots G$, denoted as the indices of the steps. $\underline{\mathbf{i}}_G(p) \in \mathbb{C}^{N_t \times 1}$ and $\underline{\boldsymbol{\delta}}_G(p) \in \mathbb{C}^{N_t \times 1}$ represent the output vectors of the feedback part and the non-linear generation part of step p, respectively. Corresponding to the data groups $\underline{\mathbf{d}}_G^{(g)}$ in (5.53),

$$
\begin{aligned}
\underline{\mathbf{i}}_G(p) &= \Big(\underbrace{\underline{i}_{G,1}(p) \ldots \underline{i}_{G,\|\mathbb{D}_1\|}(p)}_{\underline{\mathbf{i}}_G^{(1)}(p)^{\mathrm{T}}} \ldots \underbrace{\underline{i}_{G,\|\mathbb{D}_1 \cup \cdots \cup \mathbb{D}_{G-1}\|+1}(p) \ldots \underline{i}_{G,\|\mathbb{D}_1 \cup \cdots \cup \mathbb{D}_G\|}(p)}_{\underline{\mathbf{i}}_G^{(G)}(p)^{\mathrm{T}}} \Big)^{\mathrm{T}} \\
&= \left(\underline{\mathbf{i}}_G^{(1)}(p)^{\mathrm{T}} \ldots \underline{\mathbf{i}}_G^{(G)}(p)^{\mathrm{T}} \right)^{\mathrm{T}}
\end{aligned}
\tag{5.54}
$$
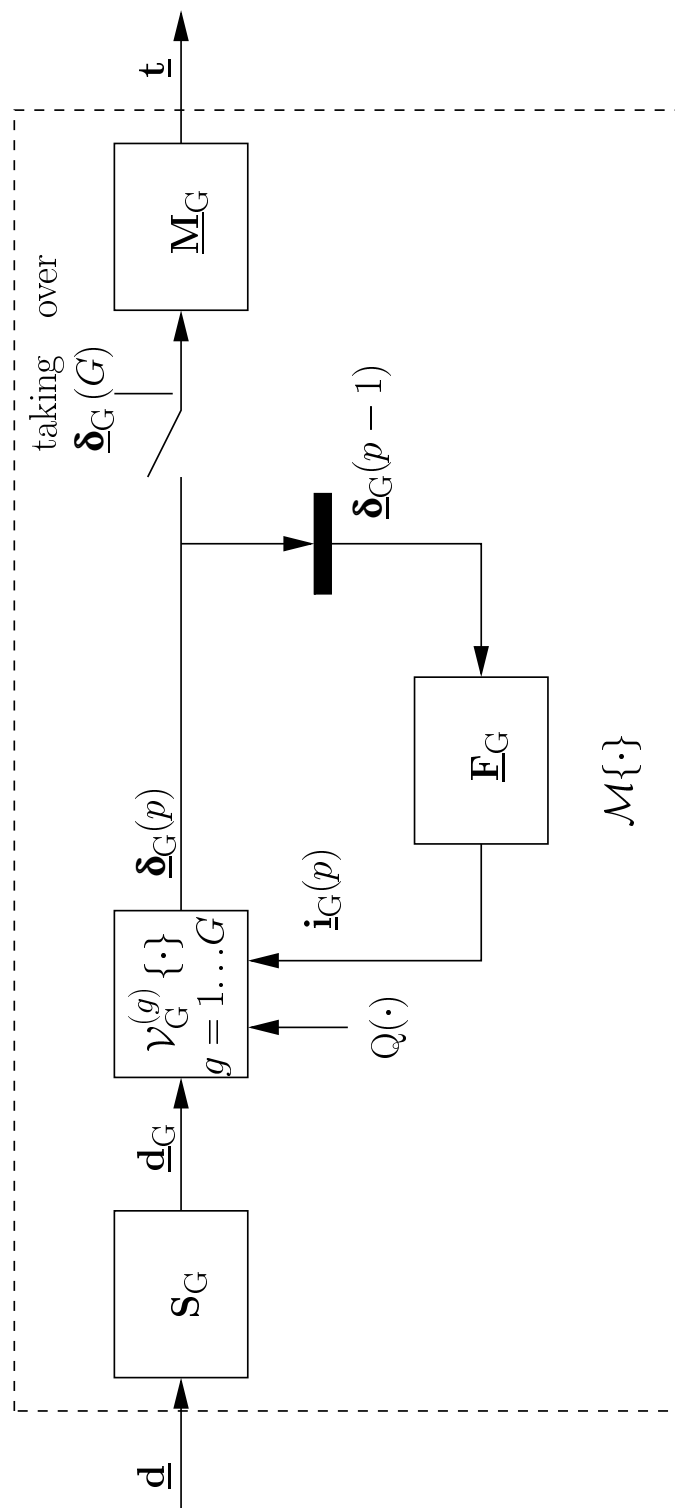
Fig. 5.16. Alternative block diagram of TxNZF described by Nassi-shneiderman diagram of Fig. 5.5

and

$$\begin{aligned}
\boldsymbol{\underline{\delta}}_{\mathrm{G}}(p) &= \Bigl(\underbrace{\underline{\delta}_{\mathrm{G},1}(p)\ldots\underline{\delta}_{\mathrm{G},\|\mathbb{D}_1\|}(p)}_{\boldsymbol{\underline{\delta}}_{\mathrm{G}}^{(1)}(p)^{\mathrm{T}}} \cdots \underbrace{\underline{\delta}_{\mathrm{G},\|\mathbb{D}_1\cup\cdots\cup\mathbb{D}_{G-1}\|+1}(p)\ldots\underline{\delta}_{\mathrm{G},\|\mathbb{D}_1\cup\cdots\cup\mathbb{D}_G\|}(p)}_{\boldsymbol{\underline{\delta}}_{\mathrm{G}}^{(G)}(p)^{\mathrm{T}}} \Bigr)^{\mathrm{T}} \\
&= \Bigl(\boldsymbol{\underline{\delta}}_{\mathrm{G}}^{(1)}(p)^{\mathrm{T}} \ldots \boldsymbol{\underline{\delta}}_{\mathrm{G}}^{(G)}(p)^{\mathrm{T}} \Bigr)^{\mathrm{T}} \qquad\qquad (5.55)
\end{aligned}$$

are also subdivided into groups with dimensions of $\boldsymbol{\underline{i}}_{\mathrm{G}}^{(g)}(p)$ and $\boldsymbol{\underline{\delta}}_{\mathrm{G}}^{(g)}(p)$ equal to the dimension of the corresponding data group $\boldsymbol{\underline{d}}_{\mathrm{G}}^{(g)}$ of (5.5), respectively. In each step p, $\boldsymbol{\underline{i}}_{\mathrm{G}}(p)$ of (5.54) is produced based on the previous output vector $\boldsymbol{\underline{\delta}}_{\mathrm{G}}(p-1)$ of the non-linear generation part and the feedback matrix $\underline{\mathbf{F}}_{\mathrm{G}}$:

$$\boldsymbol{\underline{i}}_{\mathrm{G}}(p) = \underline{\mathbf{F}}_{\mathrm{G}}\,\boldsymbol{\underline{\delta}}_{\mathrm{G}}(p-1). \qquad\qquad (5.56)$$

$\boldsymbol{\underline{\delta}}_{\mathrm{G}}(p)$ of (5.55) is group-wise generated. The group specific output vectors

$$\boldsymbol{\underline{\delta}}_{\mathrm{G}}^{(g)}(p) = \mathcal{V}_{\mathrm{G}}^{(g)}\left\{\boldsymbol{\underline{d}}_{\mathrm{G}}^{(g)}, \boldsymbol{\underline{i}}_{\mathrm{G}}^{(g)}(p), \mathrm{Q}(\cdot)\right\}, \; g = 1\ldots G, \qquad\qquad (5.57)$$

of $\boldsymbol{\underline{\delta}}_{\mathrm{G}}(p)$ of the non-linear generation part are the functions of $\boldsymbol{\underline{i}}_{\mathrm{G}}^{(g)}(p)$ in (5.54), $\boldsymbol{\underline{d}}_{\mathrm{G}}^{(g)}$ in (5.53) and the knowledge of the unconventional quantization function $\mathrm{Q}(\cdot)$. After G steps the output vector $\boldsymbol{\underline{\delta}}_{\mathrm{G}}(G)$ feeds to the forward matrix $\underline{\mathbf{M}}_{\mathrm{G}}$ and generates the transmit signal

$$\boldsymbol{\underline{t}} = \underline{\mathbf{M}}_{\mathrm{G}}\,\boldsymbol{\underline{\delta}}_{\mathrm{G}}(G). \qquad\qquad (5.58)$$

It is expected by comparing (5.58) and (5.21) that

$$\boldsymbol{\underline{\delta}}_{\mathrm{G}}(G) = \Bigl(\boldsymbol{\underline{\delta}}_{\mathrm{G}}^{(1)}(G)^{\mathrm{T}} \ldots \boldsymbol{\underline{\delta}}_{\mathrm{G}}^{(G)}(G)^{\mathrm{T}} \Bigr)^{\mathrm{T}} = \Bigl(\boldsymbol{\underline{\Delta}}_{\mathrm{G}}^{(1)\,\mathrm{T}} \ldots \boldsymbol{\underline{\Delta}}_{\mathrm{G}}^{(G)\,\mathrm{T}} \Bigr)^{\mathrm{T}} \qquad\qquad (5.59)$$

should hold. In the following we will describe these three parts in relation to the algorithm of Fig. 5.5 in detail.

Let us first consider the feedback part. With the group specific modulator matrices $\underline{\mathbf{M}}_{\mathrm{G}}^{(g)}$, $g = 1\ldots G$, of (5.60), the forward matrix is defined as

$$\underline{\mathbf{M}}_{\mathrm{G}} = \Bigl(\underline{\mathbf{M}}_{\mathrm{G}}^{(1)} \ldots \underline{\mathbf{M}}_{\mathrm{G}}^{(G)} \Bigr) \in \mathbb{C}^{Q \times N_{\mathrm{t}}}. \qquad\qquad (5.60)$$

With $\underline{\mathbf{M}}_{\mathrm{G}}$ of (5.60) and the matrix

$$\underline{\mathbf{B}}_{\mathrm{G}} = \Bigl(\underline{\mathbf{B}}_{\mathrm{G}}^{(1)\,\mathrm{T}} \ldots \underline{\mathbf{B}}_{\mathrm{G}}^{(G)\,\mathrm{T}} \Bigr)^{\mathrm{T}} \in \mathbb{C}^{N_{\mathrm{t}} \times Q} \qquad\qquad (5.61)$$

composed by the group specific system matrices $\underline{\mathbf{B}}_{\mathrm{G}}^{(g)}$, $g = 1\ldots G$, of (5.7), the feedback matrix is defined as

$$\underline{\mathbf{F}}_{\mathrm{G}} = \underline{\mathbf{B}}_{\mathrm{G}}\,\underline{\mathbf{M}}_{\mathrm{G}} - \mathbf{I} \in \mathbb{C}^{N_{\mathrm{t}} \times N_{\mathrm{t}}}. \qquad\qquad (5.62)$$

If $\underline{\boldsymbol{\delta}}_{\mathrm{G}}(p-1)$ will be fed into the forward part and the corresponding output

$$\underline{\mathbf{t}}_{\mathrm{G}}(p-1) = \underline{\mathbf{M}}_{\mathrm{G}}\,\underline{\boldsymbol{\delta}}_{\mathrm{G}}(p-1) \tag{5.63}$$

will be transmitted to the MTs. Then, the output vector

$$\underline{\mathbf{i}}_{\mathrm{G}}(p) = \underline{\mathbf{F}}_{\mathrm{G}}\,\underline{\boldsymbol{\delta}}_{\mathrm{G}}(p-1) = \underline{\mathbf{B}}_{\mathrm{G}}\,\underline{\mathbf{M}}_{\mathrm{G}}\,\underline{\boldsymbol{\delta}}_{\mathrm{G}}(p-1) - \underline{\boldsymbol{\delta}}_{\mathrm{G}}(p-1) \tag{5.64}$$

of the feedback part is the interference to $\underline{\boldsymbol{\delta}}_{\mathrm{G}}(p-1)$ foreseen at the output of MTs after step $p-1$. In this sense we term $\underline{\mathbf{i}}_{\mathrm{G}}(p)$ the interference vector of step p. With (5.61), (5.60) and (5.19), it can be obtained that the feedback matrix

$$\underline{\mathbf{F}}_{\mathrm{G}} = \begin{pmatrix} \mathbf{0}^{(\|\mathbb{D}_1\|)} & \cdots & \cdots & \mathbf{0} \\ \underline{\mathbf{B}}_{\mathrm{G}}^{(2)}\,\underline{\mathbf{M}}_{\mathrm{G}}^{(1)} & \mathbf{0}^{(\|\mathbb{D}_2\|)} & \ddots & \vdots \\ \vdots & \ddots & \ddots & \vdots \\ \underline{\mathbf{B}}_{\mathrm{G}}^{(G)}\,\underline{\mathbf{M}}_{\mathrm{G}}^{(1)} & \cdots & \underline{\mathbf{B}}_{\mathrm{G}}^{(G)}\,\underline{\mathbf{M}}_{\mathrm{G}}^{(G-1)} & \mathbf{0}^{(\|\mathbb{D}_G\|)} \end{pmatrix}. \tag{5.65}$$

is a block-wise low triangular matrix with the diagonal blocks being zero matrices. Fig. 5.17 illustrates the structure of the feedback matrix $\underline{\mathbf{F}}_{\mathrm{G}}$ corresponding to the exemplary subdivision of the data symbols of Fig. 5.2. Then, by substituting (5.65), (5.54) and (5.55) in (5.64), we obtain

$$\underline{\mathbf{i}}_{\mathrm{G}}^{(g)}(p) = \begin{cases} \mathbf{0}, & g = 1, \\ \sum_{g'=1}^{g-1} \underline{\mathbf{B}}_{\mathrm{G}}^{(g)}\,\underline{\mathbf{M}}_{\mathrm{G}}^{(g')}\,\underline{\boldsymbol{\delta}}_{\mathrm{G}}^{(g')}(p-1), & g = 1\ldots G. \end{cases} \tag{5.66}$$

(5.66) means that the transmission of $\underline{\boldsymbol{\delta}}_{\mathrm{G}}^{(g)}(p-1)$ will only experience the interferences from the transmissions of $\underline{\boldsymbol{\delta}}_{\mathrm{G}}^{(g')}(p-1)$, $g' < g$. This is equivalent to the basic principle with respect to the interference avoidance in TxNZF Filter as described in Section 5.2.

Now, let us consider the non-linear generation function $\mathcal{V}_{\mathrm{G}}^{(g)}\{\cdot\}$, $g = 1\ldots G$, of (5.57). The element $\underline{d}_{\mathrm{G},n}^{(g)}(p)$ of $\underline{\boldsymbol{\delta}}_{\mathrm{G}}^{(g)}(p)$ in (5.55) is determined in analogy to the determination of $\underline{\Delta}_{\mathrm{G},n}^{(g)}$ in (5.13), i.e.

$$\underline{d}_{\mathrm{G},n}^{(g)} = \underline{v}_m \Longrightarrow \underline{\delta}_{\mathrm{G},n}^{(g)}(p) = \underline{g}_{m,p'} - \underline{i}_{\mathrm{G},n}^{(g)}(p),\ p' = \arg\min_{p\in\{1\ldots P\}} \left\| \underline{g}_{m,p} - \underline{i}_{\mathrm{G},n}^{(g)}(p) \right\|. \tag{5.67}$$

In this sense $\underline{\boldsymbol{\delta}}_{\mathrm{G}}(p)$ is termed correction vector of step p and $\underline{\boldsymbol{\delta}}_{\mathrm{G}}^{(g)}(p)$ of (5.55) is termed group specific correction vector of step p.

Obtained from (5.66) that $\underline{\mathbf{i}}_{\mathrm{G}}^{(1)}(p)$, $p = 1\ldots G$, are all equal to zero, with (5.55) the group specific correction vectors $\underline{\boldsymbol{\delta}}_{\mathrm{G}}^{(1)}(p)$, $p = 1\ldots G$, are all identity. Comparing the generation
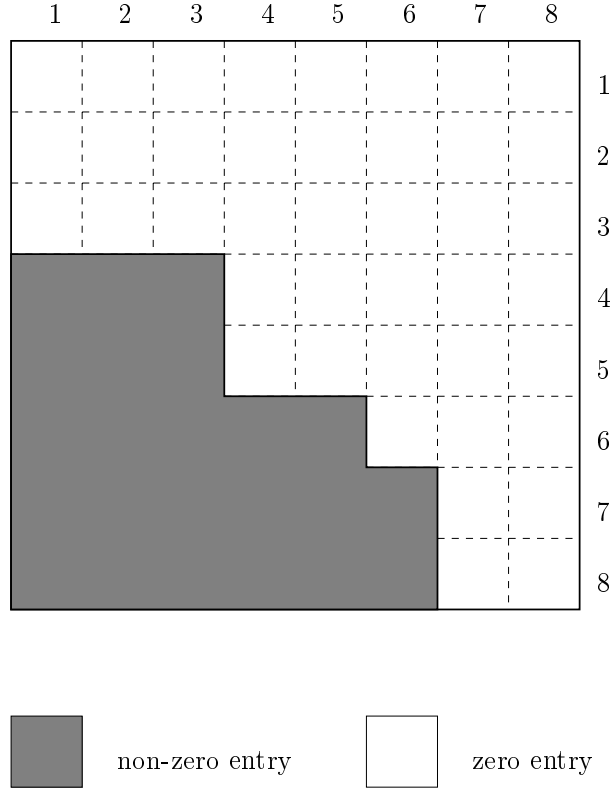
Fig. 5.17. Structure of the feedback matrix $\underline{\mathbf{F}}_G$

of $\underline{\boldsymbol{\delta}}_G^{(1)}(p)$ according to (5.67) and the generation of $\underline{\boldsymbol{\Delta}}_G^{(1)}$ according to (5.13), it is obvious that

$$\underline{\boldsymbol{\delta}}_G^{(1)}(p) = \underline{\boldsymbol{\Delta}}_G^{(1)}, \ g = 1 \ldots G, \tag{5.68}$$

hold. $\underline{\mathbf{i}}_G^{(2)}(p)$ depends only on $\underline{\boldsymbol{\delta}}_G^{(1)}(p-1)$, see (5.66). Substitution of (5.68) in (5.66) yields

$$\underline{\mathbf{i}}_G^{(2)}(p) = \underline{\mathbf{B}}_G^{(2)} \ \underline{\mathbf{M}}^{(1)} \ \underline{\boldsymbol{\Delta}}_G^{(1)}, \ g = 2 \ldots G. \tag{5.69}$$

Then, again comparing the generations of $\underline{\boldsymbol{\delta}}_G^{(2)}(p)$ according to (5.67) and $\underline{\boldsymbol{\Delta}}_G^{(2)}$ according to (5.13) we obtain

$$\underline{\boldsymbol{\delta}}_G^{(2)}(p) = \underline{\boldsymbol{\Delta}}_G^{(2)}, \ g = 2 \ldots G. \tag{5.70}$$

Continuing the iterative procedure in an analogue way, generally, after g' steps we obtain

$$\underline{\boldsymbol{\delta}}_G^{(g')}(p) = \underline{\boldsymbol{\Delta}}_G^{(g')}, \ p = g' \ldots G. \tag{5.71}$$

Finally, based on (5.71) follows the interference vector $\underline{\boldsymbol{\delta}}_G(G)$ of step G by (5.59). Then, feeding $\underline{\boldsymbol{\delta}}_G(G)$ of (5.59) to the forward part with forward matrix $\underline{\mathbf{M}}_G$ of (5.60), the transmit signal

$$\underline{\mathbf{t}} = \underline{\mathbf{M}}_G \underline{\boldsymbol{\delta}}_G(G) = \sum_{g=1}^{G} \underline{\mathbf{M}}_G^{(g)} \underline{\boldsymbol{\Delta}}_G^{(g)} = \sum_{g=1}^{G} \underline{\mathbf{t}}_G^{(g)} \tag{5.72}$$

of the TxNZF Filter is generated.

As mentioned at the beginning of this section, TxNZF Filter may serve as a flexible framework for several techniques for transmit signal design, which allows almost free balance between performance and required complexity. This flexibility is enabled by several degrees of freedoms, namely

- the number and sizes of groups,
- the assignment of data symbols $\underline{d}_n$, $n = 1 \ldots N_t$, to the groups,
- the design of the unconventional quantization scheme with quantization function $Q(\cdot)$ and
- the design of the non-linear group-wise generation functions $\mathcal{V}_G^{(g)} \{\cdot\}$.

In what follows we first present these freedoms with respect to the structure shown in Fig. 5.16, and then, some examples with consideration of these freedoms will be given to present the idea that the generalized TxNZF Filter allows almost free balance between the performance and the required complexity.

As we mentioned in Section 5.2 and alternatively described by Fig. 5.16, the transmit signal of TxNZF Filter are group-wise generated. Therefore, the data symbols are assigned to several data groups, the data symbols in the same group could be jointly processed. Concerning the block diagram of Fig. 5.16, the number and sizes of groups influence the structure of the feedback matrix $\underline{\mathbf{F}}_G$ of (5.65). In the case that

$$G = N_t, \tag{5.73}$$

hold, each data group contains only a single data symbol. Then, the feedback matrix $\underline{\mathbf{F}}_G$ of (5.62) degenerates to be a low triangular matrix, see Fig. 5.18. With respect to (5.57), each element of the interference vectors $\underline{\boldsymbol{\delta}}_G(g)$ has to be separately generated and has no chance to cooperate with other elements. In the case that

$$G = 1, \tag{5.74}$$

or

$$\mathbb{D} = \mathbb{D}_l \tag{5.75}$$

holds, all the data symbols are assigned to a single data group. Then, the feedback matrix $\underline{\mathbf{F}}_G$ of (5.62) is equal to $\mathbf{0}$ and vanishes, see Fig. 5.18. With respect to (5.57) all the elements of $\underline{\boldsymbol{\delta}}_G(p)$ are allowed to be jointly generated. Generally, the number and the sizes of data groups of TxNZF Filter can be freely adjusted and change the basic structure of $\underline{\mathbf{F}}_G$.

When the number and sizes of the data groups are fixed, there are still many choices concerning the sorting order of data symbols and as well as the data groups. These sorting order could give beneficial effect on the performance, e.g. the sorting order with respect to the channel attenuations as mentioned in Section 5.2.2.
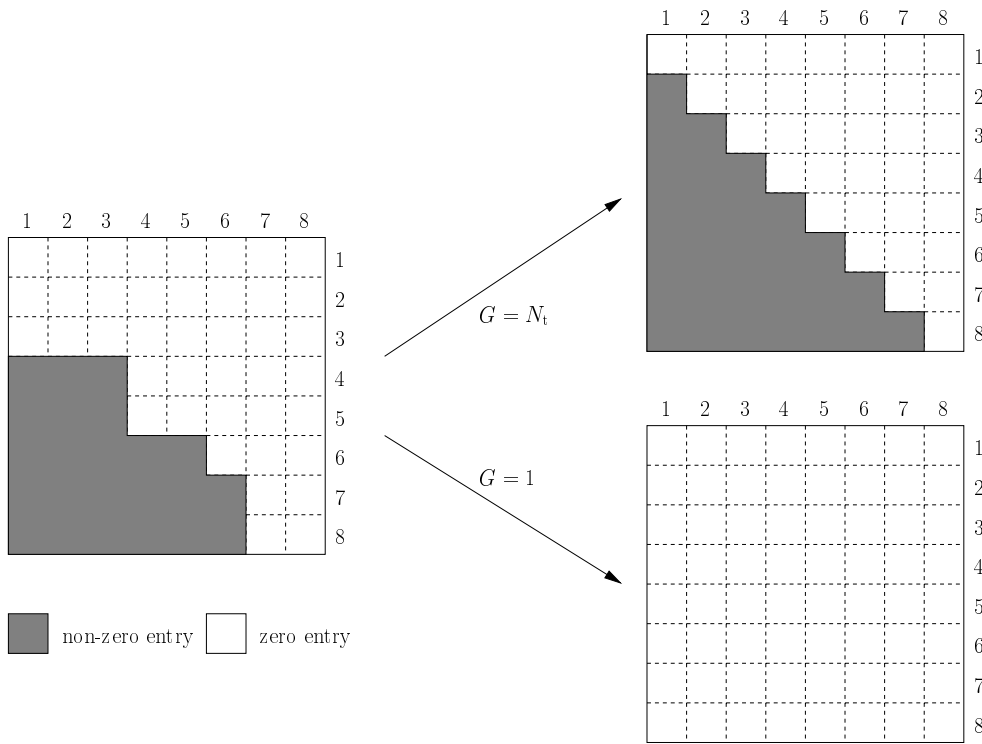
Fig. 5.18. Degeneration of the feedback matrix $\underline{\mathbf{F}}_{\mathrm{G}}$

Up to now, the available designs of the group-wise non-linear generation functions $\mathcal{V}_{\mathrm{G}}^{(g)}\{\cdot\}$, $g = 1 \ldots G$, of (5.57) are very limited. Here, we only give two examples. The first example is the one as already introduced in (5.67), which is a very simply design of these functions. Another example concerns the optimum design, in which the exhaustive search is performed to find the best group specific correction vectors $\underline{\boldsymbol{\delta}}_{\mathrm{G,\,opt}}^{(g)}(p)$ so that the corresponding transmit energy

$$T_{\mathrm{G}}^{(g)}(p) = \left\|\underline{\mathbf{M}}_{\mathrm{G}}^{(g)}\ \underline{\boldsymbol{\delta}}_{\mathrm{G,\,opt}}^{(g)}(p)\right\|^{2} \tag{5.76}$$

is minimized. The complexity of this optimum solution is very high and increases with the size of data groups.

Now, let us see some examples. If all data symbols are assigned to a single group, i.e. $\underline{\mathbf{F}}_{\mathrm{G}}$ vanishes as mentioned above, and the optimum non-linear generation function is chosen, then the TxNZF Filter becomes the overall optimum scheme. However, the complexity is prohibitively high, because the total number N_{t} of data symbols are usually very large in mobile radio systems. If each data group assigns only a single data symbol, i.e. $\underline{\mathbf{F}}_{\mathrm{G}}$ becomes a low triangular matrix as mentioned before, in this case the two exemplary non-linear generation functions are equivalent, then TxNZF Filter tends to be the well known THP scheme [Fis02]. THP has very low complexity but also great performance degradation compared to the overall optimum scheme mentioned above. In between of these two extreme examples, all data symbols are assigned to several data groups, i.e. $\underline{\mathbf{F}}_{\mathrm{G}}$ is a block-wise low triangular matrix. Then, if optimum group-wise non-linear generation

functions are used for all data groups, the performance of the resulting scheme is expected to be superior to the performance of THP but worse than that of the overall optimum scheme. However, because the size of data groups is smaller than the total number N_t of data symbols, the complexity is reduced compared to that of the overall optimum scheme. That means that a free balance between a high performance and the complexity can be realized by adjusting the number and sizes of data groups.

Chapter 6

Summary

6.1 English

In conventional radio communication systems, the system design generally starts from the transmitter (Tx), i.e. the signal processing algorithm in the transmitter is a priori selected, and then the signal processing algorithm in the receiver is a posteriori determined to obtain the corresponding data estimate. Therefore, in these conventional communication systems, the transmitter can be considered the master and the receiver can be considered the slave. Consequently, such systems can be termed transmitter (Tx) oriented. In the case of Tx orientation, the a priori selected transmitter algorithm can be chosen with a view to arrive at particularly simple transmitter implementations. This advantage has to be countervailed by a higher implementation complexity of the a posteriori determined receiver algorithm.

Opposed to the conventional scheme of Tx orientation, the design of communication systems can alternatively start from the receiver (Rx). Then, the signal processing algorithm in the receiver is a priori determined, and the transmitter algorithm results a posteriori. Such an unconventional approach to system design can be termed receiver (Rx) oriented. In the case of Rx orientation, the receiver algorithm can be a priori selected in such a way that the receiver complexity is minimum, and the a posteriori determined transmitter has to tolerate more implementation complexity.

In practical communication systems the implementation complexity corresponds to the weight, volume, cost etc of the equipment. Therefore, the complexity is an important aspect which should be taken into account, when building practical communication systems. In mobile radio communication systems, the complexity of the mobile terminals (MTs) should be as low as possible, whereas more complicated implementations can be tolerated in the base station (BS). Having in mind the above mentioned complexity features of the rationales Tx orientation and Rx orientation, this means that in the uplink (UL), i.e. in the radio link from the MT to the BS, the quasi natural choice would be Tx orientation, which leads to low cost transmitters at the MTs, whereas in the downlink (DL), i.e. in the radio link from the BS to the MTs, the rationale Rx orientation would be the favorite alternative, because this results in simple receivers at the MTs. Mobile radio downlinks with the rationale Rx orientation are of interests in the thesis.

Modern mobile radio communication systems are cellular systems, in which both the intracell and intercell interferences exist. These interferences are the limiting factors for the performance of mobile radio systems. The intracell interference can be eliminated or at least reduced by joint signal processing with consideration of all the signals in the

considered cell. However such joint signal processing is not feasible for the elimination of intercell interference in practical systems. Knowing that the detrimental effect of intercell interference grows with its average energy, the transmit energy radiated from the transmitter should be as low as possible to keep the intercell interference low. Low transmit energy is required also with respect to the growing electro-phobia of the public.

The transmit energy reduction for multi-user mobile radio downlinks by the rationale Rx orientation is dealt with in the thesis. Among the questions still open in this research area, two questions of major importance are considered here. MIMO is an important feature with respect to the transmit power reduction of mobile radio systems. Therefore, first question concerns the linear Rx oriented transmission schemes combined with MIMO antenna structures. The investigations of the MIMO benefit on the linear Rx oriented transmission schemes are studied in the thesis. Utilization of unconventional multiply connected quantization schemes at the receiver has also great potential to reduce the transmit energy. Therefore, the second question considers the designing of non-linear Rx oriented transmission schemes combined with multiply connected quantization schemes.

As just mentioned, MIMO is an important feature with respect to the transmit power reduction of mobile radio systems. For the purpose of performance evaluation of mobile radio systems with MIMO antenna structures, MIMO channel models are required. Besides the temporal dimension as in conventional SISO channel modelling, the multiple antennas introduce additionally the spatial dimension, which should also be considered in MIMO channel modelling. An important issue concerning the spatial dimension of MIMO is the degree of correlation of the impulse responses of the channels between different pairs of Tx and Rx antennas. These channel impulse responses are termed antenna specific. The correlation depends on the configuration of the antenna structures and the topography and morphography of the propagation area, etc. Although, recently, much work concerning MIMO channel modelling for different scenarios has been reported. In this thesis, we do not try to address all these MIMO channel models. Rather, we consider only two quasi extreme cases, namely on the one side scenarios with spatially totally uncorrelated and on the other side scenarios with spatially fully correlated antenna specific channel impulse responses. These two models are introduced in Chapter 2 and are used for system evaluations of the linear and non-linear Rx oriented transmission schemes considered in this thesis. Evaluating the performance of mobile radio systems for these two extreme channel models would give an impression on the performance of mobile radio systems in the case of other MIMO channel models which cover the scenarios in between of these two extreme cases.

As mentioned above, both linear and non-linear Rx oriented transmission systems are considered in this thesis. These considered linear and non-linear systems are first identified and characterized based on a general structure of a data transmission system. In Rx oriented transmission systems, for the a priori given Rx operator, there exist a variety of choices. Focusing on the application of the Rx orientation in mobile radio downlinks, the receivers are aspired to be as simple as possible. Therefore, in both considered linear and non-linear Rx oriented transmission systems the Rx operator is restricted to

a favorable structure by concatenating a linear Rx operator and a quantizer, where the latter constitutes the non-linearity of the whole Rx operator. Two types of quantizers are described in the thesis, namely quantizers with conventional simply connected and unconventional multiply connected quantization schemes. In the case of conventional simply connected quantization schemes, each element of the message set corresponds to a single point, termed representative of this message element, in the complex plane. Each representative is located in a region termed decision region. All these decision regions completely tile the complex plane to be non-overlapping. In the case of unconventional multiply connected quantization schemes, each element of the message set corresponds to, instead of a single representative as in the case of conventional quantization schemes, now multiple representatives exist for a certain message element in the complex plane. The decision regions related to the representatives of a certain message element are termed partial decision regions of this message element. Again, all these partial decision regions of all message elements completely tile the complex plane to be non-overlapping. In Rx oriented transmission systems, the Tx operator is a posteriori determined under considerations of the channel and the a priori given Rx operator. In the case of said linear such systems considered in the thesis, the Tx operator becomes a linear one and is a posteriori adapted based on the channel and only the chosen linear Rx operator, whereas non-linear quatizer is not considered and chosen as the conventional simply connected quantization scheme. In the case of considered non-linear such systems, the Tx operator is determined under considerations of the channel, the a priori given linear Rx operator and also the chosen quantizer with multiply connected quantization scheme.

The designing of the linear Rx oriented transmission schemes based on the rationale TxMF, TxZF Filter and TxMMSE Filter are well known, therefore, are only briefly recapitulated. The performance criteria energy efficiency and the related criterion Tx efficiency are introduced and formulated in detail based on the singular value decomposition of the channel matrix. A large energy efficiency means efficient transmission of the radiated energy, and, therefore, low transmit energy is required at the transmitter when a certain useful energy has to be produced at the receiver output. Based on the detailed formulation of energy efficiency, some hints concerning the choice of the a priori given linear Rx operator are given in Chapter 3.

One major goal of the thesis is the investigations of the MIMO benefit on the linear Rx oriented transmission schemes. The investigations are restricted to the linear scheme with TxZF Filter and based on the linear Rx oriented MIMO broadcast systems, where one BS employed with K_{B} Tx antennas supports simultaneously K MTs and each of the K MTs has K_{M} Rx antennas. First, the TxZF Filter algorithm and the corresponding performance criteria developed for general linear Rx oriented transmission systems are adapted to the MIMO broadcast systems. In the broadcast systems, the MTs can be discerned between two situations of cooperative and non-cooperative MTs. In the case of cooperative MTs, each MT would have the received information of all the other MTs. Although, the situation with cooperative MTs would lead to superior performance as shown by the numerical example in Section 4.4, it would be a very impractical situation which is not feasible in real world systems. In practical systems each MT disposes only

of its own received information. In this case the MTs are said to be non-cooperative, and only this case is considered for the performance study in this thesis.

For the performance study, the statistical properties, namely means and variances of the Tx efficiencies and the Tx energies are considered by analytical and/or numerical results for the two MIMO channels mentioned before, namely the situations with totally uncorrelated channel impulse responses and with fully correlated channel impulse responses.

First, the study of the Tx efficiency is performed. In the case with totally uncorrelated channel impulse responses, the closed form analytical results of the Tx efficiency can be found in literature. These analytical results are only valid for an approximate assumption. From the analytical results, it can be seen that an increasing number of Tx antennas increases both the mean and the variance of Tx efficiencies, however, the influence of multiple Rx antennas on Tx efficiency is lack due to the approximate assumption. Therefore, the validity of the assumption for the analytical results is argued and simulations are performed. It turns out from the simulation results that basically the analytical results coincide with the simulated results. However the coincidences of the mean and the variance are different. The mean of the Tx efficiency obtained by analytical and simulated results are virtually equal and do not depend on the number of Rx antennas. Whereas, its variance obtained by simulation results decreases and becomes closer to the analytical result with increasing number of Rx antennas. In the case with fully correlated channel impulse responses, the closed form solutions are not available, only the simulation results are performed. It turns out that the behaviors of the simulation curves obtained for this case and for the case with totally uncorrelated channel impulse responses are very similar and only slight degradations are observed in this case. These degradations mean the decreased mean and the increased variance of the Tx efficiencies. In summary, multiple Tx and Rx antennas can give beneficial effects on the elimination of intracell interference and the beneficial effects given by the multiple Tx antennas are more distinguished. The studies of Tx efficiency for the two extreme cases also give the impression on the Tx efficiencies for the cases in between of these two extreme cases, i.e., when going from the case with totally uncorrelated channel impulses to the case with fully uncorrelated channel impulse response, the degree of the beneficial effects obtained by the multiple Tx and Rx antennas tends to go down.

The study of Tx efficiency shows the effects of the multiple Tx and Rx antennas on the elimination of intracell interference, which is only one aspect with respect to the transmit energy reduction. Therefore, the study of the Tx energy is also performed in the thesis. In the case with totally uncorrelated channel impulse responses, again the available analytical results in literature are only valid for an approximate assumption. These results show that an increasing number of Tx antennas leads to decreased mean and variance of the Tx energy. Again, the influence of multiply Rx antennas is lack due to the approximate assumption. First, by the analysis based on a simple case, the influence of multiple Rx antennas is revealed. Then, the precise of the analytical results and the influence of multiple Rx antennas are verified by simulation results. It turns out that both the mean and the variance of the Tx energies go down with an increasing

number of Rx antennas, and such an increasing improves the coincidences of the analytical and simulation results. In the case of fully correlated channel impulse responses, by the analysis based on a simple case and the simulations, it turns out that the multiple Tx antennas show the similar but slightly degraded beneficial effect on the Tx energy as that in the case of totally uncorrelated channel impulse responses. However, multiple Rx antennas give slightly detrimental effect on the Tx energy. I.e., increasing the number of Rx antennas slightly increases the mean and the variance of the Tx energy. In summary, when going from the case with totally uncorrelated channel impulse to the case with fully correlated channel impulse responses, multiple Tx antennas always give beneficial effect on the Tx energy and the degree of the beneficial effect tends to go down. However, multiple Rx antennas do not always show the beneficial effect, this beneficial effect disappears when the channel impulse responses are highly correlated.

Another major goal of the thesis focuses on investigations of non-linear Rx oriented transmission schemes combined with unconventional multiply connected quantization schemes at the receiver. As mentioned before, in conventional simply connected quantization schemes, each of the message elements corresponds to a single decision region. For an error free transmission of a message element carried by a certain data symbol, the estimate at the receiver output should land in the corresponding decision region. In contrast to the conventional quantization schemes, multiply connected quantization schemes offer several, or even infinitely many partial decision regions for each of these message elements. Then, the estimate at the receiver landing in any one of the corresponding partial decision regions of the transmitted message will lead to an error free transmission. Consequently, if a certain number of data symbols carrying a set of message elements have to be transmitted, instead of only one, as in the case of conventional quantization schemes, now many possible transmit signals aiming at different combinations of the corresponding partial decision regions exist. Each of them requires a different value of the transmit energy. Now, the crux of the non-linear Rx oriented scheme with multiply connected quantization schemes consists in finding a specific transmit signal out of all these possible transmit signals so that the required transmit energy becomes as low as possible. In the optimum case, one could determine the transmit energies for all possible transmit signals and then, finally use the signal with smallest transmit energy. However, such an exhaustive search would be exhibitively expensive. In this thesis a less complex suboptimum solution for finding a superior transmit signal following the group-wise signal processing is proposed and described. The proposed suboptimum scheme is termed TxNZF Filter. Simulation results show that the TxNZF Filter outperforms its linear counterpart TxZF Filter. Particularly, when the channel attenuations between the BS and the different MTs differ significantly from each other, the superiority of the TxNZF Filter becomes significant. Some implementation aspects are presented to show that the TxNZF Filter can be implemented in a very cost efficient way. Generally, as shown in this thesis, the TxNZF Filter can be served as a framework of several techniques combined with multiply connected quantization schemes, which allows a free balance between the performance and the complexity. Some well known schemes, e.g. THP, can be treated as a special case of TxNZF Filter.

6.2 Deutsch

Bei konventionellen Funkübertragungssystemen beginnt man beim Systementwurf mit dem Sender. Dies bedeutet, daß man a priori den senderseitig verwendeten Algorithmus der Sendesignalerzeugung (Sendeoperator) auswählt, und dann a posteriori den im Empfänger zur Datenschätzung verwendeten Algorithmus (Empfangsoperator) festlegt. Bei dieser herkömmlichen Vorgehensweise kann man den Sender als den Meister (engl. master) und den Empfänger als den Sklaven (engl. slave) ansehen. Man kann deshalb solche Systeme auch als senderorientiert bezeichnen. Im Fall der Senderorientierung kann man bei der Wahl des Sendeoperators anstreben, zu möglichst einfachen Senderimplementierungen zu kommen. Dieser Vorteil muß aufgewogen werden durch eine höhere Implementierungskomplexität des a posteriori festzulegenden Empfangsoperators.

Anstelle des herkömmlichen Schemas der Senderorientierung kann man den Systementwurf auch auf der Empfängerseite beginnen. In diesem Fall werden die empfängerseitig verwendeten Algorithmen der Signalverarbeitung (Empfangsoperator) a priori festgelegt, und die senderseitig zu einzusetzenden Algorithmen (Sendeoperator) ergeben sich dann a posteriori. Eine derartige Vorgehensweise ist unkonventionell und kann als empfängerorientiert bezeichnet werden. Im Fall der Empfängerorientierung kann man bei der a priori getroffenen Auswahl des Empfangsoperators anstreben, möglichst einfache Empfänger zu erhalten, und muß dafür auf der Sendeseite höhere Komplexität tolerieren.

In praktischen Übertragungssystemen steigen Gewicht, Volumen und Kosten der Hardware mit der Implementierungskomplexität. Deshalb ist das Erzielen möglichst geringer Implementierungskomplexität beim praktischen Systementwurf ein wichtiger Gesichtspunkt. In Mobilfunksystemen sollte hierbei die Komplexität der Mobilstationen (MS) möglichst gering sein, während die Basisstationen (BS) komplexer sein dürfen. Angesichts der oben erwähnten Komplexitätscharakteristika der Vorgehensweisen Senderbzw. Empfängerorientierung bedeutet dies,

- daß die quasi natürliche Wahl für die Strecken von den MSen zur BS, d.h. für die Aufwärtsstrecke, die zu einfachen Sendern in den MSen führende Senderorientierung wäre, während

- in den Strecken von der BS zu den MSen, d.h. in der Abwärtsstrecke, die zu einfachen Empfängern in den MSen führende Empfängerorientierung zu wählen wäre.

In dieser Arbeit interessieren Mobilfunk-Abwärtsstrecken, die nach dem Schema der Empfängerorientierung arbeiten.

Moderne Mobilfunksysteme sind zellulare Systeme, in denen sowohl Intrazell- als auch Interzellinterferenz auftreten. Diese Interferenzen sind der eigentlich begrenzende Faktor für die Systemperformanz. Intrazellinterferenz kann durch gemeinsame Verarbeitung bzw. Erzeugung aller in einer Zelle auftretenden Signale eliminiert oder zumindest reduziert werden. Gegen die Interzellinterferenz kann man dagegen durch eine solche gemeinsame Behandlung in praktischen Systemen nichts ausrichten. Es ist offensichtlich, daß

die schädliche Wirkung der Interzellinterferenz um so größer ist, je höher die von den
Sendern des Systems abgestrahlten Leistungen sind. Im Interesse geringer Interzellinter-
ferenz ist es deshalb erstrebenswert, die abgestrahlten Leistungen möglichst klein zu hal-
ten. Geringe abgestrahlte Leistungen sind im übrigen auch wünschenswert im Hinblick
auf die zunehmende Elektrophobie der Bevölkerung.

Anliegen der Dissertation ist die Sendeleistungsreduktion in Mehrteilnehmer-
Abwärtsstrecken des Mobilfunks durch Einsatz des Schemas Empfängerorientierung.
Unter den in diesem Zusammenhang noch offenen Fragen wird zwei bedeutenderen solchen
Fragen nachgegangen:

- MIMO-Antennensysteme sind eine Möglichkeit, die erforderlichen Sendeleistun-
  gen zu verringern. Deshalb wird in der Arbeit die Kombination von MIMO-
  Antennensystemen mit dem Schema Empfängerorientierung betrachtet; hier-
  bei interessieren die durch eine solche Kombination erzielbaren Performanzver-
  besserungen.

- Ein zweiter interessanter Gesichtspunkt ist das Verwenden empfängerseitiger De-
  tektoren mit mehrfach zusammenhängenden und damit unkonventionellen Entschei-
  dungsgebieten, die bekanntlich ebenfalls das Potential einer Sendeleistungsreduktion
  beinhalten. In der Arbeit wird untersucht, wie diese Technik vorteilhaft mit dem
  Schema der Empfängerorientierung zusammengebracht werden kann.

Wie gerade erwähnt, sind MIMO-Antennenstrukturen ein wichtiger Ansatzpunkt, wenn
es um die Reduzierung der erforderlichen Sendeleistungen geht. Um Mobilfunksy-
steme mit MIMO-Antennenstrukturen untersuchen zu können, benötigt man MIMO-
Kanalmodelle. Neben der zeitlichen Dimension, die bereits bei herkömmlichen SISO-
Antennensystemen eine Rolle spielt, erfordern MIMO-Kanalmodelle das Einführen einer
zusätzlichen räumlichen Dimension. Ein wichtiger Aspekt beim Einführen einer solchen
räumlichen Dimension ist der Grad der Korrelation der Impulsantworten der Funkkanäle
zwischen den einzelnen Paaren von Sende- und Empfangsantennen. Diese Kanalimpuls-
antworten werden mit dem Attribut "antennenspezifisch" bezeichnet. Der Grad der Kor-
relation hängt ab von der Konfiguration der Antennenstrukturen, von der Topographie
und Morphologie des Ausbreitungsgebiets usw. In jüngerer Zeit wurde an verschiede-
nen Stellen viel Arbeit in die MIMO-Kanalmodellierung für eine Vielfalt von Ausbrei-
tungsgebieten investiert. In der vorliegenden Dissertation werden nicht alle diese MIMO-
Kanalmodelle angesprochen. Wir konzentrieren uns vielmehr auf zwei quasi extreme Fälle,
nämlich auf den Fall der räumlich total unkorrelierten und den Fall der räumlich voll korre-
lierten antennenspezifischen Kanalimpulsantworten. Diese beiden MIMO-Kanalmodelle
werden in Kapitel 2 eingeführt und dann bei der Evaluation linearer und nichtlinearer
empfängerorientierter Übertragungssysteme in dieser Arbeit verwendet. Derartige Evalu-
ationen für die genannten Extremfälle geben auch einen Eindruck von der Systemperfor-
manz für Szenarien, deren MIMO-Kanalmodelle zwischen den beiden genannten Extremen
liegen.

Wie bereits angedeutet, werden in der Arbeit sowohl lineare als auch nichtlineare
empfängerorientierte Übertragungssysteme betrachtet. Diese linearen bzw. nichtlinearen

Systeme werden zunächst auf der Basis eines Übertragungssystems mit einer sehr allgemeinen generischen Struktur definiert und charakterisiert. In empfängerorientierten Übertragungssystemen gibt es für den a priori zu wählenden Empfangsoperator eine große Auswahl. Mit Blick auf die Anwendung in Mobilfunkabwärtsstrecken sollten die Empfänger wie oben schon gesagt möglichst aufwandsgünstig sein. Deshalb wird sowohl bei den linearen als auch bei den nichtlinearen Systemansätzen dieser Arbeit eine Empfängerstruktur gewählt, die aus der Verkettung eines linearen Empfangsoperators und eines Quantisierers besteht. Letzterer macht die Nichtlinearität des gesamten Empfangsoperators aus. In der Arbeit werden zwei Quantisierertypen betrachtet, nämlich solche mit herkömmlichen einfach zusammenhängenden und solche mit unkonventionellen, d.h. mehrfach zusammenhängenden Entscheidungsgebieten. Im Falle der herkömmlichen einfach zusammenhängenden Entscheidungsgebiete entspricht jede Realisierung eines Nachrichtenelements (Datensymbol) der übertragenen Nachricht eindeutig einem einzigen Punkt in der komplexen Ebene, der als Repräsentant des betreffenden Nachrichtenelements bezeichnet wird. Jeder solche Repräsentant liegt in einer gewissen, als Entscheidungsgebiet bezeichneten Region der komplexen Ebene. Alle diese Entscheidungsgebiete pflastern die komplexe Ebene vollständig und ohne Überlappungen. Im Falle unkonventioneller, d.h. mehrfach zusammenhängender Entscheidungsgebiete entsprechen jeder Realisation eines Nachrichtenelements nicht ein einziger, sondern mehreren Repräsentanten in der komplexen Ebene, von denen jeder wieder in einem ihn umgebenden Entscheidungsgebiet liegt. Alle Entscheidungsgebiete, die einer gewissen Realisierung eines Nachrichtenelements zugeordnet sind, werden Teilentscheidungsgebiete dieser Realsierung genannt. Alle Teilentscheidungsgebiete aller möglicher Realisierungen der Nachrichtenelemente pflastern die gesamte komplexe Ebene wieder vollständig und ohne Überlappungen. In empfängerorientierten Übertragungssystemen ist der Sendeoperator unter Berücksichtigung des a priori festgelegten Empfangsoperators und des Kanals a posteriori festgelegt. Im Falle der in der Arbeit betrachteten linearen empfängerorientierten Übertragungssysteme ist der Sendeoperator linear, und die durch den Quantisierer eingebrachte Nichtlinearität bleibt beim Festlegen des Sendeoperators außer acht; in diesem Fall werden in der Arbeit einfach zusammenhängende Quantisierungsgebiete vorausgesetzt. Im Falle der betrachteten nichtlinearen empfängerorientierten Übertragungssysteme wird der Sendeoperator unter Beachten des Kanals, des a priori festgelegten Empfangsoperators und auch des Quantisierungsschemas – dieses sei nun mehrfach zusammenhängend – bestimmt.

Der Entwurf linearer empfängerorientierter Übertragungssysteme nach den Verfahren TxMF (Transmit Matched Filter), TxZF (Transmit Zero Forcing)–Filter und TxMMSE (Transmit Minimum Mean Square Error)–Filter sind aus dem Schrifttum wohlbekannt und werden in der Arbeit deshalb nur kurz rekapituliert. Als für die erforderliche Sendeleistung relevante Performanzkriterien werden die Energieeffizienz und die mit dieser zusammenhängende Sendeeffizienz eingeführt und erläutert, wobei die Herleitung dieser Kriterien auf der Singulärwertzerlegung der MIMO-Kanalmatrix basiert. Eine hohe Energieeffizienz bedeutet, daß ein Großteil der abgestrahlten Sendeleistung als nutzbringende Leistung im Empfänger ankommt, so daß bei einer gewissen geforderten

Übertragungsqualität die Sendeleistung relativ klein gehalten werden kann. Anhand des Kriteriums Energieeffizienz können in Kapitel 3 der Arbeit ein paar Hinweise zur günstigen A-priori-Wahl des Empfangsoperators gegeben werden.

Ein Hauptanliegen der vorliegenden Dissertation ist das Herausarbeiten der Vorteile, die MIMO-Antennensysteme in Kombination mit linearen empfängerorientierten Mobilfunk-Abwärtsstrecken bieten. Hierbei werden nur Systeme mit TxZF-Filter betrachtet, bei denen die BS eine Anzahl von K_B Sendeantennen und jede der K MSen eine Anzahl von K_M Empfangsantennen hat. Zunächst werden der Algorithmus des TxZF-Filters und die entsprechenden Performanzkriterien für ein generisches lineares empfängerorientiertes Übertragungssystem formuliert und an die Kombination mit MIMO-Antennenstrukturen angepaßt. Bei den dadurch entstehenden Abwärtsstrecken kann man unterscheiden zwischen den beiden Situationen der kooperativen bzw. der nicht kooperativen MSen. Im Fall kooperativer MSen kennt jede einzelne MS auch die Empfangssignale der anderen $K - 1$ MSen. Wie in Abschnitt 4.4 der Arbeit an einem numerischen Beispiel gezeigt wird, hätte man in einer solchen Situation eine besonders günstige Systemperformanz; allerdings wäre das hierzu erforderliche Verfügbarmachen aller K Empfangssignale an allen K MSen nicht praktikabel. In praktischen Systemen verfügt jede MS nur über ihr eigenes Empfangssignal, und nur dieser Fall der nicht kooperativen MSen wird in der Arbeit betrachtet.

Bei den Performanzstudien werden die statistischen Eigenschaften, nämlich Mittelwert und Varianz, der Sendeeffizienz und der erforderlichen Sendeleistungen in analytischen und/oder numerischen Untersuchungen ermittelt. Hierbei werden die beiden Fälle der total unkorrelierten bzw. voll korrelierten Kanäle, siehe Kapitel 2, betrachtet.

Zunächst wird die Sendeeffizienz untersucht. Für den Fall total unkorrelierter Kanäle findet man analytische Ergebnisse zur Sendeeffizienz im Schrifttum. Allerdings gelten diese Ergebnisse nur näherungsweise, weil sie auf der Annahme der statistischen Unabhängigkeit gewisser, im Verlauf der Betrachtungen auftretenden Größen basieren. Der entsprechende analytische Ausdruck zeigt, daß mit einer Zunahme der Anzahl K_B der Sendeantennen sowohl Mittelwert als auch Varianz der Sendeeffizienz steigen. Allerdings berücksichtigt der analytische Ausdruck nicht den Einfluß der Anzahl K_M der Empfangsantennen pro MS. Dieses Defizit hängt mit der gerade erwähnten Vernachlässigung des Effekts statistischer Bindungen zusammen. In Simulationen wird untersucht, wie schwerwiegend dieser Effekt ist. Es zeigt sich, daß der analytische Ausdruck im wesentlichen die richtigen Ergebnisse liefert, Ergebnisse also, die mit den Simulationsergebnissen gut übereinstimmen. Allerdings ergeben sich bei der Varianz der Sendeeffizienz gewisse, von der Anzahl K_M der Empfangsantennen pro MS abhängige Abweichungen. Mit zunehmendem K_M nähern sich die analytischen und simulativen Ergebnisse auch bezüglich der Varianz der Sendeeffizienz immer mehr aneinander an. Im Falle völlig korrelierter Kanäle ist kein analytischer Ausdruck für die Sendeeffizienz verfügbar. Durch Simulationen zeigt sich jedoch, daß der Unterschied der Sendeeffizienz in den beiden Fällen der total unkorrelierten und der völlig korrelierten Kanäle nicht gravierend ist, wobei im letzteren Fall eine gewisse Degradation im Sinne eines geringeren Mittelwerts und einer

höheren Varianz der Sendeeffizienz zu beobachten ist. Zusammenfassend kann man feststellen, daß sich MIMO-Antennenstrukturen als vorteilhaft für die Reduzierung der erforderlichen Sendeleistung erweisen, und daß sich hierbei das Erhöhen der Anzahl K_B der Sendeantennen mehr auszahlt als das Erhöhen der Anzahl K_M der Empfangsantennen pro MS. Das Studium der Sendeeffizienz für die beiden Extremfälle der total unkorrelierten bzw. völlig korrelierten Kanäle scheint auch zur Vermutung zu berechtigen, daß bei gegebenen Werten K_B und K_M die Sendeeffizienz mit zunehmender Korrelation der Kanäle abnimmt.

Das Untersuchen der Sendeeffizienz zeigt die günstige Auswirkung einer Erhöhung der Anzahl der Sende- und Empfangsantennen auf die erforderliche Sendeleistung. Das Studium dieses Effekt wird in der Dissertation weiter vertieft durch das direkte Betrachten der erforderlichen Sendeleistung. Im Fall total unkorrelierter Kanäle gibt es im Schrifttum wieder einen geschlossenen Näherungsausdruck. Dieser zeigt, daß mit zunehmender Anzahl K_B der Sendeantennen Mittelwert und Varianz der erforderlichen Sendeleistung abnehmen. Wieder berücksichtigt der genannte Näherungsausdruck nicht die Anzahl K_M an Empfangsantennen pro MS. Zum geschlossenen Erfassen dieses Effekts wird vom Verfasser zunächst ein einfaches Beispiel betrachtet. Dann wird durch Simulationen der genannte analytische Näherungsausdruck verifiziert. Hierbei zeigt sich, daß beim Erhöhen von K_M im Fall total unkorrelierter Kanäle Mittelwert und Varianz der erforderlichen Sendeleistung zurückgehen, und daß das analytische und das simulative Ergebnis mit wachsendem K_M immer besser übereinstimmen. Im Falle völlig korrelierter Kanäle zeigen ein einfaches, geschlossen behandelbares Beispiel sowie die Simulationsergebnisse, daß ein Erhöhen von K_B einen ähnlich günstigen, aber etwas weniger ausgeprägten Effekt auf die erforderliche Sendeleistung haben wie im Fall völlig korrelierter Kanäle. Größer ist bei den beiden Kanalmodellen der Unterschied des Einflusses der Anzahl K_M an Empfangsantennen pro MS; im Falle völlig korrelierter Kanäle führt ein Erhöhen von K_M sogar zu einer geringfügigen Zunahme von Mittelwert und Varianz der erforderlichen Sendeleistung. Zusammenfassend kann man sagen, daß eine Zunahme von K_B sich stets günstig auf Mittelwert und Varianz der erforderlichen Sendeleistung auswirkt, während der günstige Effekt einer Zunahme von K_M mit zunehmender Korrelation der Kanäle abnimmt und sich sogar ins Gegenteil verkehren kann.

Ein wichtiges Ziel der Arbeit ist das Erforschen nichtlinearer empfängerorientierten Mobilfunkabwärtsstrecken mit MIMO-Antennenstrukturen und mehrfach zusammenhängenden Entscheidungsgebieten in den empfängerseitigen Quantisierern. Wie oben schon bemerkt, entspricht bei herkömmlichen Quantisierern mit einfach zusammenhängenden Entscheidungsgebieten jede Realsierung eines Nachrichtenelements einem einfach zusammenhängenden Quantisierungsgebiet. Im Fall einer fehlerfreien Übertragung eines Nachrichtenelements kommt der entsprechende empfängerseitige Schätzwert in das korrekte Entscheidungsgebiet zu liegen. Im Gegensatz zu herkömmlichen Quantisierern mit einfach zusammenhängenden Entscheidungsgebieten haben unkonventionelle Quantisierer mit mehrfach zusammenhängenden Entscheidungsgebieten für jede Realisierung eines Nachrichtenelements mehrere, u.U. sogar unendlich viele Teilquantisierungsgebiete. Wenn der empfängerseitig gewonnene Schätzwert in irgendeinem dieser Gebiete liegt, wird

er fehlerfrei detektiert. Hat man nun eine Folge zu übertragenden Nachrichtenelemente, so gibt es demnach nicht nur ein einziges mögliches Sendesignal, sondern vielmehr ein ganzes Sortiment solcher Signale. Jedes dieser möglichen Sendesignale hat hierbei i.a. eine andere Energie. Der springende Punkt der in der vorliegenden Dissertation betrachteten nichtlinearen empfängerorientierten Mobilfunkabwärtsstrecken besteht nun darin, daß man von den vielen möglichen Sendesignalen genau dasjenige der geringsten Energie sendet. Zum Ermitteln dieses optimalen Sendesignals ist im bis dato verfügbaren Schrifttum nur das Vorgehen einer erschöpfenden Suche durch alle möglichen Sendesignale bekannt, eine prohibitiv aufwendige Methode. In der vorliegenden Dissertation wird nun ein weniger aufwendiger Weg zur Auswahl des Sendesignals vorgestellt. Dieser führt zwar nicht zum optimalen Sendesignal, d.h. zum Sendesignal der absolut geringstmöglichen Energie, ergibt jedoch trotzdem ein energiemäßig recht attraktives Sendesignal. Bei dem vorgeschlagenen Verfahren wird das gesamte Sendesignal aus iterativ gebildeten Sendesignalen für die einzelnen MSen zusammengesetzt, wobei die MSen in der Ordnung abnehmender Kanaldämpfung abgehandelt werden. Das Verfahren wird in der Dissertation als TxNZF (Transmit Non-linear Zero Forcing) Filter bezeichnet. Simulationen zeigen, daß das TxNZF-Filter zu wesentlich geringeren erforderlicher Sendeleistungen führt als das TxZF-Filter, und zwar insbesondere dann, wenn die Kanaldämpfungen von der BS zu den einzelnen MSen sich stark voneinander unterscheiden. Die Untersuchungen zum TxNZF-Filter werden ergänzt durch Betrachtungen zu dessen aufwandgünstiger Implementierung. Abschließend stellt der Autor das neue Konzept des TxNZF-Filters in einen allgemeinen Rahmen verschiedener Übertragungstechniken, bei denen in den empfängerseitigen Quantisierern mehrfach zusammenhängende Entscheidungsgebiete verwendet werden, und bei denen günstige Balancen zwischen Implementierungskomplexität und Performanz gefunden werden können. Eines dieser Konzepte ist unter der Bezeichnung Tomlinson-Harashima-Precoding bekannt.

6.3 中文

本篇论文的重点是对多用户移动通信中下行链路 (multi-user mobile radio downlinks) 的基带算法的研究。传统的算法多是基于面向发射端 (transmitter oriented) 的设计原理的，也即优先给出发射端的算法，然后根据估测的信道信息 (channel information) 和已知的发射端算法确定接收端的算法，比如联合检测算法 (Joint Detection, JD)。在这种设计原理下，接收端需要承受相当大的算法复杂度。对于所研究的下行链路来说，这意味着移动终端 (Mobile Terminal, MT) 的复杂度将大大提高。相对与传统的设计原理，本文着重与基于面向接收端 (receiver oriented) 的设计原理的算法研究，也即优先给出简单的接收端的算法，然后根据估测的信道信息和已知的接收端算法确定发射端的算法。在这种设计原理下，主要的算法复杂度将由发射端来承受，接收端变得相当简单。考虑到在发射端信道信息必须提前获得，这在一定程度上使得基于接收端设计原理的算法更适用于使用时分复用 (Time Division Duplexing, TDD) 的移动通信系统。在设计算法的同时，另一个重要的考虑因素是使得发射端的发射功率尽量的低，从而有效的降低蜂窝移动通信系统中的小区间干扰 (intercell interference)，同时也可以降低电磁波对人体带来的可能的伤害性。基于以上的考虑，本文的研究主要集中与以下两方面:

- 系统的分析多入多出 (multiple-input multiple-output, MIMO) 天线系统对已有的线性算法的有益影响，作为一个重要的例子，本文只考虑对与 TxZF (Transmit Zero Forcing) 算法的影响;

- 基于接收端使用多联结量化器 (multiply connected quantizer) 的非线性算法的设计以及特性的研究。

在本文的研究中，系统的理论和数据分析表明多入多出天线系统在多数通信环境下能够提高传输功率的利用率，从而达到降低发射功率的目的。接收端多联结量化器的使用给发射端算法的设计提供了额外的自由度。建立在这种自由度的基础上，作者设计出了 TxNZF (Transmit Non-linear Zero Forcing) 算法。研究表明，与线性算法相比 TxNZF 算法能更有效的降低发射功率。尤其是在各移动终端与发射端间的信道衰减差异很大的情况下，这种发射功率的降低更为显著。

Appendix A
Derivations

A.1 Derivations of mean and variance of a Tx energy related variable for scenarios with totally uncorrelated channel impulse responses

Substitution (4.48) into X in (4.54) yields

$$X = \sum_{k_B=1}^{K_B} \sum_{q=1}^{Q_t} \left| \sum_{k_M=1}^{K_M} \sum_{w=1}^{W} D_{1,w+q-1}^{(1,\,k_M)} \underline{h}_w^{(1,\,k_B,\,k_M)} \right|^2. \tag{A.1}$$

For the sake of brevity, we neglect some indices of all quantities, which indicate the numbering of MTs and the numbering of rows of matrices when deriving the mean and the variance of X in the following. Then, (A.1) is expressed as

$$X = \sum_{k_B=1}^{K_B} \sum_{q=1}^{Q_t} \left| \sum_{k_M=1}^{K_M} \sum_{w=1}^{W} D_{w+q-1}^{(k_M)} \underline{h}_w^{(k_B,\,k_M)} \right|^2. \tag{A.2}$$

(A.2) can be rewritten as

$$\begin{aligned}
X &= \sum_{k_B=1}^{K_B} \sum_{q=1}^{Q_t} \left(\sum_{k_M=1}^{K_M} \sum_{w=1}^{W} D_{w+q-1}^{(k_M)} \underline{h}_w^{(k_B,\,k_M)} \sum_{k'_M=1}^{K_M} \sum_{w'=1}^{W} D_{w'+q-1}^{(k'_M)} \underline{h}_{w'}^{(k_B,\,k'_M)\,\mathrm{H}} \right) \\
&= \sum_{w=1}^{W} \sum_{w'=1}^{W} \sum_{k_B=1}^{K_B} \sum_{q=1}^{Q_t} \sum_{k_M=1}^{K_M} \sum_{k'_M=1}^{K_M} D_{w+q-1}^{(k_M)} D_{w'+q-1}^{(k'_M)} \underline{h}_w^{(k_B,\,k_M)} \underline{h}_{w'}^{(k_B,\,k'_M)\,\mathrm{H}}.
\end{aligned} \tag{A.3}$$

We first consider the mean value

$$\begin{aligned}
\mathrm{E}\{X\} &= \mathrm{E}\left\{ \sum_{w=1}^{W} \sum_{w'=1}^{W} \sum_{k_B=1}^{K_B} \sum_{q=1}^{Q_t} \sum_{k_M=1}^{K_M} \sum_{k'_M=1}^{K_M} D_{w+q-1}^{(k_M)} D_{w'+q-1}^{(k'_M)} \underline{h}_w^{(k_B,\,k_M)} \underline{h}_{w'}^{(k_B,\,k'_M)\,\mathrm{H}} \right\} \\
&= \sum_{w=1}^{W} \sum_{w'=1}^{W} \sum_{k_B=1}^{K_B} \sum_{q=1}^{Q_t} \sum_{k_M=1}^{K_M} \sum_{k'_M=1}^{K_M} \mathrm{E}\left\{ D_{w+q-1}^{(k_M)} D_{w'+q-1}^{(k'_M)} \underline{h}_w^{(k_B,\,k_M)} \underline{h}_{w'}^{(k_B,\,k'_M)\,\mathrm{H}} \right\}
\end{aligned} \tag{A.4}$$

of X of (A.3). As assumed in Subsection 4.5.2, $D_{w+q-1}^{(k_M)}$, $k_M = 1 \ldots K_M$, are i.i.d. binary variables, for these variables

$$\mathrm{E}\left\{ D_p^{(k_M)} D_{p'}^{(k'_M)} \right\} = \begin{cases} \frac{1}{K_M(Q_t+W-1)} & (p=p') \bigcap (k_M = k'_M), \\ 0 & \text{else}, \end{cases} \tag{A.5}$$

holds. The channel impulse responses $\underline{h}_w^{(k_B, k_M)}$ are i.i.d. complex Gaussian variables, for which the relation

$$
\mathrm{E}\left\{ \underline{h}_w^{(k_B, k_M)} \underline{h}_{w'}^{(k_B, k'_M)\,\mathrm{H}} \right\} = \begin{cases} 2\sigma_w^2 & (w = w') \bigcap (k_M = k'_M), \\ \\ 0 & \text{else}, \end{cases} \tag{A.6}
$$

is valid. $D_{w+q-1}^{(k_M)}$ of (A.5) and $\underline{h}_w^{(k_B, k_M)}$ of (A.6) are independently distributed. Now, with (A.5) and (A.6), the mean value $\mathrm{E}\{X\}$ of (A.4) can be written as

$$
\begin{aligned}
\mathrm{E}\{X\} &= \sum_{w=1}^{W} \sum_{w'=1}^{W} \sum_{k_B=1}^{K_B} \sum_{q=1}^{Q_t} \sum_{k_M=1}^{K_M} \sum_{k'_M=1}^{K_M} \mathrm{E}\left\{ D_{w+q-1}^{(k_M)} D_{w'+q-1}^{(k'_M)} \underline{h}_w^{(k_B, k_M)} \underline{h}_{w'}^{(k_B, k'_M)\,\mathrm{H}} \right\} \\
&= \sum_{k_B=1}^{K_B} \sum_{q=1}^{Q_t} \sum_{w=w'=1}^{W} \sum_{k_M=k'_M=1}^{K_M} \mathrm{E}\left\{ D_{w+q-1}^{(k_M)} D_{w'+q-1}^{(k'_M)} \right\} \mathrm{E}\left\{ \underline{h}_w^{(k_B, k_M)} \underline{h}_{w'}^{(k_B, k'_M)\,\mathrm{H}} \right\} \\
&= \sum_{k_B=1}^{K_B} \sum_{q=1}^{Q_t} \sum_{w=1}^{W} \sum_{k_M=1}^{K_M} \mathrm{E}\left\{ D_{w+q-1}^{(k_M)} D_{w+q-1}^{(k_M)} \right\} \mathrm{E}\left\{ \underline{h}_w^{(k_B, k_M)} \underline{h}_w^{(k_B, k_M)\,\mathrm{H}} \right\}.
\end{aligned} \tag{A.7}
$$

Finally, with (A.5) and (A.6) we obtain the mean value

$$
\begin{aligned}
\mathrm{E}\{X\} &= \sum_{k_B=1}^{K_B} \sum_{q=1}^{Q_t} \sum_{w=1}^{W} \sum_{k_M=1}^{K_M} \frac{1}{K_M(Q_t + W - 1)} \cdot 2\sigma_w^2 \\
&= \frac{2K_B Q_t}{(Q_t + W - 1)} \sum_{w=1}^{W} \sigma_w^2
\end{aligned} \tag{A.8}
$$

of X of (A.2).

Noticing that for the variance of X

$$
\mathrm{var}\{X\} = \mathrm{E}\left\{X^2\right\} - (\mathrm{E}\{X\})^2 \tag{A.9}
$$

is valid, only the calculation of the 2nd moment $\mathrm{E}\{X^2\}$ of X is necessary. Substituting (A.3) into the 2nd moment $\mathrm{E}\{X^2\}$, and then, expanding it, we can obtain

$$
\begin{aligned}
\mathrm{E}\left\{X^2\right\} &= \mathrm{E}\left\{ \left(\sum_{k_B=1}^{K_B} \sum_{q=1}^{Q_t} \left| \sum_{k_M=1}^{K_M} \sum_{w=1}^{W} D_{w+q-1}^{(k_M)} \underline{h}_w^{(k_B, k_M)} \right|^2 \right)^2 \right\} \\
&= \sum_{k_B=1}^{K_B} \sum_{k'_B=1}^{K_B} \sum_{q=1}^{Q_t} \sum_{q'=1}^{Q_t} \sum_{k_M=1}^{K_M} \sum_{w=1}^{W} \sum_{k'_M=1}^{K_M} \sum_{w'=1}^{W} \sum_{k''_M=1}^{K_M} \sum_{w''=1}^{W} \sum_{k'''_M=1}^{K_M} \sum_{w'''=1}^{W} \\
&\quad \cdot \mathrm{E}\left\{ D_{w+q-1}^{(k_M)} D_{w'+q-1}^{(k'_M)} D_{w''+q'-1}^{(k''_M)} D_{w'''+q'-1}^{(k'''_M)} \right\} \\
&\quad \cdot \mathrm{E}\left\{ \underline{h}_w^{(k_B, k_M)} \underline{h}_{w'}^{(k_B, k'_M)\,\mathrm{H}} \underline{h}_{w''}^{(k'_B, k''_M)} \underline{h}_{w'''}^{(k'_B, k'''_M)\,\mathrm{H}} \right\}.
\end{aligned} \tag{A.10}
$$

(A.10) contains a lot of terms, we classify all the terms to simplify the calculation of (A.10). Let us first look at all the means $\mathrm{E}\left\{\underline{h}_w^{(k_{\mathrm{B}},k_{\mathrm{M}})}\underline{h}_{w'}^{(k_{\mathrm{B}},k_{\mathrm{M}}')^{\mathrm{H}}}\underline{h}_{w''}^{(k_{\mathrm{B}}',k_{\mathrm{M}}'')}\underline{h}_{w'''}^{(k_{\mathrm{B}}',k_{\mathrm{M}}''')^{\mathrm{H}}}\right\}$ in (A.10). With (A.6) only the terms with the indices classified into the following four cases are not equal to zero:

$$
\begin{cases}
\text{case 1:} & (k_{\mathrm{B}}=k_{\mathrm{B}}')\bigcap(w=w')\bigcap(k_{\mathrm{M}}=k_{\mathrm{M}}')\bigcap(w''=w''')\bigcap(k_{\mathrm{M}}''=k_{\mathrm{M}}''') \\
& \bigcap\left[(w,k_{\mathrm{M}})\neq(w'',k_{\mathrm{M}}'')\right], \\[4pt]
\text{case 2:} & (k_{\mathrm{B}}=k_{\mathrm{B}}')\bigcap(w=w''')\bigcap(k_{\mathrm{M}}=k_{\mathrm{M}}''')\bigcap(w'=w'')\bigcap(k_{\mathrm{M}}'=k_{\mathrm{M}}'') \\
& \bigcap\left[(w,k_{\mathrm{M}})\neq(w',k_{\mathrm{M}}')\right], \\[4pt]
\text{case 3:} & (k_{\mathrm{B}}=k_{\mathrm{B}}')\bigcap(w=w'=w''=w''')\bigcap(k_{\mathrm{M}}=k_{\mathrm{M}}'=k_{\mathrm{M}}''=k_{\mathrm{M}}'''), \\[4pt]
\text{case 4:} & (k_{\mathrm{B}}\neq k_{\mathrm{B}}')\bigcap(w=w')\bigcap(k_{\mathrm{M}}=k_{\mathrm{M}}')\bigcap(w''=w''')\bigcap(k_{\mathrm{M}}''=k_{\mathrm{M}}''').
\end{cases} \tag{A.11}
$$

Now, let us take $\mathrm{E}\left\{D_{w+q-1}^{(k_{\mathrm{M}})}D_{w'+q-1}^{(k_{\mathrm{M}}')}D_{w''+q'-1}^{(k_{\mathrm{M}}'')}D_{w'''+q'-1}^{(k_{\mathrm{M}}''')}\right\}$ into account. With the indices belonging to case 1, the terms $\mathrm{E}\left\{D_{w+q-1}^{(k_{\mathrm{M}})}D_{w'+q-1}^{(k_{\mathrm{M}}')}D_{w''+q'-1}^{(k_{\mathrm{M}}'')}D_{w'''+q'-1}^{(k_{\mathrm{M}}''')}\right\}$ are also not equal to zero, therefore, we can obtain the sum

$$
\begin{aligned}
\Sigma_{\text{case1}} &= \sum_{k_{\mathrm{B}}=1}^{K_{\mathrm{B}}}\sum_{q=1}^{Q_{\mathrm{t}}}\sum_{q'=1}^{Q_{\mathrm{t}}}\sum_{w=1}^{W}\sum_{w''=1}^{W}\sum_{k_{\mathrm{M}}=1}^{K_{\mathrm{M}}}\sum_{k_{\mathrm{M}}''=1}^{K_{\mathrm{M}}}\overset{(w,k_{\mathrm{M}})\neq(w'',k_{\mathrm{M}}'')}{\mathrm{E}\left\{\left\|D_{w+q-1}^{(k_{\mathrm{M}})}\right\|^2\right\}} \\
&\quad \cdot\mathrm{E}\left\{\left\|D_{w''+q'-1}^{(k_{\mathrm{M}}'')}\right\|^2\right\}\mathrm{E}\left\{\left\|\underline{h}_w^{(k_{\mathrm{B}},k_{\mathrm{M}})}\right\|^2\right\}\mathrm{E}\left\{\left\|\underline{h}_{w''}^{(k_{\mathrm{B}},k_{\mathrm{M}}'')}\right\|^2\right\} \\
&= \sum_{k_{\mathrm{B}}=1}^{K_{\mathrm{B}}}\sum_{q=1}^{Q_{\mathrm{t}}}\sum_{q'=1}^{Q_{\mathrm{t}}}\sum_{w=1}^{W}\sum_{w''=1}^{W}\sum_{k_{\mathrm{M}}=1}^{K_{\mathrm{M}}}\sum_{k_{\mathrm{M}}''=1}^{K_{\mathrm{M}}}\overset{(w,k_{\mathrm{M}})\neq(w'',k_{\mathrm{M}}'')}{\frac{4\sigma_w^2\sigma_{w''}^2}{K_{\mathrm{M}}^2(Q_{\mathrm{t}}+W-1)^2}}
\end{aligned} \tag{A.12}
$$

of all the terms with the indices belonging to case 1. In the case 2, only when

$$
q=q' \tag{A.13}
$$

holds, the terms $\mathrm{E}\left\{D_{w+q-1}^{(k_{\mathrm{M}})}D_{w'+q-1}^{(k_{\mathrm{M}}')}D_{w''+q'-1}^{(k_{\mathrm{M}}'')}D_{w'''+q'-1}^{(k_{\mathrm{M}}''')}\right\}$ do not vanish, therefore, the sum of all the terms with the indices belonging to case 2 becomes

$$
\begin{aligned}
\Sigma_{\text{case2}} &= \sum_{k_{\mathrm{B}}=1}^{K_{\mathrm{B}}}\sum_{q=1}^{Q_{\mathrm{t}}}\sum_{w=1}^{W}\sum_{w'=1}^{W}\sum_{k_{\mathrm{M}}=1}^{K_{\mathrm{M}}}\sum_{k_{\mathrm{M}}'=1}^{K_{\mathrm{M}}}\overset{(w,k_{\mathrm{M}})\neq(w',k_{\mathrm{M}}')}{\mathrm{E}\left\{\left\|D_{w+q-1}^{(k_{\mathrm{M}})}\right\|^2\right\}} \\
&\quad \cdot\mathrm{E}\left\{\left\|D_{w'+q-1}^{(k_{\mathrm{M}}')}\right\|^2\right\}\mathrm{E}\left\{\left\|\underline{h}_w^{(k_{\mathrm{B}},k_{\mathrm{M}})}\right\|^2\right\}\mathrm{E}\left\{\left\|\underline{h}_{w'}^{(k_{\mathrm{B}},k_{\mathrm{M}}')}\right\|^2\right\} \\
&= \sum_{k_{\mathrm{B}}=1}^{K_{\mathrm{B}}}\sum_{q=1}^{Q_{\mathrm{t}}}\sum_{w=1}^{W}\sum_{w'=1}^{W}\sum_{k_{\mathrm{M}}=1}^{K_{\mathrm{M}}}\sum_{k_{\mathrm{M}}'=1}^{K_{\mathrm{M}}}\overset{(w,k_{\mathrm{M}})\neq(w',k_{\mathrm{M}}')}{\frac{4\sigma_w^2\sigma_{w'}^2}{K_{\mathrm{M}}^2(Q_{\mathrm{t}}+W-1)^2}}.
\end{aligned} \tag{A.14}
$$

Similarly, we can obtain the sum

$$
\begin{aligned}
\Sigma_{\text{case3}} &= \sum_{k_{\text{B}}=1}^{K_{\text{B}}} \sum_{w=1}^{W} \sum_{q=1}^{Q_{\text{t}}} \sum_{q'=1}^{Q_{\text{t}}} \sum_{k_{\text{M}}=1}^{K_{\text{M}}} \\
&\quad \text{E}\left\{ D_{w+q-1}^{(k_{\text{M}})} D_{w+q-1}^{(k_{\text{M}})} D_{w+q'-1}^{(k_{\text{M}})} D_{w+q'-1}^{(k_{\text{M}})} \right\} \text{E}\left\{ \|\underline{h}_{w}^{(k_{\text{B}}, k_{\text{M}})}\|^{4} \right\} \\
&= \sum_{k_{\text{B}}=1}^{K_{\text{B}}} \sum_{w=1}^{W} \sum_{q=1}^{Q_{\text{t}}} \sum_{q'=1}^{Q_{\text{t}}} \sum_{k_{\text{M}}=1}^{K_{\text{M}}} \frac{8\sigma_{w}^{4}}{K_{\text{M}}^{2}\left(Q_{\text{t}}+W-1\right)^{2}}
\end{aligned} \tag{A.15}
$$

of the terms with indices belonging to case 3 and the sum

$$
\begin{aligned}
\Sigma_{\text{case4}} &= \sum_{k_{\text{B}}=1}^{K_{\text{B}}} \sum_{k_{\text{B}}'=1, k_{\text{B}}'\neq k_{\text{B}}}^{K_{\text{B}}} \sum_{q=1}^{Q_{\text{t}}} \sum_{q'=1}^{Q_{\text{t}}} \sum_{k_{\text{M}}=1}^{K_{\text{M}}} \sum_{w=1}^{W} \sum_{k_{\text{M}}''=1}^{K_{\text{M}}} \sum_{w''=1}^{W} \\
&\quad \text{E}\left\{ \|D_{w+q-1}^{(k_{\text{M}})}\|^{2} \right\} \text{E}\left\{ \|D_{w''+q'-1}^{(k_{\text{M}}'')}\|^{2} \right\} \text{E}\left\{ \|\underline{h}_{w}^{(k_{\text{B}}, k_{\text{M}})}\|^{2} \right\} \text{E}\left\{ \|\underline{h}_{w''}^{(k_{\text{B}}', k_{\text{M}}'')}\|^{2} \right\} \\
&= \sum_{k_{\text{B}}=1}^{K_{\text{B}}} \sum_{k_{\text{B}}'=1, k_{\text{B}}'\neq k_{\text{B}}}^{K_{\text{B}}} \sum_{q=1}^{Q_{\text{t}}} \sum_{q'=1}^{Q_{\text{t}}} \sum_{k_{\text{M}}=1}^{K_{\text{M}}} \sum_{w=1}^{W} \sum_{k_{\text{M}}''=1}^{K_{\text{M}}} \sum_{w''=1}^{W} \frac{4\sigma_{w}^{2}\sigma_{w'}^{2}}{K_{\text{M}}^{2}\left(Q_{\text{t}}+W-1\right)^{2}} \\
&= \frac{4Q_{\text{t}}^{2}\left(K_{\text{B}}^{2}-K_{\text{B}}\right)}{\left(Q_{\text{t}}+W-1\right)^{2}} \sum_{w=1}^{W} \sum_{w''=1}^{W} \sigma_{w}^{2}\sigma_{w'}^{2}
\end{aligned} \tag{A.16}
$$

of the terms with the indices belonging to case 4. Consequently, with (A.12), (A.14), (A.15) and (A.16), (A.10) becomes

$$
\text{E}\left\{ X^{2} \right\} = \frac{4K_{\text{B}}Q_{\text{t}}}{K_{\text{M}}\left(Q_{\text{t}}+W-1\right)^{2}} \left[K_{\text{M}}(K_{\text{B}}Q_{\text{t}}+1) \sum_{w=1}^{W} \sum_{w'=1}^{W} \sigma_{w}^{2}\sigma_{w'}^{2} + (Q_{\text{t}}-1) \sum_{w=1}^{W} \sigma_{w}^{4} \right]. \tag{A.17}
$$

Substitution (A.17) and (A.8) in (A.9) yields

$$
\begin{aligned}
\text{var}\left\{ X \right\} &= \text{E}\left\{ X^{2} \right\} - \left(\text{E}\left\{ X \right\}\right)^{2} \\
&= \frac{4K_{\text{B}}Q_{\text{t}}}{K_{\text{M}}\left(Q_{\text{t}}+W-1\right)^{2}} \left[(Q_{\text{t}}-1) \sum_{w=1}^{W} \sigma_{w}^{4} + K_{\text{M}} \sum_{w=1}^{W} \sum_{w'=1}^{W} \sigma_{w}^{2}\sigma_{w'}^{2} \right].
\end{aligned} \tag{A.18}
$$

A.2 Derivations of mean and variance of a Tx energy related variable for scenarios with fully correlated channel impulse responses

As presented in Section 2.3.3, the channel impulse responses for the considered scenarios can be written as

$$
\underline{\mathbf{h}}^{(k, k_{\text{B}}, k_{\text{M}})} = \underline{a}_{\text{Tx}}^{(k, k_{\text{B}})}\, \underline{a}_{\text{Rx}}^{(k, k_{\text{M}})}\, \underline{\mathbf{h}}_{\text{R}}^{(k)} = e^{\text{j}\phi^{(k, k_{\text{B}}, k_{\text{M}})}}\, \underline{\mathbf{h}}_{\text{R}}^{(k)}. \tag{A.19}
$$

$\phi^{(k,k_\mathrm{B},k_\mathrm{M})}$ in (A.19) depends on the geometrical configurations of the corresponding Tx antenna, Rx antenna and MT. Again, we neglect the indices for the numbering of MTs and the rows of matrices as done in A.1.

Under the assumptions made in Section 4.5.3, the elements $\underline{h}_{\mathrm{R},\,w}$ of reference channel impulse responses $\underline{\mathbf{h}}_\mathrm{R}$ of (A.19) are i.i.d. complex Gaussian variables, for which the relation

$$\mathrm{E}\left\{\underline{h}_{\mathrm{R},\,w}\underline{h}_{\mathrm{R},\,w'}^\mathrm{H}\right\} = \begin{cases} 2\sigma_w^2 & w = w', \\ \\ 0 & \text{else,} \end{cases} \tag{A.20}$$

is valid. $D_{w+q-1}^{(k_\mathrm{M})}$ follows the relation of (A.5). $\phi^{(k_\mathrm{B},k_\mathrm{M})}$ are random variables uniformly distributed within $[-\pi,\pi)$, therefore,

$$\mathrm{E}\left\{e^{\mathrm{j}\phi^{(k_\mathrm{B},k_\mathrm{M})}}\right\} = 0 \tag{A.21}$$

is valid. Although $\phi^{(k_\mathrm{B},k_\mathrm{M})}$ are not independently distributed, to simplify the derivation made in what follows, we assume that the independencies exist among them. Because we are only interested in the basic behavior revealed by the analysis, this approximate assumption is not so bad. $\phi^{(k_\mathrm{B},k_\mathrm{M})}$, $D_{w+q-1}^{(k_\mathrm{M})}$ and $\underline{h}_w^{(k_\mathrm{B},k_\mathrm{M})}$ are independently distributed.

Substitution (4.48) and (A.19) into (4.54) yields

$$\begin{aligned} X &= \sum_{k_\mathrm{B}=1}^{K_\mathrm{B}}\sum_{q=1}^{Q_\mathrm{t}}\left|\sum_{k_\mathrm{M}=1}^{K_\mathrm{M}}\sum_{w=1}^{W}D_{w+q-1}^{(k_\mathrm{M})}\underline{h}_w^{(k_\mathrm{B},k_\mathrm{M})}\right|^2 \\ &= \sum_{k_\mathrm{B}=1}^{K_\mathrm{B}}\sum_{q=1}^{Q_\mathrm{t}}\left|\sum_{k_\mathrm{M}=1}^{K_\mathrm{M}}\sum_{w=1}^{W}D_{w+q-1}^{(k_\mathrm{M})}e^{\mathrm{j}\phi^{(k_\mathrm{B},k_\mathrm{M})}}\underline{h}_{\mathrm{R},\,w}\right|^2. \end{aligned} \tag{A.22}$$

Expanding (A.22) we obtain

$$\begin{aligned} X &= \sum_{k_\mathrm{B}=1}^{K_\mathrm{B}}\sum_{q=1}^{Q_\mathrm{t}}\left(\sum_{k_\mathrm{M}=1}^{K_\mathrm{M}}\sum_{w=1}^{W}D_{w+q-1}^{(k_\mathrm{M})}e^{\mathrm{j}\phi^{(k_\mathrm{B},k_\mathrm{M})}}\underline{h}_{\mathrm{R},\,w}\sum_{k_\mathrm{M}'=1}^{K_\mathrm{M}}\sum_{w'=1}^{W}D_{w'+q-1}^{(k_\mathrm{M}')}e^{-\mathrm{j}\phi^{(k_\mathrm{B},k_\mathrm{M}')}}\underline{h}_{\mathrm{R},\,w'}^\mathrm{H}\right) \\ &= \sum_{w=1}^{W}\sum_{w'=1}^{W}\sum_{k_\mathrm{B}=1}^{K_\mathrm{B}}\sum_{q=1}^{Q_\mathrm{t}}\sum_{k_\mathrm{M}=1}^{K_\mathrm{M}}\sum_{k_\mathrm{M}'=1}^{K_\mathrm{M}}D_{w+q-1}^{(k_\mathrm{M})}D_{w'+q-1}^{(k_\mathrm{M}')}e^{\mathrm{j}\phi^{(k_\mathrm{B},k_\mathrm{M})}-\mathrm{j}\phi^{(k_\mathrm{B},k_\mathrm{M}')}}\underline{h}_{\mathrm{R},\,w}\underline{h}_{\mathrm{R},\,w'}^\mathrm{H}. \end{aligned} \tag{A.23}$$

Let us first consider the mean

$$
\begin{aligned}
\mathrm{E}\left\{X\right\} \;=\; & \sum_{w=1}^{W}\sum_{w'=1}^{W}\sum_{k_{\mathrm{B}}=1}^{K_{\mathrm{B}}}\sum_{q=1}^{Q_{\mathrm{t}}}\sum_{k_{\mathrm{M}}=1}^{K_{\mathrm{M}}}\sum_{k'_{\mathrm{M}}=1}^{K_{\mathrm{M}}} \\
& \cdot\mathrm{E}\left\{D_{w+q-1}^{(k_{\mathrm{M}})}D_{w'+q-1}^{(k'_{\mathrm{M}})}e^{\mathrm{j}\phi^{(k_{\mathrm{B}},k_{\mathrm{M}})}-\mathrm{j}\phi^{(k_{\mathrm{B}},k'_{\mathrm{M}})}}\underline{h}_{\mathrm{R},w}\underline{h}_{\mathrm{R},w'}^{\mathrm{H}}\right\} \\
=\; & \sum_{w=1}^{W}\sum_{w'=1}^{W}\sum_{k_{\mathrm{B}}=1}^{K_{\mathrm{B}}}\sum_{q=1}^{Q_{\mathrm{t}}}\sum_{k_{\mathrm{M}}=1}^{K_{\mathrm{M}}}\sum_{k'_{\mathrm{M}}=1}^{K_{\mathrm{M}}} \\
& \cdot\mathrm{E}\left\{D_{w+q-1}^{(k_{\mathrm{M}})}D_{w'+q-1}^{(k'_{\mathrm{M}})}\right\}\mathrm{E}\left\{e^{\mathrm{j}\phi^{(k_{\mathrm{B}},k_{\mathrm{M}})}-\mathrm{j}\phi^{(k_{\mathrm{B}},k'_{\mathrm{M}})}}\right\}\mathrm{E}\left\{\underline{h}_{\mathrm{R},w}\underline{h}_{\mathrm{R},w'}^{\mathrm{H}}\right\} \quad \text{(A.24)}
\end{aligned}
$$

of X of (A.23). It is obvious from (A.5), (A.20) and (A.21) that only these terms in
(A.24) with the indices satisfying

$$
w = w' \tag{A.25}
$$

and

$$
k_{\mathrm{M}} = k'_{\mathrm{M}} \tag{A.26}
$$

do not vanish. Consequently, we obtain

$$
\begin{aligned}
\mathrm{E}\left\{X\right\} \;=\; & \sum_{w=1}^{W}\sum_{k_{\mathrm{B}}=1}^{K_{\mathrm{B}}}\sum_{q=1}^{Q_{\mathrm{t}}}\sum_{k_{\mathrm{M}}=1}^{K_{\mathrm{M}}}\mathrm{E}\left\{D_{w+q-1}^{(k_{\mathrm{M}})}D_{w+q-1}^{(k_{\mathrm{M}})}\right\}\mathrm{E}\left\{e^{\mathrm{j}\phi^{(k_{\mathrm{B}},k_{\mathrm{M}})}-\mathrm{j}\phi^{(k_{\mathrm{B}},k_{\mathrm{M}})}}\right\}\mathrm{E}\left\{\underline{h}_{\mathrm{R},w}\underline{h}_{\mathrm{R},w}^{\mathrm{H}}\right\} \\
=\; & \sum_{w=1}^{W}\sum_{k_{\mathrm{B}}=1}^{K_{\mathrm{B}}}\sum_{q=1}^{Q_{\mathrm{t}}}\sum_{k_{\mathrm{M}}=1}^{K_{\mathrm{M}}}\frac{2\sigma_{w}^{2}}{K_{\mathrm{M}}(Q_{\mathrm{t}}+W-1)} \\
=\; & \frac{2K_{\mathrm{B}}Q_{\mathrm{t}}}{Q_{\mathrm{t}}+W-1}\sum_{w=1}^{W}\sigma_{w}^{2}. \tag{A.27}
\end{aligned}
$$

As mentioned in Appendix A.1, only the 2nd moment

$$
\mathrm{E}\left\{X^{2}\right\} = \mathrm{E}\left\{\left(\sum_{k_{\mathrm{B}}=1}^{K_{\mathrm{B}}}\sum_{q=1}^{Q_{\mathrm{t}}}\left|\sum_{k_{\mathrm{M}}=1}^{K_{\mathrm{M}}}\sum_{w=1}^{W}D_{w+q-1}^{(k_{\mathrm{M}})}e^{\mathrm{j}\phi^{(k_{\mathrm{B}},k_{\mathrm{M}})}}\underline{h}_{\mathrm{R},w}\right|^{2}\right)\right\} \tag{A.28}
$$

of X of (A.22) is necessary to be calculated to obtain the variance of X. Because $\phi^{(k_{\mathrm{B}},k_{\mathrm{M}})}$,

$D_{w+q-1}^{(k_{\mathrm{M}})}$ and $\underline{h}_w^{(k_{\mathrm{B}},k_{\mathrm{M}})}$ are independently distributed, (A.28) can be written as

$$
\mathrm{E}\left\{X^2\right\} = \sum_{k_{\mathrm{B}}=1}^{K_{\mathrm{B}}} \sum_{k_{\mathrm{B}}'=1}^{K_{\mathrm{B}}} \sum_{q=1}^{Q_{\mathrm{t}}} \sum_{q'=1}^{Q_{\mathrm{t}}} \sum_{k_{\mathrm{M}}=1}^{K_{\mathrm{M}}} \sum_{w=1}^{W} \sum_{k_{\mathrm{M}}'=1}^{K_{\mathrm{M}}} \sum_{w'=1}^{W} \sum_{k_{\mathrm{M}}''=1}^{K_{\mathrm{M}}} \sum_{w''=1}^{W} \sum_{k_{\mathrm{M}}'''=1}^{K_{\mathrm{M}}} \sum_{w'''=1}^{W}
$$

$$
\cdot \mathrm{E}\left\{ D_{w+q-1}^{(k_{\mathrm{M}})} D_{w'+q-1}^{(k_{\mathrm{M}}')} D_{w''+q'-1}^{(k_{\mathrm{M}}'')} D_{w'''+q'-1}^{(k_{\mathrm{M}}''')} \right\}
$$

$$
\cdot \mathrm{E}\left\{ e^{\mathrm{j}\left(\phi^{(k_{\mathrm{B}},k_{\mathrm{M}})} - \phi^{(k_{\mathrm{B}},k_{\mathrm{M}}')} + \phi^{(k_{\mathrm{B}}',k_{\mathrm{M}}'')} - \phi^{(k_{\mathrm{B}}',k_{\mathrm{M}}''')} \right)} \right\}
$$

$$
\cdot \mathrm{E}\left\{ \underline{h}_{\mathrm{R},\,w} \underline{h}_{\mathrm{R},\,w'}^{\mathrm{H}} \underline{h}_{\mathrm{R},\,w''} \underline{h}_{\mathrm{R},\,w'''}^{\mathrm{H}} \right\}. \tag{A.29}
$$

(A.29) contains a lot of terms, we try to classify all the terms to simplify the calculation of (A.29). Let us first look at all the expectations $\mathrm{E}\left\{ e^{\mathrm{j}\left(\phi^{(k_{\mathrm{B}},k_{\mathrm{M}})} - \phi^{(k_{\mathrm{B}},k_{\mathrm{M}}')} + \phi^{(k_{\mathrm{B}}',k_{\mathrm{M}}'')} - \phi^{(k_{\mathrm{B}}',k_{\mathrm{M}}''')} \right)} \right\}$. $\mathrm{E}\left\{ \underline{h}_{\mathrm{R},\,w} \underline{h}_{\mathrm{R},\,w'}^{\mathrm{H}} \underline{h}_{\mathrm{R},\,w''} \underline{h}_{\mathrm{R},\,w'''}^{\mathrm{H}} \right\}$. With (A.20) and (A.21) only the terms with the indices classified into the following six cases are not equal to zero:

$$
\begin{cases}
\text{case 1:} & (k_{\mathrm{B}} = k_{\mathrm{B}}') \bigcap (w = w') \bigcap (w'' = w''') \bigcap (k_{\mathrm{M}} = k_{\mathrm{M}}') \bigcap (k_{\mathrm{M}}'' = k_{\mathrm{M}}''') \\
& \bigcap (w \neq w''), \\[2pt]
\text{case 2:} & (k_{\mathrm{B}} = k_{\mathrm{B}}') \bigcap (w = w') \bigcap (w'' = w''') \bigcap (k_{\mathrm{M}} = k_{\mathrm{M}}''') \bigcap (k_{\mathrm{M}}' = k_{\mathrm{M}}'') \\
& \bigcap (w \neq w'') \bigcap (k_{\mathrm{M}} \neq k_{\mathrm{M}}'), \\[2pt]
\text{case 3:} & (k_{\mathrm{B}} = k_{\mathrm{B}}') \bigcap (w = w''') \bigcap (w' = w'') \bigcap (k_{\mathrm{M}} = k_{\mathrm{M}}') \bigcap (k_{\mathrm{M}}'' = k_{\mathrm{M}}'''), \\[2pt]
\text{case 4:} & (k_{\mathrm{B}} = k_{\mathrm{B}}') \bigcap (w = w''') \bigcap (w' = w'') \bigcap (k_{\mathrm{M}} = k_{\mathrm{M}}''') \bigcap (k_{\mathrm{M}}' = k_{\mathrm{M}}'') \\
& \bigcap (k_{\mathrm{M}} \neq k_{\mathrm{M}}'), \\[2pt]
\text{case 5:} & (k_{\mathrm{B}} \neq k_{\mathrm{B}}') \bigcap (w = w') \bigcap (w'' = w''') \bigcap (k_{\mathrm{M}} = k_{\mathrm{M}}') \bigcap (k_{\mathrm{M}}'' = k_{\mathrm{M}}'''), \\[2pt]
\text{case 6:} & (k_{\mathrm{B}} \neq k_{\mathrm{B}}') \bigcap (w = w''') \bigcap (w' = w'') \bigcap (k_{\mathrm{M}} = k_{\mathrm{M}}') \bigcap (k_{\mathrm{M}}'' = k_{\mathrm{M}}''') \\
& \bigcap (w \neq w').
\end{cases} \tag{A.30}
$$

The calculations of each partial sum of the terms with the indices within the six cases are listed in the following, which are obvious with respect to (A.5), (A.20) and (A.21) and self-explained by the calculations.

Case 1:

$$
\begin{aligned}
\Sigma_{\text{case1}} \quad = \quad & \sum_{k_{\text{B}}=1}^{K_{\text{B}}} \sum_{k_{\text{M}}=1}^{K_{\text{M}}} \sum_{k_{\text{M}}''=1}^{K_{\text{M}}} \sum_{w=1}^{W} \sum_{w''=1}^{W} \sum_{q=1}^{Q_{\text{t}}} \sum_{q'=1}^{Q_{\text{t}}} {}^{(w \neq w'')} \\
& \text{E} \left\{ D_{w+q-1}^{(k_{\text{M}})} D_{w+q-1}^{(k_{\text{M}})} D_{w''+q'-1}^{(k_{\text{M}}'')} D_{w''+q'-1}^{(k_{\text{M}}'')} \right\} \text{E} \left\{ \underline{h}_{\text{R},w} \underline{h}_{\text{R},w}^{\text{H}} \right\} \text{E} \left\{ \underline{h}_{\text{R},w''} \underline{h}_{\text{R},w''}^{\text{H}} \right\} \\
= \quad & \sum_{k_{\text{B}}=1}^{K_{\text{B}}} \sum_{k_{\text{M}}=1}^{K_{\text{M}}} \sum_{k_{\text{M}}''=1}^{K_{\text{M}}} \sum_{q=1}^{Q_{\text{t}}} \sum_{q'=1}^{Q_{\text{t}}} \\
& \cdot \left(\sum_{w=1}^{W} \sum_{w''=1}^{W} \frac{4\sigma_w^2 \sigma_{w''}^2}{K_{\text{M}}^2 \left(Q_{\text{t}} + W - 1 \right)^2} - \sum_{w=1}^{W} \frac{4\sigma_w^4}{K_{\text{M}}^2 \left(Q_{\text{t}} + W - 1 \right)^2} \right) \\
= \quad & \frac{4 K_{\text{B}} Q_{\text{t}}^2}{\left(Q_{\text{t}} + W - 1 \right)^2} \left(\sum_{w=1}^{W} \sum_{w''=1}^{W} \sigma_w^2 \sigma_{w''}^2 - \sum_{w=1}^{W} \sigma_w^4 \right) .
\end{aligned}
\tag{A.31}
$$

Case 2:

$$
\begin{aligned}
\Sigma_{\text{case2}} \quad = \quad & \sum_{k_{\text{B}}=1}^{K_{\text{B}}} \sum_{k_{\text{M}}=1}^{K_{\text{M}}} \sum_{k_{\text{M}}'=1}^{K_{\text{M}}} \sum_{w=1}^{W} \sum_{w''=1}^{W} \sum_{q=1}^{Q_{\text{t}}} \sum_{q'=1}^{Q_{\text{t}}} {}^{(w \neq w'') \bigcap (k_{\text{M}} \neq k_{\text{M}}')} \\
& \text{E} \left\{ D_{w+q-1}^{(k_{\text{M}})} D_{w+q-1}^{(k_{\text{M}}')} D_{w''+q'-1}^{(k_{\text{M}}')} D_{w''+q'-1}^{(k_{\text{M}})} \right\} \text{E} \left\{ \underline{h}_{\text{R},w} \underline{h}_{\text{R},w}^{\text{H}} \right\} \text{E} \left\{ \underline{h}_{\text{R},w''} \underline{h}_{\text{R},w''}^{\text{H}} \right\} \\
= \quad & \sum_{k_{\text{B}}=1}^{K_{\text{B}}} \sum_{k_{\text{M}}=1}^{K_{\text{M}}} \sum_{k_{\text{M}}'=1}^{K_{\text{M}}} \sum_{w=1}^{W} \sum_{w''=1}^{W} \sum_{q=1}^{Q_{\text{t}}} \sum_{q'=1}^{Q_{\text{t}}} {}^{(w''+q'=w+q) \bigcap (w \neq w'') \bigcap (k_{\text{M}}' \neq k_{\text{M}})} \\
& \text{E} \left\{ D_{w+q-1}^{(k_{\text{M}})} D_{w+q-1}^{(k_{\text{M}}')} D_{w''+q'-1}^{(k_{\text{M}}')} D_{w''+q'-1}^{(k_{\text{M}})} \right\} \text{E} \left\{ \underline{h}_{\text{R},w} \underline{h}_{\text{R},w}^{\text{H}} \right\} \text{E} \left\{ \underline{h}_{\text{R},w''} \underline{h}_{\text{R},w''}^{\text{H}} \right\} \\
= \quad & \sum_{k_{\text{B}}=1}^{K_{\text{B}}} \sum_{k_{\text{M}}=1}^{K_{\text{M}}} \sum_{k_{\text{M}}'=1}^{K_{\text{M}}} \sum_{w=1}^{W} \sum_{w''=1}^{W} \sum_{q=1}^{Q_{\text{t}}} \sum_{q'=1}^{Q_{\text{t}}} {}^{(w''+q'=w+q) \bigcap (w \neq w'') \bigcap (k_{\text{M}}' \neq k_{\text{M}})} \\
& \frac{4\sigma_w^2 \sigma_{w''}^2}{K_{\text{M}}^2 \left(Q_{\text{t}} + W - 1 \right)^2} \\
= \quad & \frac{4 K_{\text{B}} (K_{\text{M}} - 1)}{K_{\text{M}} \left(Q_{\text{t}} + W - 1 \right)^2} 2(Q_{\text{t}} - W)(W - 1) \sum_{w=1}^{W} \sum_{w''=1}^{W} \sigma_w^2 \sigma_{w''}^2 .
\end{aligned}
\tag{A.32}
$$

Case 3:

$$
\begin{aligned}
\Sigma_{\text{case3}} \quad = \quad & \sum_{k_{\text{B}}=1}^{K_{\text{B}}} \sum_{k_{\text{M}}=1}^{K_{\text{M}}} \sum_{k_{\text{M}}''=1}^{K_{\text{M}}} \sum_{w=1}^{W} \sum_{w'=1}^{W} \sum_{q=1}^{Q_{\text{t}}} \sum_{q'=1}^{Q_{\text{t}}} \\
& \mathrm{E}\left\{ D_{w+q-1}^{(k_{\text{M}})} D_{w'+q-1}^{(k_{\text{M}})} D_{w'+q'-1}^{(k_{\text{M}}'')} D_{w+q'-1}^{(k_{\text{M}}'')} \right\} \mathrm{E}\left\{ \underline{h}_{\text{R},\,w} \underline{h}_{\text{R},\,w'}^{\text{H}} \underline{h}_{\text{R},\,w'} \underline{h}_{\text{R},\,w}^{\text{H}} \right\} \\
= \quad & \sum_{k_{\text{B}}=1}^{K_{\text{B}}} \sum_{k_{\text{M}}=1}^{K_{\text{M}}} \sum_{k_{\text{M}}''=1}^{K_{\text{M}}} \sum_{w=w'=1}^{W} \sum_{q=1}^{Q_{\text{t}}} \sum_{q'=1}^{Q_{\text{t}}} \\
& \mathrm{E}\left\{ D_{w+q-1}^{(k_{\text{M}})} D_{w+q-1}^{(k_{\text{M}})} D_{w'+q'-1}^{(k_{\text{M}}'')} D_{w+q'-1}^{(k_{\text{M}}'')} \right\} \mathrm{E}\left\{ \underline{h}_{\text{R},\,w} \underline{h}_{\text{R},\,w}^{\text{H}} \underline{h}_{\text{R},\,w} \underline{h}_{\text{R},\,w}^{\text{H}} \right\} \\
= \quad & \sum_{k_{\text{B}}=1}^{K_{\text{B}}} \sum_{k_{\text{M}}=1}^{K_{\text{M}}} \sum_{k_{\text{M}}''=1}^{K_{\text{M}}} \sum_{q=1}^{Q_{\text{t}}} \sum_{q'=1}^{Q_{\text{t}}} \sum_{w=1}^{W} \frac{8\sigma_w^4}{K_{\text{M}}^2 (Q_{\text{t}} + W - 1)^2} \\
= \quad & \frac{8 K_{\text{B}} Q_{\text{t}}^2}{(Q_{\text{t}} + W - 1)^2} \sum_{w=1}^{W} \sigma_w^4.
\end{aligned}
\tag{A.33}
$$

Case 4:

$$
\begin{aligned}
\Sigma_{\text{case4}} \quad = \quad & \sum_{k_{\text{B}}=1}^{K_{\text{B}}} \sum_{k_{\text{M}}=1}^{K_{\text{M}}} \sum_{k_{\text{M}}'=1}^{K_{\text{M}}} \sum_{w=1}^{W} \sum_{w'=1}^{W} \sum_{q=1}^{Q_{\text{t}}} \sum_{q'=1}^{Q_{\text{t}}} {}^{(k_{\text{M}} \neq k_{\text{M}}')} \\
& \mathrm{E}\left\{ D_{w+q-1}^{(k_{\text{M}})} D_{w'+q-1}^{(k_{\text{M}}')} D_{w'+q'-1}^{(k_{\text{M}}')} D_{w+q'-1}^{(k_{\text{M}})} \right\} \mathrm{E}\left\{ \underline{h}_{\text{R},\,w} \underline{h}_{\text{R},\,w'}^{\text{H}} \underline{h}_{\text{R},\,w'} \underline{h}_{\text{R},\,w}^{\text{H}} \right\} \\
= \quad & \sum_{k_{\text{B}}=1}^{K_{\text{B}}} \sum_{k_{\text{M}}=1}^{K_{\text{M}}} \sum_{k_{\text{M}}'=1}^{K_{\text{M}}} \sum_{w=1}^{W} \sum_{w'=1}^{W} \sum_{q=1}^{Q_{\text{t}}} {}^{(k_{\text{M}} \neq k_{\text{M}}')} \\
& \mathrm{E}\left\{ D_{w+q-1}^{(k_{\text{M}})} D_{w'+q-1}^{(k_{\text{M}}')} D_{w'+q-1}^{(k_{\text{M}}')} D_{w+q-1}^{(k_{\text{M}})} \right\} \mathrm{E}\left\{ \underline{h}_{\text{R},\,w} \underline{h}_{\text{R},\,w'}^{\text{H}} \underline{h}_{\text{R},\,w'} \underline{h}_{\text{R},\,w}^{\text{H}} \right\} \\
= \quad & \sum_{k_{\text{B}}=1}^{K_{\text{B}}} \sum_{k_{\text{M}}=1}^{K_{\text{M}}} \sum_{k_{\text{M}}'=1}^{K_{\text{M}}} \sum_{q=1}^{Q_{\text{t}}} {}^{(k_{\text{M}} \neq k_{\text{M}}')} \\
& \cdot \left(\sum_{w=1}^{W} \sum_{w'=1}^{W} \frac{4\sigma_w^2 \sigma_{w'}^2}{K_{\text{M}}^2 (Q_{\text{t}} + W - 1)^2} + \sum_{w=1}^{W} \frac{4\sigma_w^4}{K_{\text{M}}^2 (Q_{\text{t}} + W - 1)^2} \right) \\
= \quad & \frac{4(K_{\text{M}} - 1) K_{\text{B}} Q_{\text{t}}}{K_{\text{M}} (Q_{\text{t}} + W - 1)^2} \left(\sum_{w=1}^{W} \sum_{w'=1}^{W} \sigma_w^2 \sigma_{w'}^2 + \sum_{w=1}^{W} \sigma_w^4 \right).
\end{aligned}
\tag{A.34}
$$

Case 5:

$$
\begin{aligned}
\Sigma_{\text{case5}} &= \sum_{k_{\text{B}}=1}^{K_{\text{B}}} \sum_{k_{\text{B}}'=1}^{K_{\text{B}}} \sum_{k_{\text{M}}=1}^{K_{\text{M}}} \sum_{k_{\text{M}}''=1}^{K_{\text{M}}} \sum_{w=1}^{W} \sum_{w''=1}^{W} \sum_{q=1}^{Q_{\text{t}}} \sum_{q'=1}^{Q_{\text{t}}}{}^{(k_{\text{B}} \neq k_{\text{B}}')} \\
&\quad \text{E}\left\{ D_{w+q-1}^{(k_{\text{M}})} D_{w+q-1}^{(k_{\text{M}})} D_{w''+q'-1}^{(k_{\text{M}}'')} D_{w''+q'-1}^{(k_{\text{M}}'')} \right\} \text{E}\left\{ \underline{h}_{\text{R},w} \underline{h}_{\text{R},w}^{\text{H}} \underline{h}_{\text{R},w''} \underline{h}_{\text{R},w''}^{\text{H}} \right\} \\
&= \sum_{k_{\text{B}}=1}^{K_{\text{B}}} \sum_{k_{\text{B}}'=1}^{K_{\text{B}}} \sum_{k_{\text{M}}=1}^{K_{\text{M}}} \sum_{k_{\text{M}}''=1}^{K_{\text{M}}} \sum_{q=1}^{Q_{\text{t}}} \sum_{q'=1}^{Q_{\text{t}}}{}^{(k_{\text{B}} \neq k_{\text{B}}')} \\
&\quad \left(\sum_{w=1}^{W} \sum_{w''=1}^{W} \frac{4\sigma_w^2 \sigma_{w'}^2}{K_{\text{M}}^2 (Q_{\text{t}} + W - 1)^2} + \sum_{w=1}^{W} \frac{4\sigma_w^4}{K_{\text{M}}^2 (Q_{\text{t}} + W - 1)^2} \right) \\
&= \frac{4K_{\text{B}}(K_{\text{B}} - 1)Q_{\text{t}}^2}{(Q_{\text{t}} + W - 1)^2} \left(\sum_{w=1}^{W} \sum_{w''=1}^{W} \sigma_w^2 \sigma_{w'}^2 + \sum_{w=1}^{W} \sigma_w^4 \right).
\end{aligned}
\tag{A.35}
$$

Case 6:

$$
\begin{aligned}
\Sigma_{\text{case6}} &= \sum_{k_{\text{B}}=1}^{K_{\text{B}}} \sum_{k_{\text{B}}'=1}^{K_{\text{B}}} \sum_{k_{\text{M}}=1}^{K_{\text{M}}} \sum_{k_{\text{M}}''=1}^{K_{\text{M}}} \sum_{w=1}^{W} \sum_{w'=1}^{W} \sum_{q=1}^{Q_{\text{t}}} \sum_{q'=1}^{Q_{\text{t}}}{}^{(k_{\text{B}} \neq k_{\text{B}}') \bigcap (w \neq w')} \\
&\quad \text{E}\left\{ D_{w+q-1}^{(k_{\text{M}})} D_{w'+q-1}^{(k_{\text{M}})} D_{w'+q'-1}^{(k_{\text{M}}'')} D_{w+q'-1}^{(k_{\text{M}}'')} \right\} \text{E}\left\{ \underline{h}_{\text{R},w} \underline{h}_{\text{R},w'}^{\text{H}} \underline{h}_{\text{R},w'} \underline{h}_{\text{R},w}^{\text{H}} \right\} \\
&= \sum_{k_{\text{B}}=1}^{K_{\text{B}}} \sum_{k_{\text{B}}'=1}^{K_{\text{B}}} \sum_{k_{\text{M}}=1}^{K_{\text{M}}} \sum_{k_{\text{M}}''=1}^{K_{\text{M}}} \sum_{w=1}^{W} \sum_{w'=1}^{W} \sum_{q=1}^{Q_{\text{t}}} \sum_{q'=1}^{Q_{\text{t}}}{}^{(k_{\text{B}} \neq k_{\text{B}}') \bigcap (w \neq w')} \\
&\quad 0 \cdot \text{E}\left\{ \underline{h}_{\text{R},w} \underline{h}_{\text{R},w'}^{\text{H}} \underline{h}_{\text{R},w'} \underline{h}_{\text{R},w}^{\text{H}} \right\} \\
&= 0.
\end{aligned}
\tag{A.36}
$$

Then, with (A.31), (A.32), (A.33), (A.34), (A.35), (A.36) and (A.27), the variance

$$
\begin{aligned}
\text{var}\{X\} &= \text{E}\left\{ X^2 \right\} - \left(\text{E}\{X\} \right)^2 \\
&= \frac{4K_{\text{B}}Q_{\text{t}}^2}{(Q_{\text{t}} + W - 1)^2} \left[\frac{K_{\text{M}} - 1}{K_{\text{M}}Q_{\text{t}}} \left(1 + \frac{2(Q_{\text{t}} - W)(W - 1)}{Q_{\text{t}}} \right) \sum_{w=1}^{W} \sum_{w''=1}^{W} \sigma_w^2 \sigma_{w'}^2 \right. \\
&\quad \left. + \left(K_{\text{B}} + \frac{K_{\text{M}} - 1}{K_{\text{M}}Q_{\text{t}}} \right) \sum_{w=1}^{W} \sigma_w^4 \right]
\end{aligned}
\tag{A.37}
$$

of X of (A.22) is obtained.

A.3   Derivation of the group specific modulator matrix for the TxNZF Filter

As mentioned in Subsection 5.2.1, the group specific transmit signal $\underline{\mathbf{t}}_{\mathrm{G}}^{(g)}$ of group g should produce no interferences to all data symbols $\underline{d}_n \in \mathbb{D}_{g'}$, $g' < g$, of the previous processed groups, i.e.,

$$\underline{\mathbf{B}}_{\mathrm{G}}^{(g')} \underline{\mathbf{t}}_{\mathrm{G}}^{(g)} = \mathbf{0}, \ g' = 1 \ldots g - 1, \tag{A.38}$$

have to be fulfilled. $\underline{\mathbf{t}}_{\mathrm{G}}^{(g)}$ should also produce no interferences to all data symbols $\underline{d}_n \in \mathbb{D}_g$ assigned to that group, then,

$$\underline{\mathbf{B}}_{\mathrm{G}}^{(g)} \underline{\mathbf{t}}_{\mathrm{G}}^{(g)} = \underline{\boldsymbol{\Delta}}_{\mathrm{G}}^{(g)} \tag{A.39}$$

has to be satisfied. Stacking all the equations of (A.38) and (A.39), we obtain

$$\begin{pmatrix} \underline{\mathbf{B}}_{\mathrm{G}}^{(1)} \\ \vdots \\ \underline{\mathbf{B}}_{\mathrm{G}}^{(g-1)} \\ \underline{\mathbf{B}}_{\mathrm{G}}^{(g)} \end{pmatrix} \underline{\mathbf{t}}_{\mathrm{G}}^{(g)} = \begin{pmatrix} \mathbf{0} \\ \vdots \\ \mathbf{0} \\ \underline{\boldsymbol{\Delta}}_{\mathrm{G}}^{(g)} \end{pmatrix}. \tag{A.40}$$

With (5.18), (A.40) can be written as

$$\underline{\mathbf{B}}_g \underline{\mathbf{t}}_{\mathrm{G}}^{(g)} = \begin{pmatrix} \mathbf{0} \\ \vdots \\ \mathbf{0} \\ \underline{\boldsymbol{\Delta}}_{\mathrm{G}}^{(g)} \end{pmatrix}. \tag{A.41}$$

Following the rationale TxZF [BMWT00], the solution of (A.41) becomes

$$\begin{aligned} \underline{\mathbf{t}}_{\mathrm{G}}^{(g)} &= \underline{\mathbf{B}}_g^{\mathrm{H}} \left(\underline{\mathbf{B}}_g \underline{\mathbf{B}}_g^{\mathrm{H}} \right)^{-1} \begin{pmatrix} \mathbf{0} \\ \vdots \\ \mathbf{0} \\ \underline{\boldsymbol{\Delta}}_{\mathrm{G}}^{(g)} \end{pmatrix} \\ &= \left[\underline{\mathbf{B}}_g^{\mathrm{H}} \left(\underline{\mathbf{B}}_g \underline{\mathbf{B}}_g^{\mathrm{H}} \right)^{-1} \right]_{\|\mathbb{G}_1 \cup \mathbb{G}_g\|}^{\|\mathbb{G}_1 \cup \mathbb{G}_{g-1}\|+1} \underline{\boldsymbol{\Delta}}_{\mathrm{G}}^{(g)}. \end{aligned} \tag{A.42}$$

Then, we obtain the group specific modulator matrix

$$\underline{\mathbf{M}}_{\mathrm{G}}^{(g)} = \left[\underline{\mathbf{B}}_g^{\mathrm{H}} \left(\underline{\mathbf{B}}_g \underline{\mathbf{B}}_g^{\mathrm{H}} \right)^{-1} \right]_{\|\mathbb{G}_1 \cup \mathbb{G}_g\|}^{\|\mathbb{G}_1 \cup \mathbb{G}_{g-1}\|+1} \tag{A.43}$$

for group g.

Appendix B

Frequently used abbreviations and symbols

B.1 Abbreviations

BS	Base Station
CDMA	Code Division Multiple Access
DL	Downlink
FDD	Frequency Division Duplexing
FDMA	Frequency Division Multiple Access
FEC	Forward Error Correction
EVD	Eigenvalue Decomposition
ISI	Intersymbol Interference
JD	Joint Detection
JT	Joint Transmission
LOS	Line-of-Sight
MAI	Multiple Access Interference
MIMO	Multiple Input Multiple Output
MT	Mobile Terminal
QPSK	Quadrature Phase Shift Keying
RAE	Receive Antenna Element
RP	Reference Point
SNR	Signal–to–Noise Ratio
SNIR	Signal–to–Noise–plus–Interference Ratio
SISO	Single Input Single Output
SVD	Singular Value Decomposition
TDD	Time Division Duplexing
TDMA	Time Division Multiple Access
THP	Tomlinson-Harashima Precoding
TAE	Transmit Antenna Element
TxMF	Transmit Matched Filter
TxMMSE	Transmit Minimum Mean Square Error
TxZF	Transmit Zero Forcing
TxNZF	Transmit Non-linear Zero Forcing
UL	Uplink

B.2 Symbols

$\underline{\mathbf{B}}$	total system matrix
$\underline{\mathbf{B}}^{(k)}$	MT specific system matrix
$\underline{\mathbf{B}}_{\mathrm{G}}^{(g)}$	group specific system matrix
$\underline{\mathbf{B}}_{\mathrm{G}}$	permutated total system matrix $\underline{\mathbf{B}}$
$\underline{\mathbf{d}}^{(k)}$	MT specific data vector
$\underline{d}_n^{(k)}$	element of MT specific data vector $\underline{\mathbf{d}}^{(k)}$
$\underline{\mathbf{d}}$	total data vector
$\underline{d}_n$	element of the total data vector $\underline{\mathbf{d}}$
$\underline{\mathbf{d}}^{(R)}$	realization of the total data vector $\underline{\mathbf{d}}$
$\underline{\mathbf{d}}_{\mathrm{G}}^{(g)}$	group specific data vector
$\underline{\mathbf{d}}_{\mathrm{G}}$	permutated total data vector of $\underline{\mathbf{d}}$
$\underline{\widehat{\mathbf{d}}}$	total continuous valued data estimate
$\underline{\widehat{d}}_n$	element of total continuous valued data estimate vector $\underline{\widehat{\mathbf{d}}}$
$\underline{\widehat{\mathbf{d}}}^{(k)}$	MT specific continuous valued data estimate
$\underline{\widehat{\mathbf{d}}}_{\mathrm{dis}}$	total discrete valued data estimate
$\underline{\widehat{d}}_{\mathrm{dis},\,n}$	element of the total discrete valued data estimate $\underline{\widehat{\mathbf{d}}}_{\mathrm{dis}}$
$\mathcal{D}_{\mathrm{dis}}\{\cdot\}$	Rx operator
$\underline{\mathbf{D}}^{(k)}$	MT specific demodulator matrix
$\underline{\mathbf{D}}$	total demodulator matrix
$\mathbb{D}$	set of all data symbols $\underline{d}_1 \ldots \underline{d}_{N_{\mathrm{t}}}$ to be transmitted from BS to K MTs
$\mathbb{D}_g$	data group
$\underline{\mathbf{e}}$	total undisturbed receive signal
$\underline{\mathbf{e}}^{(k)}$	MT specific undisturbed receive signal
$\underline{\mathbf{e}}_{\mathrm{opt}}$	undisturbed receive signal resulting in $\underline{\mathbf{t}}_{\mathrm{opt}}$
$\underline{\mathbf{F}}_{\mathrm{G}}$	forward matrix
$\underline{g}_{m,\,p}$	representative of data realization $\underline{v}_m$ in multiply connected decision regions
$\mathbb{G}_{m,\,p}$	partial decision region of data realization $\underline{v}_m$ corresponding to representative $\underline{g}_{m,\,p}$
$\mathbb{G}_m$	decision region of data realization $\underline{v}_m$
$\underline{\mathbf{h}}^{(k,\,k_{\mathrm{B}},\,k_{\mathrm{M}})}$	MT and antenna specific channel impulse response
$\underline{h}_w^{(k,\,k_{\mathrm{B}},\,k_{\mathrm{M}})}$	element of MT and antenna specific channel impulse response $\underline{\mathbf{h}}^{(k,\,k_{\mathrm{B}},\,k_{\mathrm{M}})}$
$\underline{\mathbf{h}}_{\mathrm{R}}^{(k)}$	MT specific reference channel impulse response
$\underline{h}_{\mathrm{R},\,w}^{(k)}$	element of MT specific reference channel impulse response $\underline{\mathbf{h}}_{\mathrm{R}}^{(k)}$
$\underline{\mathbf{H}}^{(k,\,k_{\mathrm{B}},\,k_{\mathrm{M}})}$	MT and antenna specific channel matrix
$\underline{\mathbf{H}}^{(k)}$	MT specific channel matrix
$\underline{\mathbf{H}}$	total channel matrix

$\mathbf{I}^{(N_t)}$	$N_t \times N_t$ identity matrix
$\underline{\mathbf{i}}_G^{(g)}$	group specific interference vector
$\underline{i}_{G,n}^{(g)}$	element of group specific interference vector $\underline{\mathbf{i}}_G^{(g)}$
$\underline{\mathbf{i}}_G^{(g)}(p)$	group specific interference vector of step p
$\underline{\mathbf{i}}_G(p)$	total interference vector of step p
K	number of MTs
K_B	number of transmit antennas
K_M	number of receive antennas
$\mathcal{M}\{\cdot\}$	Tx operator
$\underline{\mathbf{M}}$	total modulator matrix
$\underline{\mathbf{M}}_G^{(g)}$	group specific modulator matrix
$\underline{\mathbf{M}}_G$	permutated total modulator matrix $\underline{\mathbf{M}}$
N	number of data symbols to be transmitted per MT
N_t	total number of data symbols to be transmitted
$\underline{\mathbf{n}}$	total noise vector
$\underline{n}_z$	element of total noise vector $\underline{\mathbf{n}}$
$\underline{\mathbf{n}}^{(k)}$	MT specific noise vector
P_b	bit error rate
$Q\{\cdot\}$	quantization function
Q_t	temporal spreading factor
Q	total spreading factor
$\underline{\mathbf{r}}$	total disturbed receive signal
$\underline{\mathbf{r}}^{(k)}$	MT specific disturbed receive signal
$\mathbf{R}_n$	covariance matrix of total noise vector $\underline{\mathbf{n}}$
$\mathbf{R}_d$	covariance matrix of total data vector $\underline{\mathbf{d}}$
R_{opt}	maximum possible receive energy
$R_{MF,n}$	receive energy of the data symbol $\underline{d}_n$ in the case of TxMF
$R_{ZF,n}$	receive energy of the data symbol $\underline{d}_n$ in the case of TxZF Filter
$r_{MF,n}$	energy ratio of receive energy $R_{MF,n}$ and transmit energy $T_{MF,n}$ of the data symbol $\underline{d}_n$ in the case of TxMF
$r_{ZF,n}$	energy ratio of receive energy $R_{ZF,n}$ and transmit energy $T_{ZF,n}$ of the data symbol $\underline{d}_n$ in the case of TxZF Filter
r_{opt}	maximum energy ratio
$\mathbf{S}_G^{(g)}$	group specific selection matrix
$\mathbf{S}_G$	permutation matrix
$\underline{\mathbf{t}}$	total transmit signal
$\underline{\mathbf{t}}_G^{(g)}$	group specific transmit signal
$\underline{\mathbf{t}}_{opt}$	optimum transmit signal
T	total transmit energy

T_n	data symbol specific transmit energy
$T_{\mathrm{MF},n}$	transmit energy of the data symbol $\underline{d}_n$ in the case of TxMF
$T_{\mathrm{ZF},n}$	transmit energy of the data symbol $\underline{d}_n$ in the case of TxZF Filter
$t_{\mathrm{ZF},n}$	normalized transmit energy of the data symbol $\underline{d}_n$ in the case of TxZF Filter
$\underline{v}_m$	data symbol realization
$\mathbb{V}$	set of data symbol realizations
$\mathbb{V}_{\mathrm{q},m}$	data symbol realization specific set
W	number of taps of channel impulse response
$\underline{\boldsymbol{\Delta}}_{\mathrm{G}}^{(g)}$	group specific correction vector
$\underline{\boldsymbol{\delta}}_{\mathrm{G}}^{(g)}(p)$	group specific correction vector of step p
$\underline{\boldsymbol{\delta}}_{\mathrm{G}}(p)$	total correction vector of step p
η_n	energy efficiency of data symbol $\underline{d}_n$
$\eta_{\mathrm{Rx},n}$	Rx efficiency of data symbol $\underline{d}_n$
$\eta_{\mathrm{Tx},n}$	Tx efficiency of data symbol $\underline{d}_n$
σ_{d}^2	variance of real and imaginary parts of the data symbol $\underline{d}_n$
σ^2	variance of real and imaginary parts of the noise element $\underline{n}_z$
σ_w^2	variance of real and imaginary parts of channel impulse response $\underline{h}_w^{(k,k_{\mathrm{B}},k_{\mathrm{M}})}$ or $\underline{h}_{\mathrm{R},w}^{(k)}$

References

[AS65]   Abramowitz, M.; Stegun, I. A.: *Handbook of mathematical functions.* New York: Dover, 1965.

[Asc84]   Aschoff, V.: *Geschichte der Nachrichtentechnik.* Berlin: Springer-Verlag, 1984.

[Bai86]   Baier, A.: *Digitale signalangepaßte Filter und Korrelatoren zur Detektion von Bandpaßsignalen.* Fortschrittberichte VDI, Reihe 10, Nummer 74, VDI-Verlag, Düsseldorf, 1986.

[Bai94]   Baier, P. W.: CDMA or TDMA? CDMA for GSM? *Proc. IEEE 5th International Symposium on Personal, Indoor and Mobile Radio Communications (PIMRC'94)*, vol. 4, The Hague, 1994, pp. 1280–1284.

[Bai96]   Baier, P. W.: A critical review of CDMA. *Proc. IEEE 46th Vehicular Technology Conference (VTC'96)*, vol. 1, Atlanta, 1996, pp. 6–10.

[BAWT01]   Buehrer, R. M.; Arunachalam, S.; Wu, K. H.; Tonello, A.: Spatial channel model and measurements for IMT-2000 systems. *Proc. IEEE 53rd Vehicular Technology Conference (VTC'01)*, vol. 1, 2001, pp. 342–346.

[Bel63]   Bello, P. A.: Characterization of randomly time-variant linear channels. *IEEE Transactions on Communications Systems*, vol. 11, 1963, pp. 360–393.

[BJK96]   Baier, P. W.; Jung, P.; Klein, A.: Taking the challenge of multiple access for third-generation cellular mobile radio systems – a European view. *IEEE Communications Magazine*, vol. 34, 1996, pp. 82–89.

[BK95]   Baier, P. W.; Klein, A.: Flexible hybrid multiple access schemes for 3rd generation mobile radio systems. *Mobile and Personal Communications*, 1995, pp. 31–43.

[Bla98]   Blanz, J. J.: *Empfangsantennendiversität in CDMA-Mobilfunksystemen mit gemeinsamer Detektion der Teilnehmersignale.* Fortschrittberichte VDI, Reihe 10, Nr. 535. Düsseldorf: VDI-Verlag, 1998.

[BM03]   Baier, P. W.; Meurer, M.: Receiver Orientation, an Unconventional Approach to Mobile Radio Downlink Design. *Proc. European Conference on Wireless Technology 2003 (ECWT'2003)*, Munich, 2003, pp. 11–14.

[BMWT00]   Baier, P. W.; Meurer, M.; Weber, T.; Tröger, H.: Joint transmission (JT), an alternative rationale for the downlink of time division CDMA using multi-element transmit antennas. Invited paper in *Proc. IEEE 6th International Symposium on Spread Spectrum Techniques & Applications (ISSSTA'00)*, vol. 1, Parsippany, 2000, pp. 1–5.

[BPJ97]   Berens, F.; Plechinger, J.; Jung, P.: Uplink coverage analysis of multi-carrier joint detection code division multiple access based macrocellular radio systems. *Proc. IEEE 8th International Symposium on Personal, Indoor and Mobile Radio Communications (PIMRC'97)*, Helsinki, 1997, pp. 105–109.

[BQT+03]   Baier, P. W.; Qiu, W.; Tröger, H.; Jötten, C. A.; Meurer, M.: Modelling and optimization of receiver oriented multi-user MIMO downlinks for frequency selective channels. *Proc. 10th International Conference on Telecommunications (ICT'03)*, vol. 2, Papeete, 2003, pp. 1547–1554.

[BT04]   Byers, G.; Takawira, F.: Spatially and temporally correlated MIMO channels: modeling and capacity analysis. *IEEE Transactions on Vehicular Technology*, vol. 53, 2004, pp. 634–643.

[BZT+04]   Burr, A.; Zacharov, Y.; Tröger, H.; Qiu, W.; Meurer, M.; Stimming, C.; Vanaev, A.; Tauboeck, G.; Shen, J.; Mai, H. H.: *Selected MIMO Techniques and their Performance.* Deliverable 14, IST-2001-32125 FLOWS (Flexible Convergence of Wireless Standards and Services), http://www.flows-ist.org/main/outputs/list.htm, 2004.

[Cal88]   Calhoun, G.: *Digital cellular radio.* Norwood: Artech House, 1988.

[CLM01]   Choi, R. L.-U.; Letaief, K. B.; Murch, R. D.: MISO CDMA Transmission with Simplified Receiver for Wireless Communication Handsets. *IEEE Transactions on Communications*, vol. 49, 2001, pp. 888–898.

[CS82]   Conway, J.; Sloane, N.: Voronoi Regions of Lattices, Second Moments of Polytopes, and Quantization. *IEEE Transactions on Information Theory*, vol. 28, 1982, pp. 211–226.

[CS85]   Conway, J.; Sloane, N.: A Lower Bound on the Average Error of Vector Quantizers. *IEEE Transactions on Information Theory*, vol. 31, 1985, pp. 106–109.

[EN93]   Esmailzadeh, R.; Nakagawa, M.: Pre-RAKE diversity combination for direct sequence spread spectrum communications systems. *Proc. IEEE International Conference on Communications (ICC'93)*, vol. 1, Geneva, 1993, pp. 463–467.

[ESN95]   Esmailzadeh, R.; Sourour, E.; Nakagawa, M.: Pre-RAKE diversity combining in time division duplex CDMA mobile communications. *Proc. IEEE 6th International Symposium on Personal, Indoor and Mobile Radio Communications (PIMRC'95)*, vol. 2, Toronto, 1995, pp. 431–435.

[ESN99]   Esmailzadeh, R.; Sourour, E.; Nakagawa, M.: PreRAKE diversity combining in time-division duplex CDMA mobile communications. *IEEE Transactions on Vehicular Technology*, vol. 48, 1999, pp. 795–801.

[FG98]   Foschini, G.; Gans, M.: On limits of wireless communications in a fading environment when using multiple antennas. *Wireless Personal Communications*, vol. 6, 1998, pp. 311–335.

[Fis02]   Fischer, R. F. H.: *Precoding and Signal Shaping for Digital Transmission.* New York: John Wiley & Sons, 2002.

[FST+96]   Fukasawa, A.; Sato, T.; Takizawa, Y.; Kato, T.; Kawabe, M.; Fisher, R. R.: Wideband CDMA system for personal radio communications. *IEEE Communications Magazine*, vol. 34, 1996, pp. 116–123.

[FWLH02a]   Fischer, R. F. H.; Windpassinger, C.; Lampe, A.; Huber, J. B.: MIMO Precoding for Decentralized Receivers. *Proc. IEEE International Symposium on Information Theory (ISIT'02)*, Lausanne, Switzerland, 2002, pp. 496.

[FWLH02b]   Fischer, R. F. H.; Windpassinger, C.; Lampe, A.; Huber, J. B.: Space-Time Transmission using Tomlinson-Harashima Precoding. *Proc. 4th ITG Conference on Source and Channel Coding*, Berlin, 2002, pp. 139–147.

[FWLH02c]   Fischer, R. F. H.; Windpassinger, C.; Lampe, A.; Huber, J. B.: Tomlinson-Harashima Precoding in Space-Time Transmission for Low-Rate Backward Channel. *Proc. International Zurich Seminar on Broadband Communications (IZS'02)*, Zurich, 2002.

[GBP02]   Gesbert, D.; Bolcskei, H.; Paulraj, A.: Outdoor MIMO wireless channels: Models and performance prediction. *IEEE Transactions on Communications*, vol. 50, 2002, pp. 1926–1934.

[GSS+03]   Gesbert, D.; Shafi, M.; Shiu, D. S.; Smith, P. J.; Naguib, A.: From theory to practice: an overview of MIMO space–time coded wireless systems. *IEEE Journal on Selected Areas in Communications*, vol. 21, 2003, pp. 281–302.

[HKK+00]   Haardt, M.; Klein, A.; Koehn, R.; Oestreich, S.; Purat, M.; Sommer, V.; Ulrich, T.: The TD-CDMA based UTRA TDD mode. *IEEE Journal on Selected Areas in Communications*, vol. 18, 2000, pp. 1375–1385.

[HM72]   Harashima, H.; Miyakawa, H.: Matched-transmission technique for channels with intersymbol interference. *IEEE Transactions on Communications*, vol. 20, 1972, pp. 774–780.

[HNP+99]   Hardell, L.; Nasman, A.; Pahlson, A.; Hallquist, A.; Mild, K. H.: Use of cellular telephones and the risk for brain tumors: a case-control study. *International Journal of Oncology*, vol. 15, 1999, pp. 113–116.

[IEE01]   Human exposure to radio frequency and microwave radiation from portable and mobile telephones and other wireless communication devices–a comar technical information statement. *IEEE Engineering in Medicine and Biology Magazine*, vol. 20(1), 2001, pp. 128–131.

[IHRF03]   Irmer, R.; Habendorf, R.; Rave, W.; Fettweis, G.: Noninear Multiuser Transmission using Multiple Antennas for TDD-CDMA. *Proc. IEEE 6th International Symposium on Wireless Personal Multimedia Communications 2003 (WPMC'03)*, vol. 3, Yokosuka, 2003, pp. 251–255.

[IRF03]   Irmer, R.; Rave, W.; Fettweis, G.: Minimum BER transmission for TDD-CDMA in frequency-selective channels. *Proc. IEEE 14th International Symposium on Personal, Indoor and Mobile Radio Communications (PIMRC'03)*, vol. 2, Beijing, 2003, pp. 1260–1264.

[JBMW02] Jötten, C. A.; Baier, P. W.; Meurer, M.; Weber, T.: Cost efficient representation and signalling of channel information in MIMO systems. *Proc. IEEE 56th Vehicular Technology Conference (VTC'02-Fall)*, vol. 1, Vancouver, 2002, pp. 175–179.

[JKG⁺02] Joham, M.; Kusume, K.; Gzara, M. H.; Utschick, W.; Nossek, J. A.: Transmit Wiener Filter for the Downlink of TDD DS-CDMA Systems. *Proc. IEEE 7th International Symposium on Spread Spectrum Techniques & Applications (ISSSTA'02)*, vol. 1, Prague, 2002, pp. 9–13.

[JKUN02] Joham, M.; Kusume, K.; Utschick, W.; Nossek, J. A.: Transmit Matched Filter and Transmit Wiener Filter for the Downlink of FDD DS-CDMA Systems. *Proc. IEEE 13th International Symposium on Personal, Indoor and Mobile Radio Communications (PIMRC'02)*, vol. 5, Lisboa, 2002, pp. 2312–2316.

[JN98] Jeong, I.; Nakagawa, M.: A Novel Transmission Diversity System in TDD-CDMA. *IEICE Transactions on Communications*, vol. E81-B, 1998, pp. 1409–1416.

[JU00] Joham, M.; Utschick, W.: Downlink Processing for Mitigation of Intracell Interference in DS-CDMA Systems. *Proc. IEEE 6th International Symposium on Spread Spectrum Techniques & Applications (ISSSTA'00)*, vol. 1, Parsippany, 2000, pp. 15–19.

[KBL97] Kuster, N.; Balzano, Q.; Lin, J. C.: *Mobile Communications Safety*. London, UK: Chapman & Hall, 1997.

[Kle96] Klein, A.: *Multi-user detection of CDMA signals – algorithms and their application to cellular mobile radio*. Fortschrittberichte VDI, Reihe 10, Nr. 423. Düsseldorf: VDI-Verlag, 1996.

[Lee90] Lee, W. C. Y.: *Mobile cellular telecommunications systems*. New York: McGraw-Hill, 1990.

[LNSE01] Lucent; Nokia; Siemens; Ericsson: A standardized set of MIMO radio propagation channels. *3GPP, TSG RAN WG1, R1-01-1179*, Jeju, Korea, 2001.

[Lue96] Luetkepohl, H.: *Handbook of Matrices*. England: John Wiley & Sons, 1996.

[MBL⁺00] Meurer, M.; Baier, P. W.; Lu, Y.; Papathanassiou, A.; Weber, T.: TD-CDMA downlink: Optimum transmit signal design reduces receiver complexity and enhances system performance. *Proc. 7th International Conference on Telecommunications (ICT'00)*, vol. 1, Acapulco, 2000, pp. 300–305.

[MBQ04] Meurer, M.; Baier, P. W.; Qiu, W.: Receiver Orientation versus Transmitter Orientation in Linear MIMO Transmission Systems. *EURASIP Journal on Applied Signal Processing*, vol. 9, 2004, pp. 1191 – 1198.

[MBW⁺00] Meurer, M.; Baier, P. W.; Weber, T.; Lu, Y.; Papathanassiou, A.: Joint transmission, advantageous downlink concept for CDMA mobile radio systems using time division duplexing. *IEE Electronics Letters*, vol. 36, 2000, pp. 900–901.

[Meh91]   Mehta, M. L.: *Random matrices: Revised and Enlarged Second Edition*. New York: Academic Press, 1991.

[MM80]   Monzingo, R. A.; Miller, W. T.: *Introduction to adaptive arrays*. New York: John Wiley & Sons, 1980.

[MTJ02]   Meurer, M.; Tröger, H.; Jötten, C. A.: A novel generalized optimization criterion for transmit signal design in joint transmission (JT) multiuser downlinks. *Proc. 9th International Conference on Telecommunications (ICT'02)*, vol. 1, Beijing, 2002, pp. 26–31.

[MTWB01]   Meurer, M.; Tröger, H.; Weber, T.; Baier, P. W.: Synthesis of joint detection (JD) and joint transmission (JT) in CDMA downlinks. *IEE Electronics Letters*, vol. 37, 2001, pp. 919–920.

[MWQ04]   Meurer, M.; Weber, T.; Qiu, W.: A random matrix approach to performance evaluation of receiver-oriented transmission. *Proc. 4. Diskussionssitzung der ITG-Fachgruppe Angewandte Informationstheorie*, Kiel, 2004.

[Naß95]   Naßhan, M. M.: *Realitätsnahe Modellierung und Simulation nachrichtentechnischer Systeme, gezeigt am Beispiel eines CDMA-Mobilfunksystems*. Fortschrittberichte VDI, Reihe 10, Nr. 384. Düsseldorf: VDI-Verlag, 1995.

[NB01]   Noll-Barreto, A.: *Signal Pre-Processing in the Downlink of Spread-Spectrum Communications Systems*. Fortschrittberichte VDI, Reihe 10, Nr. 687. Düsseldorf: VDI-Verlag, 2001.

[NBF00]   Noll-Barreto, A.; Fettweis, G.: Performance improvement in DS-spread spectrum CDMA systems using a pre- and a post-rake. *Proc. 2000 International Zurich Seminar on Broadband Communications (IZS'00)*, Zurich, 2000, pp. 39–46.

[NS73]   Nassi, I.; Shneiderman, B.: Flowchart techniques for structured programming. *ACM SIGPLAN Notices*, vol. 8, 1973, pp. 12–26.

[OP98]   Ojanpera, T.; Prasad, R.: *Wideband CDMA for Third Generation Mobile Communications*. Artech House Publishers, 1998.

[Pap00]   Papathanassiou, A.: *Adaptive antennas for mobile radio systems using Time Division CDMA and joint detection*. Forschungsberichte Mobilkommunikation Band 6. Universität Kaiserslautern, 2000.

[Par92]   Parsons, J. D.: *The mobile radio propagation channel*. London: Pentech Press, 1992.

[PHS03]   Peel, C.; Hochwald, B.; Swindlehurst, L.: A Vector-Perturbation Technique for Near-Capacity Multi-antenna Multi-User Communication: Part 1 & 2. *Proc. 41st Allerton Conference on Communication, Control, and Computing*, Monticello, Illinois, 2003.

[Pro95]   Proakis, J. G.: *Digital Communications*. 3. Auflage. New York: McGraw-Hill, 1995.

[QMBW04] Qiu, W.; Meurer, M.; Baier, P. W.; Weber, T.:   Power efficient
          CDMA broadcast system doing without any channel knowledge at the re-
          ceivers, a non-obvious modification of THP. *Proc. IEEE joint conference
          (APCC/MDMC'04) of 10th Asia-Pacific Conference on Communications
          (APCC2004) and 5th International Symposium on Multi-Dimensional Mo-
          bile Communications (MDMC2004)*, Beijing, 2004, pp. 793–799.

[QTM02]   Qiu, W.; Tröger, H.; Meurer, M.: System model of joint transmission (JT)
          in multi-user MIMO transmission systems. *COST 273 TD(02) 008*, London,
          2002.

[QTMJ03] Qiu, W.; Tröger, H.; Meurer, M.; Jötten, C. A.:   Performance analysis
          of a channel oriented concept for multi-user MIMO downlinks with fre-
          quency selective channels. *Proc. IEEE 57th Vehicular Technology Conference
          (VTC'03-Spring)*, vol. 1, Jeju, Korea, 2003, pp. 539–543.

[Rup93]   Rupprecht, W.: *Signale und Übertragungssysteme*. Berlin: Springer-Verlag,
          1993.

[SBE+02] Soma, P.; Baum, D. S.; Erceg, V.; Krishnamoorthy, R.; Paulraj, A. J.: Ana-
          lysis and modeling of multiple-input multiple-output (MIMO) radio channel
          based on outdoor measurements conducted at 2.5 GHz for fixed BWA appli-
          cations. *Proc. IEEE International Conference on Communications (ICC'02)*,
          vol. 25, New York, 2002, pp. 272–276.

[SJ67]   Stein, S.; Jones, J. J.:   *Modern Communication Principles*. New York:
          McGraw-Hill, 1967.

[Ste92]   Steele, R.: *Mobile Radio Communications*. London: Pentech Press, 1992.

[Ste95]   Steiner, B.:   *Ein Beitrag zur Mobilfunk-Kanalschätzung unter besonderer
          Berücksichtigung synchroner CDMA-Mobilfunksysteme mit Joint Detection*.
          Fortschrittberichte VDI, Reihe 10, Nr. 337. Düsseldorf: VDI-Verlag, 1995.

[Tel99]   Telatar, I. E.:   Capacity of multi-antenna Gaussian channels.   *European
          Transactions on Telecommunications*, vol. 10, 1999, pp. 585–595.

[Tom71]   Tomlinson, M.: New automatic equalizer employing modulo arithmetic. *IEE
          Electronics Letters*, vol. 7, 1971, pp. 138–139.

[Trö03]   Tröger, H.:   *Empfängerorientierte Mehrteilnehmer-Übertragungsverfahren
          für die Abwärtsstrecke zellularer Mobilfunksysteme*. Forschungsberichte Mo-
          bilkommunikation Band 13. Universität Kaiserslautern, 2003.

[TWMB01] Tröger, H.; Weber, T.; Meurer, M.; Baier, P. W.: Performance assessment of
          Joint Transmission (JT) multi-user downlinks with multi-element transmit
          antennas. *European Transactions on Telecommunications*, vol. 12, 2001, pp.
          407–415.

[Ver98]   Verdú, S.: *Multiuser detection*. Cambridge: Cambridge University Press,
          1998.

[VM98]   Vojcic, B. R.; Mee, J. W.: Transmitter precoding in synchronous multiuser communications. *IEEE Transactions on Communications*, vol. 46, 1998, pp. 1346–1355.

[Wec02]   Weckerle, M.: *Utilization of Correlation Matrices in Adaptive Array Processors for Time Slotted CDMA Uplinks.* Forschungsberichte Mobilkommunikation Band 11. Universität Kaiserslautern, 2002.

[WF03a]   Windpassinger, C.; Fischer, R. F. H.: Low-Complexity Near-Maximum-Likelihood Detection and Precoding for MIMO Systems using Lattice Reduction. *Proc. IEEE Information Theory Workshop 2003 (ITW2003)*, Paris, France, 2003, pp. 345–348.

[WF03b]   Windpassinger, C.; Fischer, R. F. H.: Optimum and Sub-Optimum Lattice-Reduction-Aided Detection and Precoding for MIMO Communications. *Proc. 2003 Canadian Workshop on Information Theory*, Ontario, Canada, 2003, pp. 83–87.

[WM03]   Weber, T.; Meurer, M.: Optimum Joint Transmission: Potentials and Dualities. *Proc. 6th International Symposium on Wireless Personal Multimedia Communications 2003 (WPMC'03)*, vol. 1, Yokosuka, 2003, pp. 79–83.

[WMS03]   Weber, T.; Meurer, M.; Sklavos, A.: Optimum Nonlinear Joint Transmission. *COST 273 TD(03)008*, Barcelona, 2003.

[XCHV04]   Xu, H.; Chizhik, D.; Huang, H.; Valenzuela, R.: A generalized space-time multiple-input multiple-output (MIMO) channel model. *IEEE Transactions on Wireless Communications*, vol. 3, 2004, pp. 966–975.

[XWL+04]   Xiao, C.; Wu, J.; Leong, S.-Y.; Zheng, Y.; Letaief, K. B.: A Discrete-Time Model for Triply Selective MIMO Rayleigh Fading Channels. *IEEE Transactions on Wireless Communications*, vol. 3, 2004, pp. 1678–1688.

[YBO+04]   Yu, K.; Bengtsson, M.; Ottersten, B.; McNamara, D.; Karlsson, P.; Beach, M.: Modeling of wide-band MIMO radio channels based on NLoS indoor measurements. *IEEE Transactions on Vehicular Technology*, vol. 53, 2004, pp. 655–665.

Tabellarischer Lebenslauf

Name:	Wei Qiu
Adresse:	Kurt-Schumacher-Str. 48
	67663 Kaiserslautern
	Deutschland
Geburtsdatum:	5. Juli 1975
Geburtsort:	Jiangsu / V.R.China
Familienstand:	verheiratet
Nationalität:	V.R.China
Schulbildung:	1988–1994
	Gymnasium in Jiangsu
Hochschulaufnahmenprüfung:	Juli 1994
1. Studium:	1994–1999
	Studium der Elektrotechnik/Nachrichtentechnik
	an der Tsinghua Universität, Peking
Studienabschluß:	Bachelor
2. Studium:	1999–2001
	Studium der Elektrotechnik/Nachrichtentechnik
	an der Universität Kaiserslautern
Studienabschluß:	Master of Science (M.Sc.)
Berufstätigkeit:	seit September 2001
	wissenschaftlicher Mitarbeiter
	am Lehrstuhl für hochfrequente Signalübertragung
	und -verarbeitung
	an der Technischen Universität Kaiserslautern